

2015

# Discovery and analysis of genes important in kidney development and disease

---

<https://hdl.handle.net/2144/13984>

*Boston University*

BOSTON UNIVERSITY

SCHOOL OF MEDICINE

Dissertation

**DISCOVERY AND ANALYSIS OF GENES IMPORTANT IN KIDNEY  
DEVELOPMENT AND DISEASE**

by

**HILA MILO RASOULY**

B.A., University of Tel Aviv, 2003  
M.Sc., Hebrew University of Jerusalem, 2005

Submitted in partial fulfillment of the  
requirements for the degree of  
Doctor of Philosophy

2015



Approved by

First Reader

---

Weining Lu, M.D.  
Associate Professor of Medicine

Second Reader

---

David J. Salant, M.D.  
Professor of Medicine

“If we knew what it was we were doing, it would not be called research, would it?”

Albert Einstein

## **DEDICATION**

I would like to dedicate this work to my spouse Aviram, my daughters Tahel and Oriane,  
and my parents Daniel and Lee.

## ACKNOWLEDGMENTS

I would like to express my thanks and appreciation to my thesis advisor, Dr. Weining Lu, for giving me the opportunity to perform my thesis research in his laboratory. Dr. Lu's enthusiasm, optimism, support, kindness, generosity, teaching and encouragements were instrumental in the completion of this work. Dr. Lu's office was always open during the past five years for me, and our conversations gave me the confidence that he believes in me and cares for my career. Dr. Lu also gave me the freedom to take part in the GMS curriculum development committee for the Program in Biomedical Sciences (PiBS), in the genetic counseling seminar and international scientific conferences, and gave me the opportunity to mentor three summer students over the years, all these were very gratifying.

I wish to thank all members of my thesis committee, Dr. Kenneth Albrecht, Dr. David Salant, Dr. Marc Lenburg and Dr. Matthew Layne for their time and scientific advice to my research projects. In particular, I would like to thank Dr. Salant for agreeing to take on the task of being the second reader of my dissertation and Dr. Albrecht who chaired my thesis committee.

A special thanks to Dr. Shoumita Dasgupta, director of the Graduate Program in Genetics and Genomics at Boston University School of Medicine. Dr. Dasgupta's support throughout the years filled me with a sense of belonging to the Boston University community. I would like to especially thank her for giving me the opportunity to be part

of the PiBS curriculum development committee, which was an amazing experience and introduced me to many great faculty members at Boston University and to the dilemma of graduate training. It was also an honor to be a teacher assistant in her class, which I admire.

I want also to thank my friends and colleagues in Dr. Lu's laboratory. Special thanks to Anna Pisarek-Horowitz, my fellow graduate student, who had the patience to teach me how to dissect mice and embryos, how to use a microscope, and introduced me to the world of electron microscopy. Anna has been a great friend throughout these five years, and I am so happy that we shared this experience. I would also like to thank Dr. Xueping Fan for his scientific inputs during lab meetings and beyond, as well as for his willingness to perform biochemistry experiments for one of my projects. I would like to thank Stefanie Chan who became a friend during her two years in the lab, and helped me a lot with the mouse colonies, especially during the time of my maternity leave. I also thank Juan Liu, who taught me all she knew about mice, took care of the mice for me during my first years in the lab, and was also a great companion at that time. Many thanks to Dr. Sudhir Kumar and Dr. Richa Sharma, who recently joined our lab, for their help with several experiments.

I would also like to thank the Renal department for providing such a nurturing environment for me in the past five years. Special thanks to Kathleen Dashner, the lab operation manager in the department, not only for her help to cut so many tissue samples for my projects, but also for our long discussion, she is one of the most generous persons



I have ever met. I would also like to thank Theresa Nguyen, the administrator of the Renal department, and Dr. Laurence Beck, who organizes an impressive renal research seminar series that introduced me to the research of many leading nephrologists.

I would like to acknowledge the GSI initiatives and Yuriy Alekseyev and Adam Gower from the microarray core facility at Boston University School of Medicine for helping me with the microarray experiment.

I would also like to express my gratitude to all members in the laboratory animal science center (LASC) at BU Medical School, who took care of all the mice I generated in the past five years.

I am also grateful to MaryAnn Champion, the program director of the genetic counseling program, who invited me to join their seminar and always made me feel that I am more than welcomed. These seminars kept my mood up when the experiments in the lab were not going well.

On a personal note, I would like to thank my family, my father Daniel, my mother Lee and my sister Laura, who organized themselves to help me finishing my PhD research, despite all the difficulties. Their support, especially with my daughters and home tasks as well as their interest in my research was instrumental. I would not have been able to finish this thesis work without their help during their long visits in the past 18 months.

Finally, I would like to thank my husband, Aviram, for so many things: convincing me ten years ago to try and get into an American graduate program; being an

amazing father, never complaining about my long hours of study during the weekends since Tahel was a baby; relentlessly boosting my self-esteem even when asked to answer the most basic scientific questions. Thank you Aviram for all the support, love and friendship, I am so happy that we are together.

**DISCOVERY AND ANALYSIS OF GENES IMPORTANT IN KIDNEY  
DEVELOPMENT AND DISEASE**

**HILA MILO RASOULY**

Boston University School of Medicine, 2015

Major Professor: Weining Lu, M.D., Associate Professor of Medicine

**ABSTRACT**

Abnormal kidney development is a relatively prevalent health issue; however, the genetic basis is mostly unknown. The aim of this thesis is to identify genes important in kidney development and disease and to study their molecular functions. We hypothesized that human diseases associated with kidney anomalies can uncover novel genes important in kidney development and disease. The thesis is divided into three independent projects that examined three genes (i.e. *Zeb2*, *Ilk*, *Robo2*) at three stages of mouse kidney development: nephrogenesis, glomerular podocyte, and early ureteric bud outgrowth.

In the first project, we identified *Zeb2*, a gene encoding the zinc finger E-box binding homeobox 2 transcription factor that is mutated in the Mowat Wilson syndrome, as a novel gene important in nephrogenesis. *Zeb2* conditional knockout mice (*Zeb2 cKO*) develop glomerulocystic kidney disease with many atubular glomeruli and decreased expression of proximal tubular markers before cyst formation. These data suggest that abnormal nephrogenesis leads to the congenital atubular glomeruli and primary

glomerular cysts in the *Zeb2 cKO* mice. This study implies that *ZEB2* is a novel candidate gene for glomerular cystic disease in patients. Additionally we found that *Pkd1*, the gene mutated in autosomal dominant polycystic kidney disease, is upregulated in non-cystic glomeruli and knockout of one copy of the *Pkd1* gene exacerbates the cystic phenotype of the *Zeb2 cKO* mice. These findings suggest a genetic interaction between *Zeb2* and *Pkd1* and that *Zeb2* might be a novel *PKD1* modifier.

In the second project, we studied the roles of integrin-linked kinase (ILK) and roundabout 2 (ROBO2) in glomerular podocytes. We found that ILK and ROBO2 form a protein complex, and that loss of *Robo2* improves survival and alleviates the podocyte and basement membrane abnormalities seen in *Ilk* knockout mice. In the third project, using microarray gene expression analysis, we found lower gene expression levels of extracellular matrix proteins during early ureteric bud outgrowth in the *Robo2* homozygous knockout embryos as compared to wild type controls. These findings suggest that ROBO2 may regulate extracellular matrix components in the kidney.

In conclusion, we found a new role for *Zeb2* in nephrogenesis, and identified a novel function of *Robo2* in regulating extracellular matrix gene expression in podocytes and during early kidney development.

## TABLE OF CONTENTS

TITLE .....	i
APPROVAL PAGE .....	iii
QUOTE.....	iv
DEDICATION .....	v
ACKNOWLEDGMENTS .....	vi
ABSTRACT.....	x
TABLE OF CONTENTS.....	xii
LIST OF TABLES .....	xix
LIST OF FIGURES .....	xxi
LIST OF ILLUSTRATIONS.....	xxiv
LIST OF ABBREVIATIONS.....	xxv
CHAPTER ONE: Introduction .....	1
1.1 Kidney and urinary tract development and function.....	3
1.1.1 Kidney and urinary tract anatomy.....	3
1.1.2 Kidney and urinary tract development.....	4
1.1.3 The renal corpuscle structure .....	7
1.2 Human Genetics of CAKUT.....	8

1.2.1 Genetic heterogeneity of CAKUT impedes linkage and association studies in CAKUT families .....	9
1.2.2 Genomic imbalances and chromosomal rearrangements as a tool to uncover genes associated with CAKUT. ....	10
1.3 Mouse models as a tool to study birth defects of the kidney .....	11
1.3.1 Mouse models for urinary tract development .....	11
1.3.2 Genetic tools in mouse genetics.....	11
1.3.3 Genetic interaction analysis .....	13
1.4 Genes and pathways associated with kidney development and disease .....	14
1.5 Examples of birth defects of the kidney .....	15
1.5.1 Renal cystic diseases.....	15
1.5.2 Congenital Podocytopathies.....	16
1.5.3 Glomerular basement membrane diseases .....	16
1.6 Human syndromes associated with an increased risk for CAKUT.....	16
1.7 General Hypothesis and Specific Aims .....	22
1.7.1 General Hypothesis .....	22
1.7.2 Specific Aims.....	22
CHAPTER TWO: Loss of <i>Zeb2</i> causes glomerulocystic kidney disease in mice.....	23
2.1 Summary .....	23
2.2 Background and Introduction .....	24
2.2.1 Mowat Wilson syndrome.....	24
2.2.2 ZEB2 protein.....	25

2.2.3 Role of ZEB2 in development and cancer. ....	26
2.2.4 Glomerulocystic kidney disease (GCKD) as a specific form of renal cystic disease.....	28
2.2.5 Genes associated with glomerular cysts in mice.....	29
2.3 Hypothesis.....	30
2.4 Materials and Methods.....	31
2.4.1 Mice Strains .....	31
2.4.2 Mouse DNA extraction and genotyping .....	32
2.4.3 Tissue collection and preparation .....	33
2.4.4 Histological analysis .....	33
2.4.5 Immunohistochemistry .....	33
2.4.6 Immunofluorescence staining .....	34
2.4.7 Urine protein and renal function analysis .....	35
2.4.8 Glomerular count and cysts assessment.....	35
2.4.9 Assessment of glomerulotubular integrity .....	36
2.4.10 TaqMan real-time PCR gene expression analysis .....	37
2.4.11 Statistical analysis.....	37
2.5 Results.....	38
2.5.1 ZEB2 is broadly expressed in the developing kidney.....	38
2.5.2 Loss of Zeb2 leads to glomerular kidney cysts formation.....	42
2.5.3 GCKD in Zeb2 knockout mice is due to atubular glomeruli formation .....	60
2.5.4 Zeb2 knockout mice have abnormal tubular development.....	62

2.5.5 Decreased apoptosis in the early stages of glomerular development of Zeb2 conditional knockout embryos .....	64
2.5.6 Elevated levels of Pkd1 mRNA and protein in the kidneys of Zeb2 conditional knockout mice .....	67
2.5.7 Heterozygous deletion of Pkd1 in the kidneys of Zeb2 conditional knockout mice exacerbates renal cystic phenotype .....	71
2.6 Discussion .....	72
2.6.1 Interpretations .....	72
2.6.2 Future research opportunities .....	78
2.7 Conclusions .....	82
 CHAPTER THREE: Loss of <i>Robo2</i> alleviates the glomerular phenotype of <i>Ilk</i> podocyte-specific knockout mice. ....	 84
3.1 Summary .....	84
3.2 Background and Introduction .....	85
3.2.1 The glomerular basement membrane .....	86
3.2.2 The integrin linked kinase (ILK) function in the podocytes .....	88
3.2.3 ROBO2 functions in the podocytes .....	91
3.2.4 Both ILK and ROBO2 form complexes with Nephrin through NCK .....	95
3.3 Hypothesis .....	96
3.4 Materials and Methods .....	97
3.4.1 Biochemical analysis of protein-protein interaction and complex formation ..	97
3.4.2 Mice strains .....	97



3.4.3 Mouse DNA extraction and genotyping .....	99
3.4.4 Tissue collection and preparation .....	99
3.4.5 Ultrastructural analysis of the glomeruli.....	99
3.4.6 Survival analysis .....	100
3.4.7 Urine protein analysis .....	100
3.4.8 Histological analysis .....	100
3.5 Results.....	101
3.5.1 ILK and ROBO2 form a protein complex through PINCH and NCK.....	101
3.5.2 Generation of Robo2-Ilk double conditional knockout mice .....	103
3.5.3 Loss of Robo2 improves the podocyte ultrastructure of 4 weeks old Ilk cKO mice.....	105
3.5.4 Loss of Robo2 alleviates the thickening and splitting phenotype of the glomerular basement membrane in young Ilk knockout mice.....	109
3.5.5 Loss of Robo2 increases the median survival of Ilk cKO mice.....	111
3.5.6 Loss of Robo2 did not significantly affect proteinuria prevalence and renal histology in 4-6 weeks old Ilk podocyte-specific knockout mice.....	113
3.5.7 Loss of Robo2 does not affect the podocyte loss phenotype in 4 weeks old Ilk podocyte-specific knockout mice .....	115
3.6 Discussion.....	116
3.6.1 Loss of Robo2 improved the survival of the Ilk single cKO .....	117
3.6.2 Loss of ROBO2 improves the GBM phenotype of the Ilk cKO mice. ....	117
3.6.3 Loss of ROBO2 improve the life span of the Ilk cKO mice.....	118

3.6.4 ILK and ROBO2 may have opposite effects on cytoskeleton remodeling, cell adhesion and glomerular basement membrane composition .....	119
3.7 Limitations .....	122
3.8 Conclusions.....	124
 CHAPTER FOUR: SLIT2/ROBO2 signaling regulates extracellular matrix gene expression during early ureteric bud outgrowth .....	
4.1 Summary .....	125
4.2 Background and Introduction .....	126
4.2.1 Ureteric bud outgrowth.....	126
4.2.2 Genes associated with abnormal UB outgrowth.....	130
4.3 Hypothesis.....	134
4.4 Materials and Methods.....	135
4.4.1 General experimental design.....	135
4.4.2 Mice strains .....	135
4.4.3 Tissue collection and RNA isolation .....	136
4.4.4 Microarray experimental design .....	136
4.4.5 Microarray experiment.....	137
4.4.6 Microarray quality control .....	137
4.4.7 Gene Set Enrichment Analysis (GSEA) .....	139
4.4.8 Ingenuity pathway analysis overview .....	140
4.5 Results.....	141

4.5.1 No single gene expression is significantly altered in Slit2 and Robo2 knockout kidney at E10.5 and E11.5 .....	141
4.5.2 Genes coding for extracellular matrix proteins are coordinately downregulated in the Robo2 and the Slit2 knockouts compared to wild-type littermates .....	150
4.5.3 Pathways related to the extracellular matrix proteins are downregulated in the Robo2 and the Slit2 knockout compared to wild-type littermates.....	158
4.6 Discussion .....	162
4.6.1 Interpretations .....	162
4.6.2 Limitations .....	169
4.7 Conclusions.....	170
5. SUMMARY AND CONCLUSIONS .....	172
JOURNALS LIST AND ABBREVIATIONS .....	175
BIBLIOGRAPHY.....	181
CURRICULUM VITAE.....	213

## LIST OF TABLES

Table 1.1: Syndromes Associated with increased risk for CAKUT .....	19
Table 2.1: Kidney samples collected from the <i>Zeb2</i> conditional knockout mice in project one.....	44
Table 2.2: Cystic phenotype observed in H&E stained histological samples of <i>Zeb2</i> <sup><i>fllox/fllox</i></sup> ; <i>Pax2-cre</i> <sup>+</sup> and wild-type littermates between E16.5 and E18.5 .....	47
Table 2.3: Percentage of cysts with glomerular tuft analyzed on H&E stained histological samples between E16.5 and E18.5.....	47
Table 2.4: Mendelian distribution of <i>Zeb2</i> conditional knockout using <i>Pax2-cre</i> . .....	51
Table 3.1: Number of mice analyzed for phenotype and survival studies in <i>Ilk</i> and <i>Robo2</i> cKO mice .....	105
Table 3.2: Statistical analysis of the survival in the first set of mice (n>20).....	112
Table 4.1: Mutations in genes controlling early ureteric buds outgrowth in human and mouse .....	128
Table 4.2: Embryonic kidney tissues from F1 crossing used in microarray experiments .....	142
Table 4.3: No significant differential expression of any gene in any group was detected in E10.5-E11.5 <i>Robo2</i> and <i>Slit2</i> embryonic kidney tissues .....	147
Table 4.4: The expression of candidate genes controlling UB outgrowth in the microarray dataset .....	149
Table 4.5: Sets of genes significantly coordinately down-regulated in <i>Slit2</i> and <i>Robo2</i> knockouts compared to the wild-type controls .....	151

Table 4.6: Sets of genes significantly coordinately up-regulated in E10.5 knockout compared to the wild-type .....	152
Table 4.7: Most differential expressed Laminin coding genes at E10.5-E11.5 in the UBand MM (Mean log <sub>2</sub> >8).....	154
Table 4.8: Table 4.6: Most differential expressed Collagen coding genes at E10.5-E11.5 in the UB and MM (Mean log <sub>2</sub> >8).....	155
Table 4.9: Upstream regulators analysis by IPA .....	161
Table 4.10: Top genes encoded metallopeptidase that are expressed in E10.5 and E11.5 UB and MM tissues from Slit2 and Robo2 knockout mice.....	168

## LIST OF FIGURES

Figure 2.1: <i>Zeb2</i> mRNA is broadly expressed in the developing mouse kidney and urinary tract. ....	39
Figure 2.2: ZEB2 is highly expressed in developing mouse kidney.....	41
Figure 2.3: Loss of <i>Zeb2</i> in the metanephric mesenchyme and the ureteric bud leads to renal cysts development.....	46
Figure 2.4: No glomerular cysts were observed in E15.5 <i>Zeb2<sup>fllox/fllox</sup>;Six2-cre<sup>+</sup></i> kidney...	48
Figure 2.5: Deletion of <i>Zeb2</i> in the metanephric mesenchyme and the ureteric bud leads to glomerular cysts formation. ....	50
Figure 2.6: Deletion of <i>Zeb2</i> in the tubular epithelial cells, podocytes and glomerular parietal cells using <i>Six2-cre<sup>+</sup></i> leads to glomerular cysts development. ....	53
Figure 2.7: Deletion of <i>Zeb2</i> in the tubular epithelial cells does not cause tubular cysts.	54
Figure 2.8: Cystic kidney disease in adult <i>Zeb2<sup>fllox/fllox</sup>;Six2-Cre<sup>+</sup></i> mice.....	56
Figure 2.9: Glomerulosclerosis in adult <i>Zeb2<sup>fllox/fllox</sup>;Six2-Cre<sup>+</sup></i> mice .....	57
Figure 2.10: No glomerulosclerosis is observed at E18.5 in <i>Zeb2<sup>fllox/fllox</sup>;Pax2-Cre<sup>+</sup></i> mice	58
Figure 2.11: Proteinuria and renal failure in adult <i>Zeb2<sup>fllox/fllox</sup>; Six2-cre<sup>+</sup></i> mice .....	59
Figure 2.12: Congenital atubular glomeruli in the <i>Zeb2</i> nephron-specific knockout mice. ....	61
Figure 2.13: Decreased tubular markers' expression in the <i>Zeb2</i> nephron-specific knockout mice. ....	63
Figure 2.14: Reduced kidney size in the <i>Zeb2</i> nephron-specific knockout mice. ....	64

Figure 2.15: Decreased apoptosis in the C- and S-shaped bodies in <i>Zeb2</i> knockout mice. .....	65
Figure 2.16: No significant change in cell proliferation in the Bowman’s capsule of <i>Zeb2</i> knockout mice.....	67
Figure 2.17: Abnormal expression levels of genes associated with GCKD after the appearance of the glomerular cysts.....	69
Figure 2.18: Increased <i>Pkd1</i> expression in the kidney of <i>Zeb2</i> conditional knockout mice. .....	70
Figure 3.1: Robo2 and Ilk form a protein complex through Nck and Pinch. ....	102
Figure 3.2: Podocyte ultrastructure (SEM) in 2 weeks old <i>Ilk</i> and <i>Robo2</i> cKO mice....	106
Figure 3.3: Loss of Robo2 improves the podocyte ultrastructure of the 4 weeks old <i>Ilk<sup>lox/lox</sup>;Pod-cre<sup>+</sup></i> mice. ....	107
Figure 3.4: Podocyte ultrastructure (SEM) in 6 weeks old <i>Ilk</i> and <i>Robo2</i> cKO mice....	108
Figure 3.5: Loss of Robo2 decreases GBM thickening and splitting in 4 weeks old <i>Ilk<sup>lox/lox</sup>;Pod-cre<sup>+</sup></i> single cKO mice.....	110
Figure 3.6: Intermediate analysis of survival showed that loss of <i>Robo2</i> improves the survival of <i>Ilk</i> cKO Mice. ....	112
Figure 3.7: Loss of <i>Robo2</i> improves the median survival of podocyte-specific single <i>Ilk</i> knockout mice.....	113
Figure 3.8: No significant difference in proteinuria between the <i>Ilk-Robo2</i> DKO mice and the <i>Ilk</i> single cKO mice at 4 weeks.....	115
Figure 4.1: Probe-level expression of <i>Robo2</i> .....	144

Figure 4.2: Probe-level expression of <i>Slit2</i> .....	145
Figure 4.3: Principal Component Analysis.....	146
Figure 4.4: Heatmaps from leading edges for gene-sets downregulated in E10.5 <i>Robo2</i> and <i>Slit2</i> knockout kidneys .....	157
Figure 4.5: Pathway analysis with IPA on E10.5 combined dataset .....	159
Figure 4.6: Targets of IGF1R and their differential expressions in E10.5 ureteric buds ( <i>Slit2</i> <sup>-/-</sup> and <i>Robo2</i> <sup>-/-</sup> combined).....	161
Figure 4.7: Targets of TGFB1 and their differential expressions in E10.5 ureteric buds ( <i>Slit2</i> <sup>-/-</sup> and <i>Robo2</i> <sup>-/-</sup> combined).....	162



## LIST OF ILLUSTRATIONS

Illustration 1.1: Urinary tract development and Structure .....	5
Illustration 1.2: Scheme of the Cre-lox system.....	13
Illustration 2.1: The ZEB2 protein structure.....	26
Illustration 2.2: <i>Zeb2</i> floxed allele.....	43
Illustration 3.1: Robo2 inhibits Nephrin-induced actin polymerization. ....	92
Illustration 3.2: Alleles used to analyze genetic interaction between ILK and ROBO2 in the podocytes. ....	98
Illustrations 3.3: Generation of the <i>Robo2<sup>fllox/+</sup>;Ilk1<sup>fllox/+</sup>;Pod-cre<sup>+</sup></i> mice.....	104
Illustration 3.4: ILK and ROBO2 have opposite roles on podocyte structure and function. .....	121
Illustration 4.1: Ureteric bud outgrowth .....	127
Illustration 4.2 : Genes and signaling pathways involved in UB outgrowth. ....	131
Illustration 4.3: Generation of a hypothesis.....	164

## LIST OF ABBREVIATIONS

ANH.....	Antenatal Hydronephrosis
BUN.....	Blood Urea Nitrogen
CAKUT.....	Congenital Anomalies of the Kidney and the Urinary Tract
cKO.....	conditional Knockout
CSB.....	Comma-Shaped bodies
CC.....	Coiled Coil
DBA.....	Dolichos biflorus agglutinin
DKO.....	Double Knockout
EMT.....	Epithelial to Mesenchymal Transition
ESRD.....	End Stage Renal Disease
GBM.....	Glomerular Basement Membrane
GCKD.....	Glomerular Cystic Kidney Disease
GUDMAP.....	GenitoUrinary Development Molecular Anatomy Project
H&E.....	Hematoxylin and Eosin
IF.....	Immunofluorescence
IHC.....	Immunohistochemistry
ILK.....	Integrin Linked Kinase
LTL.....	Lotus Tetragonolobus Lectin
MM.....	Metanephric Mesenchyme
MWS.....	Mowat Wilson Syndrome
MET.....	Mesenchymal to Epithelial Transition

MTS .....	Masson Trichrome Stain
OMIM .....	Online Mendelian Inheritance in Man
PAS .....	Periodic acid–Schiff–diastase stain
PC1.....	Polycystin-1
PCR.....	Polymerase Chain Reaction
PKD.....	Polycystic kidney disease
PKD1.....	Polycystic kidney disease gene 1
ROBO2 .....	roundabout 2
RT .....	Reverse Transcription
SSB .....	S-Shaped Bodies
SLIT2 .....	Slit guidance ligand 2
UB.....	Ureteric Bud
UUO.....	Unilateral Ureteral Obstruction
VUR.....	Vesicoureteral Reflux
ZEB2.....	zinc finger E-box binding homeobox 2

## **CHAPTER ONE: Introduction**

Each year about 6% of infants worldwide (~ 8 million children) including 3% of all live births in the United States (>120,000 babies) are born with a serious birth defect of genetic origin (CDC, 2008; MOD, 2006; Yoon et al., 1997). Kidney and urinary tract developmental disorders account for 20-30% of all birth defects identified in the prenatal period, with limited diagnostic options (Deshpande and Hennekam, 2008; Pohl et al., 2002; Woolf, 2000). Congenital Anomalies of the Kidney and Urinary Tract (CAKUT) (Sargent, 2000; Williams et al., 2008a) are a group of renal tract birth defects that includes congenital kidney anomalies such as duplex multicystic dysplastic kidneys, renal cystic diseases, and congenital podocytopathies, and ureteric defects such as obstructive uropathy and vesicoureteral reflux (VUR) (Toka et al., 2010). The overall incidence of CAKUT in children is estimated over 1% and they are among the most common problems encountered by pediatric nephrologists and urologists (Peters et al., 2010; Sargent, 2000; Williams et al., 2008a). CAKUT is also the leading cause of chronic kidney disease and renal failure in children (Neild, 2010; Sanna-Cherchi et al., 2009; Toka et al., 2010).

During pregnancy, routine prenatal ultrasound examination enables early detection of many urinary tract anomalies in fetuses (Nguyen et al., 2010). Although some CAKUT phenotypes will resolve spontaneously in many babies after birth, the prenatal diagnosis of CAKUT during pregnancy brings a heavy psychological burden on the parents. When an anomaly is detected during obstetric ultrasound scan, the decision

regarding the pregnancy is strongly influenced by the definitive diagnosis and prognosis of the condition (Deshpande and Hennekam, 2008). Since a long list of genetic syndromes and chromosomal abnormalities is associated with CAKUT, the decision regarding diagnosis and intervention can be difficult. The decision becomes all the more difficult as only few causative genes have been identified so far in patients with isolated or non-syndromic CAKUT. Therefore, it is important to discover novel causative genes for CAKUT. A better understanding of kidney development is also necessary to the elucidation of the genetic basis of these disorders, which can also lead to new treatments, as exemplified by the use of CoQ10 to treat congenital podocytopathy in patients with mutations in the *ADCK4* gene (Ashraf et al., 2013).

In this thesis, I performed three research projects using mouse genetic approaches to better understand the molecular functions of three genes (i.e. *Zeb2*, *Ilk*, *Robo2*) that play important roles at three different stages of kidney development and their associated kidney diseases. The first project focused on the identification of *Zeb2* as a novel gene important in nephrogenesis and glomerulocystic kidney disease. The second project studied the genetic interaction between integrin linked kinase (*Ilk*) and roundabout 2 (*Robo2*) in kidney podocyte development and congenital podocytopathy. The third project explored the molecular abnormalities that lead to abnormal ureteric bud outgrowth, the formation of multiple ureteric buds and the associated CAKUT phenotype in *Robo2* and Slit guidance ligand 2 (*Slit2*) knockout mice.

To better understand these three projects, I will first summarize here some background information regarding kidney development and disease, as well as the human

genetics and mouse genetics tools available today to explore the pathogenesis of CAKUT. More detailed background information will be provided in each project separately.

## **1.1 Kidney and urinary tract development and function**

### *1.1.1 Kidney and urinary tract anatomy*

The urinary system is a multi-component organ system, whose primary function is to produce, transport, store, and eliminate urine in order to maintain body homeostasis by controlling the water and ionic balance of the blood (Rasouly and Lu, 2013). The kidney eliminates nitrogenous waste, maintains the volume, composition, and pressure of the blood, and the density of the bones (Bover and Cozzolino, 2011). Anatomically, the urinary system can be subdivided into an upper unit, the kidney, which filters and modifies the blood to produce urine, and a lower unit consisting of the ureter, the bladder, and the urethra, which transports, stores and eliminates the urine from the body (Rasouly and Lu, 2013). The nephron is the major component of the kidney, which filters the blood and maintains body homeostasis. A human kidney contains average 1 million nephrons (ranging between 200,000 and 1.8 million), which comprise intricately patterned and functionally compartmentalized epithelial structures (Hughson et al., 2003). The nephron can be further divided into the glomerulus, the proximal tubule, the loop of Henle, and the distal tubule.

### *1.1.2 Kidney and urinary tract development.*

The kidney and ureter originate from the intermediate mesoderm in early embryos when an epithelial outpouching called the ureteric bud (UB) sprouts from the caudal region of the Wolffian duct (also called the nephric duct) and invades adjacent metanephric mesenchyme (MM) (Illustration 1.1A) (Davidson, 2008). After the UB invasion into the MM, a reciprocal induction between the tip of the UB and the MM results in multiple rounds of UB branching morphogenesis to form the collecting system (the collecting duct), while mesenchymal-to-epithelial transition (MET) of the MM leads to the formation of the nephron (Saxen, 1987). These developmental processes ultimately give rise to a functional kidney that starts to produce urine at ~10 weeks of gestation in human and ~E16.5 in mice. At the same time, the trunk of the UB (i.e. the UB portion remaining outside of the MM) elongates without branching to form the ureter, a muscular tube structure transporting urine from the kidney to the bladder (Illustration 1.1C) (Airik and Kispert, 2007). Together with the differential growth in the caudal part of the body during fetal development, the elongation of the ureter leads to the ascent of the kidney to its final position in the retroperitoneal space behind the abdominal cavity.

At each round of ureteric branching, the MM becomes compacted and forms aggregates that undergo mesenchymal-to-epithelial transition. The aggregates of MM first form spheres of polarized epithelia with *de novo* generation of a central lumen, called renal vesicles. Each sphere then elongates to form the comma-shaped body (C-shaped body), and then the S-shaped body during nephrogenesis. The proximal end of the

S-shaped body forms the glomerulus, which connects to the proximal tubule that is derived from the mid-region of the S-shaped body, and the distal tubule that is derived from the distal-region of the S-shaped body. The distal tubule ultimately fuses with the tip of the adjacent ureteric bud to complete the connection of developing nephron to the collecting duct.

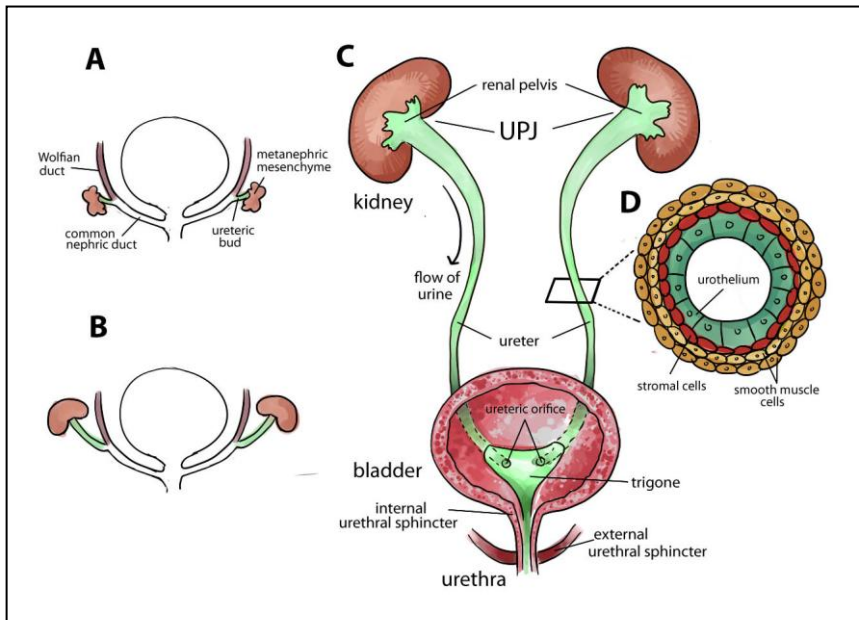


### Illustration 1.1: Urinary tract development and Structure

(A) Early development of the urinary tract (4th week of gestation in human and E10.5 in mice). An epithelial diverticulum called ureteric bud (UB) emanates from the Wolffian duct and grows into an adjacent group of mesenchymal cells (metanephric mesenchyme). (B) Elongation of the ureter and formation of the kidney (metanephros) during development. The common nephric ducts shorten, expand and integrate into the urogenital sinus (the future bladder) close to the region where the future bladder neck is located. (C) Structure of mature urinary tract in human and mice. Urine flows from the renal pelvis in the kidney through the ureter to the bladder for storage and eliminates to the outside through the urethra. The ureter is connected to the kidney at the ureteropelvic junction (UPJ) and connected to the bladder at the ureterovesical junction (UVJ). Inside the bladder, two ureteric orifices and the internal urethral orifice form the trigone. The urethral sphincter complex includes the lissosphincter which is a continuation of the bladder smooth muscle and the rhabdosphincter which consists of striated muscles. (D)



Transverse section of the mature ureter depicts four layers of cells: urothelium, stromal cells, smooth muscle cells and adventitial fibroblasts (Rasouly and Lu, 2013).

### *1.1.3 The renal corpuscle structure*

The glomerular filtration barrier is the major structure that filters the blood to produce the primary urine. The glomerulus receives the blood from an afferent arteriole and drains into an efferent arteriole. The high pressure in the glomerulus capillaries enables blood filtration. The interior surface of the capillaries comprises the fenestrated endothelial cells. Numerous endothelial cell fenestrae of 60-80nm diameter enable the first filtration of plasma solutes and small molecular weight proteins. The endothelial cells sit on a thick (250-350nm) glomerular basement membrane (GBM) that also filters the blood. The podocytes line the other side of the GBM. The podocytes extend their cell bodies to form long filopodia structures called foot processes that interdigitate and wrap around the capillaries. The foot processes of neighboring podocytes are separated by filtration slits that are bridged by a cell adhesion structure called the slit diaphragm through which the blood is filtered to form the primary urine in the Bowman's space. The Bowman's space is enclosed by the Bowman's capsule that is lined by parietal epithelial cells. The capsule has two poles: the vascular pole, where the afferent and the efferent arterioles enter into and exist from the sphere, and the urinary pole which is connected to the proximal tubule and enable the drainage of the urine. The glomerular filtrate (i.e. primary urine) then passes through the renal tubules where it is modified and partially reabsorbed into the blood stream and ultimately enters into the collecting ducts to form the final concentrated urine.

## 1.2 Human Genetics of CAKUT

CAKUT is a genetically heterogeneous developmental disorder with a variable phenotype that can be caused by mutations in one single gene that controls early kidney and urinary tract development (Lu et al., 2007b; Sanyanusin et al., 1995; Ulinski et al., 2006).

Linkage analysis has been used to uncover monogenic disease causal genes in CAKUT. For example, *SIX1* (SIX homeobox 1) mutations were identified by linkage analysis in a large family with branchiootorenal (BOR) syndrome (Ruf et al., 2003). Another type of linkage analysis that requires less family members is homozygosity mapping, which relies on the assumption that the disorder is recessive and the patients inherited the same mutation linked to the same haplotype from both parents. Homozygosity mapping tools combined with next-generation sequencing tools has led to the discovery of *TRAF1* (TNF receptor-associated protein 1) mutations in individuals with CAKUT and VACTERL association (vertebral defects, anal atresia, cardiac defects, tracheo-esophageal fistula, renal anomalies, and limb abnormalities) (Saisawat et al., 2014) and *SDCCAG8* (serologically defined colon cancer antigen 8) mutations as the cause of a retinal-renal ciliopathy (Otto et al., 2010). However, when large families are not available, a combination of several smaller pedigrees with similar phenotypes needs to be used to perform linkage analysis.

### *1.2.1 Genetic heterogeneity of CAKUT impedes linkage and association studies in CAKUT families*

Several genome-wide linkage and association studies in CAKUT families did not find evidence of linkage nor detect any association with functional candidate genes (Cordell et al., 2010; van Eerde et al., 2007). Since many studies support a genetic basis for these developmental disorders (as opposed to environmental and non genetic causes) (Connolly et al., 1997; Feather et al., 2000; Kaefer et al., 2000; Noe, 1992; Noe et al., 1992; Peeden and Noe, 1992; Scott et al., 1997; Van den Abbeele et al., 1987), the genetic heterogeneity is probably one of the explanations for such negative results. When families with a similar phenotype but different genetic etiologies are combined, the linkage analysis cannot identify the different loci. Another potential challenge for these studies is the variability of the manifestations and high rates of spontaneous resolution of the CAKUT phenotype (e.g. VUR and hydronephrosis) during the life of an individual. In addition, the penetrance of the mutations may be incomplete. Therefore, disease-free individuals cannot necessarily be classified in the linkage or association studies as unaffected (Eccles et al., 1996). Finally, mutations in the same gene can cause both syndromic and non-syndromic forms of CAKUT, which further complicates the research approach in combining families with variable CAKUT phenotypes. However, sequencing candidate genes that cause syndromic forms of CAKUT (e.g. *FRAS1*, *FREM2*, *GRIP1*, *FREM1*, *ITGA8*, and *GREM1*), has recently led to the identification of mutations in familial cases of isolated CAKUT (Kohl et al., 2014).

*1.2.2 Genomic imbalances and chromosomal rearrangements as a tool to uncover genes associated with CAKUT.*

Another approach to identify new CAKUT genes is to look for genes disrupted by genomic imbalances in patients with a CAKUT phenotype. Translocations can disrupt genes that are important in kidney development and enable the discovery of those genes (Higgins et al., 2008). The hypothesis in this case is that these genes might be mutated in other patients with CAKUT without genomic imbalances. For example, mutant *EYA1* was discovered as the cause of the BOR syndrome thanks to a translocation disrupting it in one patient (Kalatzis et al., 1996). Similarly, the associations between *ROBO2* and *NFIA* with CAKUT were originally identified in patients with chromosomal translocations (Lu et al., 2007a; Lu et al., 2007b).

Other types of genomic imbalances are microdeletions and microduplications. According to the literature, 10-17% of CAKUT patients carry microdeletions (Bachmann-Gagescu et al., 2010; Sampson et al., 2010; Weber et al., 2011) and several microdeletion syndromes were reported with an increased risk for CAKUT. The analysis of these genomic imbalances is however more challenging since the microdeletions and microduplications usually encompass multiple genes.

### **1.3 Mouse models as a tool to study birth defects of the kidney**

#### *1.3.1 Mouse models for urinary tract development*

Mice genetics provide excellent tools to study genes and signaling pathways important for the urinary tract development (Mendelsohn, 2009). The mouse is the model of preference for CAKUT research because the developmental structures of the urinary tract in lower model organisms (e.g. zebrafish) are too different from the human's. The high similarity between human and mouse genomes and the advanced genetic engineering technologies plus large accessible mutant mouse resources, provide excellent research tools to characterize the effects of human mutations in mouse models in vivo (Blake et al., 2011; Diez-Roux et al., 2011; Finger et al., 2011; McMahon et al., 2008).

However, several cases have been reported in which the knockout mice reproduce only some of the human disease phenotype, or exhibit a more severe phenotype, or no phenotype at all (Elsea and Lucas, 2002; Routtenberg, 1995). Therefore, the extrapolation from mice models to patients needs to be done with caution.

#### *1.3.2 Genetic tools in mouse genetics*

Spatially and temporally controlled gene deletions and gene expressions in mice can be done using the Cre-lox system (Sauer, 1998). Cell-specific deletions of genes of

interest in the mouse urinary tract enable studying the function of genes that cause early embryonic lethal phenotype in germline knockout mice before kidney initiation. The Cre recombinase recognizes specific DNA sequences named loxP sites and can excise the DNA between these loxP sites. The activity of the Cre-recombinase is regulated by the promoter of the targeted genes. Since the excision is at the DNA level, it introduces genomic changes that will be retained in all the descendants of the cells expressing the Cre (Illustration 1.2). For example, the *Pax2-Cre* transgene enables to specifically delete genes in the entire urinary tract (MM and the UB tissue lineages) (Ohyama and Groves, 2004). Additional kidney and urinary tract specific Cre lines include the *Six2-Cre* in the MM nephron lineage (Kobayashi et al., 2008), the *Nphs2-Cre* in the podocytes (Moeller et al., 2003), the *Hoxb7-Cre* in the Wolffian duct and UB (Yu et al., 2002), and the *Tbx18-Cre* in the ureteral mesenchymal cells (Wang et al., 2009). The research presented in this thesis used three different Cre recombinases (*Pax2-cre*, *Six2-cre* and *Nphs2-cre*).

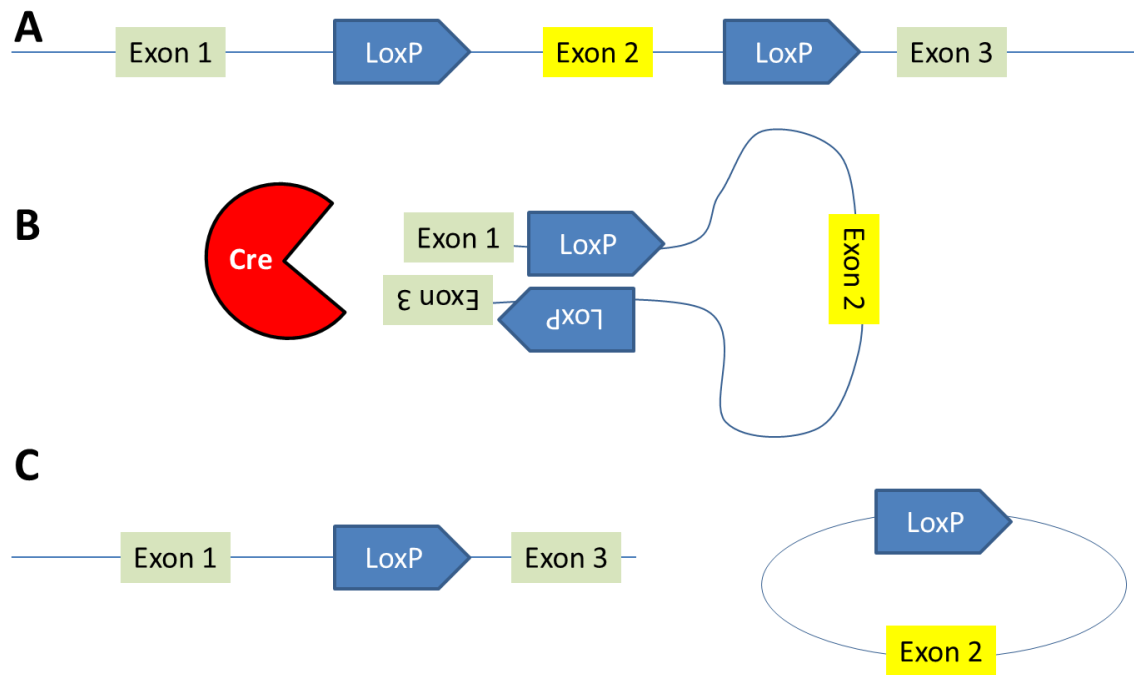


**Illustration 1.2: Scheme of the Cre-lox system.**

The Cre recombinase (red) recognizes specific DNA sequences named loxP sites. The Cre recombinase excises the DNA between two loxP sites.

### *1.3.3 Genetic interaction analysis*

In genetic interaction, or epistasis, the phenotypic effects of one gene are modified by one or several other genes. Genetic interaction is defined as a deviation from the expected additive effect of the combination of two mutations. Genetic interaction can reveal the relationship between genes and pathways. Genetic interactions can be alleviating or aggravating. They can reflect different molecular mechanisms such as physical complex formation between the proteins encoded by different genes, redundancy in the function of those proteins, linear and non-linear regulatory relationships, or activity



in the same pathway (Lehner, 2011). Experiments using mutations in genes of interest have identified numerous examples of epistasis such as genetic interaction among *Hnf1b*, the Wilms' tumor suppressor-1 (WT1) transcription factor and the canonical Notch signaling during the formation of podocytes (Naylor et al., 2013). Genetic interaction analysis also revealed that *Frem1*, which encodes an extracellular protein, genetically interacts with *Slit3* in the development of renal agenesis phenotype (Beck et al., 2013).

#### **1.4 Genes and pathways associated with kidney development and disease**

The combined analysis of patients with CAKUT and animal models has led to the discovery of many genes and pathways important in kidney development and disease. Many common molecular signaling pathways important in other organ system development have also been shown to play significant roles in the development of the kidney and urinary tract. These include the receptor tyrosine kinase (RTK) signaling pathway (e.g. *Gdnf*, *Ret*) (Costantini, 2010), the Wnt signaling pathway (e.g. *Ctnnb1*, *Wnt7b*, *Wnt9b*, *Fzd1*) (Trowe et al., 2012), the Hedgehog signaling pathway (e.g. *Shh*, *Gli3*, *Smo*, *Tshz3*) (Cain et al., 2011; Caubit et al., 2008; Yu et al., 2002), the TGF- $\beta$  signaling pathway (e.g. *Bmp4*, *Smad4*) (Brenner-Anantharam et al., 2007; Miyazaki et al., 2000; Tripathi et al., 2012), the retinoic acid mediated nuclear receptor signaling pathway (e.g. *Rara*, *Rarb*) (Batourina et al., 2005; Kam et al., 2012; Mendelsohn, 2009), and the renin-angiotensin system (e.g. *Agt*, *Ren*, *Agtr1*, *Agtr2*) (Gribouval et al., 2005; Nishimura et al., 1999; Oliverio et al., 1998; Tsuchida et al., 1998). The thesis research presented

here discusses the roles of several CAKUT genes in pathways such as the TGF- $\beta$  signaling pathway, the receptor tyrosine kinase (RTK) signaling pathway, the integrin and extracellular matrix pathway, and the Wnt signaling pathway, in pathogenesis of the CAKUT phenotypes observed.

## **1.5 Examples of birth defects of the kidney**

In this thesis, several types of birth defects of the kidneys are discussed, including renal cystic disease, congenital podocytopathies, and glomerular basement membrane diseases. I will give here a short overview of these groups of disorders and detailed information is provided in the introduction of each specific project in relevant chapters.

### *1.5.1 Renal cystic diseases*

Renal cystic disease is a relatively frequent disorder and its prevalence increases with age (Eknoyan, 2009). However, the etiology and significance of different renal cystic diseases is highly variable. Renal cystic diseases can be classified based on the timing of cyst appearance, the location that forms the cyst in the kidney (e.g. collecting ducts, tubules, glomeruli), and whether they are inherited or acquired.

### *1.5.2 Congenital Podocytopathies*

Podocytopathies are the diseases attributed to damage or dysfunction of the podocytes. They are characterized by the presence of a large amount of protein in the urine (proteinuria) (Singh et al., 2015). The functional or structural alteration in the podocytes can be caused by inherited or acquired disorders.

### *1.5.3 Glomerular basement membrane diseases*

Since the components of the glomerular basement membrane are produced both by the podocytes and the endothelial cells, some of the GBM diseases may also be classified as podocytopathies. Diseases of the GBM can be inherited or secondary to other diseases which include the nail patella syndrome, Alport syndrome, thin GBM disease, membranous nephropathy, Goodpasture's disease, fibrillary glomerulonephritis, and diabetic nephropathy.

## **1.6 Human syndromes associated with an increased risk for CAKUT**

CAKUT phenotype has been reported in many syndromes. To understand the scope of the problem in a systematic way for syndromes associated with an increased risk for CAKUT, I searched the Online Mendelian Inheritance in Man (OMIM) and compiled a list of CAKUT associated syndromes (syndromes with an increased risk for CAKUT

compared to the general population, but in which the renal anomalies are not the major symptom) (Table 1.1). Many of the syndromes are caused by mutations in genes known to play a role in kidney development (marked in yellow in Table 1.1). Other syndromes are caused by mutations in genes encoding proteins playing roles in the cilia, which role has been extensively studied in normal kidney development (Arts and Knoers, 2013) (marked in blue in Table 1.1). These known genes were good positive controls supporting our hypothesis that syndromes associated with CAKUT can be caused by genes important in kidney development.

Some other CAKUT associated syndromes are caused by microdeletion/microduplication encompassing a large number of genes. The microdeletion/microduplication syndromes are more challenging to study because the CAKUT phenotype might be caused by a combined effect of loss of several genes. We have performed some preliminary analysis on the genes deleted in patients with CAKUT phenotype such as the 1q21.1 microdeletion-microduplication syndrome. After a review of the genes in the minimal critical region deleted in this syndrome, we studied the *Bcl9* gene and its closest family member *Bcl9-2*. This research is still in progress and not presented here.

Finally, some syndromes with an increased risk for CAKUT are caused by mutations in a single gene and its functions in kidney development are often unknown. For example, Mowat Wilson syndrome is a CAKUT associated syndrome caused by

mutations in *ZEB2*. Although the function of *ZEB2* has been relatively well characterized, little is known in terms of its function in kidney development. This also led us to hypothesize that *ZEB2* plays a role in kidney development and that loss of *ZEB2* results in congenital renal anomalies. The detailed analysis of *Zeb2* conditional knockout mice will be presented in the project one of my thesis research and is described in the Chapter two below.

**Table 1.1: Syndromes Associated with increased risk for CAKUT**

Gene	Chr	Human disease	OMIM	Ref
MBTPS2	Xp22.12-p22.11	BRESEK/BRESHECK syndrome	308205	(Naiki et al., 2012)
<b>OFD1</b>	<b>Xp22.2</b>	<b>Orofaciodigital syndrome I</b>	<b>311200</b>	<b>(Feather et al., 1997)</b>
ATRX	Xq21.1	Alpha-thalassemia/mental retardation syndrome	301040	(Cole et al., 1991)
AGTR2	Xq22-q23	X-linked mental retardation-88	300852	(Nishimura et al., 1999)
	Xq27-q28	Microphthalmia, syndromic 1	309800	(Forrester et al., 2001)
<b>NOTCH2</b>	<b>1p12-p11</b>	<b>Hajdu-Cheney syndrome</b>	<b>102500</b>	
<b>NFIA</b>	<b>1p31.3-p31.2</b>	<b>Deletion syndrome</b>	<b>613735</b>	(Lu et al., 2007a)
	1p32-p31	Microdeletion syndrome	613735	(Lu et al., 2007a)
	1q21.1	Microdeletion syndrome	612474	
	1q21.1	Microduplication syndrome	612475	(Brunetti-Pierri et al., 2008; Mefford et al., 2008; Rosenfeld et al., 2012)
TMCO1	1q24.1	Craniofacial dysmorphism, skeletal anomalies, and mental retardation syndrome	213980	(Xin et al., 2010)
<b>IFT172</b>	<b>2p23.3</b>	<b>Short-rib thoracic dysplasia 10 with or without polydactyly</b>	<b>615630</b>	<b>(Halbritter et al., 2013)</b>
ZEB2	2q22.3	Mowat Wilson syndrome	235730	(Garavelli and Mainardi, 2007)
	3pter-p25	3p- syndrome	613792	(Mowrey et al., 1993)
<b>IFT122</b>	<b>3q21.3-q22.1</b>	<b>Cranioectodermal dysplasia 1</b>	<b>218330</b>	<b>(Eke et al., 1996)</b>
<b>WDR19</b>	<b>4p14</b>	<b>Short-rib thoracic dysplasia 5 with or without polydactyly</b>	<b>614376</b>	<b>(Huber and Cormier-Daire, 2012)</b>
WFS1	4p16.1	Wolfram syndrome	222300	(Salih and Tuvemo, 1991)
NIPBL	5p13.2	Cornelia de Lange syndrome 1	122470	(Selicorni et al., 2005)
OCLN	5q13.2	Band-like calcification with simplified gyration and polymicrogyria	251290	(LeBlanc et al., 2013)
TFAP2A	6p24.3	Branchio-oculo-facial syndrome	113620	(Lin et al., 2000)
<b>FOXC1</b>	<b>6p25</b>	<b>Axenfeld-Rieger syndrome type 3</b>	<b>602482</b>	<b>(Kume et al., 2000; Weisschuh et al., 2008)</b>
RMND1	6q25.1	Combined oxidative phosphorylation deficiency 11	614922	(Taylor et al., 2014)
BMPER	7q14.3	Diaphanospondylodysostosis	608022	(Funari et al., 2010)
<b>GLI3</b>	<b>7p13</b>	<b>Pallister-Hall syndrome</b>	<b>146510</b>	<b>(Cain et al., 2011; Narumi et al., 2010)</b>

	7q11.23	Williams syndrome	194050	(Schulman et al., 1996)
	7q11.2-q21.3	EEC1 syndrome	129900	(Tucker and Lipson, 1990)
	8p11.23-p11.22	Kallmann syndrome 2	147950	(Levy and Knudtzon, 1993)
<b>GLIS3</b>	<b>9p24.2</b>	<b>Diabetes mellitus, neonatal, with congenital hypothyroidism</b>	<b>610199</b>	<b>(Kang et al., 2009; Senee et al., 2006)</b>
<b>LMX1B</b>	<b>9q33.3</b>	<b>Nail-patella syndrome</b>	<b>161200</b>	<b>(Dreyer et al., 1998)</b>
	10q24	Split-hand/foot malformation 3, duplication syndrome	246560	(Keymolen et al., 2000)
	11p15-p14	Microdeletion syndrome	606528	(Bitner-Glindzicz et al., 2000)
<b>LRP4</b>	<b>11p11.2</b>	<b>Cenani-Lenz syndactyly syndrome</b>	<b>212780</b>	<b>(Li et al., 2010)</b>
DHCR7	11q13.4	Smith-Lemli-Opitz syndrome	270400	(Goldenberg et al., 2004)
KMT2D	12q13.12	Kabuki syndrome 1	147920	(Hannibal et al., 2011)
<b>PTPN11</b>	<b>12q24.13</b>	<b>LEOPARD syndrome 1</b>	<b>151100</b>	<b>(Swanson et al., 1971)</b>
	14q32	Hemifacial microsomia	164210	(Castori et al., 2006)
INF2	14q32.33	Charcot-Marie-Tooth disease, dominant intermediate E	614455	(Boyer et al., 2011)
<b>IFT43</b>	<b>14q24.3</b>	<b>Cranioectodermal dysplasia 3</b>	<b>614099</b>	<b>(Arts et al., 2011)</b>
STRA6	15q24.1	Microphthalmia	601186	(Pasutto et al., 2007)
WDR73	15q25.2	Galloway-Mowat syndrome	251300	(Colin et al., 2014)
TBC1D24	16p13.3	DOOR syndrome	220500	(Le Merrer et al., 1992)
THOC6	16p13.3	Microcephaly, mental retardation, and distinctive facies, with cardiac and genitourinary malformations	613680	(Beaulieu et al., 2013)
PMM2	16p13.2	Congenital disorder of glycosylation, type Ia	212065	(Chang et al., 1993)
<b>SALL1</b>	<b>16q12.1</b>	<b>Townes-Brocks syndrome</b>	<b>107480</b>	<b>(Albrecht et al., 2004)</b>
	16p11.2	Microdeletion syndrome	613444	(Bachmann-Gagescu et al., 2010)
KANSL1	17q21.31	Microdeletion syndrome	610443	(Tan et al., 2009)
RAI1	17p11.2	Smith-Magenis syndrome	182290	(Greenberg et al., 1996)
WNT3	17q21.31	Tetra-amelia syndrome	273395	(Bermejo-Sanchez et al., 2011)
KCTD1	18q11.2	Scalp-ear-nipple syndrome	181270	(Plessis et al., 1997)
ATP5A1	18q21.1	Mitochondrial complex (ATP synthase) deficiency, nuclear type 4	615228	(Jonckheere et al., 2013)
CCBE1	18q21.32	Hennekam lymphangiectasia-	235510	(Cormier-Daire et al.,

		lymphedema syndrome 1		1995)
RLP11	19q13.2	Diamond-Blackfan anemia 1	105650	(Willig et al., 1999)
<b>SALL4</b>	<b>20q13.2</b>	<b>Duane-radial ray syndrome</b>	<b>607323</b>	<b>(Sakaki-Yumoto et al., 2006)</b>
PIGT	20q13.32	Multiple congenital anomalies-hypotonia-seizures syndrome 3	615398	(Kvarnung et al., 2013)
TBX1	22q11.21	Velocardiofacial syndrome	192430	(Ryan et al., 1997)
	22q11.2	Opitz GBBB syndrome	145410	(Wilson and Oliver, 1988)
	22q11	Cat eye syndrome	115470	
		Hardikar syndrome	612726	(Poley and Proud, 2008)
		Fryns syndrome	229850	(Slavotinek, 2004)

Abbreviation: Chr: chromosomal location. Yellow: genes known to play a role in kidney development, Blue: genes encoding ciliary proteins



## 1.7 General Hypothesis and Specific Aims

### 1.7.1 General Hypothesis

The general hypothesis of this thesis is that human syndromes associated with an increased risk for CAKUT are caused by mutations of genes important in kidney development and disease.

The specific hypotheses for each of the projects presented in this thesis are described in each relevant chapter.

### 1.7.2 Specific Aims

**Aim 1:** To determine whether the *Zeb2* gene plays a role in kidney development and whether loss of *Zeb2* in mice causes congenital renal disease.

**Aim 2:** To explore the potential genetic interaction between *Ilk* and *Robo2* in glomerular podocytes.

**Aim 3:** To explore the molecular defects during early ureteric bud outgrowth in *Slit2* and *Robo2* knockout mice.

## CHAPTER TWO: Loss of *Zeb2* causes glomerulocystic kidney disease in mice

### 2.1 Summary

ZEB2 is a zinc finger E-box binding homeobox transcription factor. Mutations in *ZEB2* cause Mowat-Wilson syndrome, an autosomal dominant disorder associated with kidney disease. Here we show that *Zeb2* conditional knockout mice with either *Pax2-cre* or *Six2-cre* developed primary glomerulocystic kidney disease starting at embryonic day E16.5. *Zeb2<sup>flox/flox</sup>;Pax2-cre<sup>+</sup>* mice died at birth and *Zeb2<sup>flox/flox</sup>;Six2-cre<sup>+</sup>* mice developed renal failure by 8 weeks of age. Atubular glomeruli were observed in *Zeb2* knockout mice, explaining the presence of glomerular cysts in the absence of tubular dilatation. Decreased expression of early renal proximal tubular markers was detected in *Zeb2* knockout embryonic kidneys at E14.5 preceding glomerular cyst formation, suggesting that primary renal tubule defects in early nephrogenesis contribute to the formation of congenital atubular glomeruli. Furthermore, gene expression analysis revealed an upregulation of PKD1 expression in the glomeruli of *Zeb2* knockout mice. Together, our results suggest that *Zeb2* plays an important role in normal nephron development and loss of *Zeb2* leads to primary glomerulocystic kidney disease in mice. Our findings may be added to the ill-described kidney phenotype in Mowat-Wilson syndrome, and suggest that *ZEB2* might be a novel candidate gene in patients with glomerular cystic disease.

## 2.2 Background and Introduction

In order to identify a novel gene associated with abnormal kidney development in human patients, we first reviewed the syndromes that include CAKUT as part of their clinical presentation (OMIM clinical synopsis), which have been described in the introduction chapter (Table 1.1). In this project, we focused on the *ZEB2* gene that causes the Mowat Wilson syndrome (MWS), a human syndrome associated with ill-defined kidney birth defects.

### *2.2.1 Mowat Wilson syndrome.*

MWS is a rare syndrome characterized by distinctive facial features, moderate to severe intellectual disability, large intestine blockage (Hirschsprung disease), congenital heart defects, and renal anomalies (OMIM 235730) (Garavelli and Mainardi, 2007). At least 13% of the MWS patients were found to have renal anomalies including hydronephrosis and vesicoureteral reflux (Garavelli and Mainardi, 2007), however, the specific kidney phenotype is not well described. The prevalence of MWS is estimated to be 1:50,000-1:70,000 live births although it may be under-diagnosed (Engenheiro et al., 2008; Ghoumid et al., 2013; Wenger et al., 2014). The MWS is a dominant disorder caused by heterozygous loss-of-function mutations (e.g. non-sense, frameshift or deletion) in the *ZEB2* gene (Garavelli and Mainardi, 2007). Atypical presentations of MWS were also reported in patients with *ZEB2* heterozygous missense mutations

(Heinritz et al., 2006). In sum, MWS is due to reduced levels of the ZEB2 protein, suggesting that the level of ZEB2 is important for normal development.

### *2.2.2 ZEB2 protein*

ZEB2, also called Smad Interacting Protein 1 (SIP1), is a member of the ZEB family of two-handed zinc finger/homeodomain transcription factors. ZEB2 is a 1214-amino acid protein and is highly conserved in vertebrates with 92% identity between humans and *Xenopus*. It also shares 69% similarity to its closest family member, ZEB1 (Grabitz and Duncan, 2012).

ZEB transcription factors have two separate clusters of zinc fingers at the N-terminus and at the C-terminus (Illustration 2.1), which bind the DNA for transcriptional regulation. Both ZEB2 and ZEB1 bind a 5'-CACCT sequence (Verschueren et al., 1999). As its name suggests, ZEB2/SIP1 can bind activated R-SMADs. Specifically, SMAD1, SMAD2 and SMAD3 have been experimentally shown to bind ZEB2 after TGF- $\beta$  activation (Verschueren et al., 1999). ZEB2 also has a CID repressor domain that interacts with CtBP (Postigo and Dean, 1999). Post-transcriptional modification of ZEB2 by sumoylation at Lys-391 and Lys-866 can reduce its transcriptional activity (Long et al., 2005).



### Illustration 2.1: The ZEB2 protein structure

The ZEB2 transcription factor has two zinc finger domains on the N and the C ends of the protein enabling its binding to the DNA. ZEB2 has a SMAD Binding domain (SBD), a CtBP interacting domain (CID), a homeobox domain (HD) and 2 sumoylation sites (K391 and K866).

#### 2.2.3 Role of ZEB2 in development and cancer.

ZEB2 plays a role in ocular lens development, brain development and neural crest migration, as well as in cancer progression (Comijn et al., 2001; Miquelajauregui et al., 2007; Seuntjens et al., 2009; Van de Putte et al., 2003b; Yoshimoto et al., 2005).

At embryonic day E8.5, two cell populations express *Zeb2* mRNA, the neuroepithelium and the neural crests (Van de Putte et al., 2003a). *Zeb2* homozygous null mouse embryos exhibit severe defects at E8.5 and die at E9.5 before organogenesis, impeding research on the role of *Zeb2* in the development of most organs (Van de Putte et al., 2003a). Therefore, a conditional *Zeb2* allele was generated to investigate the role of *Zeb2* during organogenesis (Higashi et al., 2002).

As opposed to the activating function of *Zeb2* on *Foxe3* during lens development (Yoshimoto et al., 2005), ZEB2 represses the expression of *Sfrp1* (an extracellular inhibitor of Wnt signaling) during hippocampal development (Miquelajauregui et al.,

2007). ZEB2 also modulates CNS myelination, where it activates *Smad7* expression (Weng et al., 2012). Interestingly, SMAD7 represses the Wnt signaling pathway, suggesting an opposite effect of ZEB2 activity on the Wnt pathway during myelination and hippocampus development.

In post-mitotic neurons of the embryonic neocortex, ZEB2 regulates neuron progenitors non-cell autonomously via direct repression of *neurotrophin-3* (*Ntf3*) in the post-mitotic neurons (Seuntjens et al., 2009).

In the cancer field, ZEB2 is a mesenchymal marker and is associated with epithelial to mesenchymal transition (EMT) (Comijn et al., 2001; Vandewalle et al., 2005). ZEB2 regulates and is regulated by the miR-200 family (Bracken et al., 2008), which also regulates EMT. However, EMT rarely occurs during normal development, accordingly, deletion of *Zeb2* during lens development in the epithelial layer leads to the dysregulation of genes distinct from those discovered in the cancer field (Manthey et al., 2014a; Manthey et al., 2014b).

In sum, ZEB2 can have many functions depending on the cell types and the developmental stages. ZEB2 can be both an activator and a repressor of gene expression. It can bind activated Smads but its activity does not always depend on it. ZEB2 can regulate the expression of *Foxe3* in the lens, *Sfrp1* in the hippocampus, *Ntf3* in the neurons and *E-cadherin* in cancer cells. Interestingly, ZEB2 target gene *Sfrp1* (Leimeister et al., 1998), *Ntf3* (Good and George, 2001), *Smad7* (Banas et al., 2007) and the miR-200

family (Patel et al., 2012) are all expressed in the kidney. However, the function of ZEB2 during kidney development is unknown. This thesis research is the first study of the impact of loss of *Zeb2* on kidney development.

#### *2.2.4 Glomerulocystic kidney disease (GCKD) as a specific form of renal cystic disease*

Most of the renal cystic diseases are characterized by primary renal tubular dilatation. Glomerulocystic kidney disease (GCKD) is a special form of renal cystic disease characterized by the dilatation of the Bowman's space (Wood et al., 2015). In 1993, Bernstein defined GCKD as a disease entity (Bernstein, 1993). Two- to threefold dilatation of Bowman's space in more than 5% of identifiable glomeruli in the plane of a kidney section define GCKD (Bernstein, 1993; Lennerz et al., 2010). Although most of the glomerular cysts are associated with tubular dilatation, a subset of "primary" (also called "isolated") glomerular cystic disease does not display tubular dilatations (Lennerz et al., 2010), and the glomerular cysts are mainly located in the subcapsular area of the renal cortex (Romero et al., 1993; Wood et al., 2015). Ultrasound and nonenhanced CT have limited capacity to identify glomerular cysts, and only nonenhanced T2-weighted MR imaging enables their detection, limiting the diagnosis of GCKD in the population (Wood et al., 2015). Nevertheless, several syndromes have glomerular cysts as part of their phenotype. These include tuberous sclerosis complex (TSC1 – OMIM 191100 and TSC2 – OMIM 613254) (Murakami et al., 2012), Zellweger syndrome (also called cerebrohepatorenal syndrome that is mainly caused by mutations in the PEX1 gene -

OMIM 214100) (Bernstein, 1993), and the X-linked dominant oral-facial-digital syndrome type 1 (OFD1 – OMIM 311200) (Feather et al., 1997). In addition, mutations in *UMOD* (Rampoldi et al., 2003) and *HNF1 $\beta$*  genes are reported to cause glomerular cysts (Bingham et al., 2001; Loftus and Ong, 2013). Glomerular cysts can also be found in patients with ciliopathies (e.g. polycystic kidney disease, Bardet-Biedl Syndrome, nephronophthisis, etc.) and obstructive uropathy (Bissler et al., 2010).

#### 2.2.5 Genes associated with glomerular cysts in mice

Glomerular cysts have been reported in several mouse models such as the *Wwtr1*, *Glis3*, *Ofd1* and *Pkhd1* germline knockout mice, the *Hnf1 $\beta$*  and *Dicer* conditional knockout mice, and the *Pkd1* overexpression transgenic mice (Ferrante et al., 2006; Hossain et al., 2007; Kang et al., 2009; Massa et al., 2013; Patel et al., 2012; Pritchard et al., 2000a; Williams et al., 2008b). In the *Hnf1 $\beta$ <sup>flox/flox</sup>;Six2-cre<sup>+</sup>* model, the glomerular cysts develop because of a lack of proximal tubules development (Massa et al., 2013). In other models, both glomerular cysts and tubular cysts are observed.

Interestingly, two of the genes that cause glomerular cysts in knockout mice also interact with SMADs (Hossain et al., 2007; Kang et al., 2009; Makita et al., 2008). The *Wwtr1* gene encodes the TAZ protein that can shuttle SMADs between the cytoplasm and the nucleus and, like ZEB2, TAZ can also induce EMT (Varelas et al., 2008; Yang et al., 2012). One of transcription factors interacting with TAZ is the Kruppel-like zinc finger



protein (encoded by *Glis3* gene). Knockout of *Glis3* in mice also cause glomerular cysts (Kang et al., 2009).

In both *Pkd1* transgenic mice and *Dicer* conditional knockout mice (using *Ksp-cre*), increased *Pkd1* levels are associated with glomerular cyst formation (Patel et al., 2012; Thivierge et al., 2006). Interestingly, in the *Dicer* cKO, the same microRNA family that is repressed by ZEB2, miR200, was shown to regulate *Pkd1* levels (Brabletz and Brabletz, 2010; Patel et al., 2012).

### **2.3 Hypothesis.**

Although abnormalities of the kidneys are relatively common in Mowat Wilson syndrome (Garavelli and Mainardi, 2007), they have not been well characterized and the potential pathogenic role of *ZEB2* mutations in kidney development has not been examined. In this research project, we hypothesized that *ZEB2* plays a role in kidney development and loss of *ZEB2* results in congenital renal anomalies. To test this hypothesis, we analyzed a *Zeb2* floxed conditional knockout (cKO) mouse line (Higashi et al., 2002) as *Zeb2* null mice die at E9.5 before kidney development begins (Van de Putte et al., 2003a).

## 2.4 Materials and Methods

### 2.4.1 Mice Strains

*Zeb2* conditional knockout mice with two LoxP sites flanking the exon seven (*Zeb2*<sup>flox/flox</sup>) were kindly provided by Dr. Yujiro Higashi (Osaka University, Osaka, Japan) (Higashi et al., 2002). Mice with the *Pax2-cre*<sup>+</sup> allele were obtained from the Mutant Mouse Regional Resource Centers (MMRRC) (Stock number: 010569-UNC) (Ohyama and Groves, 2004). Mice with the *Six2-cre*<sup>+</sup> allele (Stock number 009606) (Kobayashi et al., 2008) and *Pkd1* floxed allele (Stock number 010671) were purchased from the Jackson laboratories (Stock number 009606) (Piontek et al., 2004).

Briefly, the *Zeb2* (*Zeb2*<sup>flox/flox</sup>) mice were crossed with the *Pax2-cre* mice to generate *Zeb2*<sup>flox/+</sup>;*Pax2-cre*<sup>+</sup>, which were then bred with *Zeb2*<sup>flox/flox</sup> and *Zeb2*<sup>flox/+</sup>;*Pax2-cre*<sup>+</sup> mice to produce *Zeb2*<sup>flox/flox</sup>;*Pax2-cre*<sup>+</sup> conditional knockout (cKO) offspring and controls (*Zeb2*<sup>flox/+</sup> and *Zeb2*<sup>flox/flox</sup> mice without the *Pax2-cre* allele and *Zeb2*<sup>+/+</sup>;*Pax2-cre*<sup>+</sup> mice).

The *Zeb2* (*Zeb2*<sup>flox/flox</sup>) mice were also crossed with the *Six2-cre* mice to generate *Zeb2*<sup>flox/+</sup>;*Six2-cre*<sup>+</sup> mice. The *Zeb2*<sup>flox/+</sup>;*Six2-cre*<sup>+</sup> mice were bred with *Zeb2*<sup>flox/flox</sup> homozygotes and *Zeb2*<sup>flox/+</sup> heterozygote mice (without the *Six2-cre* allele because *Six2-cre* homozygotes are lethal) to produce *Zeb2*<sup>flox/flox</sup>;*Six2-cre*<sup>+</sup> conditional knockout offspring and controls (*Zeb2*<sup>flox/+</sup> and *Zeb2*<sup>flox/flox</sup> mice without the *Six2-cre* transgene and *Zeb2*<sup>+/+</sup>;*Six2-cre*<sup>+</sup> mice).

Mouse embryos were staged by designating the day that the vaginal plug was observed in the dam as E0.5. The conditional knockout mice were analyzed from embryonic stage E14.5 to postnatal 8 weeks old. All animal studies were approved by the Institutional Animal Care and Use Committee of Boston University Medical Campus (#14388).

#### 2.4.2 Mouse DNA extraction and genotyping

Mice were genotyped using DNA samples that were extracted from mouse tails using hotshot NaOH method as previously described (Truett et al., 2000).

All genotyping was performed using a PCR method on thermal cycler Veriti FAST (Life Technologies) or MyClycler (BioRad). The presence of the *Pax2-cre* allele was detected using primers designed specifically to the *Pax2-cre* transgene. The presence of the *Six2-cre* allele was detected using generic primers for “Cre recombinase”. The presence of the *Zeb2* floxed allele was detected as previously described (Higashi et al., 2002). The presence of *Pkd1* floxed or mutant alleles were detected as previously described (Piontek et al., 2004).

### *2.4.3 Tissue collection and preparation*

The mouse kidneys at defined ages and embryonic stages were dissected and fixed overnight in 4% paraformaldehyde. The samples were then washed 2 times in PBS on ice and preserved in 70% EtOH until they were processed for paraffin embedding. Serial 4-7  $\mu\text{m}$  tissue sections were cut using a MT-920 microtome (Microm). For immunofluorescence staining, mouse kidneys were fixed in 4% formaldehyde followed by incubation in 30% sucrose /PBS overnight at 4°C, embedded in OCT compound (Tissue-Tek), and cryosectioned at 10  $\mu\text{m}$  using a Microm HM 550 cryostat (Thermo Scientific).

### *2.4.4 Histological analysis*

Paraffin embedded kidney sections were stained by hematoxylin and eosin, Periodic acid–Schiff (PAS) stain and Masson Trichrome stain, and were examined using a Nikon or Olympus light microscope.

### *2.4.5 Immunohistochemistry*

For immunohistochemistry, sections were pretreated to quench endogenous peroxidase (3.0% hydrogen peroxide in PBS) and endogenous biotin (Avidin-Biotin

blocking kit, Vector Laboratories, Burlingame, CA). Mitotic cells were detected with phospho-histone H3 (ser 10) (pHH3) antibody (Cell Signaling Technology #9701, Beverly MA) at 1:200 dilution. Proximal tubules were stained with biotinylated *Lotus tetragonolobus* agglutinin (LTL) (Cat #B1325, Vector Labs), distal tubules and collecting ducts were stained with biotinylated *Dolichos biflorus* agglutinin (DBA) (Cat #B-1035, Vector Labs). Apoptosis was detected as previously described using the TUNEL reaction (terminal deoxynucleotidyl transferase [TdT]-mediated dUTP-biotin nick-end labeling). (Omori et al., 2000). Fragmented DNA was detected using Apoptag® (Chemicon, Temecula, CA) with DAB development (Biogenex, San Ramon, CA) and hematoxylin counterstaining. To quantify apoptosis in the C-shaped body (CSB) and S-shaped body (SSB) in developing kidney, all CSB and SSB were counted first and then all CSB and SSB with at least one TUNEL positive cell were counted again in one slide per kidney. The counting was performed without the knowledge of the genotypes of the slides.

To quantify the proliferation in the Bowman's capsules, all glomeruli were counted first and then all the glomeruli with at least one pHH3 positive cell on their Bowman's capsules were counted again in one slide per kidney.

#### *2.4.6 Immunofluorescence staining*

For immunofluorescence staining, frozen sections of mouse kidneys were permeabilized with 0.1% PBS- Triton X-100 for 10 min and blocked in 5% goat serum

for 1hr. Primary antibodies were incubated overnight at 4°C followed by secondary antibodies incubated at RT for 1hr. The following primary antibodies were used: WT1 (Cat# sc-192, Santa Cruz Biotechnology), Polycystin-1 (Cat# sc-130554, Santa Cruz Biotechnology), Laminin (Cat# L9393, Sigma), GFP (Cat# GFP-1020, Aves). Tissue sections were mounted in media containing DAPI and imaged by a Zeiss confocal microscope. The immunofluorescent TUNEL staining was performed using the ApopTag® Red *In Situ* Apoptosis Detection Kit (Millipore, S7165).

#### *2.4.7 Urine protein and renal function analysis*

Urine protein excretion was detected by SDS-PAGE followed by Coomassie blue staining and quantified using ImageJ. Urine creatinine was measured using the Crystal Chem Kit (Crystal Chem, Catalog# 80350). Urine albumin/creatinine ratios were calculated. Serum values were obtained from blood samples at time of euthanasia for blood urea nitrogen using the Catalyst Dx® Chemistry Analyzer by IDEXX.

#### *2.4.8 Glomerular count and cysts assessment*

Bowman's space dilatation was defined when the glomerular tuft occupied less than two third of the bowman space. To compare the number of glomeruli with and without cysts between wild-type and conditional knockout mice, H&E-stained median

sagittal sections from one or two kidneys were analyzed for each animal. A total of 8 *Zeb2<sup>flox/flox</sup>; Pax2-cre<sup>+</sup>* kidneys and 7 littermate controls at E18.5 were analyzed for glomerular cystic phenotype. The ratio of glomerular cysts (i.e. glomeruli with identifiable glomerular tuft and Bowman's space dilatation) to the total number of glomeruli was calculated in mouse embryonic kidneys between E16.5 and E18.5.

#### *2.4.9 Assessment of glomerulotubular integrity*

Since the proximal tubular cells encroach the Bowman capsule, the connection between the proximal tubule and the glomerulus can be visualized using the proximal specific marker LTL. Glomerulotubular integrity was assessed by analyzing the connection between the proximal tubules and the glomeruli on LTL stained kidney sections as described previously (Forbes et al., 2011; Galarreta et al., 2014). All glomeruli were counted on the kidney sections and scored on the basis of presence (positive) or absence (negative) of LTL staining in the Bowman's capsule. Quantification of glomerulotubular integrity was presented as the percentage of LTL-positive glomeruli in total glomeruli as previously described (Forbes et al., 2011). A total of 5 *Zeb2<sup>flox/flox</sup>; Six2-cre<sup>+</sup>* kidneys and 5 littermate controls at 12 days old of age were analyzed. Results were presented as the percentage of LTL-positive glomeruli as previously described (Forbes et al., 2011).

#### 2.4.10 TaqMan real-time PCR gene expression analysis

Total RNA was extracted from E14.5, E18.5 and P8 kidneys of control and *Zeb2* cKO using the miRNeasy Micro kit (Cat# 217084, Qiagen). cDNA was synthesized from total RNA using the Verso cDNA Synthesis Kit (Cat# AB-1453, Life Technologies) and the TaqMan MicroRNA Reverse Transcription kit (Cat# 4366596, Life Technologies). Gene expression was analyzed using the 7500FAST real-time PCR machine with TaqMan probes purchased from Life Technologies. Relative gene expression data were analyzed by the delta-delta-Ct method and were normalized to the either *Gapdh* or *Ppp1r3c*. A total of three E14.5, five E18.5 and five P8 knockout mice and littermate controls were analyzed.

#### 2.4.11 Statistical analysis

A minimum of three mice were used for each analysis, unless stated otherwise. Data are represented as means +/- standard deviation. Statistical analysis was performed by using the Student t-test; significance was determined at  $p < 0.05$ .



## 2.5 Results

### *2.5.1 ZEB2 is broadly expressed in the developing kidney*

Based on the in situ hybridization (ISH) data from publically available databases (e.g. GUDMAP and GenePaint), *Zeb2* is broadly expressed in mouse developing kidney between E13.5 and E15.5. The microarray gene expression data from the GUDMAP also reveal that *Zeb2* is expressed at a high level in the developing medullary interstitium, the developing podocytes and the tissues of the urinary tract such as the ureter (Figure 2.1) (Harding et al., 2011; McMahon et al., 2008; Visel et al., 2004).

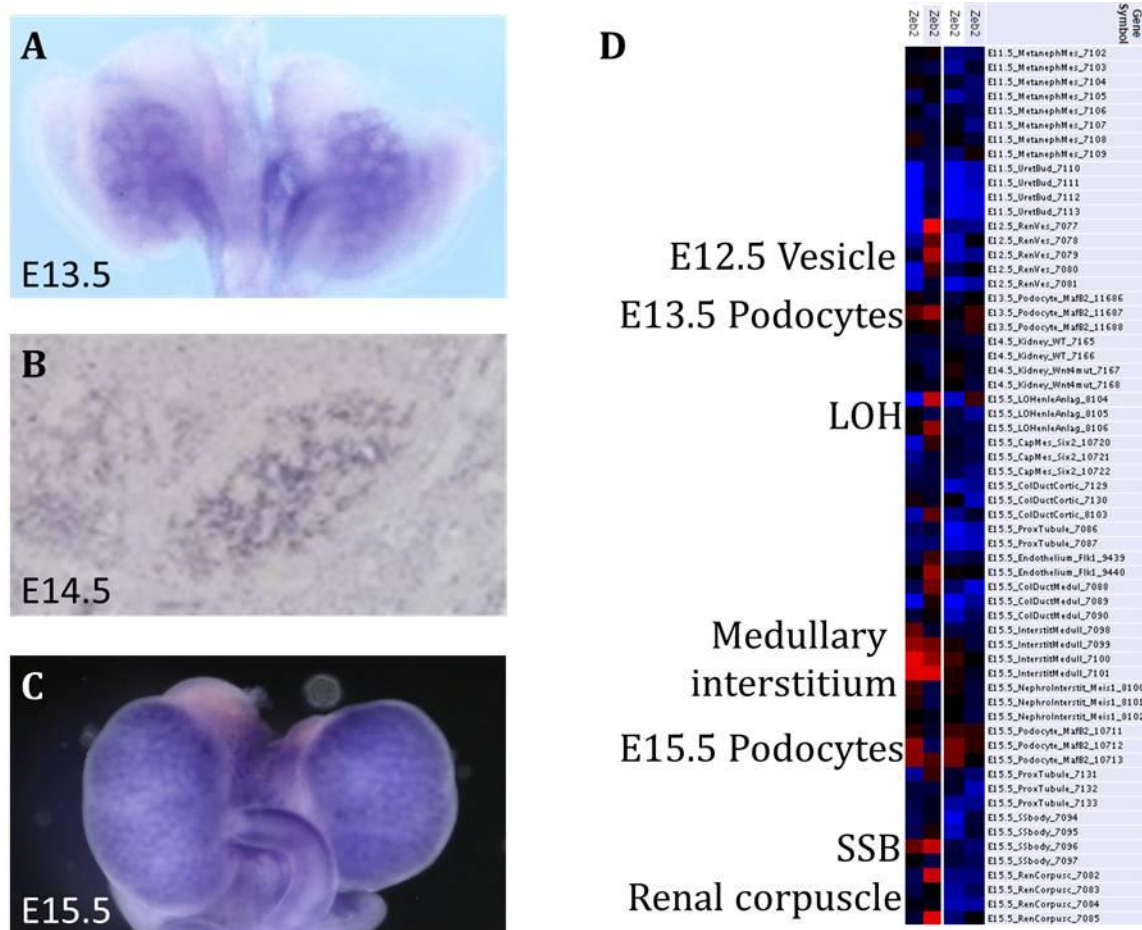


**Figure 2.1: *Zeb2* mRNA is broadly expressed in the developing mouse kidney and urinary tract.**

ISH data show that *Zeb2* mRNA is expressed in (A) mouse E13.5 kidney (whole mount ISH from GUDMAP), (B) mouse E14.5 kidney (section ISH from Gene Paint) and (C) mouse E15.5 kidney (whole mount ISH from GUDMAP). (D) Microarray gene expression heatmap data from GUDMAP show that *Zeb2* mRNA is expressed in the renal vesicles, the podocytes, the medullary interstitium and the S-shaped body of developing kidney.

To study *Zeb2* expression in mouse kidney, we confirmed the expression of *Zeb2* mRNA during murine development using real-time RT-PCR on kidney extract from wild-type mice. *Zeb2* mRNA was expressed throughout kidney development and in adult kidneys (Figure 2.2, A). We then used a *Zeb2*-EGFP reporter mouse to visualize the expression pattern of *Zeb2* in the kidney. The *Zeb2*-EGFP reporter mouse was generated by knocking in a *Zeb2-Egfp* fusion element in the *Zeb2* locus, generating a ZEB2-EGFP fusion protein (Nishizaki et al., 2014). In the mouse brain, the GFP expression pattern is consistent with *Zeb2* mRNA expression as previously reported (Nishizaki et al., 2014), validating this *Zeb2*-EGFP reporter stain. Using an anti-GFP antibody to enhance the GFP signal, ZEB2 was detected in the developing kidney at E16.5 (Figure 2.2, B-J). In addition to the stromal cells, ZEB2 was detected in a subset of cells in the nephron, including the S-shaped bodies (Figure 2.2D), glomeruli (Figure 2.2G) and renal tubules (Figure 2.2J).

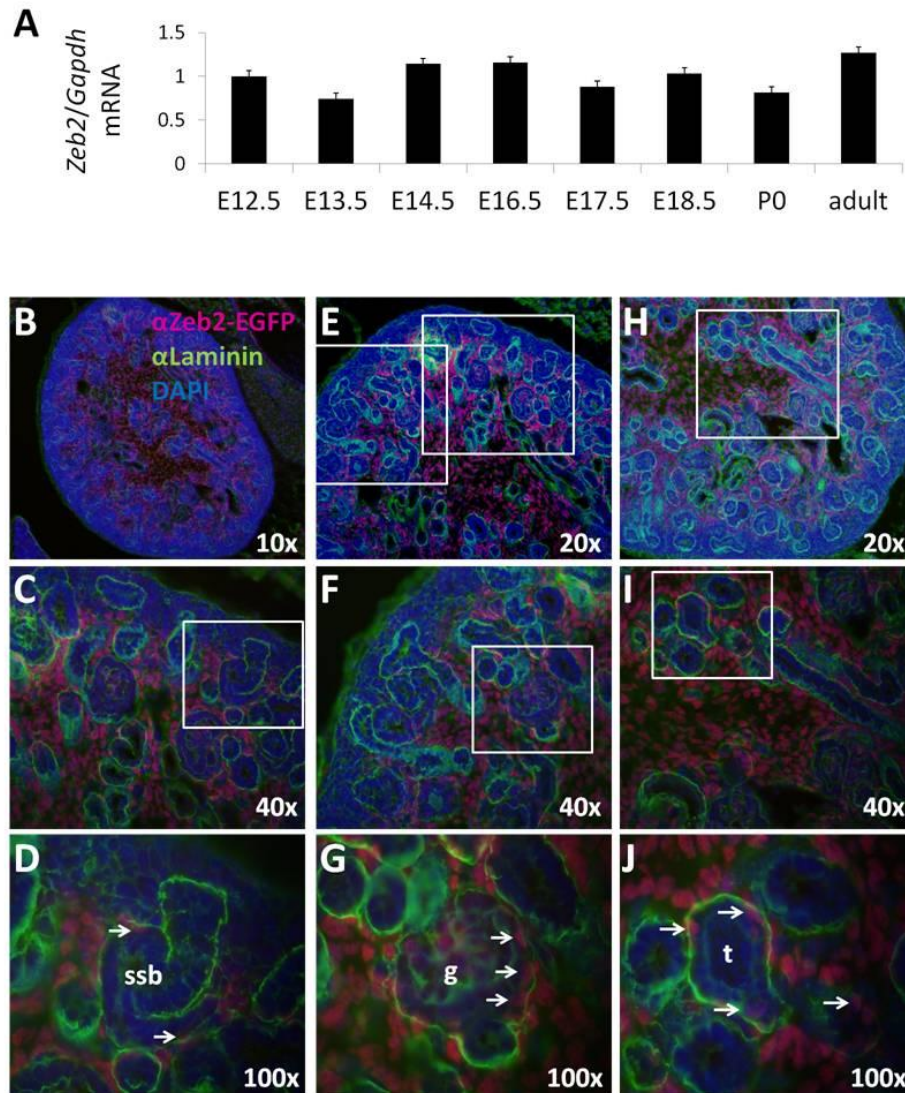


**Figure 2.2: ZEB2 is highly expressed in developing mouse kidney**

(A) *Zeb2* mRNA is expressed throughout development and adulthood by RT-PCR. (B-J) ZEB2 expression (red) was detected using the ZEB2-EGFP reporter mouse at E16.5 with an antibody against GFP. The nephrons and collecting ducts were delineated with a laminin antibody (green). (B) Transverse section of the whole kidney at low magnification (10x). (C and F) Higher magnification of the white box in (E) shows ZEB2 expression in the kidney cortex, 20x magnification. (D) Higher magnification of the white box in (C) shows an S-shaped body (SSB) and ZEB2 positive cells (arrows), 40x magnification. (G) Higher magnification of the white box in (F) shows a glomerulus (g) and ZEB2 positive cells (arrows), 100x magnification. (J) Higher magnification of the white box in (I) shows a tubule (t) and ZEB2 positive cells (arrows).

### 2.5.2 Loss of *Zeb2* leads to glomerular kidney cysts formation

#### ***Generation of a kidney specific *Zeb2* knockout mouse***

*Zeb2* null mice die at E9.5 before kidney development initiation (Higashi et al., 2002; Van de Putte et al., 2003a). To determine the role of *Zeb2* in kidney development, we crossed a *Zeb2* floxed conditional knockout mouse line (*Zeb2*<sup>fl<sup>ox</sup>/fl<sup>ox</sup></sup>) with a *Pax2-cre*<sup>+</sup> deleter strain that expresses *Cre* recombinase in both the ureteric bud and the metanephric mesenchyme (Illustration 2.2) (Levinson et al., 2005; Narlis et al., 2007; Ohyama and Groves, 2004). Kidney samples were collected between E14.5 and P0 (Table 2.1).

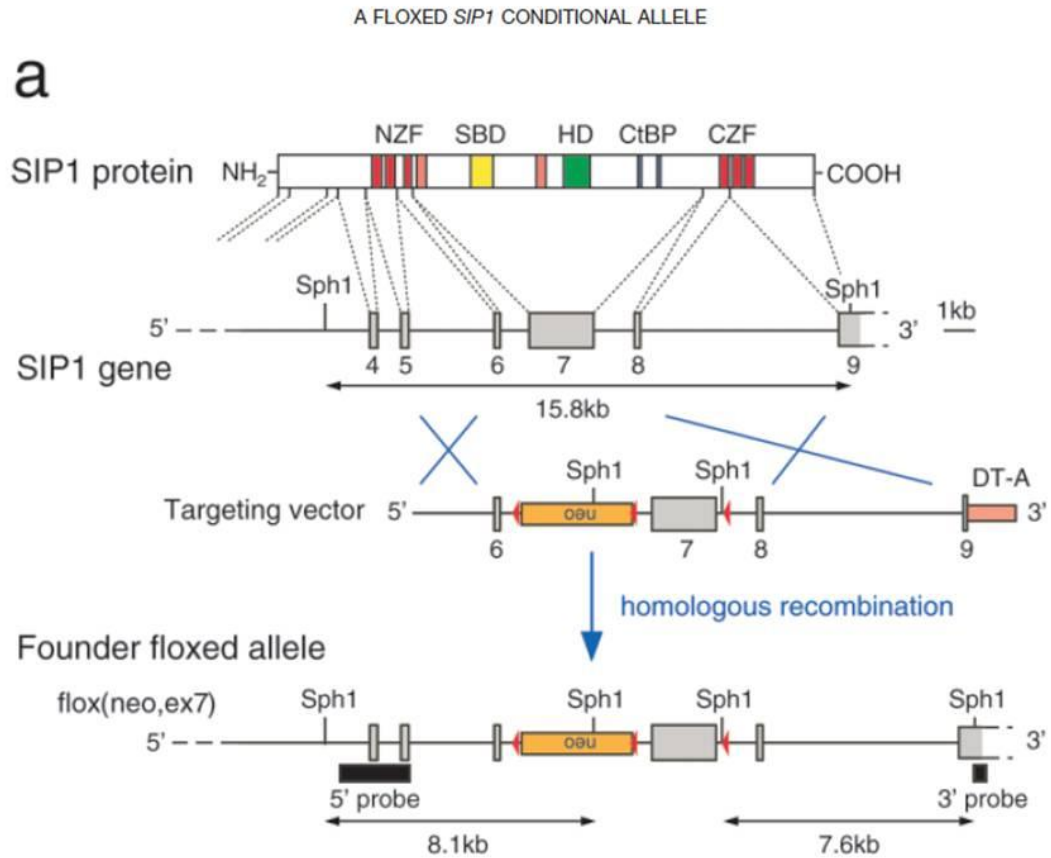


### Illustration 2.2: *Zeb2* floxed allele

The *Zeb2* floxed allele used in project one: the exon 7 of *Zeb2* is flanked by two loxP sites (red arrows). Exon 7 encodes the middle part of the ZEB2 protein with the Zinc Fingers located on the N terminus of the protein (Higashi et al., 2002).

**Table 2.1: Kidney samples collected from the *Zeb2* conditional knockout mice in project one.**

Embryonic kidney samples collected.

A. Frozen kidneys (OCT)					
Genotype	E14.5	E15.5	E16.5	E17.5	E18.5
<i>Zeb2</i> <sup>fl<sup>ox</sup>/fl<sup>ox</sup></sup> and <i>Zeb2</i> <sup>fl<sup>ox</sup>/+</sup> (wt)		10			2
<i>Zeb2</i> <sup>fl<sup>ox</sup>/fl<sup>ox</sup></sup> ; <i>Pax2-cre</i> <sup>+</sup>		2			3
<i>Zeb2</i> <sup>fl<sup>ox</sup>/+</sup> ; <i>Pax2-cre</i> <sup>+</sup>		5			1
<i>Zeb2</i> <sup>fl<sup>ox</sup>/fl<sup>ox</sup></sup> and <i>Zeb2</i> <sup>fl<sup>ox</sup>/+</sup> (wt)	19	5	7	6	
<i>Zeb2</i> <sup>fl<sup>ox</sup>/fl<sup>ox</sup></sup> ; <i>Six2-cre</i> <sup>+</sup>	5	3	3	3	
<i>Zeb2</i> <sup>fl<sup>ox</sup>/+</sup> ; <i>Six2-cre</i> <sup>+</sup>	5	5	1	0	

B. Paraffin embedding (PFA fixed)					
Genotype	E14.5	E15.5	E16.5	E17.5	E18.5
<i>Zeb2</i> <sup>fl<sup>ox</sup>/fl<sup>ox</sup></sup> and <i>Zeb2</i> <sup>fl<sup>ox</sup>/+</sup> (wt)	3	4		9	13
<i>Zeb2</i> <sup>fl<sup>ox</sup>/fl<sup>ox</sup></sup> ; <i>Pax2-cre</i> <sup>+</sup>	2	1		3	8
<i>Zeb2</i> <sup>fl<sup>ox</sup>/+</sup> ; <i>Pax2-cre</i> <sup>+</sup>	2	5		0	4
<i>Zeb2</i> <sup>fl<sup>ox</sup>/fl<sup>ox</sup></sup> and <i>Zeb2</i> <sup>fl<sup>ox</sup>/+</sup> (wt)	7	18	8		
<i>Zeb2</i> <sup>fl<sup>ox</sup>/fl<sup>ox</sup></sup> ; <i>Six2-cre</i> <sup>+</sup>	6	5	5		
<i>Zeb2</i> <sup>fl<sup>ox</sup>/+</sup> ; <i>Six2-cre</i> <sup>+</sup>	6	2	7		

C. RNA (RNAlater)					
Genotype	E14.5	E15.5	E16.5	E17.5	E18.5
<i>Zeb2</i> <sup>fl<sup>ox</sup>/fl<sup>ox</sup></sup> and <i>Zeb2</i> <sup>fl<sup>ox</sup>/+</sup> (wt)		8	5	3	8
<i>Zeb2</i> <sup>fl<sup>ox</sup>/fl<sup>ox</sup></sup> ; <i>Pax2-cre</i> <sup>+</sup>		3	2	2	8
<i>Zeb2</i> <sup>fl<sup>ox</sup>/+</sup> ; <i>Pax2-cre</i> <sup>+</sup>		1	2	0	2
<i>Zeb2</i> <sup>fl<sup>ox</sup>/fl<sup>ox</sup></sup> and <i>Zeb2</i> <sup>fl<sup>ox</sup>/+</sup> (wt)	10	8	6		
<i>Zeb2</i> <sup>fl<sup>ox</sup>/fl<sup>ox</sup></sup> ; <i>Six2-cre</i> <sup>+</sup>	6	3	5		
<i>Zeb2</i> <sup>fl<sup>ox</sup>/+</sup> ; <i>Six2-cre</i> <sup>+</sup>	3	2	1		

P8 and P12 kidney samples collected.

Genotype	Paraffin	RNA
<i>Zeb2</i> <sup>fl<sup>ox</sup>/fl<sup>ox</sup></sup> and <i>Zeb2</i> <sup>fl<sup>ox</sup>/+</sup> (wt)	34	13
<i>Zeb2</i> <sup>fl<sup>ox</sup>/fl<sup>ox</sup></sup> ; <i>Six2-cre</i> <sup>+</sup>	11	5
<i>Zeb2</i> <sup>fl<sup>ox</sup>/+</sup> ; <i>Six2-cre</i> <sup>+</sup>	15	7

***Kidney specific Zeb2 knockout embryos develop cysts (using the Pax2-cre allele)***

The E18.5  $Zeb2^{\text{flox/flox}};Pax2\text{-cre}^+$  homozygous embryos did not display discernible gross structural defects of the kidney or the ureter. However, the histological examination of kidneys from 14  $Zeb2^{\text{flox/flox}};Pax2\text{-cre}^+$  homozygous embryos between E16.5 and E18.5 revealed that 14/14 (100%) homozygotes developed renal cysts (Figure 2.3 and Table 2.2), while none of the 12 littermate controls developed renal cysts (Figure 2.3 and Table 2.2). The  $Zeb2^{\text{flox/flox}};Pax2\text{-cre}^+$  embryos had a similar number of glomeruli as their wild-type littermate controls (Table 2.2), indicating that there was no reduction in nephron number. Accordingly, the renal cysts were initiated at E16.5 as no cysts could be detected at E15.5 (Figure 2.4). In the *Zeb2* conditional knockout embryos the renal cysts were apparently from a glomerular origin as 47% of the glomeruli were cystic and 30% of the cysts had a visible glomerular tuft at E16.5 (Table 2.2 and Table 2.3). This phenotype is sufficient for a diagnosis of glomerulocystic kidney disease (GCKD) according to the established criteria (Lennerz et al., 2010).



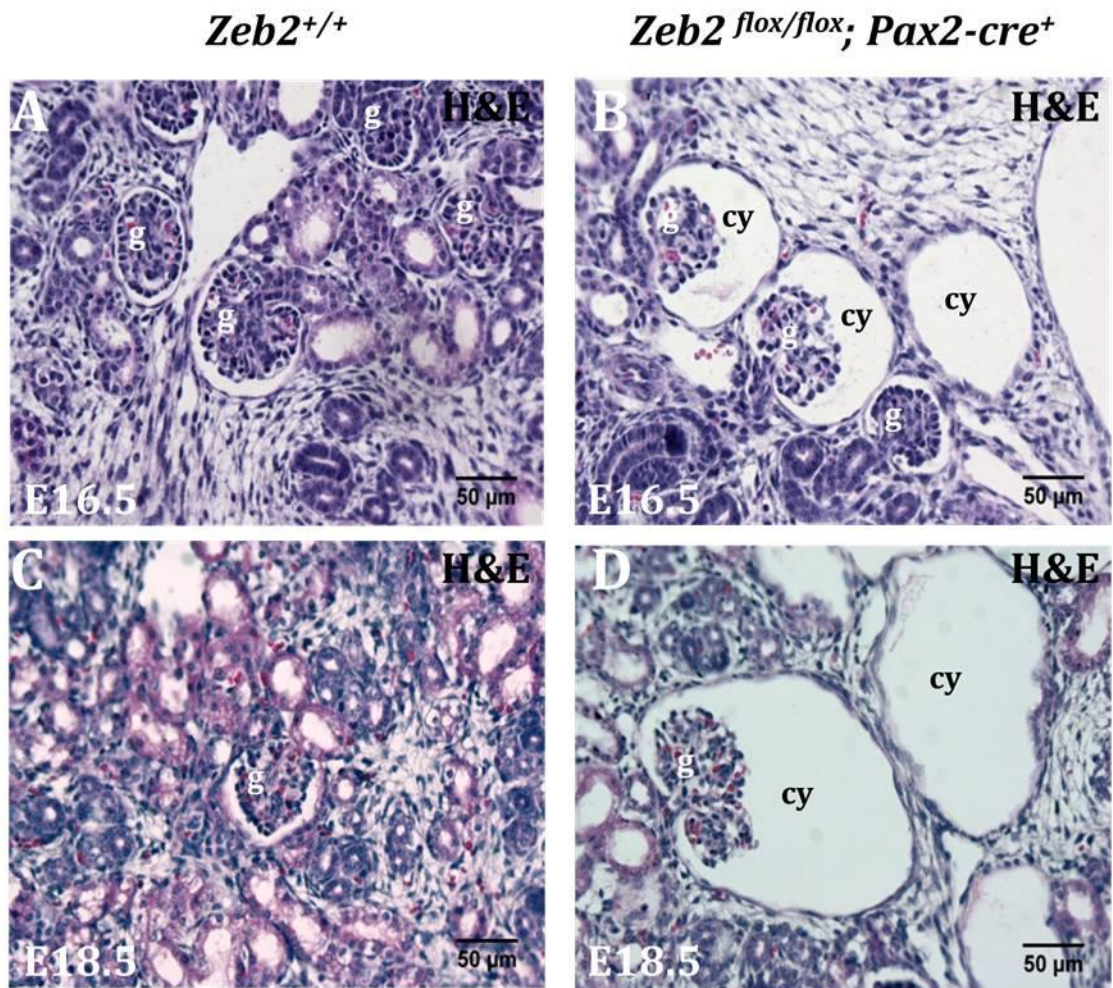


**Figure 2.3: Loss of *Zeb2* in the metanephric mesenchyme and the ureteric bud leads to renal cysts development**

Loss of *Zeb2* in the metanephric mesenchyme and the ureteric bud using the *Pax2-cre*<sup>+</sup> allele leads to renal cysts development. (A, B) Congenital kidney cysts were observed at E16.5 in the *Zeb2*<sup>flox/flox</sup>; *Pax2-Cre*<sup>+</sup> embryos and not in littermate controls. (C, D) Kidney cysts at E18.5 the *Zeb2*<sup>flox/flox</sup>; *Pax2-Cre*<sup>+</sup> embryos and not wild type littermate controls. cy- cysts, g- glomerulus (H&E staining, n<sub>≥</sub>3 in each group, 20x magnification)

**Table 2.2: Cystic phenotype observed in H&E stained histological samples of *Zeb2*<sup>flox/flox</sup>; *Pax2-cre*<sup>+</sup> and wild-type littermates between E16.5 and E18.5**

	E16.5		E17.5		E18.5	
	<i>Zeb2</i> <sup>+/+</sup>	<i>Zeb2</i> <sup>flox/flox</sup> ; <i>Pax2-cre</i> <sup>+</sup>	<i>Zeb2</i> <sup>+/+</sup>	<i>Zeb2</i> <sup>flox/flox</sup> ; <i>Pax2-cre</i> <sup>+</sup>	<i>Zeb2</i> <sup>+/+</sup>	<i>Zeb2</i> <sup>flox/flox</sup> ; <i>Pax2-cre</i> <sup>+</sup>
Embryos with kidney cysts (more than 1 cyst)	0/2 (0%)	3/3 (100%)	0/3 (0%)	3/3 (100%)	0/7 (0%)	8/8 (100%)
Glomerular Cysts/ Number of glomeruli (n= number of kidneys analyzed)	1/48 2%, (n=4)	26/55 47%, (n=5)	0/40 0%, (n=3)	18/59 30.5%, (n=4)	1/363 0.2%, (n=13)	61/391 15.6%, (n=15)

**Table 2.3: Percentage of cysts with glomerular tuft analyzed on H&E stained histological samples between E16.5 and E18.5**

	Cysts with Glomerular tuft / total cysts (n= number of kidneys analyzed)
	<i>Zeb2</i> <sup>flox/flox</sup> ; <i>Pax2-cre</i> <sup>+</sup>
E16.5	26/85 (30.6%, n=5)
E17.5	18/46 (39%, n=4)
E18.5	61/226 (27%, n=15)

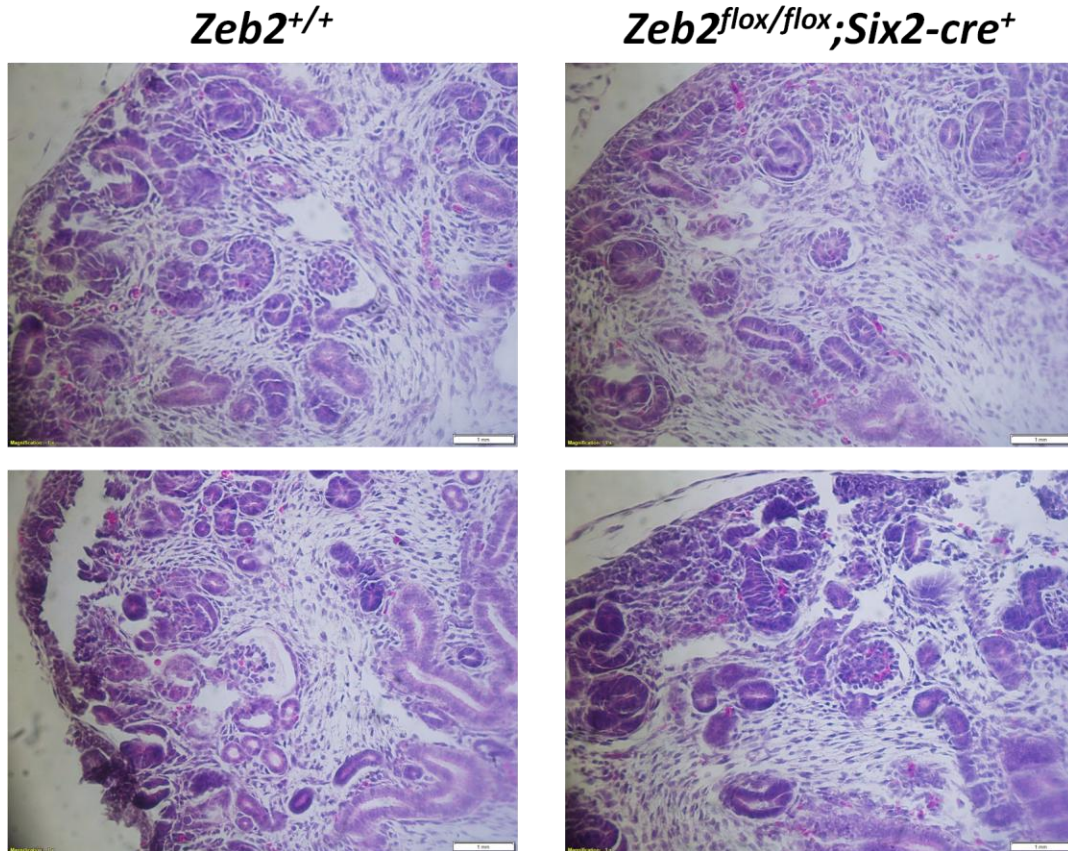


**Figure 2.4: No glomerular cysts were observed in E15.5  $Zeb2^{flox/flox};Six2-cre^+$  kidney.**

No glomerular cysts were observed in the  $Zeb2^{flox/flox};Six2-cre^+$  embryonic kidney at E15.5 compared to the  $Zeb2^{+/+}$  wild type littermate controls (n=3). 20 x magnifications.

No tubular cysts in the  $Zeb2^{flox/flox};Pax2-cre^+$  kidneys

Since glomerular cysts are usually secondary to tubular cysts, we decided to determine whether *Zeb2* mutant embryonic kidneys also developed renal tubular cysts. We examined the kidney sections with both proximal tubule specific marker *Lotus tetragonolobus lectin* (LTL) and distal tubules and collecting duct specific marker

*Dolichos biflorus agglutinin* (DBA). The cysts were negative for both LTL and DBA staining at embryonic stage E18.5, suggesting that the *Zeb2*<sup>fllox/fllox</sup>; *Pax2-cre*<sup>+</sup> homozygous embryos develop primary glomerular cysts (Figure 2.5).

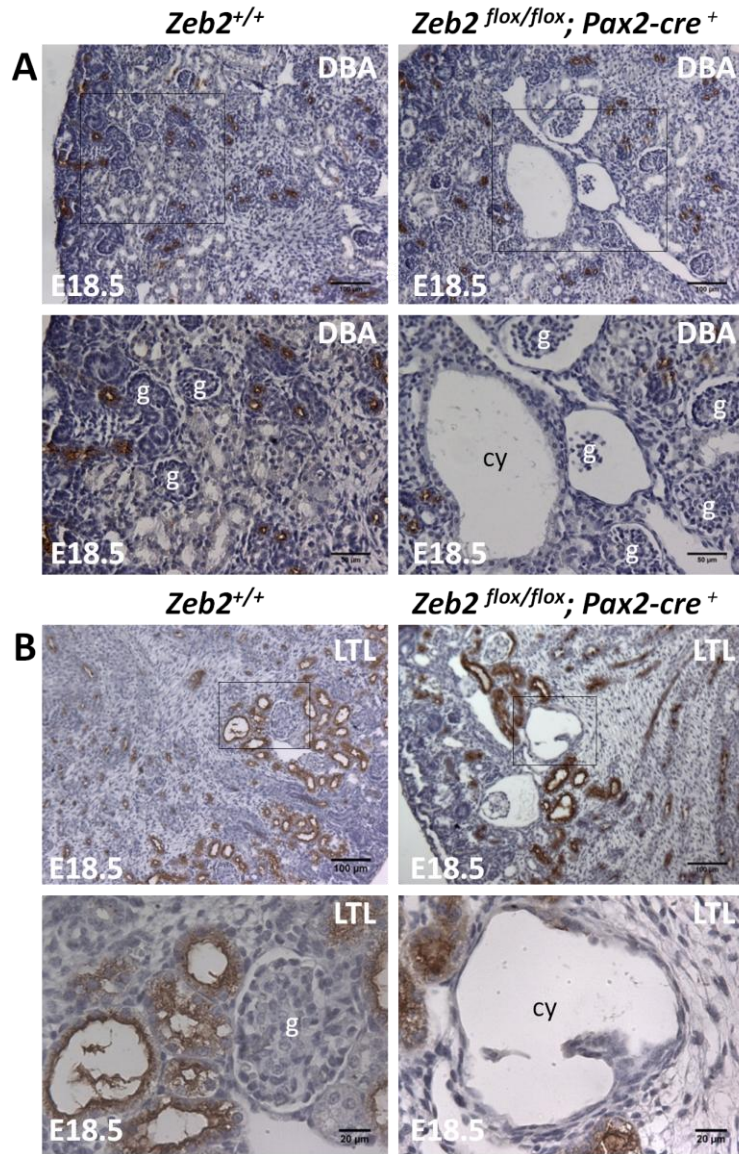


**Figure 2.5: Deletion of *Zeb2* in the metanephric mesenchyme and the ureteric bud leads to glomerular cysts formation.**

Deletion of *Zeb2* in the metanephric mesenchyme and the ureteric bud does not lead to tubular or collecting duct cysts. (A) None of the cysts in the *Zeb2*<sup>flox/flox</sup>; *Pax2-Cre*<sup>+</sup> kidneys at E18.5 is positive for the collecting duct and distal tubules marker, Dolichos biflorus agglutinin (DBA) staining (10x and 20x magnification). (B) None of the cysts in the *Zeb2*<sup>flox/flox</sup>; *Pax2-Cre*<sup>+</sup> kidneys at E18.5 is positive for the proximal tubules marker, *Lotus tetragonolobus lectin* (LTL) staining (10x and 40x magnification) ( $n \geq 3$  for each group, g-glomerulus, cy-cyst)

*Zeb2*<sup>flox/flox</sup>; *Pax2-cre*<sup>+</sup> pups die at birth

After genotyping 96 three-week old weanlings of *Zeb2*<sup>flox/+</sup>; *Pax2-cre*<sup>+</sup> heterozygous matings, I did not find any *Zeb2*<sup>flox/flox</sup>; *Pax2-cre*<sup>+</sup> homozygotes (Table 2.4). I then analyzed newborn mice and E18.5 embryos from timed-pregnant females. Five dead newborn *Zeb2*<sup>flox/flox</sup>; *Pax2-cre*<sup>+</sup> homozygotes and 21/55 (38%) E18.5 homozygous embryos were found (Table 2.4), suggesting that *Zeb2*<sup>flox/flox</sup>; *Pax2-cre*<sup>+</sup> homozygotes die at birth.

**Table 2.4: Mendelian distribution of *Zeb2* conditional knockout using *Pax2-cre*.**

Genotype	(a) 3 weeks		(b) E18.5	
	Observed	Expected	Observed	Expected (range)
<i>Zeb2</i> <sup>flox/+</sup> ; <i>Pax2-cre</i> <sup>+</sup>	23	36	10	20-21
<i>Zeb2</i> <sup>+/+</sup> ; <i>Pax2-cre</i> <sup>+</sup>	28	18	10	10-11
<i>Pax2-cre</i> <sup>-</sup>	45	24	14	13-14
<i>Zeb2</i> <sup>flox/flox</sup> ; <i>Pax2-cre</i> <sup>+</sup>	0	18	21	10-11
Total	96		55	

***Nephron-specific Zeb2 knockout embryos develop cysts (using the Six2-cre allele)***

Generation of a nephron specific *Zeb2* knockout mouse

*Zeb2<sup>flox/flox</sup>;Pax2-cre<sup>+</sup>* homozygous mice died after birth, which precludes a longitudinal analysis of glomerulocystic kidney disease progression in adult mice. To study the effect of *Zeb2* deletion and glomerular cystic phenotype on the postnatal kidney and to further delineate the role of ZEB2 in nephron development, we crossed *Zeb2<sup>flox/flox</sup>* mice with nephron-specific *Six2-cre* mice and analyzed kidney phenotype in *Zeb2<sup>flox/flox</sup>;Six2-cre<sup>+</sup>* homozygous mice. SIX2 is a nephron progenitor marker and is expressed in the cap mesenchymal cells that give rise to all segments of the nephron including the parietal and visceral epithelial cells (i.e. podocytes) in the glomeruli and the proximal and distal tubular epithelial cells (Kobayashi et al., 2008). As described in the methods, the *Zeb2<sup>flox/flox</sup>* mice were crossed with mice expressing the *Six2-cre* allele (Kobayashi et al., 2008).

***Zeb2<sup>flox/flox</sup>;Six2-cre<sup>+</sup> mice develop GCKD***

Histological examination of the kidneys from nine *Zeb2<sup>flox/flox</sup>;Six2-cre<sup>+</sup>* homozygous embryos revealed that, like the *Zeb2<sup>flox/flox</sup>;Pax2-cre<sup>+</sup>* embryos, all homozygous embryos had glomerular cysts starting at E16.5 (Figure 2.6A). At postnatal day 12 (P12), the glomerular cysts in the *Zeb2<sup>flox/flox</sup>;Six2-cre<sup>+</sup>* mice were mainly located

in the subcapsular region of the kidney that is consistent with the GCKD diagnosis (Figure 2.6B) (Lennerz et al., 2010). The cysts were also negative for both LTL and DBA staining (Figure 2.7), confirming their glomerular origin. In comparison, none of the five wild-type littermate controls had a cystic phenotype at P12 (Figure 2.6 and Figure 2.7).

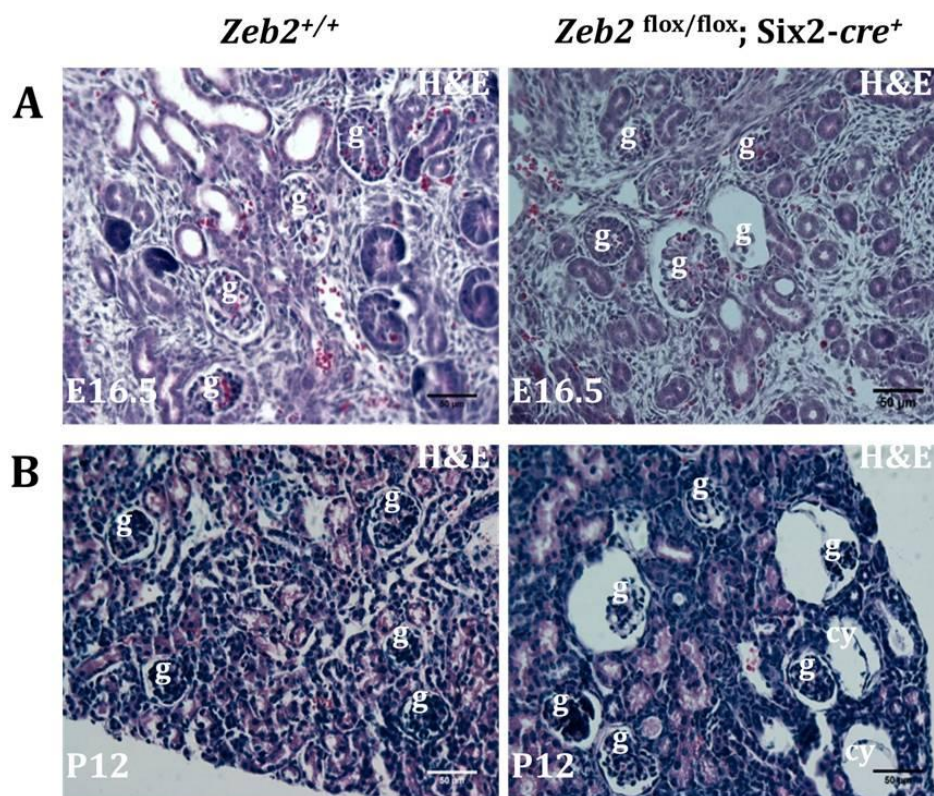


**Figure 2.6: Deletion of *Zeb2* in the tubular epithelial cells, podocytes and glomerular parietal cells using *Six2-cre*<sup>+</sup> leads to glomerular cysts development.**

Deletion of *Zeb2* in the tubular epithelial cells, podocytes and glomerular parietal cells using *Six2-cre*<sup>+</sup> leads to glomerular cysts development. (A) Congenital kidney cysts were observed in the *Zeb2*<sup>flox/flox</sup>;*Six2-Cre*<sup>+</sup> embryonic kidneys at E16.5 and not in littermate controls (H&E staining, 20x magnification). (B) Mainly subcapsular kidney cysts were observed at P12 in the *Zeb2*<sup>flox/flox</sup>;*Six2-Cre*<sup>+</sup> kidneys but not in littermate controls (H&E staining, 20x magnification).



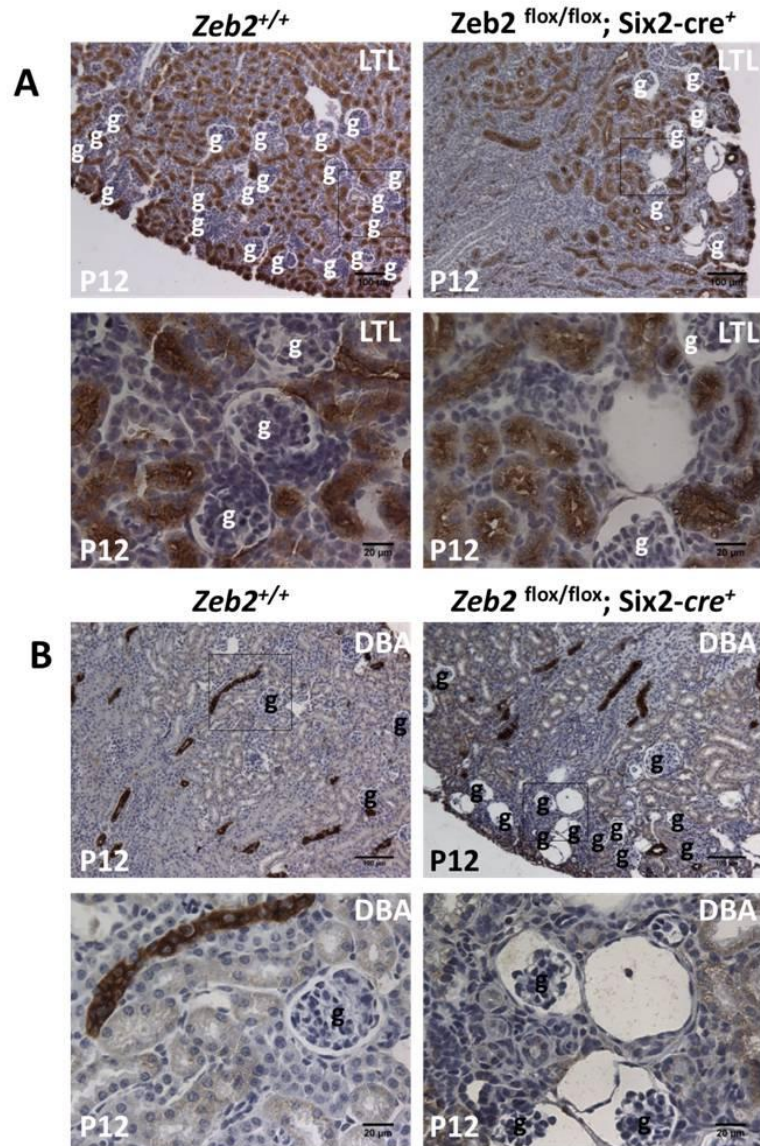


**Figure 2.7: Deletion of *Zeb2* in the tubular epithelial cells does not cause tubular cysts**

(A) At P12 none of the cysts in the *Zeb2*<sup>flox/flox</sup>; *Six2-Cre*<sup>+</sup> kidneys is positive for the proximal tubules marker, *Lotus tetragonolobus lectin* (LTL) staining (10x and 20x magnification). (B) At P12 none of the cysts in the *Zeb2*<sup>flox/flox</sup>; *Six2-Cre*<sup>+</sup> kidneys is positive for the collecting duct and distal tubules marker, Dolichos biflorus agglutinin (DBA) staining (10x and 20x magnification). (n≥3 for each group, g-glomerulus, cy-cyst)

Kidney failure before 2 months of age in *Zeb2<sup>lox/lox</sup>;Six2-cre<sup>+</sup>* mice.

To determine the longitudinal effect of glomerulocystic kidney disease on kidney structure and function, we followed the *Zeb2<sup>lox/lox</sup>;Six2-cre<sup>+</sup>* mice to adulthood. At 7 weeks of age, all *Zeb2<sup>lox/lox</sup>;Six2-cre<sup>+</sup>* mice (n=5, 100%) developed macroscopic renal cysts that were visualized on the surface of the kidney (Figure 2.8A). Histological analysis revealed the presence of numerous large glomerular cysts in the subcapsular area of the renal cortex (Figure 2.8B). Although no significant interstitial fibrosis was observed (Figure 2.9A), some remaining non-cystic glomeruli in adult *Zeb2<sup>lox/lox</sup>;Six2-cre<sup>+</sup>* mice displayed glomerulosclerosis lesions (Figure 2.9B), which were not present at E18.5 (Figure 2.10). By 8 weeks of age, all *Zeb2<sup>lox/lox</sup>;Six2-cre<sup>+</sup>* mice (n=5, 100%) developed albuminuria (Figure 2.11, A and B) with significantly elevated serum blood urea nitrogen (BUN) levels (Figure 2.11C). These data reveal that loss of *Zeb2* in developing nephrons causes glomerulocystic kidney disease, glomerulosclerosis, albuminuria and renal failure in adult mice.

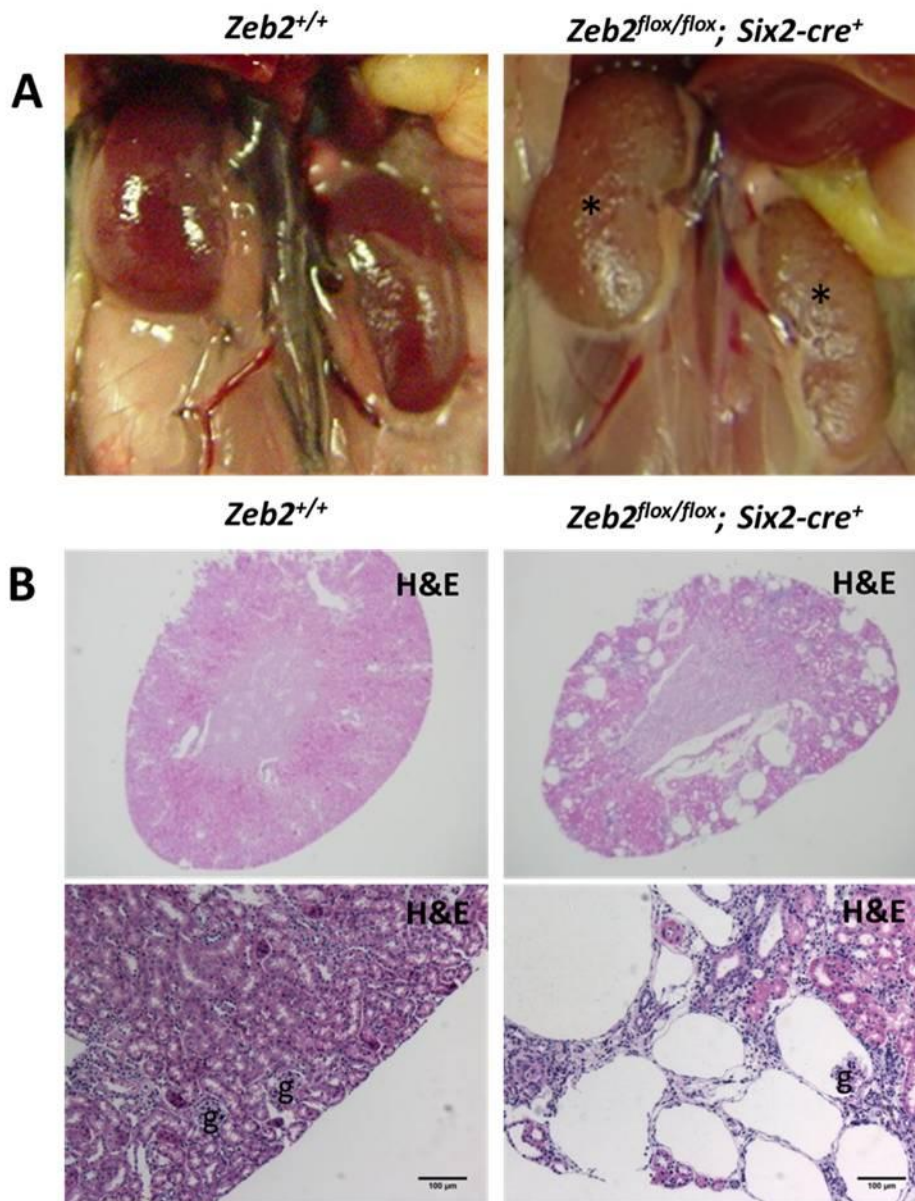


**Figure 2.8: Cystic kidney disease in adult  $Zeb2^{lox/lox};Six2-Cre^+$  mice**

(A) Macroscopic images of kidneys from 7-week old control mice and  $Zeb2^{lox/lox};Six2-Cre^+$  mice. The  $Zeb2^{lox/lox};Six2-Cre^+$  mice have pale and cystic kidneys as compared to wild-type littermate (n=5 in each group). (B) Histological images of kidneys from control mice and  $Zeb2^{lox/lox};Six2-Cre^+$  mice. Large cysts, mainly in the subcapsular area of the cortex in the 7-week old  $Zeb2^{lox/lox};Six2-Cre^+$  mice as compared to wild-type littermate (overall view at 2.5x magnification and enlargement at 10x magnification) (n=3 in each group).

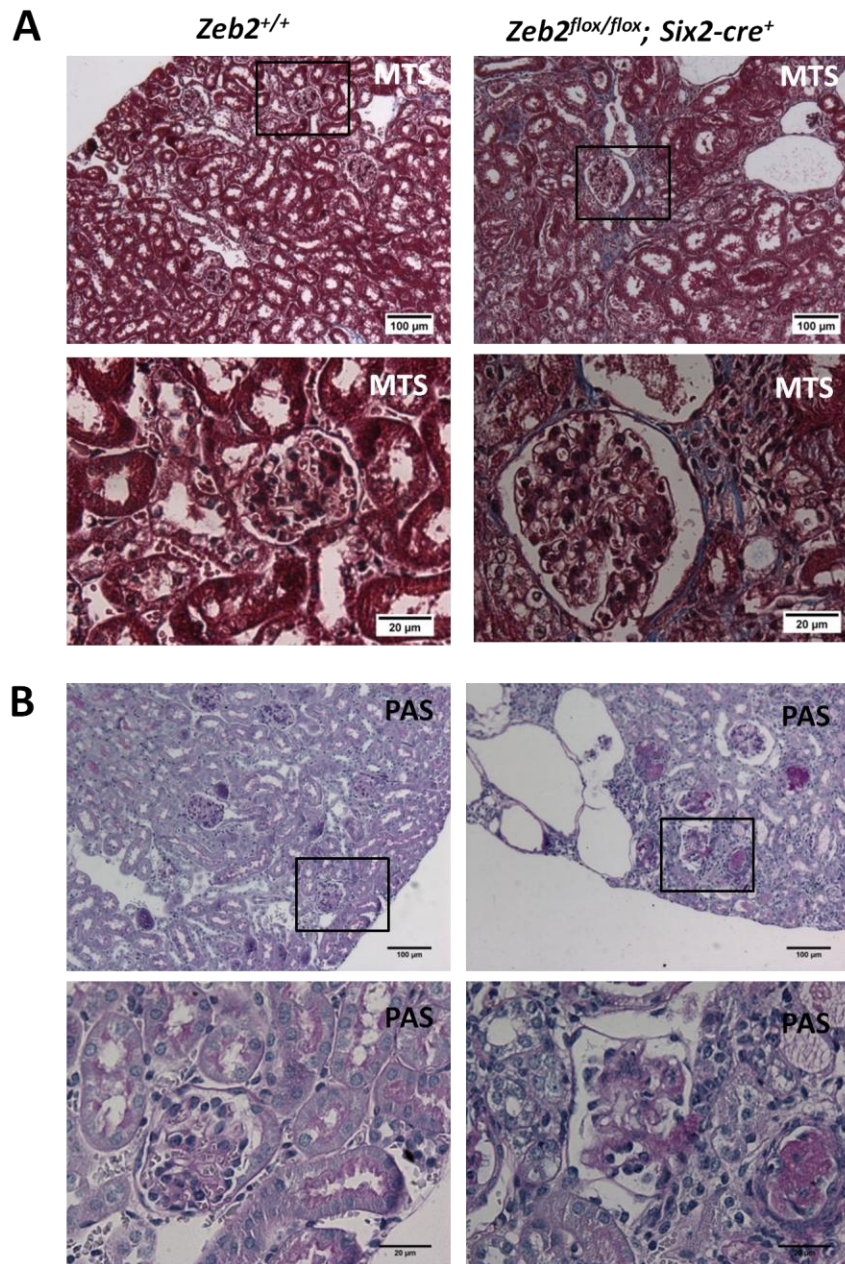


**Figure 2.9: Glomerulosclerosis in adult *Zeb2*<sup>lox/lox</sup>; *Six2-Cre*<sup>+</sup> mice**

(A) Little fibrosis is observed (blue) in the kidneys of the 7 weeks old *Zeb2*<sup>lox/lox</sup>; *Six2-Cre*<sup>+</sup> mice (Masson Trichrome staining- MTS, 10x (upper panels) and 60x (lower panels) magnifications) (B) Glomerulosclerosis is observed in pink in the non-cystic glomeruli of the 7 weeks old *Zeb2*<sup>lox/lox</sup>; *Six2-Cre*<sup>+</sup> mice (Periodic acid Schiff -PAS staining, 10x magnifications in upper panels and 60x magnifications in lower panels) (n=3 in each group).

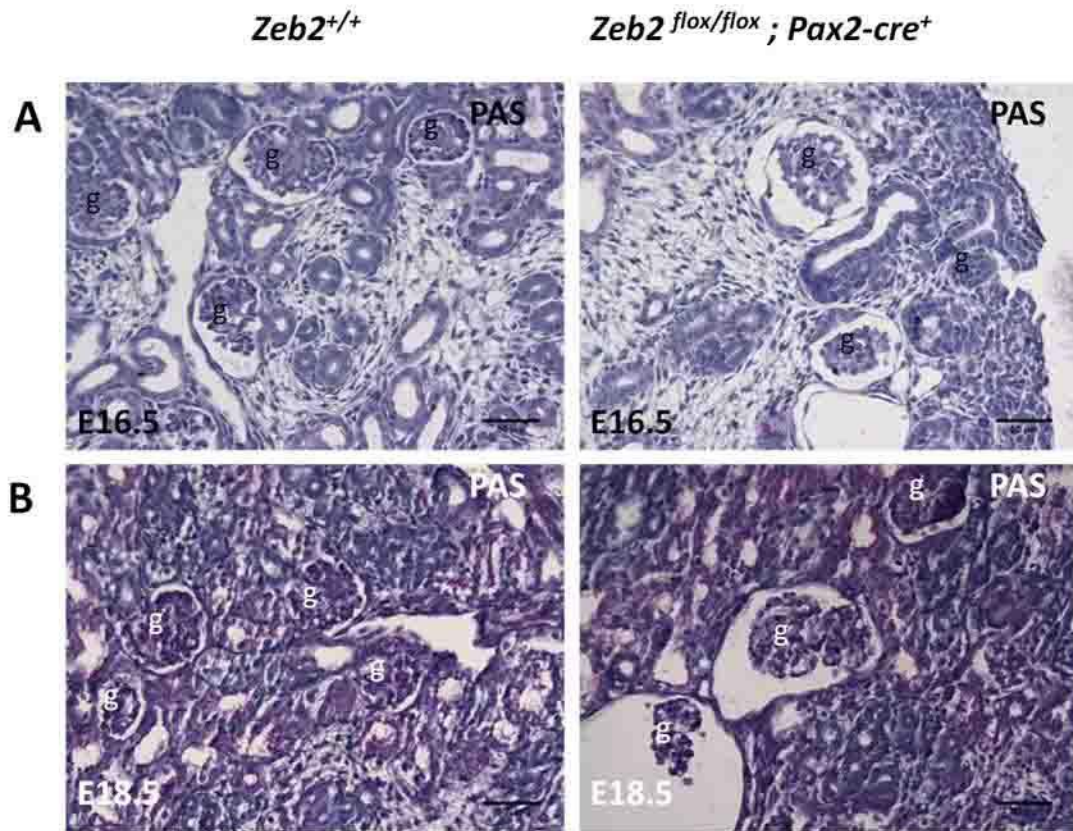


**Figure 2.10: No glomerulosclerosis is observed at E18.5 in *Zeb2*<sup>flox/flox</sup>; *Pax2-Cre*<sup>+</sup> mice**

Glomerulosclerosis was not observed in E16.5 (A) and E18.5 (B) *Zeb2*<sup>flox/flox</sup>; *Pax2-Cre*<sup>+</sup> mice (Periodic acid Schiff -PAS staining, 20x magnification).

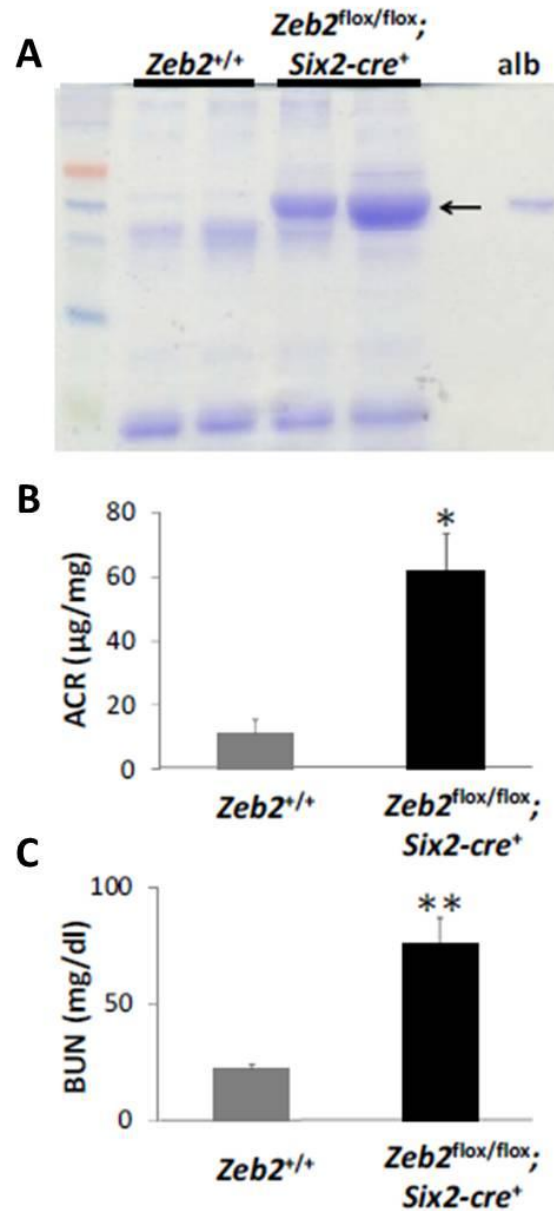


**Figure 2.11: Proteinuria and renal failure in adult *Zeb2*<sup>flox/flox</sup>; *Six2-cre*<sup>+</sup> mice**

(A-B) The *Zeb2*<sup>flox/flox</sup>; *Six2-cre*<sup>+</sup> mice develop albuminuria by 5 weeks old. (A) Representative SDS-page and Coomassie blue staining shows proteinuria/ albuminuria in two *Zeb2*<sup>flox/flox</sup>; *Six2-cre*<sup>+</sup> 5 weeks old mice as compared to two littermate controls (n=5 mice in each group). alb: albumin standard. (B) Increased urine Albumin to Creatinine Ratio-uACR in 5 weeks old *Zeb2*<sup>flox/flox</sup>; *Six2-cre*<sup>+</sup> mice (n=4 mice in each group, \*p-value < 0.05) (C) Kidney failure with significantly elevated BUN in 5 weeks old *Zeb2*<sup>flox/flox</sup>; *Six2-cre*<sup>+</sup> mice (n=3 mice in each group, \*\*p-value < 0.001). Results are represented as means +/- standard deviation.

### 2.5.3 GCKD in *Zeb2* knockout mice is due to atubular glomeruli formation

One common cause of acquired glomerular cysts is the loss of glomerulotubular junction integrity leading to atubular glomeruli (Chevalier and Forbes, 2008; Gibson et al., 1996). Glomerulotubular integrity can be quantified by examining the connection of the proximal tubule to the Bowman's capsule with the proximal tubule marker LTL (Forbes et al., 2011). To determine whether the *Zeb2* knockout mice have decreased glomerulotubular integrity, we examined glomeruli from five P12 *Zeb2*<sup>flox/flox</sup>; *Six2-cre*<sup>+</sup> mice and five littermate controls. We found that only 63/604 (10%) glomeruli had a visible LTL positive staining (i.e. glomerulotubular junction) in the *Zeb2* cKO mice as compared to 115/324 (36%) in the wild-type littermate controls (Figure 2.12), a statistically significant decrease of glomerulotubular integrity, suggesting that *Zeb2* deletion causes the formation of atubular glomeruli.

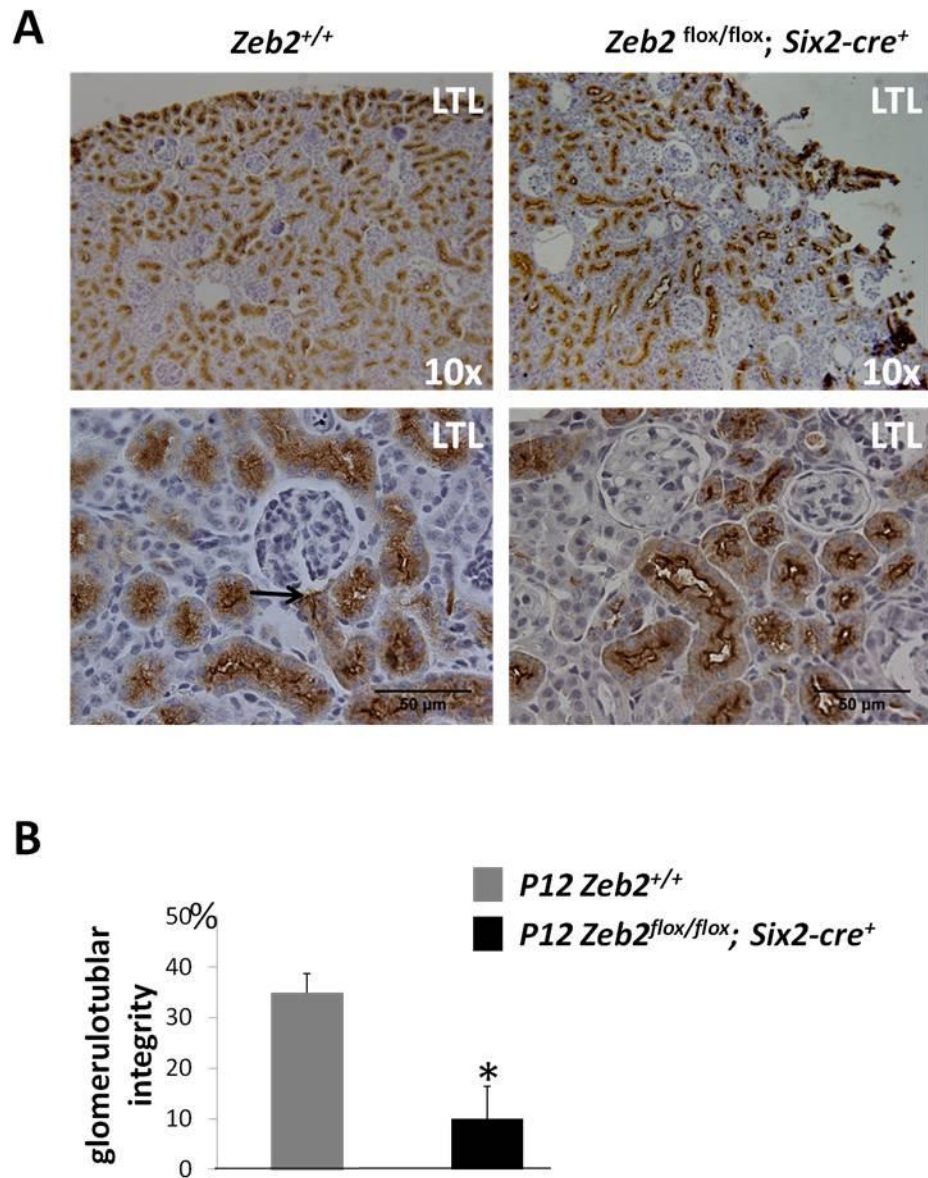


**Figure 2.12: Congenital atubular glomeruli in the *Zeb2* nephron-specific knockout mice.**

(A) LTL staining shows glomerular proximal tubule connection (arrow) in wild-type littermates but reduced in *Zeb2*<sup>fl<sup>ox</sup>/fl<sup>ox</sup></sup>; *Six2-cre*<sup>+</sup> mice (n=5 in each group). (B) Percentage of LTL-positive glomeruli out of total glomeruli counted in single sagittal kidney sections of 5 *Zeb2* cKO and 5 wild type littermates (n=604 for *Zeb2* cKO glomeruli and n=324 for wild type glomeruli). The 25% difference in LTL-positive glomerular staining in *Zeb2* conditional knockout compared to their wild-type littermates reflects loss of glomerulotubular integrity in the knockout mice.



#### 2.5.4 *Zeb2* knockout mice have abnormal tubular development

Atubular glomeruli can be caused by atrophy of the proximal tubules in polycystic kidney disease (Galarreta et al., 2014). To determine if reduced glomerulotubular integrity is associated with renal proximal tubule atrophy in *Zeb2* cKO, we analyzed the mRNA levels of markers for the proximal tubule (*Hnf1a* and *Vill*), the podocyte (*Nphs1* and *Nphs2*), and the collecting duct (*Upk3a*), all normalized to the collecting duct marker *Ppp1r3c* at postnatal day 8 (P8) (Massa et al., 2013). We found that only the proximal tubule mRNA markers were significantly reduced in the *Zeb2<sup>fllox/fllox</sup>;Six2-cre<sup>+</sup>* mice compared to the levels in the wild-type littermates (Figure 2.13A). To determine if the reduction of proximal tubule mRNA at P8 is caused by an early defect preceding the formation of glomerular cysts in *Zeb2* cKO mice, we analyzed the levels of mRNA markers in E14.5 kidneys. Similar to P8, a significant decrease of the proximal tubular markers was detected in the E14.5 *Zeb2<sup>fllox/fllox</sup>;Six2-cre<sup>+</sup>* kidneys as compared to their wild-type littermates (Figure 2.13B). Consistent with this finding, the mean kidney size of the E16.5 *Zeb2* cKO embryos was smaller than that of their wild-type littermate controls (Figure 2.14). Taken together, these data suggest that loss of *Zeb2* in the kidney causes early proximal tubule developmental defects resulting in reduced glomerulotubular integrity and congenital atubular glomeruli formation.

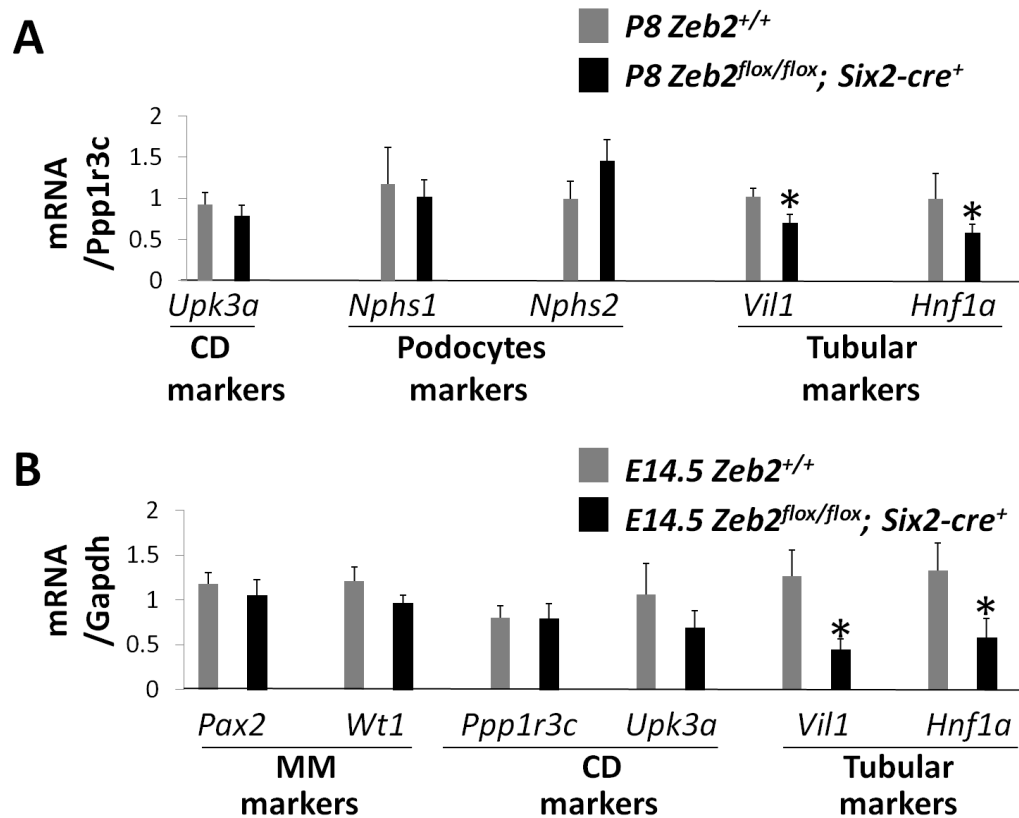


**Figure 2.13: Decreased tubular markers' expression in the *Zeb2* nephron-specific knockout mice.**

(A) At Postnatal day 8 (P8), decreased level of tubular mRNA markers (*Vil1* and *Hnf1a*) and similar levels of podocyte markers (*Nphs1* and *Nphs2*) when adjusted to a collecting duct marker (*Pppp1r3c*). An additional collecting duct marker, *Upk3a* was used as a control (n=3 in each group, mean relative quantification adjusted to *Pppp1r3c* +/- standard deviation, \*p-value < 0.05). (B) In E14.5 embryonic kidneys, decreased level of tubular mRNA markers (*Vil1* and *Hnf1a*) and similar levels of the metanephric mesenchyme markers (*Pax2* and *Wt1*) and of the collecting duct markers (*Pppp1r3c* and *Upk3a*) (mean relative quantification adjusted to *Gapdh* +/- standard deviation, n=3 in each group, \* p-value<0.05).

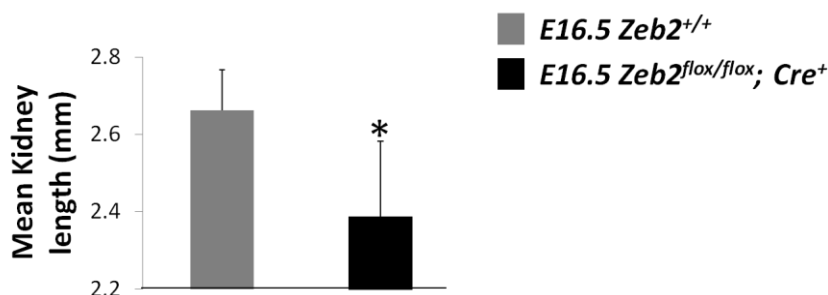


**Figure 2.14: Reduced kidney size in the *Zeb2* nephron-specific knockout mice.**

The *Zeb2* cKO embryos have reduced kidney length at E16.5 as compared to wild type littermates as measured using an Olympus microscope and the cellSens software (mean length in mm, n=14 *Zeb2* cKO kidneys from 7 embryos and n=11 wild type littermate kidneys from 6 embryos, \* p-value<10<sup>-3</sup>).

#### 2.5.5 Decreased apoptosis in the early stages of glomerular development of *Zeb2*

##### *conditional knockout embryos*

Apoptosis is part of normal kidney development during C-shaped body (CSB) and S-shaped body (SSB) formation when the connections between the glomeruli and the proximal tubules are established (Coles et al., 1993; Ho, 2014; Omori et al., 2000; Ruf et al., 2003). We hypothesized that abnormal apoptosis in CSB and SSB contributes to the congenital atubular glomeruli formation in the *Zeb2* conditional knockout mice. TUNEL assays on developing kidneys of E15.5 and E16.5 *Zeb2* cKO embryos and littermate controls were performed to test this possibility. 11/34 (32%) CSB/SSB had at least one apoptotic cell in 5 kidneys of *Zeb2* cKO embryos, while 25/39 (64%) CSB/SSB had at least one apoptotic cell in 4 kidneys of wild-type littermate controls (Figure 2.15). These

data suggest that loss of *Zeb2* causes reduced apoptosis in CSB and SSB, which may affect tubular development and ultimately result in congenital atubular glomeruli.

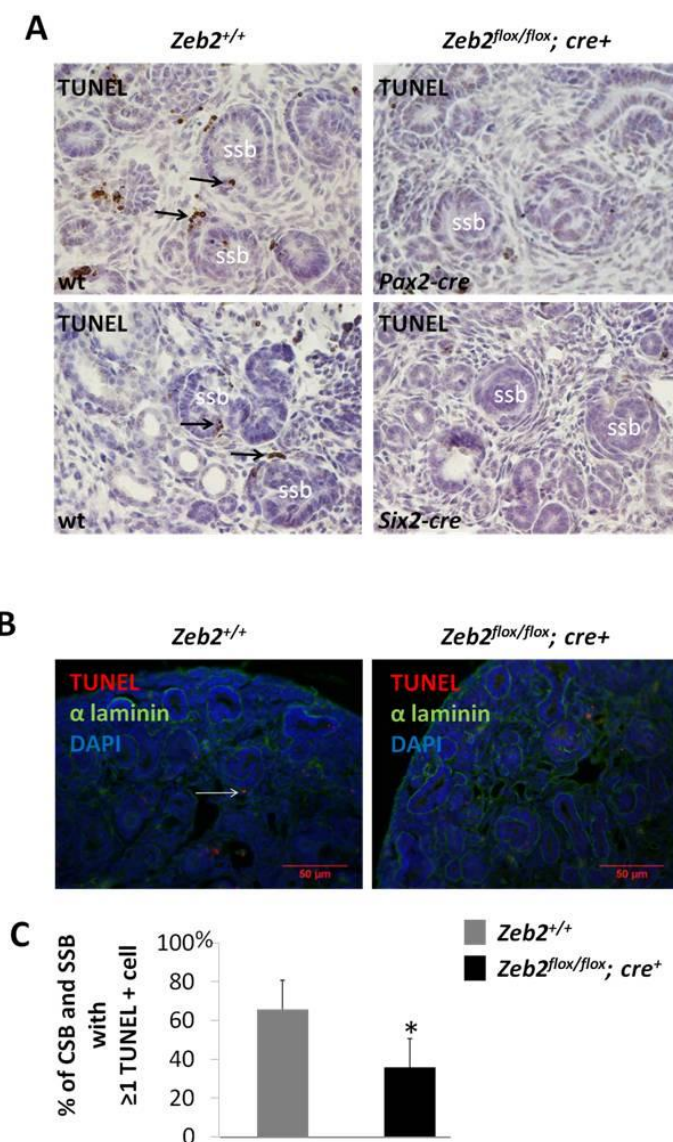


**Figure 2.15: Decreased apoptosis in the C- and S-shaped bodies in *Zeb2* knockout mice.**

(A) TUNEL staining shows reduced number of apoptotic cells (arrows) in *Zeb2* conditional knockout kidneys using both *Pax2-cre*<sup>+</sup> and *Six2-cre*<sup>+</sup> (n=5 for mutant kidneys and n=4 for wild-type kidneys). (B) Immunofluorescence with TUNEL (rhodamine fluorochrome) and an antibody against Lamal (green) to delineate the developing structures using a basement membrane marker. (C) Reduced apoptosis in the C-shaped bodies and S-shaped bodies of the *Zeb2* conditional knockouts. 11/34 (32%) CSB/SSB had  $\geq 1$  TUNEL<sup>+</sup> cell in 5 kidneys of *Zeb2* cKO embryos, and 25/39 (64%) CSB/SSB had  $\geq 1$  TUNEL<sup>+</sup> cell in 4 kidneys of wild-type littermate controls (mean percentage  $\pm$  standard deviation, \*p-value<0.01).

***No significant differences in cell proliferation in the kidneys of Zeb2 conditional knockouts compared to wild-type littermates***

Renal cystogenesis is often associated with increased cell proliferation (Paul and Vanden Heuvel, 2014). To determine if increased cell proliferation also plays a role in the formation of glomerular cysts in *Zeb2* cKO mice, I quantified the proliferation of the parietal epithelial cells lining the glomerular cysts in the kidney of *Zeb2* cKO and undilated Bowman's capsules in the wild type littermate controls. By measuring the positive signals of the cell mitotic proliferation marker phosphorylated histone H3 (pHH3), no significant difference of cell proliferation was observed in *Zeb2* knockout kidneys compared to the wild-type controls (Figure 2.16), suggesting that loss of *Zeb2* does not affect cell proliferation in the Bowman's capsule.

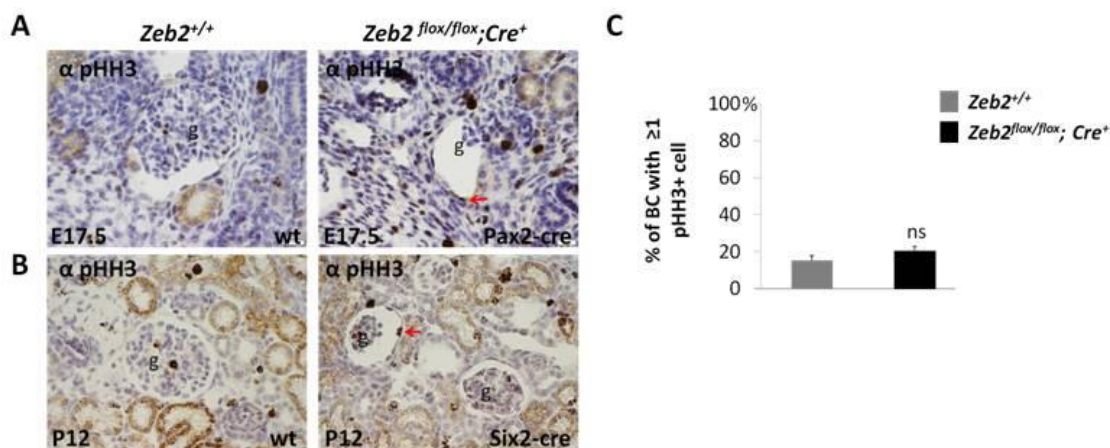


**Figure 2.16: No significant change in cell proliferation in the Bowman's capsule of *Zeb2* knockout mice.**

(A) Staining with an antibody against phosphorylated Histone H3 (pHH3) as a marker of proliferation in E17.5 *Zeb2<sup>flox/flox</sup>; Pax2-cre<sup>+</sup>* embryonic kidneys. (B) Staining with an antibody against phosphorylated Histone H3 (pHH3) as a marker of proliferation in P12 *Zeb2<sup>flox/flox</sup>; Six2-cre<sup>+</sup>* kidneys. (C) No significant difference in proliferation between the wild type and the conditional knockout mice in the Bowman's capsule layer, the percentage of glomeruli with  $\geq 1$  cell positive for pHH3 in their Bowman's capsules out of all the glomeruli in single sagittal sections (mutant n=235 glomeruli, wild-type n=220 glomeruli from 4 kidneys in each group), data are presented as mean percentage  $\pm$  standard deviation (ns- non significant)

#### 2.5.6 Elevated levels of *Pkd1* mRNA and protein in the kidneys of *Zeb2* conditional knockout mice

Glomerular cysts are reported in several mouse models of renal cystic kidney disease, including *Wwtr1*, *Glis3*, *Ofd1* and *Pkhd1* knockout mice, the *Hnf1 $\beta$*  and *Dicer* cKO mice, and *Pkd1* over expression transgenic mice (Ferrante et al., 2006; Hossain et al., 2007; Kang et al., 2009; Massa et al., 2013; Patel et al., 2012; Pritchard et al., 2000b; Williams et al., 2008b). Interestingly, the *Hnf1 $\beta$*  cKO mice develop glomerular cysts due to a drastic reduction in the levels of proximal tubular markers at E14.5 and lack of mid-

limb of the S-shaped body development, resembling the *Zeb2* cKO phenotype (Massa et al., 2013). To determine if loss of *Zeb2* affects the expression of these six genes and the microRNA miR-200, we examined mRNA and microRNA levels in the kidney tissues of E14.5 and E18.5 *Zeb2* cKO and wild-type littermate controls. Although there was no significant difference in the expression levels of any of the six genes and miR-200 at E14.5 before glomerular cyst formation (Figure 2.17A), we detected decreased expression of *Glis3* and increased expression levels of *Hnf1 $\beta$*  and *Pkd1* in the *Zeb2* cKO compared to the wild-type littermate controls at E18.5 (Figure 2.17B). Interestingly, the expression level of *Pkd1* mRNA was the most significantly upregulated in the *Zeb2* cKO kidneys at postnatal day 8 (P8) (Figure 2.18A). Consistent with the mRNA levels, PKD1 coding protein polycystin-1 (PC1) was also found to be expressed at high level in the glomeruli of postnatal day 7 (P7) *Zeb2<sup>flox/flox</sup>;Six2-cre<sup>+</sup>* mice but not at E16.5 and E17.5 when the glomerular cysts are initially observed (Figure 2.18B). Interestingly, the PC1 expression was upregulated in non-cystic glomeruli but not in the glomeruli with dilated Bowman's space (Figure 2.18C). These data suggest that loss of *Zeb2* in the kidney leads to upregulation of polycystin-1 expression in non-cystic glomeruli after the initial phase of glomerular cyst formation.

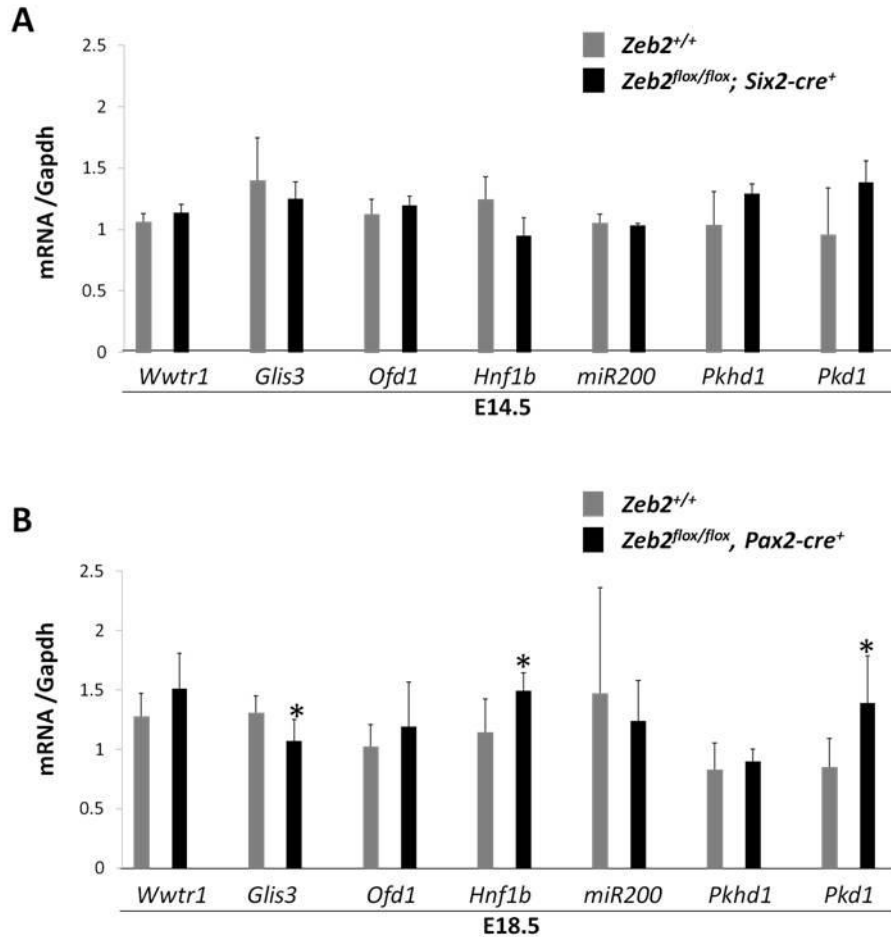


**Figure 2.17: Abnormal expression levels of genes associated with GCKD after the appearance of the glomerular cysts.**

(A) No difference at E14.5 in the mRNA levels of 6 genes and the miRNA level of miR200 which were all associated with a glomerulocystic phenotype in mice (mean relative quantification adjusted to *Gapdh* +/- standard deviation, n=3). (B) Significantly increased level of *Pkd1* mRNA at E18.5 and P8 and increased level of *Hnf1 $\beta$*  mRNA at E18.5 and decreased level of *Glis3* mRNA at E18.5 (mean relative quantification adjusted to *Gapdh* +/- standard deviation, n=5, \*p-value <0.05).



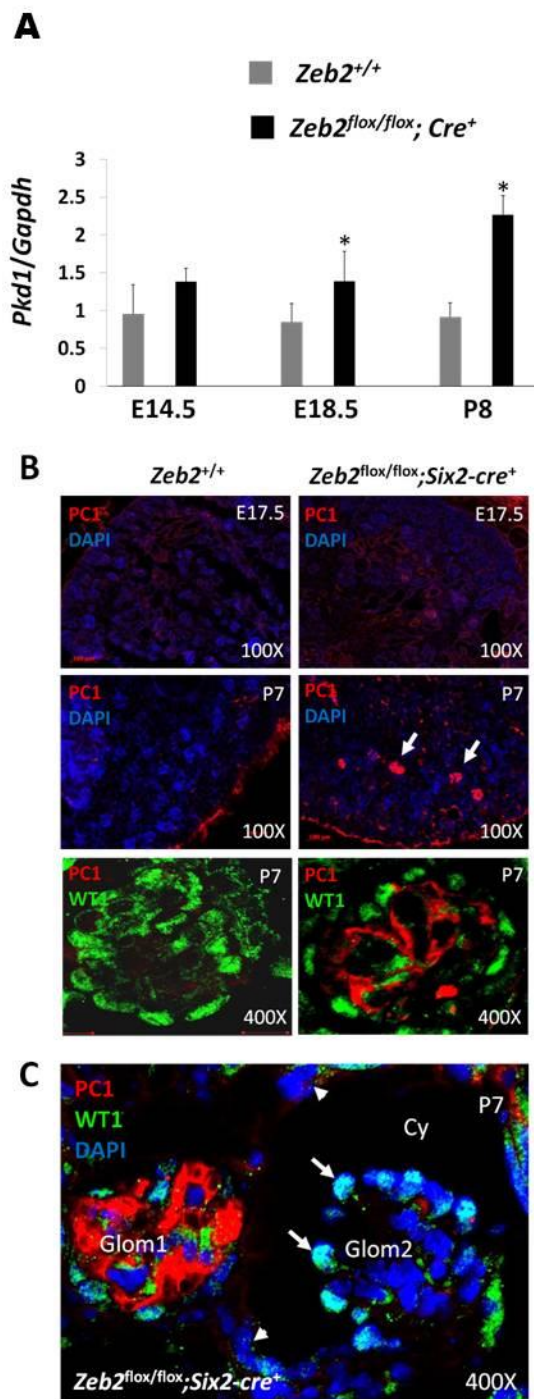


**Figure 2.18: Increased *Pkd1* expression in the kidney of *Zeb2* conditional knockout mice.**

(A) Significant upregulation of *Pkd1* mRNA at E18.5 and P8 but not E14.5 in *Zeb2* cKO kidneys compared to wild-type controls (mean relative quantification adjusted to *Gapdh*,  $n \geq 3$ , \* $p < 0.05$ ). (B) Immunofluorescence staining show increased levels of polycystin 1 (PC1) protein in the glomeruli of *Zeb2*<sup>lox/lox</sup>;*Six2-cre*<sup>+</sup> kidney at P7 (middle and lower panels), but not at E17.5 (upper panel). PC1 staining in the glomeruli was confirmed by co-expression of WT1, a glomerular podocyte marker (lower panel). (C) Double immunofluorescence staining with PC1, WT1 and DAPI in *Zeb2* cKO kidney shows increased levels of polycystin 1 (PC1) protein was detected only in non-cystic glomeruli (glom 1) but not in an adjacent glomerulus (glom 2) with significantly enlarged Bowman's space (cy). The podocytes (arrows) and parietal epithelial cells (arrowheads) are visible.

*2.5.7 Heterozygous deletion of Pkd1 in the kidneys of Zeb2 conditional knockout mice exacerbates renal cystic phenotype*

Since we observed increased levels of *Pkd1* in the *Zeb2* cKO mice, we decided to genetically reduce the expression of *Pkd1* in the nephron using a *Pkd1* conditional knockout floxed allele and the *Six2-cre* deleter mice. In summary, the data collected suggest that decreased *Pkd1* level in the nephron exacerbates the *Zeb2* cKO phenotype (data not shown). In addition, kidneys of *Pkd1<sup>flox/+</sup>;Six2-cre<sup>+</sup>* mice have higher levels of *Pkd1* mRNA (data not shown) than both the *Zeb2<sup>flox/flox</sup>;Six2-cre<sup>+</sup>* kidneys and *Zeb2<sup>flox/flox</sup>;Pkd1<sup>flox/+</sup>;Six2-cre<sup>+</sup>* kidneys, suggesting that *Pkd1* upregulation could be secondary to a decrease level of *Pkd1* in the nephrons. Therefore, loss of *Zeb2* in the nephron may decrease the levels of *Pkd1* in the nephron, while upregulating *Pkd1* expression in other cell types where *Zeb2* is not deleted.

## 2.6 Discussion

### 2.6.1 Interpretations

#### ***Proposed pathogenesis leading to kidney failure in the Zeb2 cKO mice***

In this study, we found that ZEB2 is broadly expressed in the developing kidney. Conditional deletion of *Zeb2* with *Pax2-cre* and *Six2-cre*, two Cre strains active in the developing nephron, resulted in the same glomerular cyst phenotype, indicating that ZEB2 is required for normal nephron development. Decreased levels of proximal tubular markers at E14.5, reduced kidney size at E16.5 and reduced apoptosis at the CSB and SSB phases in the *Zeb2* cKO mice suggest that an early defect of the proximal tubule development leads to congenital atubular glomeruli formation, accumulation of glomerular filtrate and cystic expansion of the Bowman's space. In addition, abnormal nephrogenesis in *Zeb2* cKO mice also result in reduced number of non-cystic functional glomeruli, which undergo hyperfiltration and hypertrophy leading to secondary FSGS and eventually renal failure. Therefore, the initial defect in nephrogenesis during embryonic kidney development in *Zeb2* cKO mice correlates with early kidney failure after birth.

### ***Zeb2 is expressed in nephron epithelial cells***

We detected ZEB2 expression only in a subset of nephron epithelial cells, and not in the cap mesenchyme (Figure 2.1 and 2.2). Since deletion of *Zeb2* in the nephron epithelial cells (e.g. tubular epithelial cells, podocytes and glomerular parietal cells) with the *Six2-cre* caused severe GCKD and renal failure phenotype (Kobayashi et al., 2008), we concluded that *Zeb2* plays an important role in the development of the epithelial layer of the nephron, as it is in the lens epithelial layer (Manthey et al., 2014a; Manthey et al., 2014b).

### ***Zeb2 is mainly expressed in the stromal cells***

Based on the expression pattern of *Zeb2* we identified in this study and the gene expression data from the GUDMAP database in the kidney, *Zeb2* is broadly expressed in the developing kidney stromal cells (Harding et al., 2011; Kobayashi et al., 2008; McMahon et al., 2008; Ohyama and Groves, 2004). Therefore, we deleted *Zeb2* in the developing mouse stromal cells using *Foxd1-cre*. These mice developed a severe growth retardation phenotype that can be observed at 3 weeks of age when they need to be euthanized due to poor body condition and renal failure (data not shown). However, at the histological level, no cysts were observed in the *Zeb2<sup>flox/flox</sup>;Foxd1-cre<sup>+</sup>* cKO mice, supporting a specific role of ZEB2 in the developing nephrons. Further analysis of these mice is needed in order to understand the role of *Zeb2* in the stromal cells.

### Early defect in tubular development

The reduced kidney size at E16.5 and the similar number of glomeruli in the *Zeb2* cKO compared to the wild-type littermates suggest abnormal development of a specific segment of the nephron. Decreased levels of tubular markers in the *Zeb2* cKO mice at E14.5, before the appearance of the cysts, imply an early defect in tubular differentiation. Consistent with our findings, haploinsufficiency of *Zeb2* was reported to be associated with delayed nephrogenesis in a transgenic rat model, however the kidney phenotype was not investigated in detail (El-Kasti et al., 2012).

Another model with a drastic reduction in the levels of tubular markers at E14.5 and lack of tubular development is the *Hnf1 $\beta$*  cKO mice, which also develops glomerular cysts (Massa et al., 2013). Unexpectedly, a slight upregulation of *Hnf1 $\beta$*  mRNA in *Zeb2* cKO E18.5 embryonic kidneys as compared to wild-type controls was observed. This upregulation of *Hnf1 $\beta$*  may reflect a compensatory mechanism in the developing nephron lacking *Zeb2*, since it was observed only after cyst formation. Our findings in this project suggest that loss of *Zeb2* is associated with primary congenital atubular glomeruli probably due to developmental defects of the glomerulotubular junction.

### Reduced apoptosis in the Comma-shaped and S-shaped bodies

At the cellular level, reduced apoptosis in C-shaped and S-shaped bodies (CSB and SSB) was observed in the *Zeb2* cKO embryonic kidneys compared to littermate

controls. Apoptosis plays an important role in normal nephrogenesis (Ahn et al., 2013; Massa et al., 2013). Here we show for the first time that decreased apoptosis during nephrogenesis, is observed in primary non-lethal GCKD. Loss of *Zeb2* during development has been shown to differently affect apoptosis in various organs (Maruhashi et al., 2005; Miquelajauregui et al., 2007; Seuntjens et al., 2009; Yoshimoto et al., 2005). Apoptosis dysregulation during nephrogenesis may lead to abnormal tubular development and ultimately to congenital atubular glomeruli.

#### Congenital Atubular glomeruli

Atubular glomeruli were first described in animal models of chronic nephropathy and then in human patients with chronic pyelonephritis (Marcussen and Olsen, 1990). In 1996, the connection between atubular glomeruli and glomerular cysts was first described (Gibson et al., 1996), yet I did not find a report investigating atubular glomeruli formation in models or patients with glomerular cysts. Proximal tubular injury and loss of tubular epithelial cells are known to cause atubular glomeruli, however they usually do not lead to glomerular cysts, but rather to small glomeruli (Forbes et al., 2011; Forbes et al., 2013; Marcussen, 1995; Xu et al., 2013). Atubular glomeruli and glomerular cysts are described in polycystic kidney disease in human, mice and rats, but are thought to be secondary to large cysts inducing tubular injury that destroys the glomerulotubular junctions (Colgin et al., 2002; Tanner et al., 2002).

In the *Zeb2* cKO model, there is no congenital urinary tract obstruction, no tubular or collecting duct cysts, but a congenital proximal tubular defect. This study produced the first viable mouse model of primary congenital atubular glomeruli, which will be valuable for the general scientific community.

The *Zeb2*<sup>fl<sub>ox</sub>/fl<sub>ox</sub></sup>; *Six2-cre* mice die from kidney failure

GCKD in *Zeb2* cKO mice leads to renal failure within 8 weeks after birth with enlarged cysts, glomerulosclerotic lesions in the non-cystic glomeruli, elevated BUN, albuminuria, but minimum renal fibrotic lesions. Considering that glomerulosclerosis was not noticed in the embryonic kidneys, it may be secondary to post-natal hyperfiltration caused by the numerous cystic glomeruli and abnormal nephrogenesis as proposed in the Illustration 2.2 above (Helal et al., 2012). Since the tubules are responsible for the reabsorption of albumin under normal conditions, the proteinuria observed in the *Zeb2* cKO mice might be a result of abnormal tubular function or damage to podocytes in the non-cystic glomerular. This early renal failure may be reminiscent of the end-stage renal disease (ESRD) found in children with congenital forms of renal cystic diseases (Hildebrandt and Otto, 2005; Kurschat et al., 2014).

Increased PC1 expression has been reported in other models of cystic kidney disease.

Increased expression of PC1 was detected in the glomeruli of *Zeb2* conditional knockout mice.

Mutations in *PKDI* cause Autosomal dominant polycystic kidney disease (ADPKD), one of the commonest monogenic diseases in patients (Torres et al., 2007). *PKDI* is located at chromosome 16p13.3 next to the *TSC2* gene and encodes a 4,302 amino acid membrane protein polycystin-1 (also called PC1) (The International Polycystic Kidney Disease Consortium, 1995) (1995). The expression pattern of PC1 in the kidney is not completely understood, and different results of PC1 immunostaining have been reported. (Geng et al., 1997; Palsson et al., 1996; Peters et al., 1996; Ward et al., 1996). However it is accepted that PC1 expression in the kidney is developmentally regulated with highest expression in the embryonic kidney and downregulated after birth.

In human patients, higher *PKDI* expression was found in both non-cystic kidney diseases (e.g. Expression data from kidney biopsies of liver disease patients: GSE50892) and ADPKD (Expression data from renal cysts of autosomal dominant polycystic kidney disease (ADPKD) patients: GSE7869) (Song et al., 2009). Previous studies have showed that the expression of polycystin-1 is significantly increased in the cyst-lining epithelium in ADPKD kidneys although it was primarily expressed intracellularly (Palsson et al., 1996). Other groups have found higher *Pkd1* levels in cystic kidney diseases in mice. For example, the *Inv* mutant mice with cystic kidney disease have an increased level of *Pkd1* expression (Expression profiling by array: GSE4462) (Sugiyama and Yokoyama, 2006). The *Dicer* conditional knockout mice also develop tubular and glomerular cyst with an increased level of *Pkd1* expression (Patel et al., 2012). Therefore, the increased expression of *Pkd1* in the *Zeb2* cKO kidneys might be secondary to kidney disease and



not directly related to the function of ZEB2 as a transcription factor in the kidney. On the other hand, other mice models of GCKD have decreased or unchanged *Pkd1* levels, suggesting that not all glomerular cysts would lead to an upregulation of *Pkd1* mRNA levels (Hossain et al., 2007; Kang et al., 2009).

### *2.6.2 Future research opportunities*

#### ***Do MWS patients develop GCKD?***

In patients, *ZEB2* heterozygous loss-of-function mutations cause the MWS. We began our research on the role of *Zeb2* in kidney development because MWS patients have an increased risk for kidney anomalies. However, a cystic phenotype has never been described in MWS patients. This discrepancy between the known phenotypes in MWS and the murine phenotype may be due to the difference between heterozygote and homozygote deletion in the kidney, or to the differences between human and mice (Elsa and Lucas, 2002; Routtenberg, 1995). It might also be related to the difficulty to detect GCKD in patients. Since nonenhanced T2-weighted magnetic resonance imaging (MRI) is the most sensitive tool to identify GCKD in patients, it might be indicated in patients with MWS (Romero et al., 1993). As more patients are diagnosed with MWS, the clinical presentation seems to be more variable than previously thought (Glessner et al., 2014; Heinritz et al., 2006) and cystic kidney disease may be eventually added to the list of

anomalies found in MWS, enabling a better differential diagnosis, both at the pediatric and the prenatal setting (Zhou et al., 2014).

***The renal phenotype of the Zeb2 heterozygote knockout mice is unknown***

The MWS is caused by heterozygote mutations in ZEB2. At the molecular level, the phenotype is probably due to haplo-insufficiency, meaning that the amount of the ZEB2 protein is not sufficient to maintain a normal development. However, the *Zeb2* heterozygous knockout mice are viable (Van de Putte et al., 2003a). Nevertheless, no renal analysis has been performed on these heterozygotes so far, especially in older mice after six months of age. Therefore, we are following a subset of heterozygotes to determine if they develop any renal tract phenotype.

***Do patients with GCKD harbor mutations in ZEB2?***

Heterozygous missense mutations in *ZEB2* were found in some atypical forms of MWS (Heinritz et al., 2006). Heterozygous missense mutations or homozygous variants in *ZEB2* may cause isolated GCKD in patients. As shown in other genetic disorders, the same gene can cause a variety of disorders both syndromic and non-syndromic (Kohl et al., 2014; Negrisol et al., 2011; Scolari et al., 2014). Because a large number of isolated congenital kidney anomalies are caused by monogenic mutations, *ZEB2* may be a new renal cystic disease gene to be added in the growing panel of genes causing kidney

anomalies in the future (Vivante et al., 2014). We have recently established a collaboration with Dr. Friedhelm Hildebrandt lab at Boston Children's Hospital to further explore this research opportunity to screen the *ZEB2* gene in patients with cystic kidney disease.

***Will ZEB2 lead to the discovery of more GCKD causal genes?***

ZEB2 is a transcription factor regulating the expression of many genes. However, it is unknown which genes are regulated by ZEB2 during kidney development. From the results generated on the ZEB2 research of other organ systems, new genes important in renal development and cystogenesis might be discovered unexpected (Manthey et al., 2014b). In addition, a well designed gene expression profiling experiment with kidney tissues isolated from *Zeb2* conditional knockout mice and wild-type controls might facilitate the discovery of new GCKD causal genes. Towards this direction, we have already started to breed *Zeb2<sup>fllox+</sup>;Six2-cre<sup>+</sup>* mice with mice carrying the *mT/mG* construct (B6.129(Cg)-Gt(ROSA)26Sor<sup>tm4(ACTB-tdTomato,-EGFP)Luo/J</sup>) to isolate cells that express *Six2-cre* in both controls and *Zeb2* cKO embryos.

Potential role of the Smad signaling pathway in cystogenesis

Studies have shown that ZEB2 binds activated SMADs at the biochemical level, (Conidi et al., 2013; Postigo, 2003). For example, ZEB2 interacts with SMAD8 during

ocular lens development (Yoshimoto et al., 2005). In addition, ZEB2 activates *Smad7* expression during CNS myelination (Weng et al., 2012). During kidney development, SMAD signaling (including SMAD7 and SMAD8) is activated in the renal vesicle stage onward to the proximal nephron tubules (Arnold et al., 2006; Blank et al., 2008; Vrljicak et al., 2004).

In addition, two gene knockout mouse models that develop glomerular cysts, the *Wwtr1* and *Glis3*, encode proteins that also interact with SMADs (Hossain et al., 2007; Kang et al., 2009; Makita et al., 2008; Varelas et al., 2008; Yang et al., 2012). The *Glis3* mRNA level was reduced in the *Zeb2* cKO embryonic kidneys at E18.5 but not at E14.5 compared to their wild type littermates. This finding raises the possibility that the pathogenesis in *Zeb2* cKO mice may be partially mediated by lower *Glis3* expression level.

Further analysis is warranted in order to define whether dysregulation of the SMAD signaling pathway is responsible for the development of atubular glomeruli and renal cystic phenotype in the *Zeb2* cKO mice.

## Potential role of the Wnt signaling pathway in the ZEB2-associated glomerular cystic phenotype

*Zeb2* represses the expression of *Sfrp1*, an inhibitor of Wnt signaling, in the mouse hippocampus (Miquelajauregui et al., 2007). Similarly, deletion of *Zeb2* during lens development, leads to the upregulation of *Dkk1*, another repressor of the Wnt signaling pathway (Manthey et al., 2014a). Wnt signaling dysregulation has been shown to cause renal cystic phenotype. Overexpression of a transgenic  $\beta$ -catenin leads to the formation of renal cysts in the collecting duct, the renal tubules and the glomeruli (Saadi-Kheddoui et al., 2001). Similarly, activation of the Wnt signaling pathway using conditional expression of *Wnt9b* in *Six2-cre* positive cells leads to renal tubular cyst formation (Kiefer et al., 2012). Although these two models upregulated the Wnt signaling and caused tubular cysts, it is possible that downregulation of the Wnt signaling pathway during nephrogenesis may also affect tubular development leading to renal cysts. However, the potential effect of *Zeb2* deletion on the Wnt signaling during nephron development remains to be determined.

## 2.7 Conclusions

In conclusion, by studying animal models of a disease gene causing a human syndrome associated with an increased risk of kidney disease, we identified *Zeb2* as a novel gene important in nephrogenesis and glomerulotubular junction formation. Loss of *Zeb2* in mice results in reduced glomerulotubular integrity, congenital atubular glomeruli

and primary glomerular cystic disease. Future studies are needed to elucidate the downstream genes regulated by *ZEB2* during kidney development and to characterize the cell type and mechanism of *Pkd1* overexpression in non-cystic glomeruli. On the human genetics side, it will be important to determine whether MWS patients also develop glomerular cysts and whether a subset of patients with glomerulocystic disease carries *ZEB2* mutations. As a transcription factor, *ZEB2* may also provide a starting point for further identification of new genes important in glomerulotubular junction development and that, when mutated, may cause GCKD in patients.

## **CHAPTER THREE: Loss of *Robo2* alleviates the glomerular phenotype of *Ilk* podocyte-specific knockout mice.**

### **3.1 Summary**

Roundabout 2 (ROBO2) is a transmembrane protein that plays an important role in kidney development. Recently we have shown that ROBO2 interacts with nephrin via an adaptor protein, NCK, and ROBO2 inhibits nephrin-induced actin polymerization. Integrin-linked kinase (ILK) is another important podocyte protein that interacts with NCK and nephrin, and promotes actin polymerization and cell adhesion. Previous studies have shown that podocyte-specific deletion of *Ilk* in mice results in proteinuria, renal failure and premature death. Here, we hypothesize that ROBO2 can form a complex with ILK in podocytes via NCK and that loss of *Robo2* in podocytes would alleviate the abnormal glomerular phenotype in *Ilk* knockout mice.

Although no direct interaction between ROBO2 and ILK was detected by yeast two-hybrid assay, co-immunoprecipitation analysis showed that ROBO2 and ILK form a protein complex through NCK and PINCH. Survival analysis of 86 mice up to one year revealed that *Robo2-Ilk* double homozygous mice survived longer than *Ilk* single homozygous mice. Electron microscopy showed that there was an improvement in podocyte and glomerular basement membrane ultrastructure of the *Robo2-Ilk* double homozygous mice in comparison to the *Ilk* single homozygous mice at 4 weeks of age.

Our results suggest that ROBO2 and ILK form a protein complex through NCK and PINCH. Loss of *Robo2* improves the glomerular ultrastructure and the survival of *Ilk* podocyte-specific knockout mice.

### 3.2 Background and Introduction

As described in Chapter One, the kidney glomerular filtration barrier is formed by a three-layered structure: the visceral epithelial cells (i.e. podocytes), the glomerular basement membrane (GBM) and the endothelial cells. The podocytes are terminally differentiated epithelial cells that form long primary processes and a complex network of interdigitating secondary processes (also called foot processes) wrapping around the glomerular capillaries. The podocyte foot processes interdigitate and form the slit diaphragm structure of approximately 40-nm width to prevent the leakage of large serum protein (e.g. albumin) into the urine (Simons and Huber, 2008). The organization and regulation of the actin cytoskeleton in the podocytes are essential for the normal foot process structure.

Nephrin (encoded by *NPHS1* gene) is the first slit diaphragm protein identified by human genetic studies: mutations in *NPHS1* cause congenital nephrotic syndrome of the Finnish type (OMIM 256300) (Kestila et al., 1998). Nephrin from the neighboring podocytes undergoes homophilic interaction and maintains the slit diaphragm structure (Wartiovaara et al., 2004). Patients and mouse models lacking nephrin exhibit severe proteinuria (i.e. leaking of large amounts of protein from the blood to the urine through



damaged glomerular filtration barrier), and foot process effacement (Kestila et al., 1998) that is caused by actin cytoskeleton rearrangements. Previous studies have shown that nephrin has an outside-in signal transducing role that affects the actin cytoskeleton of the foot process structure through phosphorylation of its intracellular domain (George and Holzman, 2012).

In addition to forming the specialized cell junctions (i.e. the slit diaphragm) between the foot processes, the podocytes also adhere to the GBM through integrins. This adhesion and attachment of the podocytes to the GBM is essential for a functional glomerular filtration barrier and loss of podocytes from the GBM can lead to proteinuria and glomerulosclerosis.

### *3.2.1 The glomerular basement membrane*

The GBM is a specialized extracellular matrix structure between the glomerular endothelia and the podocytes (Menon et al., 2012). It is especially thick because it derives from the fusion of separate extracellular matrix components produced by the podocytes and the endothelial cells during glomerulogenesis (Abrahamson, 1985; Miner, 2011). Across the GBM, water and small molecules in the blood are filtered while large plasma proteins such as albumin are restricted. The GBM contains laminin, type IV collagen, nidogen, and heparan sulfate proteoglycan agrin, components found in all basement membranes (Miner, 2011). Mutations in genes that encode laminin and type IV collagen cause inherited human kidney disease Pierson syndrome (OMIM 609049) and Alport

syndrome (OMIM 20378, 301050), which are associated with severe albuminuria and haematuria.

***The podocytes express GBM components laminins and type IV collagens***

Type IV Collagen  $\alpha3\alpha4\alpha5$  and laminin-521 are the major components of the GBM. They are secreted by both the glomerular endothelia and the podocytes. Both the type IV collagen and the laminin form the basal laminae that are about 100-200 nm thick. Although the early type IV collagen  $\alpha1\alpha2\alpha1$  is produced by both endothelial cells and podocytes, type IV collagen  $\alpha3\alpha4\alpha5$  is found in the fully mature GBM and is produced only by the podocytes (Abrahamson et al., 2009).

In the Alport syndrome, the GBM is defective due to an absence of or defective type IV collagen  $\alpha3\alpha4\alpha5$ , however the presence of type IV collagen  $\alpha1\alpha2\alpha1$  and the dysregulation of the laminins may also be part of the pathology (Abrahamson et al., 2007). The defective GBM may also convey inappropriate signals to the endothelial cells and podocytes, which, in turn, causes progressive Alport disease (Abrahamson et al., 2007). Additionally, changes in the GBM structure can also trigger intracellular signaling events that influence podocyte adhesion (Lennon et al., 2014).

Laminin is a high molecular weight protein that forms a heterotrimeric complex containing an  $\alpha$ -chain, a  $\beta$ -chain and a  $\gamma$ -chain. Laminin  $\alpha2\beta5\gamma1$  (also referred to as laminin-251 or LM-251) is the major laminin in the mature GBM, which is transitioned from laminin  $\alpha1\beta1\gamma1$  (i.e. LM-111, which is the first laminin formed in developing

GBM) and laminin  $\alpha5\beta1\gamma1$  (i.e. LM-511). The mechanisms for silencing expression of LM-111 and LM-511, and upregulating LM-521 during glomerular development are not well understood (Abrahamson, 2012).

Integrins are the major podocyte cell adhesion proteins that interact with the laminin and type IV collagen in the GBM. The laminin binds integrin  $\alpha3\beta1$ , whereas integrins  $\alpha1\beta1$  and  $\alpha2\beta1$  are the receptors for type IV collagens (Mathew et al., 2012). Interestingly, removal of these integrins in the podocytes also affects the GBM structure. Podocyte specific deletion of integrin  $\beta1$  and germline knockout of integrin  $\alpha3$  lead to a splitting GBM phenotype, while integrin  $\alpha2$  knockout mice develop irregular GBM with protrusions towards the podocytes (Girgert et al., 2010; Kreidberg et al., 1996; Pozzi et al., 2008). In addition, deletion of the integrin-linked kinase (ILK) or constitutive upregulation of the Wnt signaling in mice can also lead to abnormal GBM phenotype (Dai et al., 2006; El-Aouni et al., 2006; Kato et al., 2011).

### *3.2.2 The integrin linked kinase (ILK) function in the podocytes*

Integrin linked kinase (ILK) is a 59 kDa protein interacting with PINCH (encoded by LIMS1 gene) at its N-terminal and  $\alpha/\beta/\gamma$ -PARVIN at its C-terminal (Yamaji et al., 2001). ILK binds directly to the integrin  $\beta1$  cytoplasmic tail and is important for signal transduction at cell adhesion sites (Hannigan et al., 1996; Ishii et al., 2001). ILK also plays an important role in the podocytes as *Ilk* podocyte-specific knockout mice develop

proteinuria, abnormal splitting of GBM, renal failure and premature death (Dai et al., 2006; El-Aouni et al., 2006).

### ***ILK plays a role in actin cytoskeleton dynamics***

Increasing evidences suggest that ILK is a pseudokinase (Lange et al., 2009; Wickstrom et al., 2010), which functions as a scaffold protein and forms complexes connecting integrins to the actin cytoskeleton. ILK induces actin polymerization through a protein complex involving PARVIN, PINCH and NCK (Sakai et al., 2003; Wu and Dedhar, 2001). The interaction between ILK and the actin-binding protein  $\alpha$ - PARVIN is required for kidney development because mutations in *Ilk* disrupting  $\alpha$ -PARVIN binding cause renal agenesis in mice (Lange et al., 2009). Furthermore, a similar kidney phenotype is observed when  $\alpha$ -PARVIN is genetically deleted in mice (Lange et al., 2009). In the tracheal smooth muscle tissues, the assembly of the ILK protein complex at membrane adhesion sites regulates N-WASp-mediated actin polymerization (Zhang et al., 2007), which was shown to be important in the maintenance of podocytes' foot processes (Schell et al., 2013).

### ***ILK and cell adhesion***

The assembly of a protein complex involving ILK and PINCH is important in the formation of cell-matrix adhesion sites (Zhang et al., 2002). Disruption of the PINCH-

ILK complex reduces podocyte-matrix adhesion and foot process formation (Yang et al., 2005). Accordingly, podocyte-specific *Ilk* deletion causes podocyte depletion as shown by the reduction of podocyte number in each glomerulus (Dai et al., 2006; Kanasaki et al., 2008). This is probably due to podocyte detachment and loss in the urine as podocyte specific proteins WT1 and podocin can be detected in the urine of podocyte specific *Ilk* knockout mice (Dai et al., 2006; Kanasaki et al., 2008).

### ***ILK and GBM formation***

ILK expression also regulates extracellular matrix formation. In the lens, deletion of *Ilk* leads to a disorganized basement membrane characterized by discontinuous and diffuse expression of type IV collagen and laminin (Cammass et al., 2012). Lens-specific deletion of *Ilk* also leads to an abnormal retention of collagen reactivity within the fiber cells (Teo et al., 2014). In the mouse cortex, ILK acts as an intracellular mediator for integrin-dependent basal lamina formation (Niewmierzycka et al., 2005).

GBM phenotype in podocyte-specific *Ilk* knockout mice includes a splitting of the GBM that is similar to the phenotype reported in the integrins  $\beta 1$  and  $\alpha 3$  knockout mice (Dai et al., 2006; El-Aouni et al., 2006; Kanasaki et al., 2008). This phenotype is probably related to the role of ILK as a scaffold protein because the *Ilk* mutant mice without kinase activity do not have any abnormal GBM phenotype (Lange et al., 2009). In addition, a significant decrease of type IV collagen  $\alpha 3$ ,  $\alpha 4$  and  $\alpha 5$  chain expression was observed in 12 weeks old *Ilk* knockout mice (El-Aouni et al., 2006). Interestingly, the

GBM splitting phenotype observed in the podocyte-specific *Ilk* knockout mice is reminiscent of Alport syndrome (Kalluri et al., 1997). Taken together, these results suggest that the GBM phenotype observed in the *Ilk* cKO may be caused by the decreased adhesion of the podocytes to the GBM combined with a dysregulation of the GBM composition.

### *3.2.3 ROBO2 functions in the podocytes*

#### ***ROBO2 regulates actin cytoskeleton in the podocytes***

ROBO2 is the cell surface receptor for the repulsive guidance cue SLIT2 and plays crucial roles during early kidney development and ureteric bud outgrowth (Grieshammer et al., 2004; Lu et al., 2007b). We have recently found that SLIT2/ROBO2 signaling also play an important role in regulating actin polymerization in the podocytes. ROBO2 activation reduces nephrin-linked actin polymerization through the adaptor protein NCK (Fan et al., 2012) (Illustration 3.1). Interestingly, Slit/Robo signaling has also been shown to regulate CDC42 and downstream N-WASp-mediated actin polymerization in neurons (Wong et al., 2001).

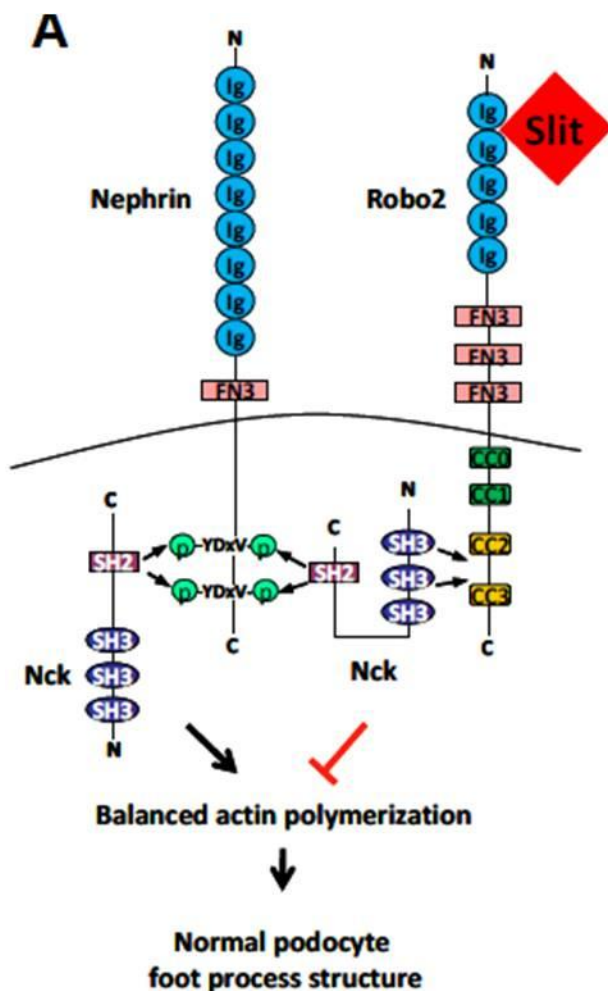


### Illustration 3.1: Robo2 inhibits Nephrin-induced actin polymerization.

A proposed model of inhibitory effects of Slit/Robo signaling on nephrin to influence podocyte foot process structure: Under physiological conditions (e.g., during foot process development), nephrin intracellular phosphorylated tyrosine domains (YDxV-p) recruit Nck through its interaction with the SH2 domain. Nck, in turn, recruits cytoskeleton regulators through its SH3 domains to promote actin polymerization. Slit2 binds Robo2 to increase Robo2 intracellular domain interaction with SH3 domains of Nck, which would prevent binding of Nck to cytoskeletal regulators and result in an inhibition of nephrin-induced actin polymerization. Balanced actin polymerization is maintained during podocyte development for a normal foot process structure. Abbreviations: Ig: Immunoglobulin domain; FN3: Fibronectin type 3 domain; SH2: Src homolog 2 domain; SH3: Src homolog 3 domain; CC0, CC1, CC2, CC3: Cytoplasmic Conserved region 0, 1, 2, 3. (published in Fan et al. Cell Reports, 2012 with permission).

### ***ROBO2 stimulation destabilizes cell adhesion***

The ROBO protein was named after the discovery of its role in repulsion (Seeger et al., 1993). In addition to its role in actin cytoskeleton regulation, SLIT-ROBO signaling also inhibits cell adhesion (Rhee et al., 2002). ROBO antagonizes E-cadherin mediated adhesion (Santiago-Martinez et al., 2008) and forms a complex with Abelson kinase (Abl) and N-cadherin, which induces  $\beta$ -catenin activation (Rhee et al., 2007). Activation of  $\beta$ -catenin in the podocytes has been shown to inhibit podocyte attachment to different matrices (Kato et al., 2011). Similarly, srGAP3, a Slit-Robo Rho GTPase activating protein, also inhibits focal adhesion (Endris et al., 2011).

### ***The Slit/Robo signaling and the ECM***

Our lab has found that ROBO2 is expressed on the basal podocyte surface adjacent to the glomerular basement membrane (Fan et al., 2012). SLIT2 is a large glycoprotein with a Laminin G-like module that is also called ALPS domain because it is present in proteins Agrin, Laminin, Perlecan and Slit (Rothberg and Artavanis-Tsakonas, 1992).

Interestingly, the LMX1B transcription factor regulates both the expression of *type IV Collagen* and *Slit2* (Morello et al., 2001; Yan et al., 2011). SLIT2 has 2 homologs in mammals, SLIT1 and SLIT3, which have about 60% homology (Brose et al., 1999). In the Zebrafish, SLIT1 binds to the type IV Collagen, Col4a5, a major component of the GBM (Xiao et al., 2011). *Slit3* has been shown to genetically interact with *Frem1*, which



encodes an extracellular protein, during renal development, suggesting a common function (Beck et al., 2013). In *Drosophila* cardiac morphogenesis, genetic interaction studies show that SLIT has a strong phenotypic interaction with integrins, laminin and collagen, as well as with ILK (MacMullin and Jacobs, 2006).

Taken together, the activation of the Slit/Robo signaling in the podocytes is probably affected by the GBM composition.

### ***Loss of Robo2 in the podocytes has a renoprotective effect from glomerular injury***

Recent results from our lab suggest that loss of *Robo2* in the podocytes has a renoprotective effect. The podocyte foot processes of the *Nephrin-Robo2* double knockout mice were relatively preserved when compared to the *Nephrin* single knockout mice (Fan et al., 2012). Similarly, the structure of podocyte foot processes in the *Robo2* knockout mice is protected after induced glomerular injury with both nephrotoxic serum (NTS) and protamine sulfate (Anna Pisarek-Horowitz, manuscript in preparation). In the wild type mice, *Slit2* and *Robo2* expression is upregulated after NTS injury, suggesting increased Slit/Robo signaling (Anna Pisarek-Horowitz, manuscript in preparation). Interestingly, NTS injury is induced by the binding of heterologous antibody that recognizes the  $\beta 1$  Integrin molecule (O'Meara et al., 1992). As described previously, podocyte-specific deletion of *integrin  $\beta 1$*  in mice leads to a splitting GBM phenotype (Pozzi et al., 2008) although NTS injury does not cause GBM splitting (Anna Pisarek-Horowitz, manuscript in preparation).

Taken together, loss of *Robo2* in the podocytes has a renoprotective effect from glomerular injury. The steadiness of the foot processes after injury indicate that these foot processes undergo less cytoskeleton remodeling when they lack ROBO2. Following injury, active Slit/Robo signaling may inhibit actin polymerization and destabilize the adhesion of the podocytes to the GBM leading to more foot process effacement and detachment.

#### *3.2.4 Both ILK and ROBO2 form complexes with Nephrin through NCK*

Podocyte cytoskeleton plasticity is necessary for maintaining a normal functional kidney filtration barrier (Greka and Mundel, 2012). We have showed that ROBO2 interacts with nephrin through NCK (Figure 3.1) (Fan et al., 2012) and NCK has been reported to interact with the ILK-PINCH complex (Wu and Dedhar, 2001). NCK is an adaptor protein that can bind an array of proteins and promote actin polymerization (Chaki and Rivera, 2013). Interestingly, ILK also forms a complex with nephrin (Dai et al., 2006) and nephrin phosphorylation regulates podocyte adhesion through the PINCH-ILK complex (Zha et al., 2013). However, it is unclear if NCK mediates the interactions between ILK and nephrin to enable the complex formation. The effect of ILK loss on nephrin expression and distribution in the podocytes is not well-defined (Dai et al., 2006).

NCK contains one SH2 domain in the C-terminus and three SH3 domains near the N-terminus. Our lab has showed that ROBO2 interacts with the first two SH3 domains of NCK (Fan et al., 2012). PINCH is known to bind the third SH3 domains of NCK (Tu et

al., 1998), while Nephrin interacts with the SH2 domain of NCK at its C-terminus (Jones et al., 2006). Therefore it is very likely that ROBO2 can also form a complex with ILK through NCK.

### 3.3 Hypothesis

Podocyte-specific deletion of *Ilk* leads to the development of a thick and split GBM. The mechanism leading to this phenotype is unclear. ILK has been shown to play a role podocyte adhesion and actin polymerization. We and others have shown that the Slit2/Robo2 signaling can destabilize cell adhesion and reduce actin polymerization. Our preliminary data also demonstrated that loss of *Robo2* in the podocytes has a renoprotective effect from glomerular injury. In addition, both ILK and ROBO2 form complexes with podocyte protein nephrin through the adaptor protein NCK, and loss of *Robo2* can alleviate the abnormal podocyte phenotype in nephrin knockout mice. Therefore, we hypothesized that ROBO2 and ILK form a protein complex, which impacts podocyte attachment and glomerular basement membrane integrity.

### 3.4 Materials and Methods

#### 3.4.1 Biochemical analysis of protein-protein interaction and complex formation

Cell culture, His-tagged protein coprecipitation, and immunoprecipitation were performed as previously described (Fan et al., 2003). Briefly, HEK cells were transfected with either a His-and Myc-tagged full length Robo2 construct or a His-and Myc-tagged mutant Robo2 construct without the NCK binding site ( $\Delta$ NBD). ROBO2 was then pulled down with Ni-NTA beads and run in a Western gel. The gel was then immune-labeled with antibodies against MYC, NCK, PINCH and ILK. The DupLEX-A yeast two-hybrid system (OriGene Tech) was used to characterize ROBO2, ILK, PINCH and NCK1 interaction according to manufacturer's instructions (these experiments were performed by Dr. Xueping Fan).

#### 3.4.2 Mice strains

The generation and genotyping of *Robo2*<sup>flox/flox</sup> and *Ilk*<sup>flox/flox</sup> mice conditional allele were described previously (Lu et al., 2007b; Terpstra et al., 2003). *Ilk*<sup>flox/flox</sup> mice were kindly provided by Dr. Kenn Albrecht. *Pod-Cre* mice harboring the p2.5P-Cre transgene under the regulation of a fragment of the human *NPHS2* promoter were purchased from the Jackson laboratories (Strain name: B6.Cg-Tg(*NPHS2*-cre)295Lbh/J,

Stock number: 008205) (Illustrations 3.2). Animal protocols were approved by the Institutional Animal Care and Use Committee (IACUC) at Boston University Medical Campus (#14388).

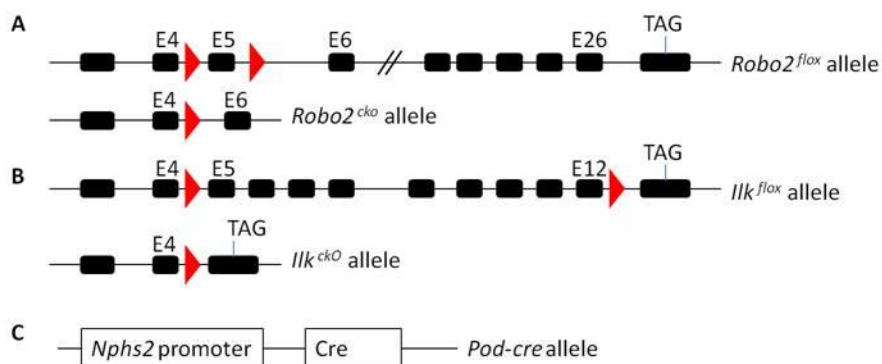


**Illustration 3.2: Alleles used to analyze genetic interaction between ILK and ROBO2 in the podocytes.**

- (A) Representation of the *Robo2* gene with the LoxP sites around exon 5 (red triangles). The Cre-recombinase creates an allele that undergoes nonsense mediated decay.
- (B) Representation of the *Ilk* gene with the LoxP sites between exons 4 and 5 and after exon 12 (red triangles). The Cre-recombinase creates an allele that undergoes nonsense mediated decay.
- (C) Illustration of the Cre-recombinase under the promoter of the podocin gene (*Nphs2*)

### *3.4.3 Mouse DNA extraction and genotyping*

Mice were genotyped from tail samples. DNA was extracted using hotshot NaOH method as previously described (Truett et al., 2000). All genotyping were performed using PCR method on a thermal cycler (MyCycler, BioRad).

### *3.4.4 Tissue collection and preparation*

The mouse kidneys at defined ages were dissected and either fixed overnight in 4% paraformaldehyde for the histology analysis, or in EM fixatives for electron microscopy analysis. For histological analysis, the samples were then washed 2 times in 1xPBS on ice and preserved in 70% EtOH until they were processed for paraffin embedding. Serial 4-7 um tissue sections were cut using a MT-920 microtome (Microm).

### *3.4.5 Ultrastructural analysis of the glomeruli*

For transmission electron microscopy, kidneys were fixed in EM fixatives containing 2% glutaraldehyde in 0.15 M sodium cacodylate, dehydrated in graded ethanol, embedded in Epon, sectioned, and stained with uranyl acetate and lead citrate. Ultrathin kidney sections were examined using a JEM-1011 electron microscope. For

scanning electron microscopy, kidneys were prepared following the standard protocol. The EM imaging was performed by Anna Pisarek-Horowitz.

#### *3.4.6 Survival analysis*

The survival rates were analyzed using the Epi Info<sup>TM</sup> software (CDC, <http://wwwn.cdc.gov/epiinfo/>) and the SPSS software.

#### *3.4.7 Urine protein analysis*

Urine protein excretion was detected by SDS-PAGE followed by Coomassie blue staining and quantified using ImageJ. ELISA for nephrin levels in the urine was performed (by Dr. Sudhir Kumar) using a commercial ELISA kit from Exocell (Cat #1019).

#### *3.4.8 Histological analysis*

Paraffin embedded kidney sections were stained by hematoxylin and eosin and visualized with a Nikon or Olympus light microscope.

## 3.5 Results

### *3.5.1 ILK and ROBO2 form a protein complex through PINCH and NCK*

We hypothesized that ROBO2 forms a complex with ILK. First, using yeast two-hybrid assay as previously described (Fan et al., 2012), we were able to confirm the interaction between ILK and PINCH, as well as between PINCH and NCK. However, no direct interaction was detected between ROBO2 and ILK or PINCH, nor between ILK and NCK either (Figure 3.1A).

We then performed co-immunoprecipitation assays to test whether ROBO2 and ILK form a complex mediated by PINCH and NCK. Since we previously identified the NCK binding site in ROBO2 intracellular domain (Fan et al., 2012), we generated a ROBO2 construct (His-myc-Robo2- $\Delta$ NBD) that does not have the NCK binding domain as a negative control. Pull-down of His-myc-Robo2, but not of His-myc-Robo2- $\Delta$ NBD, from the HEK cell lysates with Ni-NTA beads coprecipitated NCK, PINCH and ILK (Figure 3.1B). These data suggest that ROBO2 form a complex with ILK through NCK and PINCH (Figure 3.1C).



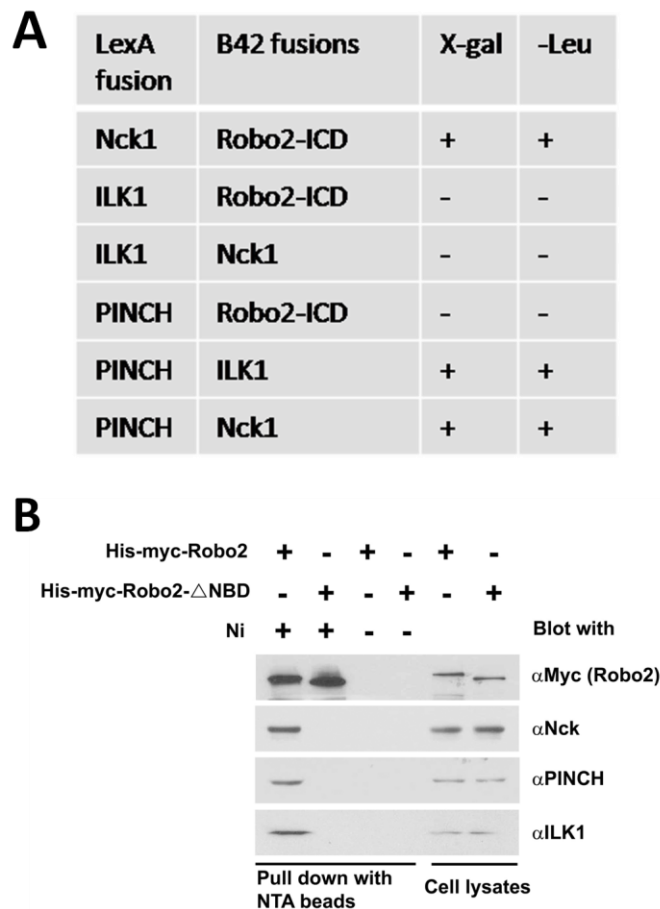
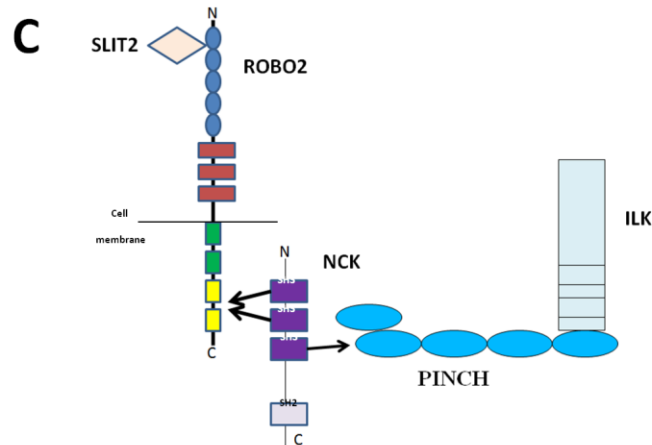


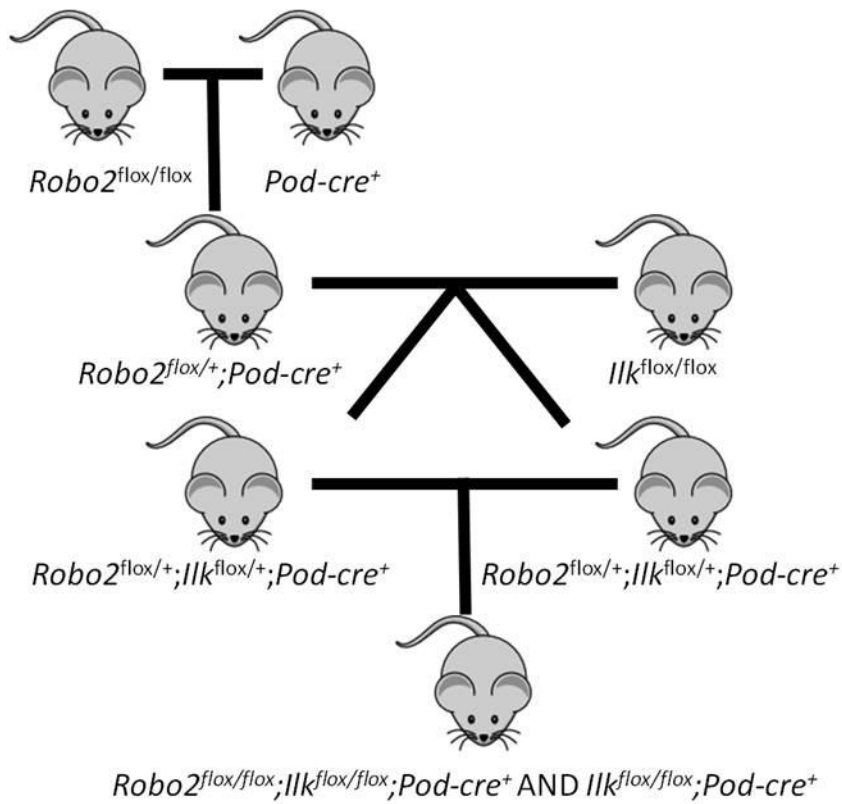
**Figure 3.1: Robo2 and Ilk form a protein complex through Nck and Pinch.**

(A) Yeast two-hybrid assay shows direct protein interactions between Robo2-ICD and Nck1; Nck1 and PINCH; PINCH and ILK1. ICD: intracellular domain. X-gal: *LacZ* reporter; -Leu: Leucine reporter; +, yeast grew; -, yeast did not grow. (B) Co-precipitation assay shows His-Myc tagged Robo2 forms protein complex with Nck, PINCH and ILK1. This protein complex is mediated by Nck as His-myc-Robo2- $\Delta$ NBD (delete Nck binding domain) does not pull down Nck, PINCH and ILK1. (C) A model of Robo2-Nck-Pinch-Ilk protein complex in podocytes.



### 3.5.2 Generation of *Robo2-Ilk* double conditional knockout mice

In order to determine if there is a genetic interaction between *Robo2* and *Ilk* in the podocytes, we generated *Robo2-Ilk* double knockout mice. Since the both *Ilk* and *Robo2* germline knockout mice are not viable after birth (Sakai et al., 2003) (Grieshammer et al., 2004; Lu et al., 2007b), we generated podocyte-specific conditional knockout mice with the podocin-cre transgene allele (*Pod-cre*) (Moeller et al., 2003) following the breeding scheme in Illustration 3.3. The mice were followed up for up to one year. A subset of the mice was euthanized at 2, 4 and 6 weeks of age which enable histological and ultrastructural analysis (Table 3.1).



### Illustrations 3.3: Generation of the $Robo2^{flox/+};Ilk1^{flox/+};Pod-cre^+$ mice

Illustration of the mice breeding scheme introducing three alleles ( $Ilk^{flox}$ ,  $Robo2^{flox}$  and  $Pod-cre^+$ ) in the same mice.

**Table 3.1: Number of mice analyzed for phenotype and survival studies in *Ilk* and *Robo2* cKO mice**

Genotype	2 weeks old	4 weeks old	6 weeks old	survival
<i>Ilk<sup>fllox/fllox</sup>;Robo2<sup>+/+</sup>;Pod-cre<sup>+</sup></i>	3	22	18	39
<i>Ilk<sup>+/+</sup>;Robo2<sup>fllox/fllox</sup>;Pod-cre<sup>+</sup></i>		10	6	
<i>Ilk<sup>fllox/fllox</sup>;Robo2<sup>fllox/fllox</sup>;Pod-cre<sup>+</sup></i>	5	19	10	47
<i>Ilk<sup>+/+</sup>;Robo2<sup>+/+</sup>;Pod-cre<sup>+</sup></i> Or no <i>Pod-cre</i> allele	11	14	14	

### 3.5.3 Loss of *Robo2* improves the podocyte ultrastructure of 4 weeks old *Ilk* cKO mice

We first analyzed the podocyte ultrastructure using scanning electron microscopy in the kidneys of 2 weeks old knockout mice. 1/3 (33%) *Ilk* single cKO mice and 1/3 (33%) *Robo2-Ilk* double cKO (dKO) mice displayed visible foot process abnormalities in comparison to *Robo2* single cKO mice and wild-type controls that did not displayed any abnormalities (Figure 3.2). None of the 2 weeks old knockout mice developed proteinuria.

We then analyzed the mice at 4 and 6 weeks of age as all *Ilk* single cKO mice developed severe proteinuria. At 4 weeks old, while 3/3 (100%) *Ilk* single cKO mice exhibited no interdigitating foot processes by scanning electron microscopy, one *Robo2-Ilk* DKO mouse displayed visible interdigitating foot processes (Figure 3.3), suggesting partial rescue of podocyte foot process defects.

However, at 6 weeks of age, both *Ilk* cKO and *Robo2-Ilk* DKO exhibited similar severe podocyte defects without normal interdigitating foot processes (Figure 3.4). These results suggest that loss of *Robo2* can only rescue podocyte foot process defects at early stage in young *Ilk* knockout mice.

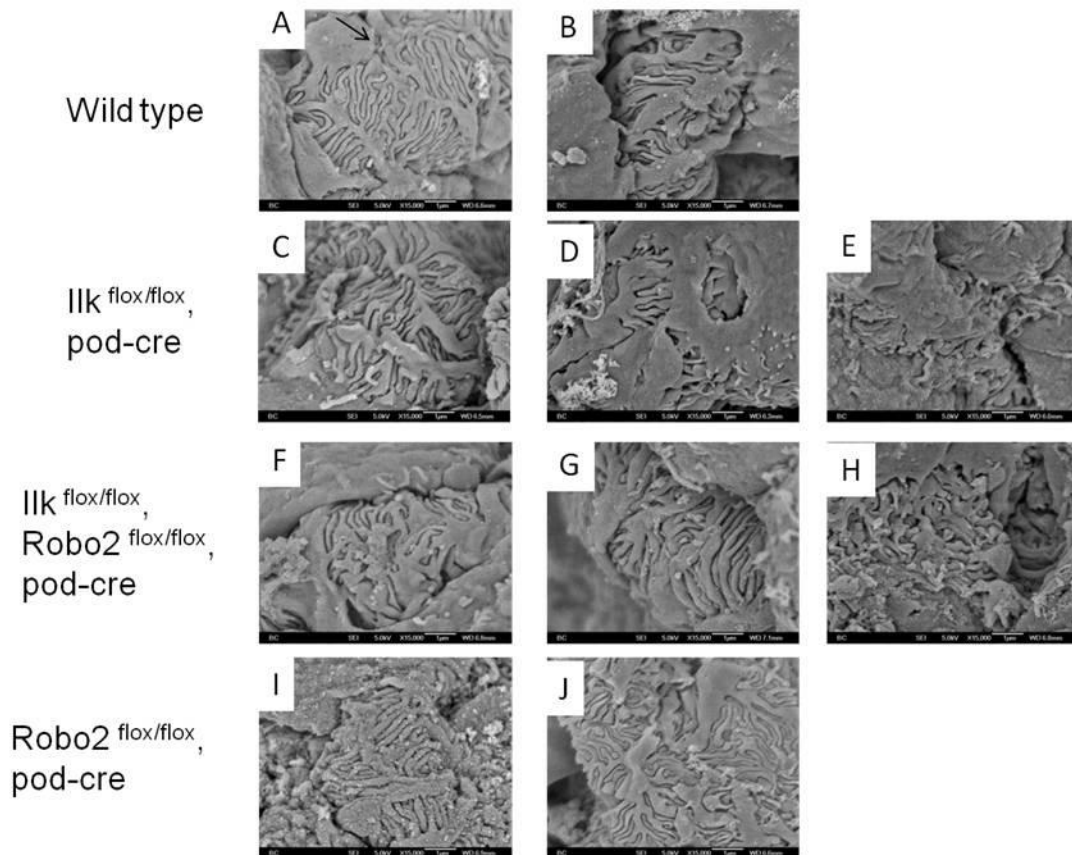


**Figure 3.2: Podocyte ultrastructure (SEM) in 2 weeks old *Ilk* and *Robo2* cKO mice**

Representative images of 2 weeks old kidneys show interdigitating foot processes in wild-type (n=2) (A, B), *Ilk* cKO (n=3) (C-E), *Ilk-Robo2* DKO (n=3) (F-H) and *Robo2* cKO mice (n=2) (I, J). All the images are obtained from scanning electron microscopy at a 15,000x magnification. Each image was taken from a different mouse.

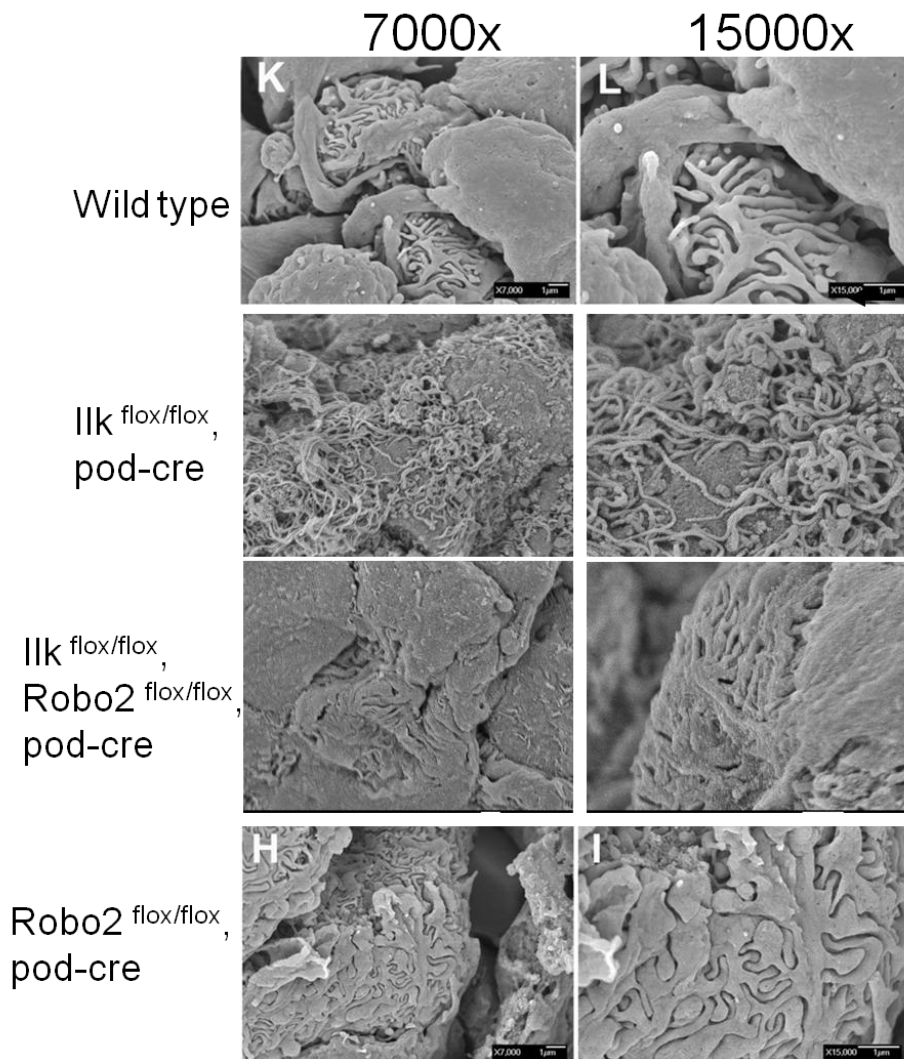


**Figure 3.3: Loss of Robo2 improves the podocyte ultrastructure of the 4 weeks old  $Ilk^{flox/flox};Pod-cre^{+}$  mice.**

(A-D) Representative images of scanning electron microscopy at 7000x magnification in 4 weeks old mouse kidneys show podocyte foot process structure in (A) wild-type, (B) *Ilk* single cKO (n=3), (C) *Robo2-Ilk* DKO (n=1), and (D) *Robo2* single cKO mice. (E-H) High 15000x magnification images of (A -D) show podocyte foot process structure. The foot processes in the *Ilk* cKO are not visible because of the abnormal long cellular protrusions or microvilli (B and F). Both *Ilk* single cKO and *Robo2-Ilk* DKO mice had severe proteinuria at 4 weeks old.

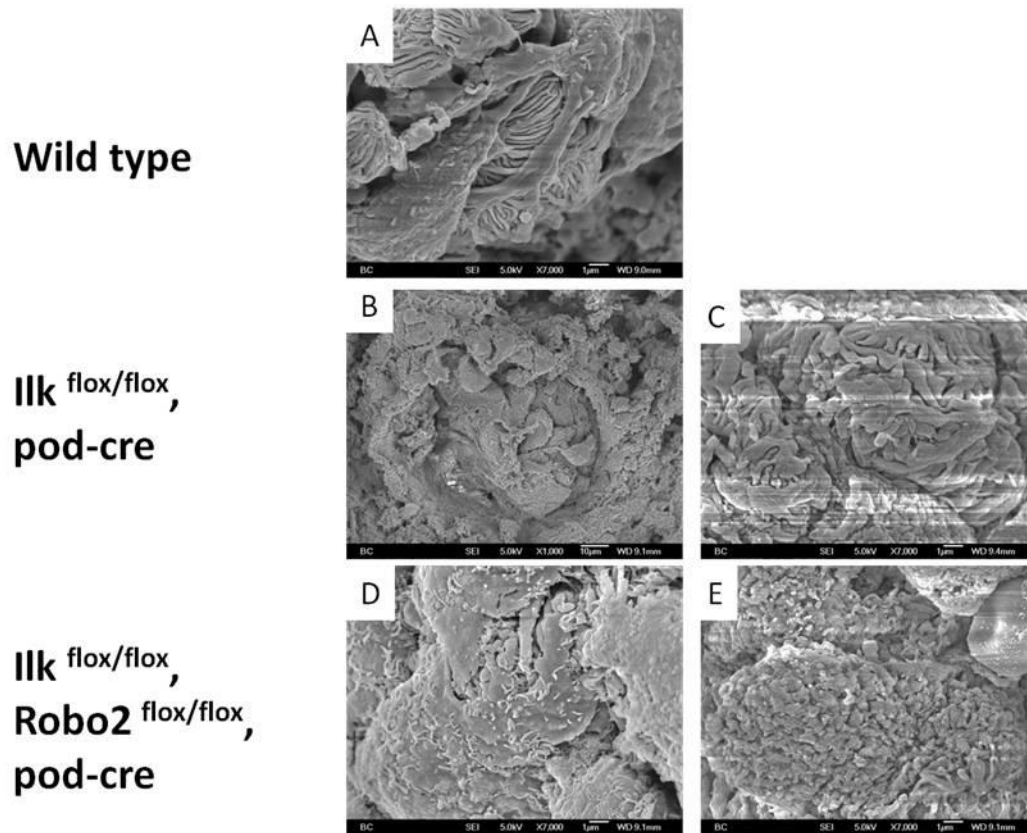


**Figure 3.4: Podocyte ultrastructure (SEM) in 6 weeks old *Ilk* and *Robo2* cKO mice**

Representative images of 6 weeks old kidneys show interdigitating foot processes in wild-type (n=1) (A), *Ilk* cKO (n=2) (B, C), DKO (n=2) (D, E). All the images are obtained from scanning electron microscopy at a 7,000x magnification. Each image was taken from a different mouse.

*3.5.4 Loss of Robo2 alleviates the thickening and splitting phenotype of the glomerular basement membrane in young Ilk knockout mice*

Previous studies show that podocyte-specific *Ilk* deletion leads to GBM thickening and splitting (Dai et al., 2006; El-Aouni et al., 2006). We performed transmission electron microscopy (TEM) analysis of *Ilk* knockout mice and found the same GBM thickening and splitting phenotype in 4 weeks old *Ilk* single cKO mice (Figure 3.5). Interestingly, the GBM width of the *Ilk*-*Robo2* double knockout mice decreased without obvious GBM splitting phenotype compared to the littermate *Ilk* single cKO mice (Figure 3.5). These data suggest that loss of *Robo2* alleviates the thickening and splitting phenotype of the GBM in young *Ilk* knockout mice.



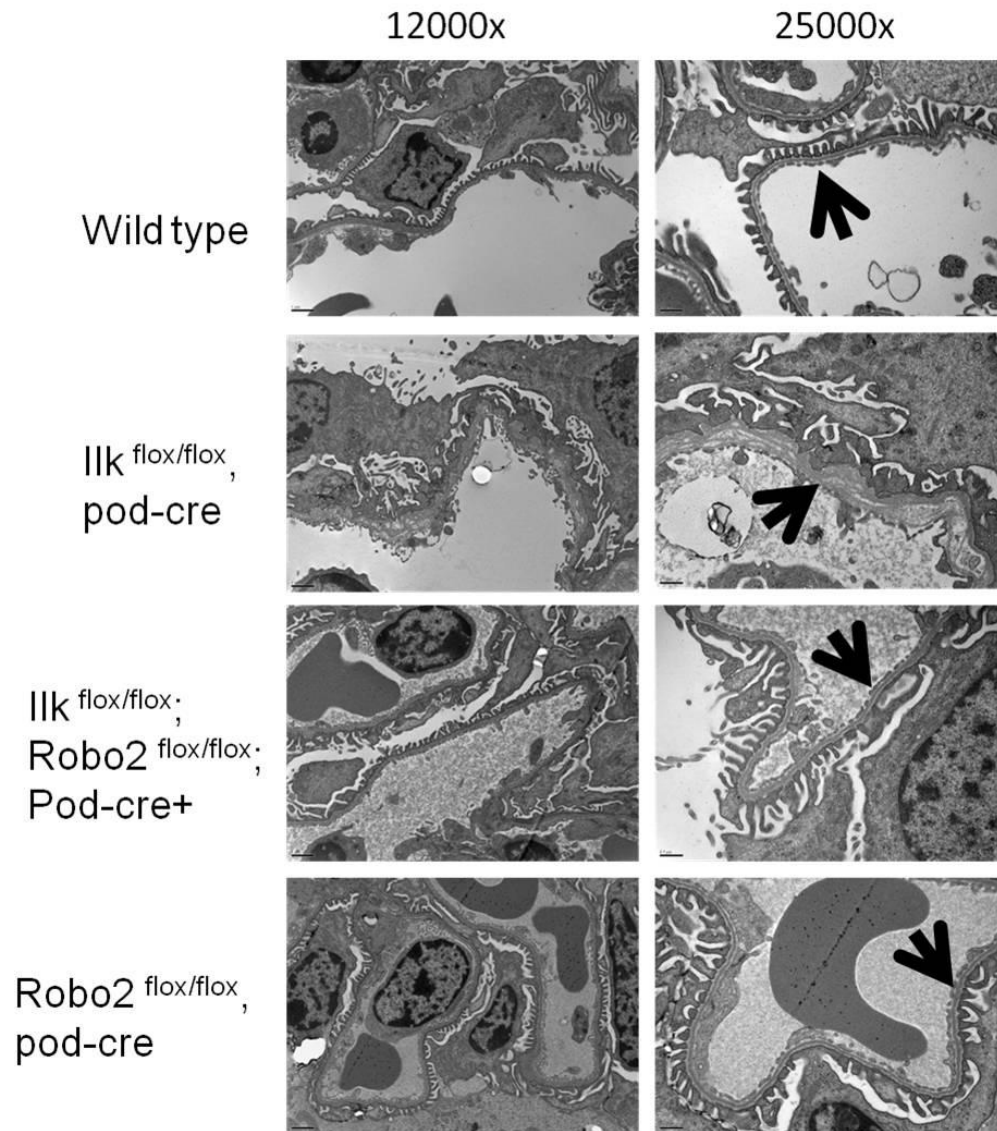


**Figure 3.5: Loss of *Robo2* decreases GBM thickening and splitting in 4 weeks old *Ilk*<sup>flx/flx</sup>;*Pod-cre*<sup>+</sup> single cKO mice.**

Transmission electron micrographs of 4 weeks old mouse glomeruli show abnormal irregular GBM thickening and splitting with electron-lucent areas (arrow) in *Ilk*<sup>flx/flx</sup>;*Pod-cre*<sup>+</sup> single cKO (n=2), while the GBM in *Ilk*<sup>flx/flx</sup>;*Robo2*<sup>flx/flx</sup>;*Pod-cre*<sup>+</sup> double knockout mice (n=2) show relatively normal thickness without GBM splitting phenotype (arrows). Mouse genotype and TEM magnifications are shown.

### 3.5.5 Loss of *Robo2* increases the median survival of *Ilk* cKO mice

To determine if loss of *Robo2* would affect the life span of *Ilk* cKO mice, we analyzed the survival of the *Ilk* cKO mice and the *Ilk-Robo2* DKO mice up to one year old. An intermediate analysis was performed when the first mice reached one year old. At this point, the survival of 21 *Ilk*<sup>flox/flox</sup>;*Robo2*<sup>flox/flox</sup>;*Pod-cre*<sup>+</sup> DKO mice and 23 *Ilk*<sup>flox/flox</sup>;*Pod-cre*<sup>+</sup> single cKO mice were analyzed. The Kaplan-Meier analysis showed that the *Ilk-Robo2* DKO survived significantly longer than the *Ilk* single cKO ( $p < 0.05$  Wilcoxon test,  $p = 0.0662$  Log-Rank test) (Figure 3.6 and Table 3.2).

To increase the power of survival analysis, we doubled the number of mice in each group and followed them up to one year. After Kaplan-Meier survival analysis, I found that 24 of the 47 (50%) *Ilk-Robo2* DKO mice survived more than 161 days while 20 of the 39 (50%) *Ilk* single cKO mice died due to renal failure by the age of 106 days (Figure 3.7A). This result indicated that loss of *Robo2* extended the median survival from 106 days in *Ilk* single knockout mice to 161 days in *Ilk-Robo2* podocyte-specific double knockout mice, a gain of 50% of life span (Figure 3.7B).

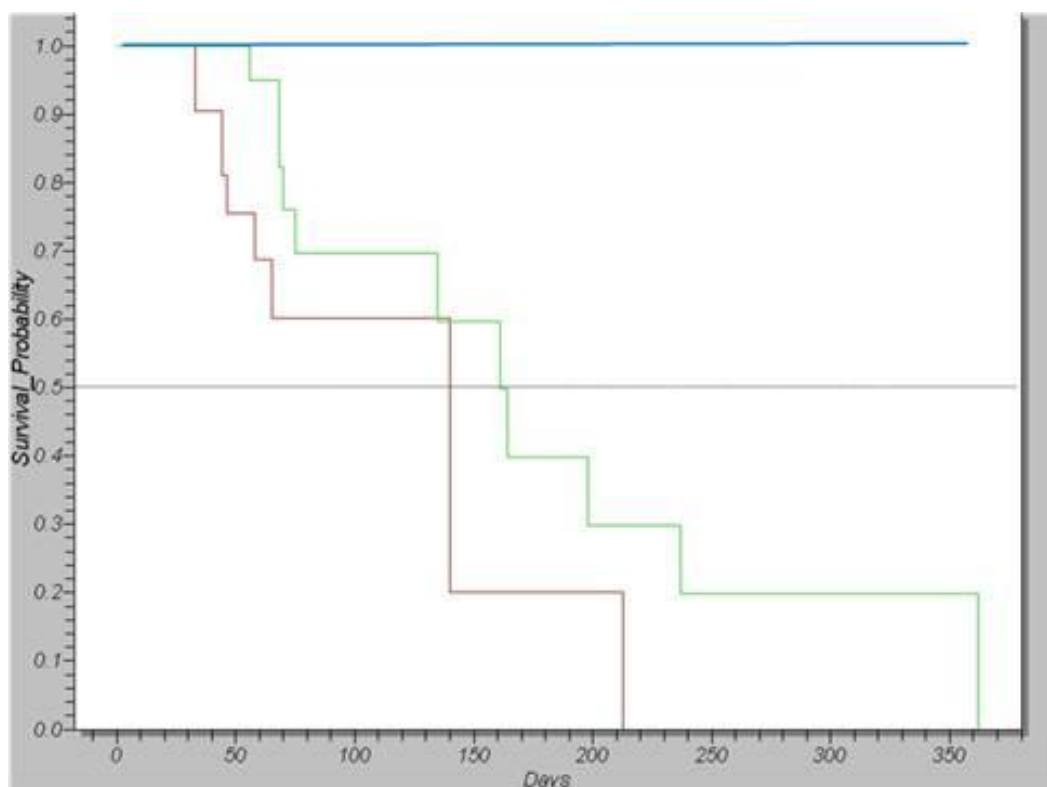


**Figure 3.6: Intermediate analysis of survival showed that loss of *Robo2* improves the survival of *Ilk* cKO Mice.**

Kaplan-Meyer analysis of the first group of mice followed up to one year showed that the *Ilk<sup>flox/flox</sup>;Robo2<sup>flox/flox</sup>;Pod-cre<sup>+</sup>* DKO (n=21 mice, green) lived longer than the *Ilk<sup>flox/flox</sup>;Pod-cre<sup>+</sup>* single cKO (n=23 mice, red).

**Table 3.2: Statistical analysis of the survival in the first set of mice (n>20)**

Test	Statistic	D.F.	P-Value
Log-Rank	3.3743	1	0.0662
Wilcoxon	4.7571	1	0.0292

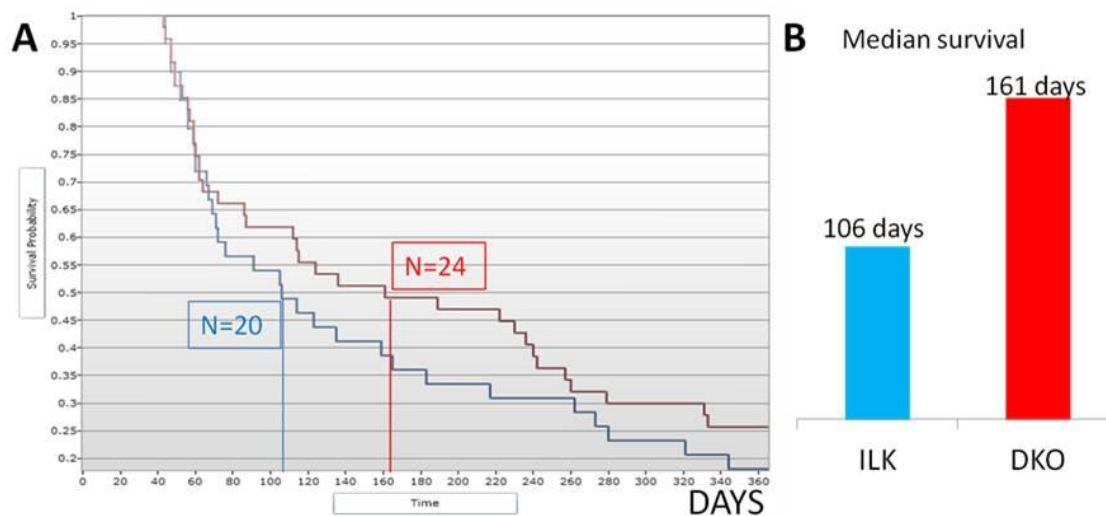


**Figure 3.7: Loss of *Robo2* improves the median survival of podocyte-specific single *Ilk* knockout mice.**

(A) Kaplan-Meier survival analysis of all the mice followed up to one year showed that 24 out of total 47 (50%) *Ilk<sup>fllox/fllox</sup>;Robo2<sup>fllox/fllox</sup>;Pod-cre<sup>+</sup>* DKO (red line) lived to 161 days while 20 out of total 39 (50%) *Ilk<sup>fllox/fllox</sup>;Pod-cre<sup>+</sup>* single cKO (blue line) lived to only 106 days. (B) The comparison of median survival of 106 days in the *Ilk<sup>fllox/fllox</sup>;Pod-cre<sup>+</sup>* single cKO mice (ILK blue bar) and 161 days in the *Ilk<sup>fllox/fllox</sup>;Robo2<sup>fllox/fllox</sup>;Pod-cre<sup>+</sup>* DKO mice, a gain of 50% life span.

### 3.5.6 Loss of *Robo2* did not significantly affect proteinuria prevalence and renal histology in 4-6 weeks old *Ilk* podocyte-specific knockout mice

To determine if loss of *Robo2* would improve the proteinuria phenotype in the *Ilk* single cKO, I analyzed the proteinuria prevalence in *Ilk* single cKO and *Ilk-Robo2* DKO mice at 4 weeks and 6 weeks old by visualizing the presence of albumin in the urine. At 4 weeks old, while 25/32 (72%) *Ilk* single cKO mice developed proteinuria, 20/29 (62%) *Ilk-Robo2* DKO mice also had similar amount of albumin in the urine. At 6 weeks, 13/20

(65%) of *Ilk* single cKO mice and 14/17 (82%) of *Ilk-Robo2* DKO mice developed proteinuria (Figure 3.8). Consistent with these results, renal histology analysis revealed that similar amounts of proteinaceous casts were observed in both *Ilk* single cKO and *Ilk-Robo2* DKO at 4 weeks and 6 weeks old (data not shown). Taken together, these findings suggest that loss of *Robo2* did not significantly affect the proteinuria prevalence and renal histology in 4-6 weeks old *Ilk* podocyte-specific knockout mice.

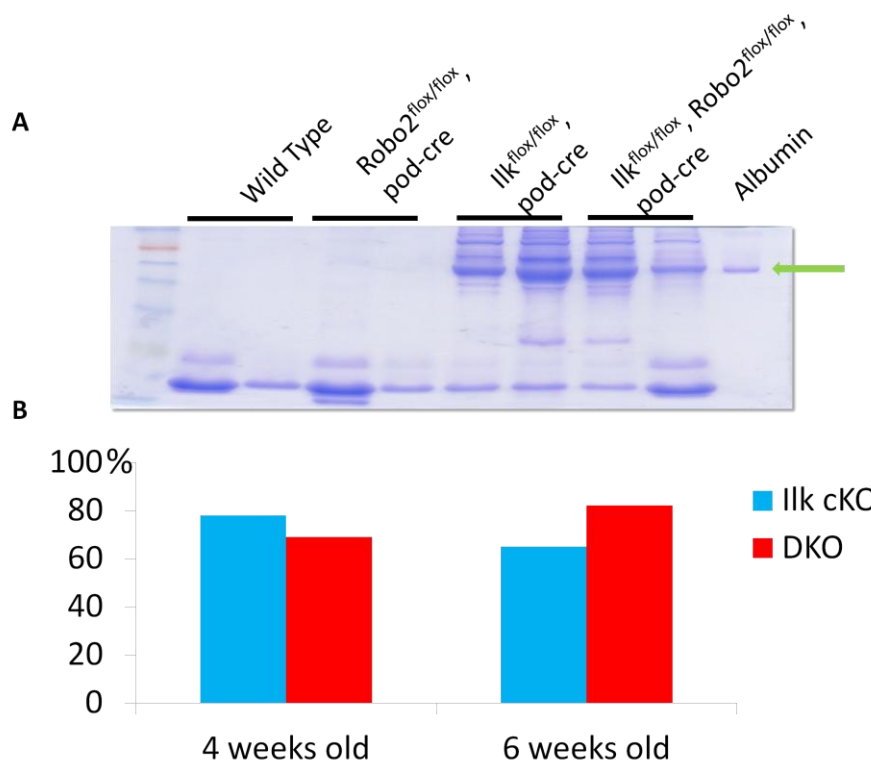


**Figure 3.8: No significant difference in proteinuria between the *Ilk-Robo2* DKO mice and the *Ilk* single cKO mice at 4 weeks.**

(A) Both *Ilk-Robo2* DKO and *Ilk* single cKO mice developed proteinuria at 4 weeks. The proteinuria was assessed by detecting urine albumin on SDS page gel and visualized by Coomassie blue staining. 1ul urine was loaded in each lane. (B) Each sample was scored as positive or negative (with or without proteinuria). No difference of proteinuria prevalence was observed at 4 weeks and 6 weeks between the  $Ilk^{fllox/fllox};Robo2^{fllox/fllox};Pod-cre^+$  double cKO mice (DKO, red, n=29 at 4 weeks and n=17 at 6 weeks) and the  $Ilk^{fllox/fllox};Pod-cre^+$  single cKO mice (Ilk cKO, blue, n=32 at 4 weeks, n=20 at 6 weeks).

### 3.5.7 Loss of *Robo2* does not affect the podocyte loss phenotype in 4 weeks old *Ilk* podocyte-specific knockout mice

*Ilk* single cKO mice have been reported to have podocyte loss (Dai et al., 2006).

To determine if loss of *Robo2* would affect the podocyte loss phenotype in the *Ilk* cKO

mice, we measured the levels of nephrin in the urine as a biomarker for podocyte loss. Preliminary analysis of nephrin levels in the urine from four 4-week old mice with proteinuria did not reveal any difference between the *Ilk* single cKO and the *Ilk-Robo2* DKO mice (data not shown). This finding suggests that loss of *Robo2* does not affect the podocyte loss phenotype in 4 weeks old *Ilk* podocyte-specific knockout mice.

### 3.6 Discussion

In this project, we found that ROBO2 forms a complex with ILK through NCK and PINCH, supporting an indirect physical interaction between ROBO2 and ILK in vitro. We then investigated the genetic interaction between ILK and ROBO2 in vivo using podocyte-specific knockout mice of both genes. Our animal model studies revealed that loss of *Robo2* improved the survival of the *Ilk* cKO mice, although the statistical significance was obvious only in a sub-group of animals between 10-35 weeks old. At the ultrastructural level, loss of *Robo2* in the podocytes alleviates the foot processes and GBM phenotype in 4 weeks old *Ilk* cKO mice. However, more samples and quantification are needed to confirm this finding. Although no clear difference of proteinuria and renal histology were found between the *Ilk* cKO and *Ilk-Robo2* DKO, our findings suggest that loss of *Robo2* alleviates the phenotype of the *Ilk* cKO mice.

### 3.6.1 Loss of *Robo2* improved the survival of the *Ilk* single cKO

Despite the large variability in the phenotype of the *Ilk* cKO mice, the median survival of the mice was 50% longer in *Ilk-Robo2* double knockout mice as compared to *Ilk* single knockout mice. This result supports a genetic interaction between ILK and ROBO2. Consistent with this finding, SLIT, ROBO ligand, has also been reported to genetically interact with ILK in *Drosophila* (MacMullin and Jacobs, 2006).

Alleviation of a phenotype in animals, in which the double-mutant phenotype is less severe than expected, often reflects that the proteins of interest act within the same pathway (Mani et al., 2008). We also found that ROBO2 and ILK can form a protein complex in vitro, which depends on the NCK-binding-site in the ROBO2 intracellular domain, further supporting the possibility that ILK and ROBO2 act within the same pathway. We may refer to the phenotype of the *Ilk-Robo2* DKO mice as a partial suppression of the *Ilk* single cKO phenotype (St Onge et al., 2007). It indicates that the deleterious effect of loss of ILK in the podocytes is partially due to the presence of ROBO2.

### 3.6.2 Loss of *ROBO2* improves the GBM phenotype of the *Ilk* cKO mice.

In addition to the survival benefit, the partial rescue of the *Ilk* cKO phenotype by the deletion of *Robo2* was also observed in the glomeruli at the ultrastructural level. At 4 weeks, loss of *Robo2* in the podocytes alleviated the GBM thickening and splitting



phenotype of *Ilk* cKO mice. Because we obtained these data with limited numbers of mice, additional studies on more kidney samples together with GBM width quantification are needed to confirm this GBM finding. Nonetheless, this alleviation of the GBM phenotype suggests that ROBO2 plays a role in the GBM phenotype of the *Ilk* cKO mice. Deletion of ILK in the podocytes may affect the GBM by decreasing podocytes adhesion to the GBM and by affecting the secretion of the extracellular matrix proteins. ROBO2 may also play a role in both processes.

### *3.6.3 Loss of ROBO2 improve the life span of the Ilk cKO mice*

Although the median survival of *Ilk-Robo2* DKO is 50% longer than the *Ilk* single cKO, we did not observe any survival advantage in *Ilk-Robo2* DKO in the first 10 weeks of life, and the survival analysis for the entire one year period using the Wilcoxon and the Log-Rank tests did not reach a statistical significance (Figure 3.7). One of the reasons for the lack of statistical difference is the wide variability in the phenotype of both the *Ilk* single cKO mice and the *Ilk-Robo2* DKO mice. The effect of *Ilk* deletion in the podocyte ranges from severe lethal phenotype (e.g. renal failure at 6 weeks old) to relative milder renal phenotype (e.g. no proteinuria at one-year old). This difference probably due to the mixed genetic background used in this study. The mice that died before the age of 10 weeks probably carried genetic variants that increased the severity of the *Ilk* deletion, while the mice that survived more than 35 weeks probably carried genetic variants attenuating the deleterious effect of lack of *Ilk* in the podocytes. Genomic comparison

between the mice surviving less than 10 weeks and those surviving more than 35 weeks may reveal important modifying genes in podocytopathies. Interestingly, sub-group analysis of mice that survived between 10 and 35 weeks showed that the life span of *Ilk-Robo2* DKO mice was significantly improved when compared to *Ilk* single cKO mice (Log Rank p-value<0.05; data not shown), suggesting that, in addition to podocyte foot process and GBM structure, loss of *Robo2* did alleviate *Ilk* knockout phenotype even when hard outcome such like survival is used as the endpoint.

*3.6.4 ILK and ROBO2 may have opposite effects on cytoskeleton remodeling, cell adhesion and glomerular basement membrane composition*

***Actin cytoskeleton remodeling***

The partial suppression of the *Ilk* single cKO phenotype by the deletion of *Robo2* may be related to their opposite roles in actin cytoskeleton remodeling. As described earlier, the podocyte cytoskeleton remodeling is a key factor in normal kidney function (Schell et al., 2013).

While ILK signaling has been shown to increase N-WASp-mediated actin polymerization (Zhang et al., 2007), Slit/Robo signaling can decrease N-WASp-mediated actin polymerization (Wong et al., 2001). Since ILK also forms a complex with nephrin (Dai et al., 2006), it may prevent ROBO2 inhibition of nephrin-mediated actin polymerization and thereby counterbalance ROBO2 activity.

### ***Cell adhesion***

Proper adhesion of the podocytes to the GBM is needed for the maintenance of the GBM structure as suggested by the phenotype of the mice lacking integrins. Both ILK and ROBO2 have been shown to affect cell adhesion. The assembly of a complex involving ILK and PINCH is important in the formation of cell-matrix adhesion sites (Zhang et al., 2002), while Slit/Robo activation inhibits cell adhesion (Rhee et al., 2002). The opposite roles of ILK and ROBO2 on cell adhesion further indicate that they can balance each other's activities. Therefore, deletion of *Robo2* in the *Ilk* deficient podocytes may partially restore the adhesion of the podocytes to the GBM because a new balance on cell adhesion signaling is reached (Illustration 3.4).

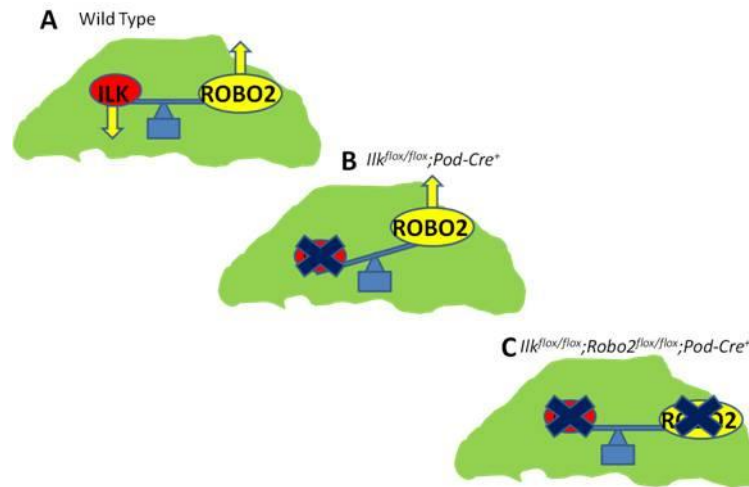


**Illustration 3.4: ILK and ROBO2 have opposite roles on podocyte structure and function.**

(A) ILK and ROBO2 have opposite roles both on cell adhesion and on actin cytoskeleton regulation. (A) The podocyte (in green color), expresses both ILK (red) and ROBO2 (yellow), which reach a balance on cell adhesion and actin cytoskeleton regulation. (B) In the *Ilk<sup>flox/flox</sup>;Pod-Cre<sup>+</sup>* podocytes, active Slit2/Robo2 signaling leads to more detachment and less active polymerization in the podocytes, resulting in foot process effacement. (C) In the absence of both ILK and ROBO2 (i.e. double knockouts), both opposing roles are lacking and a new balance is reached in the podocytes, enabling less detachment and better actin cytoskeleton structures.

***Basement membrane modeling***

In other organ systems, ILK was shown to mediate the regulation of basal lamina formation and collagen's secretion (Cammag et al., 2012; Niewmierzycka et al., 2005) (Teo et al., 2014). Changes in the GBM composition may activate ROBO2, which may have deleterious effects (Fan et al., 2012). The possible role of the Slit/Robo signaling on GBM formation or maintenance has to be further investigated.

### 3.7 Limitations

Regarding the genetic interaction analysis, the *Ilk* single cKO mice have a very heterogeneous phenotype in terms of severity of podocyte defects and life span (Dai et al., 2006; El-Aouni et al., 2006; Kanasaki et al., 2008). In this study, some of the *Ilk* single cKO mice survived up to a year without kidney failure, suggesting the role of modifier genes protecting the podocytes from the loss of ILK. ROBO2 might be one of these modifiers and its absence can further affect the phenotype in the *Ilk* cKO mice. The heterogeneity in the phenotype of the *Ilk* cKO mice may hamper the data analyses in this project as normal phenotype in *Ilk-Robo2* DKO mice could be associated with a genetic background that alleviates the effect of the ILK deletion in the podocytes. Future experiments on backcross of *Ilk* and *Robo2* KO mice into a congenic mouse strain with the same genetic background may address this limitation.

#### ***Albuminuria as a marker of kidney function***

The validity of using albuminuria as a surrogate marker for kidney function has been controversial (Levey et al., 2009). We did not find a reduced prevalence of proteinuria in the *Ilk-Robo2* DKO mice when compared to *Ilk* single cKO mice, despite an improvement in podocyte ultrastructure and survival. This discrepancy between the two observations may reflect the heterogeneity of the phenotypes as well as the lack of

sensitivity of the proteinuria analysis, as detected with Coomassie Blue staining. In order to assess its prognostic value, a sensitive proteinuria assay and a large number of urine samples are needed. We have collected all the urine samples from mice that were followed for survival analysis during the course of this project. A retrospective analysis of albuminuria using a sensitive ELISA assay on these collected urine samples may uncover its predictive value.

### ***Renal Histology***

Because of the high variability of phenotype in the *Ilk* cKO mice, and the inability to determine whether a 4 weeks old mouse would develop a severe course of disease or a relatively minor disorder, I analyzed the renal histology only in four weeks old mice with proteinuria. These mice probably represent a biased group of mice with the more severe renal phenotype as no survival benefit of *Ilk-Robo2* DKO was observed in the first 10 weeks of life compared to the *Ilk* single cKO. Together with the limited sensitivity of H&E histology analysis, we may consider to select mice between 10-35 weeks old in order to detect a difference on renal histology. In addition, a counting of the podocyte number may represent a more sensitive approach to identify differences between the *Ilk* single cKO and the *Ilk-Robo2* DKO mice.

### 3.8 Conclusions

Our results in this project suggest that ROBO2 and ILK form a protein complex through NCK and PINCH in podocytes. Loss of *Robo2* improves the podocyte and GBM ultrastructure and the survival of *Ilk* podocyte-specific knockout mice. The possible improvement of GBM thickening and splitting phenotype in the *Ilk*-*Robo2* DKO mice as compared to the *Ilk* single cKO mice may be explained by increased attachment of the podocytes to the GBM, differential cytoskeleton modeling and/or by a change in the expression of extracellular proteins. Further experiments are needed to examine these mechanisms. Together, our results suggest that ILK and ROBO2 act in a common pathway in the podocytes and loss of *Robo2* alleviates the glomerular phenotype of *Ilk* podocyte-specific knockout mice.

## **CHAPTER FOUR: SLIT2/ROBO2 signaling regulates extracellular matrix gene expression during early ureteric bud outgrowth**

### **4.1 Summary**

ROBO2 is the cell surface receptor for the repulsive guidance cue SLIT2. Mutations in *ROBO2* and *SLIT2* are associated with congenital anomalies of the kidney and urinary tract (CAKUT) in humans and mice. Previous studies show that ROBO2 is expressed in the metanephric mesenchyme (MM) and SLIT2 is expressed in the ureteric bud (UB), and SLIT2-ROBO2 signaling is required for early UB outgrowth in mice and restricts the UB to a single site on the Wolffian duct (WD). Mouse mutants without either *Slit2* or *Robo2* develop supernumerary UBs, abnormal ureterovesical junctions, multicystic dysplastic kidney, and die after birth from severe hydronephrosis and renal failure. However, the molecular mechanism of UB outgrowth defects in *Robo2* and *Slit2* knockout mice remains unknown.

To test the hypothesis that loss of SLIT2-ROBO2 signaling may affect the expression of genes that are important in controlling early UB outgrowth, we performed microarray gene expression analysis using Affymetrix GeneChip on early MM and UB tissues isolated from E10.5 and E11.5 *Robo2* and *Slit2* knockout mouse embryos.

Although we did not detect significant change in the mRNA expression of any single gene, Gene Set Enrichment Analysis (GSEA) revealed that the expression of several gene-sets, all related to the extracellular matrix (ECM) proteins, were down-regulated in E10.5 and E11.5 *Slit2* and *Robo2* knockout embryos as compared to their



wild type littermate controls. Specifically, Laminins and Collagens were significantly downregulated coordinately in the Slit2 and Robo2 knockout embryos. This result was further confirmed by the Ingenuity Pathway Analysis (IPA), a different analysis approach to identify the top canonical pathways and upstream regulators that are predicted to be associated with the dataset.

Our findings suggest that SLIT2-ROBO2 signaling may induce the expression of ECM genes in the MM during early UB outgrowth. This regulation of the ECM around the WD may prevent multiple ectopic UB formation. Further experiments are needed to confirm this novel finding.

## **4.2 Background and Introduction**

### *4.2.1 Ureteric bud outgrowth*

Development of the kidney and the ureter begins when an epithelial outpouching called ureteric bud (UB) sprouts from the caudal region of the Wolffian duct (also called mesonephric duct) and invades the adjacent metanephric mesenchyme (MM) (Illustration 4.1). This process is initiated around 4 weeks of gestation in human and at embryonic 10.5 days (E10.5) in mouse.

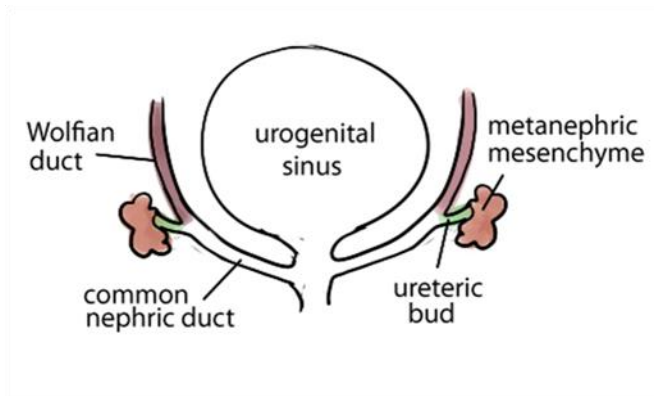


#### **Illustration 4.1: Ureteric bud outgrowth**

The ureteric bud in green grows out from the Wolffian duct into the metanephric mesenchyme (Rasouly and Lu, 2013).

The UB invasion into the MM is tightly controlled to prevent UB outgrowth defects such as ectopic ureteric buds, multiple ureteric buds or absence of budding (Dressler, 2009). Mutations in genes controlling early UB formation and positioning often cause congenital anomalies of the kidney and urinary tract (CAKUT) phenotypes, which include urinary obstruction, VUR, hydronephrosis, short duplex ureter, duplex kidney, ectopic and multicystic dysplastic kidney (MCDK) in both human and mouse (Table 4.1) (Airik and Kispert, 2007; Basson et al., 2005; Batourina et al., 2005; Grieshammer et al., 2004; Hains et al., 2010; Kume et al., 2000; Lu et al., 2007b; Lu et al., 2007c; Mackie et al., 1975; Mendelsohn, 2009; Miyazaki et al., 2000; Murawski and Gupta, 2006; Uetani and Bouchard, 2009; Wang et al., 2011).

**Table 4.1: Mutations in genes controlling early ureteric buds outgrowth in human and mouse**

Gene	Chr	Exp	Type of protein	Signaling	Human disease (OMIM)	Urinary tract defects in animal models	Ref
<i>LICAM</i>	Xq28	ue	Adhesion molecule			Ectopic UB, duplex ureters, megaureter, hydronephrosis	(Debiec et al., 2002)
<i>AGTR2</i>	Xq22-q23	um	G-protein coupled angiotensin II receptor	RAS	X-linked mental retardation-88 (OMIM 300852)	Ectopic UB, duplex ureters, hydroureter, hydronephrosis	(Nishimura et al., 1999)
<i>NFIA</i>	1p31.3-p31.2	ue, um	Nuclear Factor 1 transcription factor		Chromosome 1p32-p31 deletion syndrome (OMIM 613735)	duplex ureters, VUR, UPJ defects, hydroureter, hydronephrosis, megaureter	(Lu et al., 2007a)
<i>ROBO2</i>	3p12.3	mm	Slit receptor, Ig superfamily	Robo/Slit	Vesicoureteral reflux 2 (OMIM 610878)	Ectopic UB, multiple ureters, hydroureter, hydronephrosis	(Grieshammer et al., 2004; Lu et al., 2007b)
<i>SLIT2</i>	4p15.2	ue	Secreted protein -Robo ligand	Robo/Slit		Ectopic UB, multiple ureters, hydroureter, hydronephrosis	(Grieshammer et al., 2004)
<i>SCARB2</i>	4q21.1		glycoprotein			Kidney and ureter duplication, UPJ obstruction, hydroureter, and hydronephrosis	(Gamp et al., 2003)
<i>SPRY1</i>	4q28.1	wd, mm	Receptor Tyrosine Kinase antagonist	GDNF/RET		Ectopic UB, multiple ureters, hydroureter, hydronephrosis	(Basson et al., 2005)
<i>GGDNF</i>	5p13.2	mm	glial cell line-derived neurotrophic factor	GDNF/RET		Renal agenesis	(Sanchez et al., 1996)
<i>FOXC1</i>	6p25	um	Forkhead transcription factor	Foxc	Axenfeld-Rieger syndrome type 3 (OMIM 602482)	Ectopic UB, duplex ureters, hydroureter, hydronephrosis	(Kume et al., 2000; Weissschuh et al., 2008)
<i>Micro-deletion</i>	8p11.23-p11.22				Kallmann syndrome 2		(Levy and Knudtson, 1993)

<i>FGFR1</i>						(OMIM 147950): VUR and ureters duplication	
<i>GATA3</i>	10p15		Transcription factor	Wnt		Hypoparathyroidism-deafness-renal syndrome (OMIM 146255)	Ectopic UB, duplex kidneys, enlargement of the vas deferens, loss of uterus (Grote et al., 2008)
<i>RET</i>	10q11.21	wd	Receptor tyrosine kinase	GDNF/RET		Renal agenesis (OMIM 191830)	Renal agenesis (Schuchardt et al., 1994)
<i>PAX2</i>	10q24	wd, ue, mm	Transcription factor			Papillorrenal syndrome (OMIM 120330)	Caudal ureteric bud, reflux, hydroureter (Murawski et al., 2007)
<i>BMP4</i>	14q22-q23	um	Secreted molecule-TGF- $\beta$ family	TGF- $\beta$			Ectopic UB, duplex ureters, ectopic UVJ, hydroureter (Miyazaki et al., 2000)
<i>SALL1</i>	16q12.1	mm	Spalt-Like Transcription Factor 1	Wnt		Townes-Brocks syndrome (OMIM 107480)	incomplete ureteric bud outgrowth (Nishinaka et al., 2001)
<i>FOXC2</i>	16q24.1	um	Forkhead transcription factor	Foxc			Ectopic UB, duplex ureters, hydroureter, ureter agenesis (Kume et al., 2000)

Abbreviations: Chr: chromosomal location; Exp: expression in the urinary tract; Signaling: signaling pathway; Ref: References; UB: ureteric bud; TGF- $\beta$ : transforming growth factor- $\beta$ ; VUR: vesicoureteral reflux; RAS: Renin-angiotensin system; UVJ: ureterovesical junction; uro: urothelium; UPJ: ureteropelvic junction; wd: Wolffian duct; ub: ureteric bud; ue: ureteric epithelium; um: ureteric mesenchyme; smc: smooth muscle cells

#### 4.2.2 *Genes associated with abnormal UB outgrowth*

The Glial cell-derived neurotrophic factor (*GDNF*) encodes a highly conserved secreted protein in the MM and induces UB outgrowth during early kidney and ureter development (Costantini, 2010; Costantini and Kopan, 2010). It is the most important inducer of UB outgrowth and its activity is thought to depend on its receptor RET (Costantini, 2010; Costantini and Kopan, 2010). Loss of *Gdnf* in mice causes absence of UB formation and renal agenesis phenotype (Sanchez et al., 1996). Therefore, mutations in genes associated with the *Gdnf/Ret* pathway, like *Spry1*, *Gata3*, *Bmp4*, *Slit2/Robo2*, *Foxc1/2*, *Pax2*, *Eya1/Six1*, and *Sall1*, all cause abnormal UB outgrowth phenotypes in mice (Illustration 4.2) (Basson et al., 2005; Grieshammer et al., 2004; Grote et al., 2008; Kiefer et al., 2010; Kume et al., 2000; Lu et al., 2007b; Lu et al., 2007c; Miyazaki et al., 2000; Nie et al., 2011; Nishinakamura et al., 2001; Xu et al., 1999) .

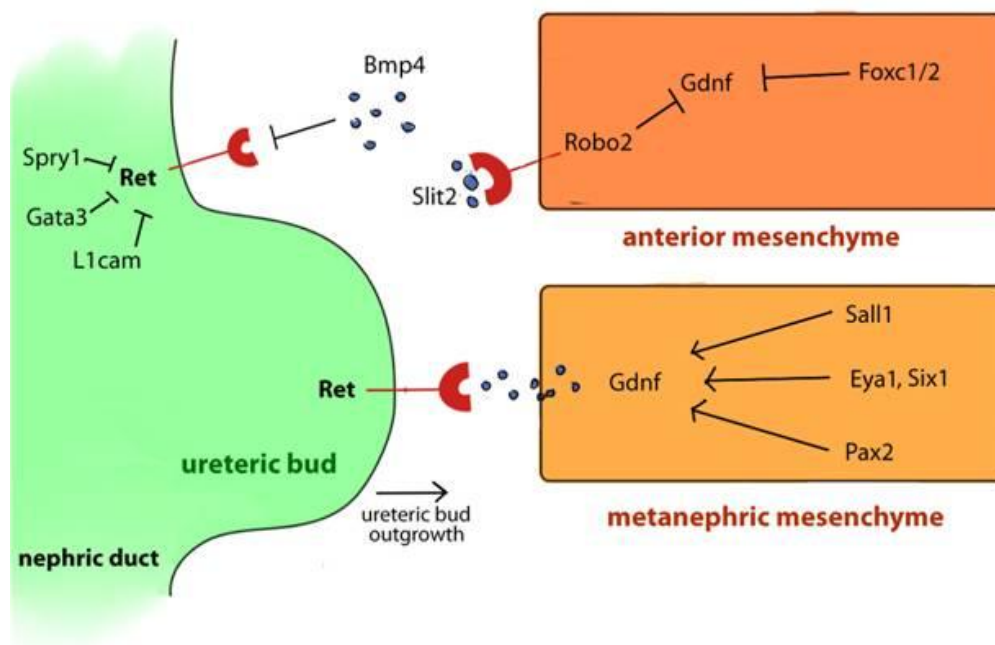


**Illustration 4.2 : Genes and signaling pathways involved in UB outgrowth.**

Genes and signaling pathways involved in UB outgrowth. Scheme of signaling pathways in and between the ureteric bud (green) and the metanephric mesenchyme (yellow-orange). The most important inducer of UB outgrowth is GDNF and its receptor RET. *Ret* is expressed by the nephric duct (green) and ureteric bud (green). GDNF is secreted by the metanephric mesenchyme (yellow). The coordination of different signaling pathways in the anterior mesenchyme and the metanephric mesenchyme play a crucial role in the development of a single ureteric bud (Rasouly and Lu, 2013).

*GDNF* is expressed in the metanephric mesenchyme (Grieshammer et al., 2004).

In human and rodents, the *GDNF* mRNA is alternatively spliced: a full-length transcript [pre-( $\alpha$ )pro-GDNF] and a shorter transcript [pre-( $\beta$ )pro-GDNF] that lacks 78 bp in the region encoding the pro-domain, and both *GDNF* mRNA are expressed during kidney development (Lonka-Nevalaita et al., 2010). GDNF is synthesized in the form of a precursor called pre-pro-GDNF that can be proteolytically cleaved (Lin et al., 1993). Interestingly, GDNF can be secreted as either cleaved or uncleaved form. It is cleaved by

FURIN inside the cell but not by matrix metalloproteases (Lonka-Nevalaita et al., 2010). The cleavage of other neurotrophic proteins has been shown to change their function, sometimes into opposite ones (Je et al., 2012). It is unknown which form of GDNF is expressed in the MM during early kidney development.

PAX2 (Paired Box 2) induces *Gdnf* expression (Brophy et al., 2001). Heterozygote mutations in *PAX2* cause the papillorenal syndrome (OMIM 120330) that is associated with a range of CAKUT phenotypes. PAX2, EYA1 and HOX11 form a complex that regulates *Gdnf* expression (Gong et al., 2007). *Pax2* is expressed in the pronephros, the UB and the MM, and *Pax2* knockout mice have a complete renal agenesis phenotype (Dressler et al., 1990).

SPRY1 (sprouty homolog 1) acts as a negative feedback molecule to inhibit the GDNF/RET signaling in the UB. In mice, mutations in *Spry1* cause multiple ureteric buds and hydronephrosis (Basson et al., 2005). Accordingly, loss of *Spry1* is able to increase GDNF/RET signaling activity and rescue mouse UB phenotype in the *Gdnf* or *Ret* knockout mice (Michos et al., 2010; Rozen et al., 2009). However, no SPRY1 mutations have been identified so far in CAKUT patients (van Eerde et al., 2007).

CAKUT like phenotype such as ureteral stenosis has been described in patients with Axenfeld-Rieger syndrome (OMIM 602482) (Weisschuh et al., 2008), which is caused by mutations in the *FOXC1* (forkhead box C1) gene. Interestingly, *Foxc1* has been found highly expressed in mouse MM and mutations of mouse *Foxc1* and its family member *Foxc2* result in expansion of *Gdnf* expression domain in the MM, leading to ectopic ureteric bud, duplex ureter, and hydronephrosis phenotype (Kume et al., 2000).

The Townes-Brocks syndrome is caused by heterozygous mutations in the *SALL1* (spalt-like transcription factor 1) gene. Homozygous *Sall1* knockout mice develop an incomplete UB outgrowth phenotype with increased apoptosis in the MM (Nishinakamura et al., 2001). *Sall1* mutant mice have a reduced expression of GDNF at E11.5, but no difference was observed at E10.5, suggesting SALL1 regulates GDNF expression indirectly in the MM after UB outgrowth (Nishinakamura et al., 2001). Overexpression of *Sall1* in mouse metanephric mesenchyme using *Six2-cre* did not result in a kidney anomaly phenotype (Jiang et al., 2010).

Slit2-Robo2 signaling also plays crucial roles in early ureteric bud outgrowth and positioning. Human *ROBO2* mutations have been identified in CAKUT patients from several unrelated families (Bertoli-Avella et al., 2008; Lu et al., 2007b). Mouse knockouts that lack either *Slit2* or *Robo2* develop supernumerary UB, duplex kidney and hydroureter phenotype (Grieshammer et al., 2004; Lu et al., 2007b). *Robo2* is a member of the immunoglobulin superfamily and encodes a cell adhesion molecule involved in axonal guidance and neurogenesis (Dickson and Gilestro, 2006; Fricke et al., 2001). It is a receptor for the SLIT2 protein (Brose et al., 1999), and the Slit2-Robo2 signaling acts as a chemorepulsive guidance cue to control axon pathfinding and neuron migration during nervous system development (Tessier-Lavigne and Goodman, 1996). Robo2 is thought to inhibit *Gdnf* expression (Grieshammer et al., 2004). Like *Gdnf*, *Robo2* is expressed in the MM of the nephrogenic zone (Grieshammer et al., 2004; Piper et al., 2000), while *Slit2* is expressed in the nephric duct and UB (Grieshammer et al., 2004). However, the function and molecular regulation of the Slit2/Robo2 signaling during



ureteric budding remain unknown. When *Robo2* was deleted specifically in the MM using either *Rarb2-cre* or *Six2-cre*, the homozygous conditional knockout mice did not develop a multiple ureteric bud phenotype (Weining Lu, unpublished data).

Since PAX2 and ROBO2 have opposite effects on *Gdnf* expression during UB outgrowth (Brophy et al., 2001; Grieshammer et al., 2004), we hypothesized that *Robo2* and *Pax2* operate *in vivo* in a common genetic pathway to regulate *Gdnf* expression and UB outgrowth during mouse kidney development. However, after examination of potential genetic interaction *in vivo* between *Robo2* and *Pax2* using three different approaches, we did not find any evidence that ROBO2 and PAX2 function in a common genetic pathway (data not shown).

### 4.3 Hypothesis

The expression of *Gdnf* is changed in MM during UB outgrowth in both *Slit2* and *Robo2* knockout mice; however the mechanism leading to such change is unknown. We hypothesized that the Slit2/Robo2 signaling affects extracellular matrix components gene expression in the metanephric mesenchyme (as it affects extracellular matrix of the GBM in *Ilk* cKO mice) to control the UB outgrowth. To test this hypothesis, we performed microarray gene expression analysis using Affymetrix GeneChip Mouse Gene 1.0 ST

Array on early MM and UB tissues collected from E10.5 and E11.5 *Robo2* and *Slit2* knockout mouse embryos.

## 4.4 Materials and Methods

### 4.4.1 General experimental design

We designed three independent experiments with biological replicates in each group (Group 1: E10.5 *Robo2* homozygous knockouts versus wild type controls; Group 2: E10.5 *Slit2* homozygous knockouts versus wild type controls; Group 3: E11.5 *Robo2* knockouts versus wild type controls) and analyzed common genes that are differentially expressed in all three groups.

### 4.4.2 Mice strains

Mouse protocols were approved by the Institutional Animal Care and Use Committee (IACUC) at Boston University Medical Center (#14388). The generation of the *Robo2*<sup>-</sup> and *Slit2*<sup>-</sup> alleles was described previously (Lu et al., 2007b; Plump et al., 2002). Adult and embryos were genotyped as previously described. Timed pregnancies were set up by checking females for vaginal plugs in the morning to determine if mating has occurred during the night. *Robo2*<sup>+/-</sup> mice were bred with *Robo2*<sup>+/-</sup> mice and *Slit2*<sup>+/-</sup>

mice were bred with *Slit2*<sup>+/-</sup> mice to generate homozygotes and wild-type littermates collected at E10.5 and E11.5.

#### *4.4.3 Tissue collection and RNA isolation*

The pregnant females were euthanized at E10.5 and E11.5 and the embryos were collected. The areas of the ureteric buds were microdissected (by Anna Pisarek-Horowitz). The microdissected tissue was preserved in RNAlater (Cat #76106, Qiagen) in -40°C and the remaining tissue was used for genotyping. RNA was extracted directly from the RNAlater solution using the RNeasy micro kit (Cat # 74004, Qiagen).

#### *4.4.4 Microarray experimental design*

Based on the genotype of the embryos, the experiment was divided into three groups as described in 4.4.1 above. Since SLIT2 is the ligand for the ROBO2 receptor, and the two knockouts abrogate the same pathway and produce the same abnormal UB phenotype, the E10.5 *Slit2*<sup>-/-</sup> and the *Robo2*<sup>-/-</sup> were considered as biological replicates for a subset of data analysis.

#### *4.4.5 Microarray experiment*

The microarray experiment was performed with the 16 GeneChip Mouse Gene 1.0 ST Arrays (Cat #901171, Affymetrix) by the microarray core facility at Boston University School of Medicine.

#### *4.4.6 Microarray quality control*

The normalization and quality assessment were performed by Adam Gower as part of the microarray core service. All microarray analyses were performed using the R environment for statistical computing (version 2.15.1).

The arrays were normalized together using the Robust Multiarray Average (RMA) algorithm (Irizarry et al., 2003) from Affymetrix (version 1.36.1) (Gautier et al., 2004). A Chip Definition File (CDF) mapped the probes on the array to unique Entrez Gene identifiers. The result was a matrix in which each row corresponds to an Entrez Gene ID and each column corresponds to a sample. The expression values were displayed as log<sub>2</sub>-transformed by default.

The technical quality of the arrays was assessed by two quality metrics: Relative Log Expression (RLE) and Normalized Unscaled Standard Error (NUSE). For each sample, median RLE values  $> 0.1$  or NUSE values  $> 1.05$  were considered as out of the usual limits, although RLE was used as the quality metric most strongly associated with technical quality.

The expression of several sex-specific genes (e.g. *Xist*, *Ddx3y*, *Eif2s3y*, *Kdm5d*, and *Uty*) was also assessed to estimate the dynamic range of the array, as the female-specific marker *Xist* and constitutively expressed Y-linked genes were served in females as positive and negative expression controls, respectively.

### ***Principal Component Analysis (PCA)***

Principal Component Analysis (PCA) is a mathematical transform that collapses the variance between samples across all ~20,000 genes on the array into a much smaller set of variables called Principal Components (PCs). These "meta-variables" are arranged such that PC1 explains the most variance in the data, followed by PC2, etc. PCA was performed using all genes, and a plot was made of PC2 vs. PC1

### ***Differential expression analysis***

Differential gene expression was assessed using Student's two-sample *t* test on the coefficients of a simple linear model (expression as a function of genotype) created using the 'lmFit' function in the *limma* Bioconductor package (version 3.14.4).

Student's two-sample *t* test with equal variance was used to identify genes that were differentially expressed with respect to knockout of *Robo2* or *Slit2* at each timepoint. Additionally, at day E10.5, the *Robo2*<sup>-/-</sup> and *Slit2*<sup>-/-</sup> embryos were pooled together (as

were the corresponding wildtype embryos) and a combined wildtype versus knockout comparison was made.

Benjamini-Hochberg False Discovery Rate (FDR) correction was then used to obtain FDR-corrected p values (a.k.a. q values), which represent the probability that a given result is a false positive based on the distribution of all p values on the array. Corrected/adjusted p values such as the FDR q are the best measure of significance for a given test when many hypotheses (e.g., ~20,000 genes) are tested at once.

#### *4.4.7 Gene Set Enrichment Analysis (GSEA)*

The GSEA was run by Adam Gower in the microarray core facility at Boston University. GSEA (version 2.0.13) (Subramanian et al., 2005) was used to identify biological terms, pathways and processes that were coordinately up- or down-regulated within each pairwise comparison. The Entrez Gene identifiers of the human homologs of the genes interrogated by the array were ranked according to the moderated  $t$  statistic computed for each knockout versus wild type comparison, producing four ranked lists. Mouse genes without a human homolog were removed, and the  $t$  statistics for multiple mouse genes with the same human homolog were averaged prior to ranking. Each list was then used to perform a pre-ranked GSEA analysis using the Entrez Gene versions of the Biocarta, KEGG, Reactome, and Gene Ontology (GO) gene sets obtained from the Molecular Signatures Database (MSigDB) -

(<http://www.broadinstitute.org/gsea/msigdb/index.jsp> ), version 4.0 (Subramanian et al., 2007).

For each ranked list, the GSEA algorithm tests each gene set in turn to determine whether its members are distributed nonrandomly within the ranked list. It then assigns a p value to each gene set based on how skewed the distribution of the gene set is towards the up- or down-regulated end of the ranked list (weighted by the ranking metric, so that the genes at the extreme end of the ranked list have more importance in computing the p value).

GSEA determines whether, on the whole, a given set of genes tends to be more up-regulated or down-regulated in a given comparison. If the set of genes is related to some biological pathway or process, then a significant GSEA result for that gene set suggests that the pathway/process is relevant to the experimental comparison.

#### *4.4.8 Ingenuity pathway analysis overview*

Ingenuity pathway analysis (IPA) is a web-based software application that enables the analysis and interpretation of data derived from microarrays experiments. The data analysis and interpretation with IPA builds on a manually curated content of the Ingenuity Knowledge Base. IPA algorithms can identify regulators and pathways that are relevant to gene expression changes observed in an analyzed dataset. The upstream regulator analysis identifies molecules, including miRNA and transcription factors, which

may cause the observed gene expression changes. The IPA software is available from the Genome Science Institute (GSI) at Boston University:

<http://www.bumc.bu.edu/gsi/initiatives/ingenuity-ipa/>

## 4.5 Results

### *4.5.1 No single gene expression is significantly altered in *Slit2* and *Robo2* knockout kidney at E10.5 and E11.5*

#### ***Samples collected***

From timed-pregnant females of *Robo2* and *Slit2* heterozygous matings, 18 homozygous *Robo2* and *Slit2* knockout embryos were identified (Table 4.2). We then performed microdissection and isolated the mRNA from tissues of UB and MM regions in 8 knockout embryos and 8 littermate controls. Total 16 microarray experiments are performed with the mRNA isolated from following embryos:

At E11.5, we were able to compare 3 *Robo2*<sup>-/-</sup> and 3 *Robo2*<sup>+/+</sup> all from the same litter, so we had 3 perfect biological replicates and 3 perfect controls.

At E10.5, we used 2 wild-type and 2 *Robo2*<sup>-/-</sup> embryos (all from one dam) and 3 wild-type and 3 *Slit2*<sup>-/-</sup> embryos (n=2 per group from one dam, n=1 per group from another dam).



**Table 4.2: Embryonic kidney tissues from F1 crossing used in microarray experiments**

Genotype	E10.5	E10.5	E11.5	E11.5
	collected	Used for microarray analysis	collected	Used for microarray analysis
<i>Robo2</i> -/-	3	2	9	3
<i>Robo2</i> +/+	2	2	10	3
Other	20	0	0	0
<i>Slit2</i> -/-	6	3	0	0
<i>Slit2</i> +/+	3	3	0	0
Other	5	0	0	0

#### Normalization and quality assessment

All the arrays had median RLE and NUSE values within the limits. The expression of *Xist* was either very high (~11 log<sub>2</sub> units) or low (~4 log<sub>2</sub> units), and varied inversely with that of the Y-linked genes, which was either high (~8-9 log<sub>2</sub> units) or low (~3-4 log<sub>2</sub> units). These results indicated that the arrays had very good dynamic range.

### Probe-level expression of *Robo2* and *Slit2*

The *Robo2* locus was disrupted by two loxP sites-mediated excision of the exon 5 (Lu et al., 2007b). To confirm that this exon deletion was present in the *Robo2*<sup>-/-</sup> samples, the probe-level expression of *Robo2* exon 5 was examined. Expression of the probe interrogating exon 5 (red) is absent in all *Robo2*<sup>-/-</sup> samples (Figure 4.1).

Similarly, the expression of probes interrogating *Slit2* exons 1 and 2 is greatly reduced in the *Slit2*<sup>-/-</sup> samples (Figure 4.2), which is consistent with the *Slit2* knockout locus that was disrupted by partial replacement of exons 1 and 2 with a GFP-Neo cassette (Plump et al., 2002). These results indicated that the quality of the microarray data is good.

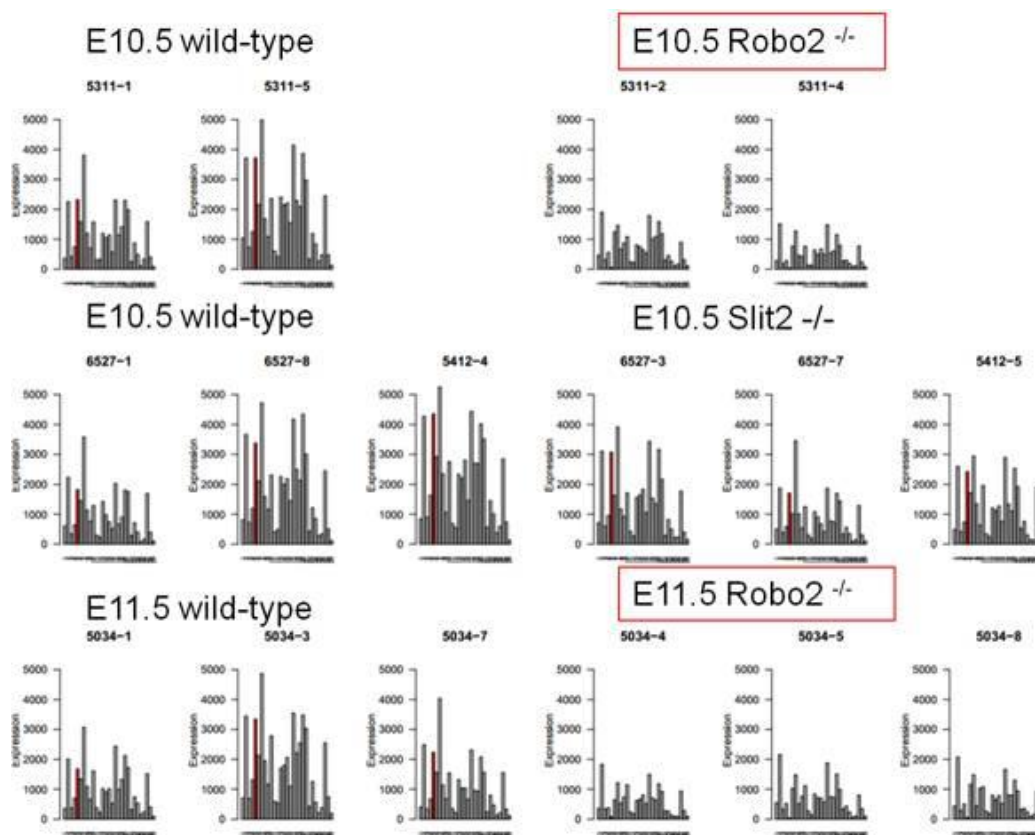


**Figure 4.1: Probe-level expression of *Robo2***

The probe-level expression of *Robo2* was examined as an internal control for the genotyping of the samples used in the microarray. Expression of the probe interrogating *Robo2* exon 5 (red – deleted in *Robo2* knockouts) is absent in all *Robo2*<sup>-/-</sup> samples.

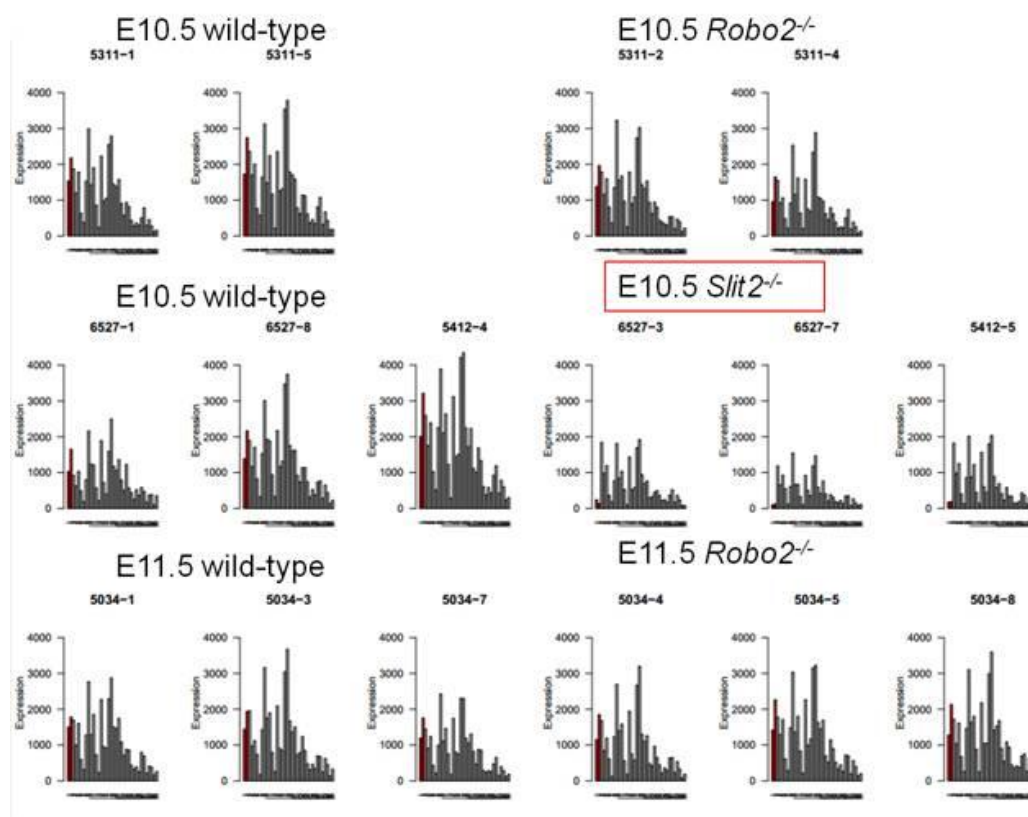


**Figure 4.2: Probe-level expression of *Slit2***

The probe-level expression of *Slit2* was examined as an internal control for the genotyping of the samples used in the microarray. Expression of the probes interrogating *Slit2* exons 1 and 2 (red - deleted in *Slit2* knockouts) are absent in all *Slit2*<sup>-/-</sup> samples.

#### Principal Component Analysis (PCA)

The PCA plot shows that there is strong separation between samples from the E10.5 and E11.5 timepoints, but within each timepoint, there is little to no separation between knockout and wildtype samples (Figure 4.3). These results suggest that there is a

strong differential gene expression with respect to time but not to genotype in this microarray experiment.

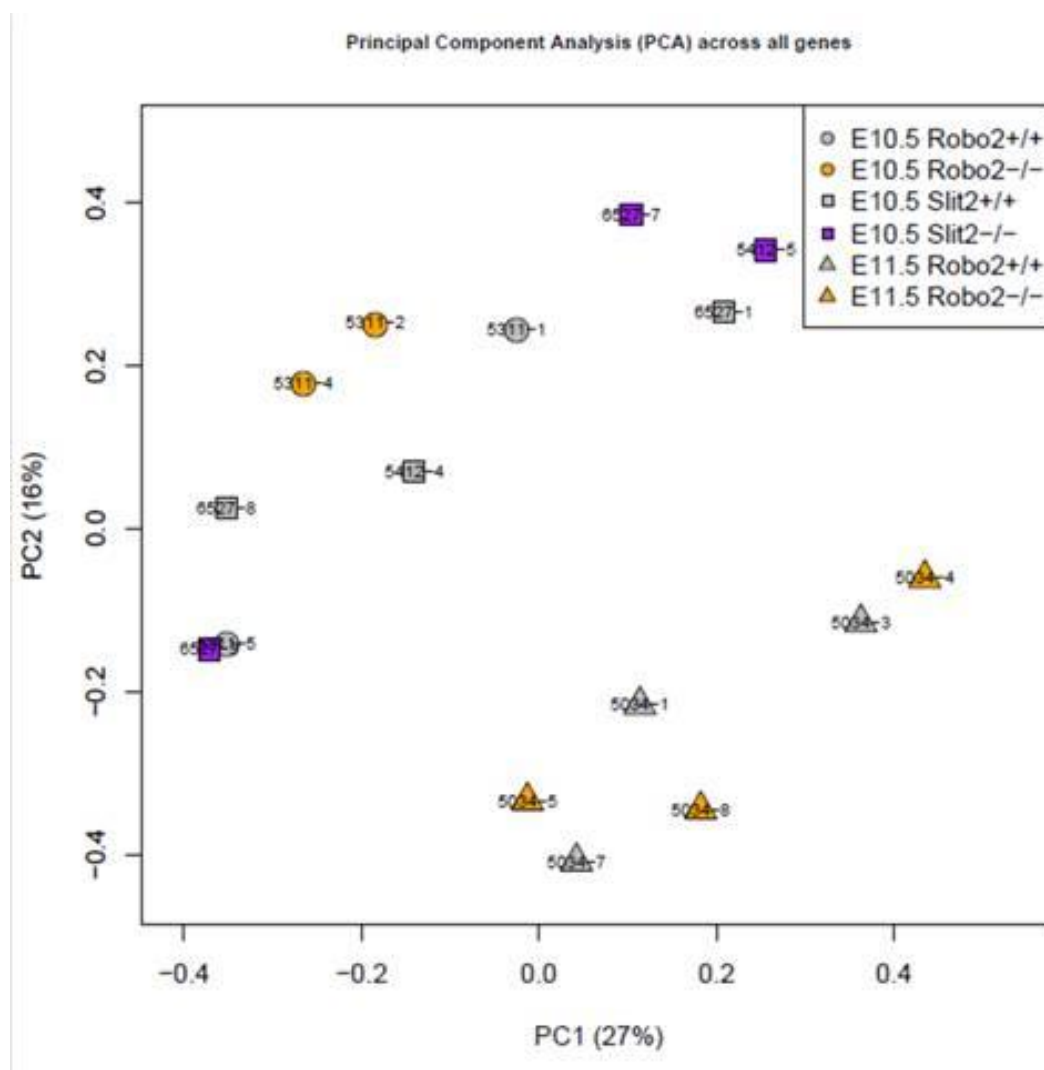


**Figure 4.3: Principal Component Analysis**

Plot of PC1 versus PC2 comparing the variance between the samples.

## Differential expression analysis

Fewer genes were differentially expressed than expected by chance at each threshold, although there were slightly more than expected by chance at E11.5 (Table 4.3). Accordingly, there were no genes with an FDR  $q < 0.25$  for any comparison other than the E11.5 *Robo2* knockout versus wild type. However, in this comparison, 5 of the 6 genes with an FDR  $q < 0.25$  were the sex-specific genes (i. e. *Xist*, *Ddx3y*, *Eif2s3y*, *Kdm5d*, and *Uty*), as all of the E11.5 *Robo2*<sup>-/-</sup> embryos were male and all of the E11.5 wildtype (*Robo2*<sup>+/+</sup>) embryos were female. The sixth gene, with FDR  $q = 0.24$ , is *Dnajc27*, which had a significant but small increase of 1.15-fold at E11.5 in the *Robo2* knockout. These data suggest that no single gene expression is significantly altered in *Slit2* and *Robo2* knockout kidney at E10.5 and E11.5.

**Table 4.3: No significant differential expression of any gene in any group was detected in E10.5-E11.5 *Robo2* and *Slit2* embryonic kidney tissues**

P threshold	expected	E10.5		E11.5	
		<i>Robo2</i> <sup>-/-</sup> vs wildtype	<i>Slit2</i> <sup>-/-</sup> vs wildtype	E10.5 Combined	<i>Robo2</i> <sup>-/-</sup> vs wildtype
0.05	1059	895	421	656	974
0.01	212	186	66	95	229
0.005	106	104	29	44	120
0.001	21	21	4	8	30

***Analysis of the expression of candidate genes controlling UB outgrowth in the microarray dataset***

Even though none of the genes was significantly differentially expressed after the FDR correction for multiple hypothesis, the analysis of gene-sets belonging to similar pathways can reveal coordinated down or upregulation based on the fold changes such as *Gdnf* and other genes known to control *Gdnf* expression during early UB outgrowth. Interestingly, the expression fold changes of *Gdnf* and *Sall1*, two genes that control UB outgrowth, had a p-value of 0.01 (Table 4.4). *Gdnf* expression was slightly increased when all the samples collected at E10.5 were analyzed (Table 4.4) and *Sall1* was slightly increased in the E10.5 *Robo2*<sup>-/-</sup> when compared to wild-type littermates (Table 4.4). However, all the genes had a FDR=1, indicating absence of differential expression after correction.

**Table 4.4: The expression of candidate genes controlling UB outgrowth in the microarray dataset**

(*Gdnf* and *Sall1*, two genes had a p-value of 0.01, are highlighted in yellow)

Gene	Description	E10.5 Robo2 <sup>-/-</sup> vs Robo2 <sup>+/+</sup>		E10.5 combined KO vs WT	
		fold change	p	fold change	p
<i>Bmp4</i>	bone morphogenetic protein 4	1.06	0.53	-1.02	0.74
<i>Eya1</i>	eyes absent 1 homolog (Drosophila)	1.31	0.26	1.05	0.48
<i>Foxc1</i>	forkhead box C1	-1.04	0.14	-1.21	0.20
<i>Foxc2</i>	forkhead box C2	-1.00	0.97	-1.13	0.31
<i>Gata3</i>	GATA binding protein 3	-1.21	0.43	-1.06	0.61
<i>Gdnf</i>	glial cell line derived neurotrophic factor	1.18	0.31	1.22	0.01
<i>Hoxa11</i>	homeobox A11	1.06	0.19	1.03	0.77
<i>Pax2</i>	paired box gene 2	-1.09	0.78	-1.02	0.95
<i>Ret</i>	ret proto-oncogene	-1.20	0.28	-1.06	0.58
<i>Sall1</i>	sal-like 1 (Drosophila)	1.19	0.01	1.12	0.11
<i>Six1</i>	sine oculis-related homeobox 1	1.82	0.36	1.71	0.12
<i>Spry1</i>	sprouty homolog 1 (Drosophila)	1.19	0.40	1.07	0.21

WT- wildtype, combined KO: *Slit2*<sup>-/-</sup> and *Robo2*<sup>-/-</sup> knockout



*4.5.2 Genes coding for extracellular matrix proteins are coordinately downregulated in the *Robo2* and the *Slit2* knockouts compared to wild-type littermates*

***GSEA analysis of Gene Sets enriched in the E10.5 and E11.5 UB and MM tissues from *Robo2* and the *Slit2* knockouts***

GSEA analysis of all gene expression data and comparisons at both E10.5 and E11.5 revealed that genes related to the extracellular matrix (ECM), collagen formation, ECM-receptor interaction, focal adhesions, actin cytoskeleton, axon guidance, and NCAM1 interactions were significantly coordinately downregulated in the E10.5 and E11.5 *Robo2* and *Slit2* knockout kidneys (Table 4.5). No gene-sets were coordinately upregulated at both E10.5 and E11.5 time points. At E10.5, many of the gene-sets most significantly upregulated were related to translation (e.g. ribosome) and metabolism (e.g. mitochondria) (Table 4.6). These results suggest that loss of *Robo2* or *Slit2* during UB outgrowth may affect the gene expression of ECM compositions in the MM and around the UB.

**Table 4.5: Sets of genes significantly coordinately down-regulated in *Slit2* and *Robo2* knockouts compared to the wild-type controls**

Gene sets related to the extracellular matrix are highlighted in yellow.

Group	Gene Set Name	Size	E10.5 Robo2 <sup>-/-</sup> vs WT			E10.5 Slit2 <sup>-/-</sup> vs WT			E10.5 combined KO vs WT			E11.5 Robo2 <sup>-/-</sup> vs WT		
			NES	p	FDR q	NES	p	FDR q	NES	p	FDR q	NES	p	FDR q
KEGG	ECM receptor interaction	82	-2.05	0.00	0.12	-2.51	0.00	0.00	-2.77	0.00	0.00	-2.39	0.00	0.00
GO	extracellular matrix part	55	-2.11	0.00	0.07	-1.71	0.01	0.06	-2.38	0.00	0.00	-2.35	0.00	0.00
GO	collagen	23	-2.05	0.00	0.09	-1.84	0.00	0.03	-2.44	0.00	0.00	-2.28	0.00	0.00
GO	proteinaceous extracellular matrix	93	-1.93	0.00	0.17	-1.74	0.00	0.05	-2.49	0.00	0.00	-2.24	0.00	0.00
GO	extracellular matrix	94	-1.87	0.00	0.19	-1.72	0.00	0.05	-2.48	0.00	0.00	-2.21	0.00	0.00
Reactome	collagen formation	57	-1.83	0.00	0.24	-2.04	0.00	0.01	-2.58	0.00	0.00	-2.17	0.00	0.00
KEGG	other glycan degradation	16	-1.72	0.02	0.24	-1.80	0.00	0.03	-1.96	0.00	0.01	-2.15	0.00	0.00
KEGG	focal adhesion	193	-1.74	0.00	0.24	-2.20	0.00	0.00	-2.44	0.00	0.00	-2.11	0.00	0.00
Reactome	extracellular matrix organization	83	-1.81	0.00	0.22	-1.63	0.00	0.08	-2.25	0.00	0.00	-1.99	0.00	0.01
Reactome	axon guidance	237	-1.87	0.00	0.19	-2.16	0.00	0.00	-2.69	0.00	0.00	-1.90	0.00	0.02
GO	actin binding	72	-1.72	0.01	0.25	-2.03	0.00	0.01	-2.30	0.00	0.00	-1.77	0.00	0.06
Reactome	a tetrasaccharide linker sequence is required for gag synthesis	25	-1.77	0.01	0.22	-1.90	0.00	0.02	-2.26	0.00	0.00	-1.75	0.00	0.07
GO	actin cytoskeleton	121	-1.88	0.00	0.20	-1.59	0.00	0.10	-2.28	0.00	0.00	-1.73	0.00	0.08
Reactome	NCAM1 interactions	39	-2.20	0.00	0.02	-1.87	0.00	0.02	-2.45	0.00	0.00	-1.67	0.00	0.11
GO	myosin complex	15	-1.81	0.01	0.21	-1.50	0.06	0.14	-1.67	0.01	0.04	-1.57	0.04	0.17
KEGG	axon guidance	128	-1.96	0.00	0.14	-1.62	0.00	0.09	-2.23	0.00	0.00	-1.54	0.00	0.18
GO	regulation of anatomical structure morphogenesis	25	-1.81	0.02	0.20	-1.55	0.04	0.12	-1.89	0.00	0.01	-1.51	0.04	0.20
Reactome	signaling by ROBO receptor	27	-1.76	0.01	0.23	-1.53	0.03	0.13	-1.90	0.00	0.01	-1.51	0.03	0.20

KEGG: Kyoto Encyclopedia of Genes and Genomes, GO: Gene Ontology, NES: Normalized Enrichment Score, p: nominal p-value, FDR q: FDR-corrected p value; FDR q < 0.25 is significant, WT- wildtype, combined KO: *Slit2*<sup>-/-</sup> and *Robo2*<sup>-/-</sup> knockout

**Table 4.6: Sets of genes significantly coordinately up-regulated in E10.5 knockout compared to the wild-type**

Group	Gene Set Name	Size	NES	p	FD R q
GO	structural constituent of ribosome	45	2.28	0.00	0.00
KEGG	Ribosome	40	2.20	0.00	0.00
Reactome	peptide chain elongation	38	2.07	0.00	0.01
	conversion from APCc CDC20 to APCc CDH1 in late				
Reactome	anaphase	16	2.00	0.00	0.02
GO	mitochondrial ribosome	20	1.99	0.00	0.02
Reactome	synthesis of glycosylphosphatidylinositol GPI	17	1.97	0.00	0.02
Reactome	mitochondrial protein import	44	1.95	0.00	0.02
GO	organellar ribosome	20	2.00	0.00	0.02
Reactome	influenza viral rna transcription and replication	54	1.95	0.00	0.02
GO	ribosomal subunit	18	2.01	0.00	0.02
	formation of the ternary complex and subsequently the				
Reactome	43s complex	29	1.89	0.00	0.04
GO	Ribosome	29	1.88	0.00	0.04
Reactome	3 UTR mediated translational regulation	57	1.87	0.00	0.04
Reactome	APC C CDC20 mediated degradation of cyclin B	16	1.85	0.00	0.05
	SRP dependent cotranslational protein targeting to				
Reactome	membrane	59	1.85	0.00	0.05
GO	Translation	146	1.85	0.00	0.05
Reactome	nucleotide like purinergic receptors	15	1.82	0.01	0.06
GO	cellular protein catabolic process	55	1.76	0.00	0.12
Reactome	phosphorylation of the APC C	16	1.74	0.01	0.13
Reactome	APC CDC20 mediated degradation of NEK2A	19	1.73	0.01	0.14
GO	mitochondrial inner membrane	58	1.72	0.00	0.15
GO	mitochondrial envelope	86	1.69	0.00	0.15
BioCarta	TH1TH2 pathway	19	1.70	0.01	0.15
Reactome	Translation	93	1.70	0.00	0.16
	inhibition of the proteolytic activity of APC c required				
	for the onset of anaphase by mitotic spindle checkpoint				
Reactome	components	18	1.70	0.01	0.16
GO	mitochondrial part	128	1.70	0.00	0.16
Reactome	respiratory electron transport	57	1.68	0.00	0.17
	respiratory electron transport atp synthesis by				
	chemiosmotic coupling and heat production by				
Reactome	uncoupling proteins	69	1.67	0.00	0.17
KEGG	oxidative phosphorylation	101	1.66	0.00	0.17
BioCarta	cytokine pathway	18	1.67	0.01	0.18
KEGG	glycosylphosphatidylinositol GPI anchor biosynthesis	25	1.66	0.02	0.18
GO	DNA dependent DNA replication	51	1.65	0.01	0.18

GO	protein catabolic process	65	1.64	0.01	0.18
GO	regulation of DNA metabolic process	44	1.64	0.00	0.18
GO	mitochondrial membrane	77	1.62	0.00	0.20
GO	mitochondrial membrane part	44	1.62	0.01	0.20
GO	anion transport	29	1.63	0.01	0.20
GO	inorganic anion transmembrane transporter activity	19	1.62	0.02	0.20
GO	integral to organelle membrane	49	1.60	0.00	0.23
GO	cytokine metabolic process	40	1.58	0.02	0.24
KEGG	parkinsons disease	97	1.58	0.00	0.24
GO	organelle inner membrane	66	1.59	0.01	0.24
GO	hydrogen ion transmembrane transporter activity	25	1.58	0.02	0.24

KEGG: Kyoto Encyclopedia of Genes and Genomes, GO: Gene Ontology, NES: Normalized Enrichment Score, p: nominal p-value, FDR q: FDR-corrected p value; FDR q < 0.25 is significant, WT- wildtype, combined KO: *Slit2*<sup>-/-</sup> and *Robo2*<sup>-/-</sup> knockout

***Laminin and collagen coding genes are coordinately downregulated in E10.5 and E11.5 Slit2 and Robo2 knockouts versus wild type controls***

I was specifically interested in the genes driving the association between the gene-sets and the differential expression in *Slit2*<sup>-/-</sup> or *Robo2*<sup>-/-</sup> knockout samples versus wildtype controls. Besides the “axon guidance” and the “actin cytoskeleton” gene-sets, all gene-sets differential expressed are related to the extracellular matrix (ECM). Analysis of the leading edges of these gene-sets revealed that genes encoded laminins and collagens are the genes driving the significant association between these gene-sets and differential expression in the dataset. Therefore I looked at the differential gene expression of genes encoded Laminins and collagens in the dataset (mean log<sub>2</sub>>8) in all the comparisons (Tables 4.7 and 4.8). Although the corrected significance has not been reached for any of these genes (FDR=1), many of the individual p-values based on the student t-test were lower than 0.05. To better visualize these results, heatmaps were

drawn using the mouse homologs of genes in the leading edges of the “GO cellular component- extracellular matrix” and the “reactome collagen formation” gene-sets at E10.5 (Figure 4.4). The intensities of the heatmaps revealed that most laminin and collagen coding genes were coordinately downregulated in E10.5 *Robo2*<sup>-/-</sup> and the *Slit2*<sup>-/-</sup> knockouts when compared to the wild-type controls (Figure 4.4).

**Table 4.7: Most differential expressed Laminin coding genes at E10.5-E11.5 in the UBand MM (Mean log<sub>2</sub> >8).**

Individual p-values based on the student t-test were lower than 0.05 are highlighted in yellow.

Gene	E10.5 <i>Robo2</i> <sup>-/-</sup> vs <i>Robo2</i> <sup>+/+</sup>		E10.5 <i>Slit2</i> <sup>-/-</sup> vs <i>Slit2</i> <sup>+/+</sup>		E10.5 Combined KO vs WT		E11.5 <i>Robo2</i> <sup>-/-</sup> vs <i>Robo2</i> <sup>+/+</sup>	
	fold change	P-value	fold change	P-value	fold change	P-value	fold change	P-value
<i>Lama1</i>	-1.55	0.11	-1.28	0.05	-1.38	0.00	-1.12	0.05
<i>Lama4</i>	-1.40	0.56	-1.03	0.83	-1.15	0.48	1.03	0.80
<i>Lama5</i>	-1.44	0.16	-1.05	0.57	-1.20	0.09	-1.14	0.01
<i>Lamb1</i>	-1.40	0.12	-1.17	0.07	-1.25	0.01	-1.11	0.00
<i>Lamb2</i>	-1.21	0.02	-1.05	0.46	-1.11	0.18	-1.05	0.35
<i>Lamc1</i>	-1.47	0.17	-1.31	0.10	-1.37	0.01	-1.12	0.00

WT- wildtype, combined KO: *Slit2*<sup>-/-</sup> and *Robo2*<sup>-/-</sup> knockout

**Table 4.8: Table 4.6: Most differential expressed Collagen coding genes at E10.5-E11.5 in the UB and MM (Mean log<sub>2</sub> >8).**

Individual p-values based on the student t-test were lower than 0.05 are highlighted in yellow.

Gene	E10.5 Robo2 <sup>-/-</sup> vs Robo2 <sup>+/+</sup> fold change P-value		E10.5 Slit2 <sup>-/-</sup> vs Slit2 <sup>+/+</sup> fold change P-value		E10.5 combined KO vs WT fold change P-value		E11.5 Robo2 <sup>-/-</sup> vs Robo2 <sup>+/+</sup> fold change P-value	
<b>Col12a1</b>	-1.87	<b>0.01</b>	-1.11	0.42	-1.36	<b>0.03</b>	-1.38	0.26
<b>Col18a1</b>	-1.28	0.22	-1.20	0.12	-1.23	<b>0.02</b>	-1.11	<b>0.00</b>
<b>Col1a1</b>	-1.57	<b>0.03</b>	-1.34	0.18	-1.42	<b>0.01</b>	-1.15	<b>0.03</b>
Col1a2	-1.42	0.15	-1.16	0.23	-1.24	0.08	-1.04	0.63
Col23a1	-1.16	0.32	-1.11	0.31	-1.13	0.17	1.01	0.84
Col2a1	-1.06	0.86	-1.09	0.49	-1.08	0.56	1.03	0.68
Col3a1	-1.32	0.07	-1.12	0.40	-1.19	0.07	-1.14	0.07
<b>Col4a1</b>	-1.37	0.18	-1.20	0.09	-1.26	<b>0.01</b>	-1.12	<b>0.04</b>
<b>Col4a2</b>	-1.36	0.18	-1.28	0.12	-1.31	<b>0.01</b>	-1.10	<b>0.01</b>
Col4a3bp	-1.05	0.85	1.05	0.72	1.02	0.86	1.08	0.17
<b>Col5a1</b>	-1.24	<b>0.03</b>	-1.10	0.33	-1.15	<b>0.04</b>	-1.12	<b>0.03</b>
<b>Col9a1</b>	-1.15	<b>0.03</b>	-1.20	0.07	-1.18	0.05	-1.06	0.59

WT- wildtype, combined KO: *Slit2*<sup>-/-</sup> and *Robo2*<sup>-/-</sup> knockout

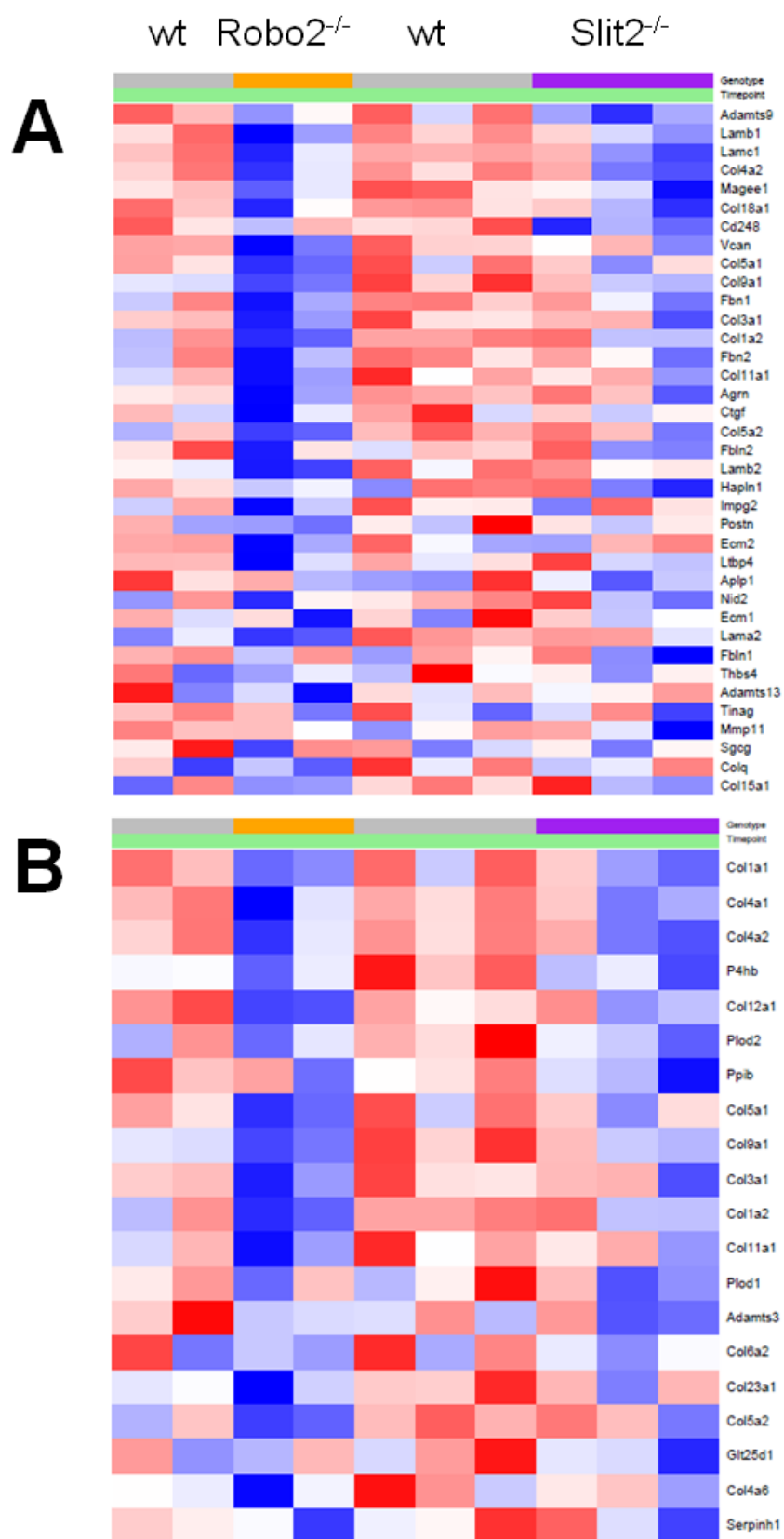


**Figure 4.4: Heatmaps from leading edges for gene-sets downregulated in E10.5 *Robo2* and *Slit2* knockout kidneys**

- (A) The leading edge genes from “extracellular matrix” visualized in a heat map. The heatmap is color-coded when compared to average, Blue is below average (downregulate), white is at average (no change) and red is above average (upregulated). The darker the color is the bigger the difference is from average. Each row represents a gene (labeled on the right). Each column represents a sample. Gray columns: wild-type, Orange columns: *Robo2*<sup>-/-</sup>, Purple columns: *Slit2*<sup>-/-</sup>.
- (B) The leading edge genes from “reactome collagen formation” visualized in a heat map. The heatmap is color-coded when compared to average, Blue is below average (downregulate), white is at average (no change) and red is above average (upregulated). The darker the color is the bigger the difference is from average. Each row represents a gene (labeled on the right). Each column represents a sample. Gray columns: wild-type, Orange columns: *Robo2*<sup>-/-</sup>, Purple columns: *Slit2*<sup>-/-</sup>.



*4.5.3 Pathways related to the extracellular matrix proteins are downregulated in the Robo2 and the Slit2 knockout compared to wild-type littermates*

***Ingenuity pathway analysis - associated pathways***

The ingenuity pathway analysis (IPA) enables to identify pathways relevant to the gene expression changes observed in the microarray dataset (IPA®, QIAGEN Redwood City, [www.qiagen.com/ingenuity](http://www.qiagen.com/ingenuity)). Canonical pathway analysis using the IPA related the gene expression changes in the combined E10.5 experiments to the following pathways: Inhibition of matrix metalloproteases; Role of JAK1, JAK2 and TYK2 in interferon signaling; iNOS signaling; ILK signaling; Glycolysis and Ubiquitin-10 biosynthesis, and Hepatic fibrosis / hepatic stellate cell activation (Figure 4.5). These IPA data is consistent with the results obtained by GESA analysis described above.

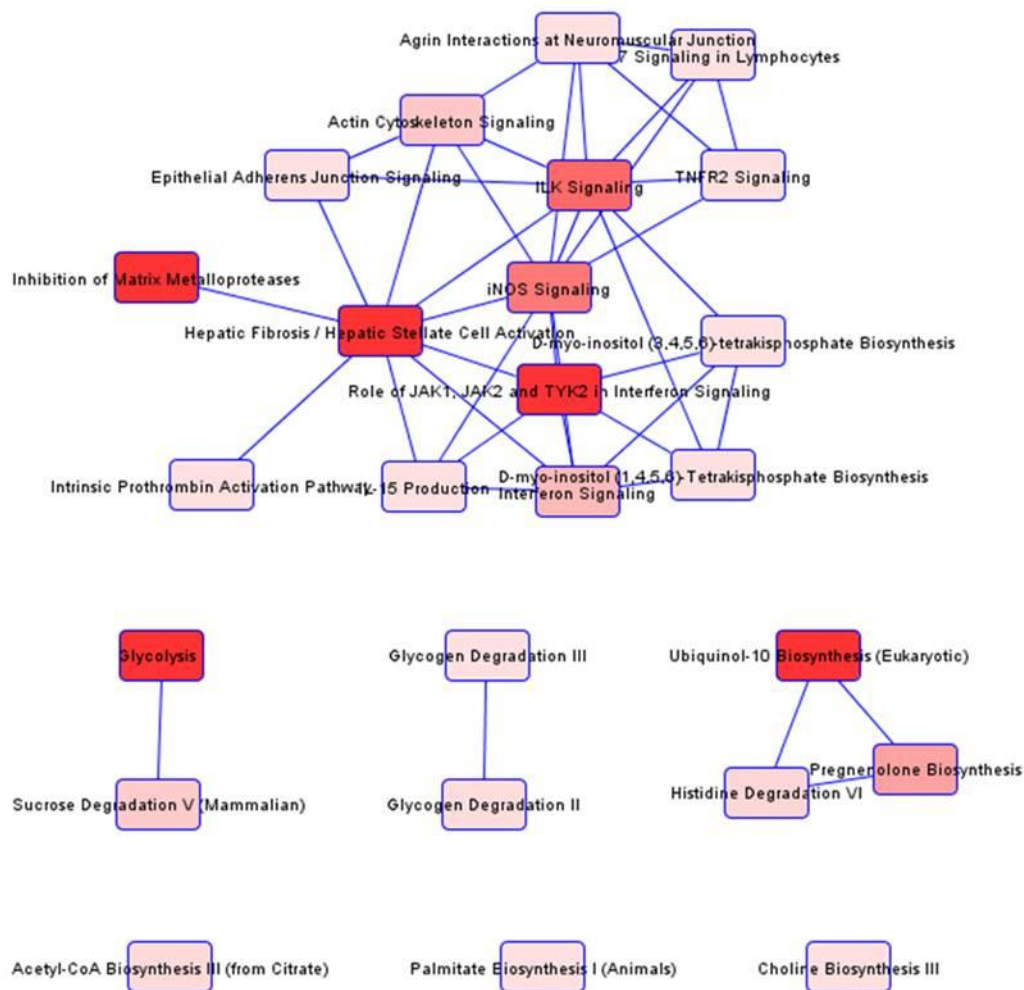


**Figure 4.5: Pathway analysis with IPA on E10.5 combined dataset**

Pathways identified by the IPA as relevant to the gene expression changes observed in the microarray dataset in the combined E10.5 experiments. As presented here, the different pathways have connection between one another. The darker the red color, the stronger the downregulation of this biological process is.

### ***Ingenuity pathway analysis - upstream regulators***

IPA can also identify upstream regulators that may cause the observed gene expression changes. By analyzing datasets from E10.5 and E11.5 kidneys, we identified following potential upstream regulators of SLIT2-ROBO2 pathway during early UB outgrowth: COL4A3, TP53, PRL, ramipril, TGFB1, LMNB1, IGF1R (Table 4.9). Both, COL4A3 and LMNB1 are ECM molecules that can affect outside-in signaling (Legate et al., 2009).

In order to understand why the IPA analysis identified IGF1R and TGF $\beta$ 1 as two upstream regulators of the gene expression changes in the dataset, I looked at the downstream targets of IGF1R and TGF $\beta$ 1. The schemes of the Further IPA analysis revealed that the association of IGF1R is also related to a downregulation of collagens. Three of the IGF1R target genes that were downregulated are *Coll1a1*, *Col14a1* and *Col4a2* (Figure 4.6). Interestingly, *Tgfb1* expression can also be regulated by IGFR1 and was found to be reduced in the knockout mice compared to wild type littermates at E10.5 (Figure 4.6). Similarly, the association of TGF $\beta$ 1 with the gene expression changes is also related to the ECM: 8 of the targets of TGFB1 are collagen and laminin (*Coll3a1*, *Lamb1*, *Col4a2*, *Col4a1*, *Coll1a1*, *Col5a1*, *Coll18a1*, *Lamc1*) and their gene expression was downregulated in this dataset (Figure 4.7).

**Table 4.9: Upstream regulators analysis by IPA**

	E10.5 Combined KO versus WT		E11.5	
	Z score	p-value	Z score	p-value
COL4A3	NA	2.13E-07	NA	2.63E-05
TP53	-1.098	3.89E-07	-1.662	2.87E-06
PRL	-1.947	1.83E-06	-1.999	1.13E-03
TGFB1	-2.582	6.63E-06	-2.572	2.13E-02
LMNB1	NA	5.47E-03	NA	1.88E-05
IGF1R	-2.076	1.97 E-04	-1.535	3.41 E-05

WT- wildtype, combined KO: *Slit2*<sup>-/-</sup> and *Robo2*<sup>-/-</sup> knockout

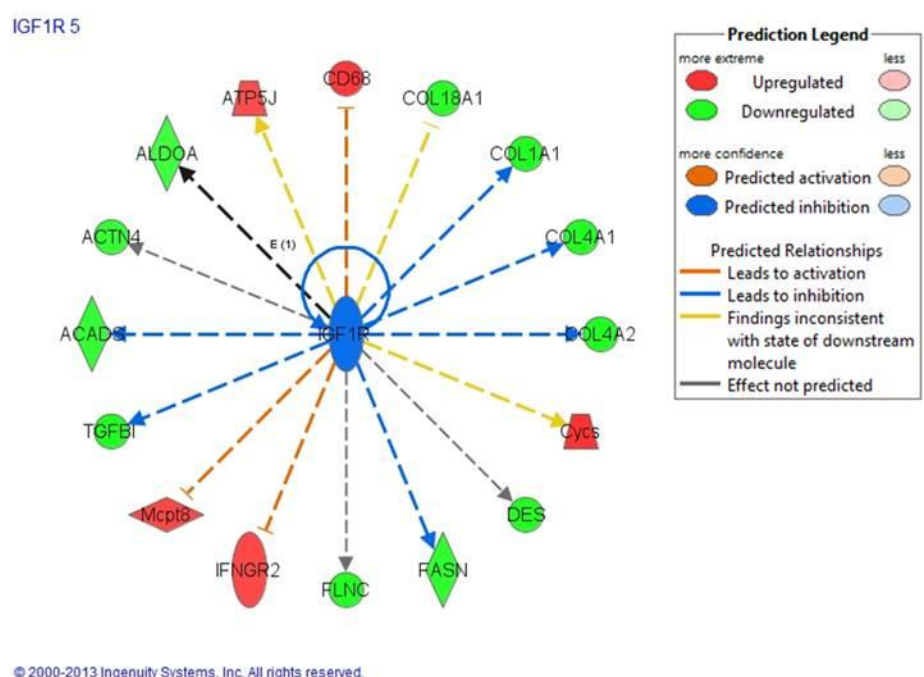


**Figure 4.6: Targets of IGF1R and their differential expressions in E10.5 ureteric buds (*Slit2*<sup>-/-</sup> and *Robo2*<sup>-/-</sup> combined).**

Illustration showing the genes that lead the IPA analysis to identify IGF1R inhibition as a possible upstream regulator controlling some of the differential gene expression pattern observed in the microarray dataset when all the E10.5 samples were combined. Six of the IGF1R target genes were downregulated (*Col1a1*, *Col4a1*, *Col4a2*, *Fasn*, *Tgfb1*, *Acads*) and three of the genes inhibited by IGF1R were upregulated in this dataset (*Cd68*, *Ifngr2*, *Mcpt8*). As illustrated here, three targets were inconsistent with the option that IGF1R is inhibited (*Col18a1*, *Cyts*, *Atp5j*).

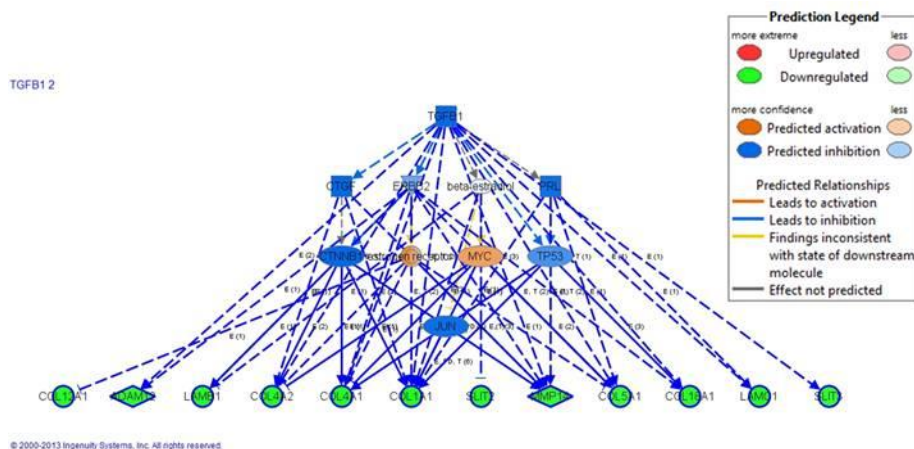


**Figure 4.7: Targets of TGFB1 and their differential expressions in E10.5 ureteric buds (*Slit2*<sup>-/-</sup> and *Robo2*<sup>-/-</sup> combined).**

Illustration showing the genes that lead the IPA analysis to identify TGFB1 inhibition as a possible upstream regulator explaining some of the differential gene expression pattern observed in the microarray dataset when all the E10.5 samples were combined. Twelve of the targets of TGFB1 were downregulated in this dataset (*Coll13a1*, *Adam12*, *Lamb1*, *Col4a2*, *Col4a1*, *Colla1*, *Slit2*, *Mmp14*, *Col5a1*, *Coll18a1*, *Lamc1*, *Slit3*). As illustrated here, many of these targets are not direct targets of TGFB1, but through mediator including CTGF, ERBB2, PRL,  $\beta$ -estradiol, estrogen receptors,  $\beta$ -catenin (CTNNB1), MYC, TP53 and JUN.

## 4.6 Discussion

### 4.6.1 Interpretations

***The Slit2/Robo2 signaling may prevent multiple ureteric buds by changing the ECM composition around the Wolffian duct***

A coordinate downregulation of ECM associated genes (e.g. collagen and laminin coding genes) in E10.5 and E11.5 *Robo2*<sup>-/-</sup> and the *Slit2*<sup>-/-</sup> UB and MM tissues was revealed by both the GSEA and the IPA analyses. These results suggest that the multiple

UB phenotype in *Slit2* and *Robo2* knockout mice might be caused by decreased expression of genes encoding extra-cellular matrix proteins. Under physiological condition (e.g. in the wild type mice), SLIT2-ROBO2 signaling may maintain a high level of ECM protein coding gene expression to strengthen the MM tissue structure and prevent ectopic UB formation (Illustration 4.3, top panel). When SLIT2-ROBO2 signaling is absent (e.g. in patients with *SLIT2/ROBO2* mutations or in *Slit2/Robo2* knockout mice), the ECM protein coding gene expression are downregulated, possibly resulting in an abnormal ECM enabling ectopic UB outgrowth (Illustration 4.3, bottom panel).

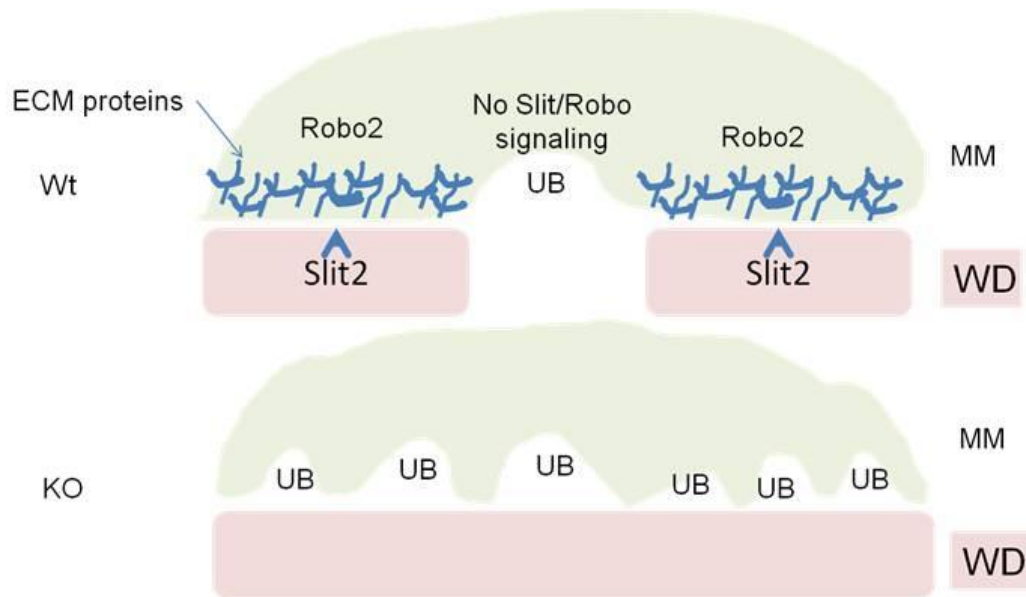


### Illustration 4.3: Generation of a hypothesis

Top panel: illustration of the wild type (wt): absence of SLIT2-ROBO2 signaling in the area of normal ureteric budding and ECM regulation by the SLIT2-ROBO2 signaling around the Wolffian duct to prevent ectopic UB formation. MM- metanephric mesenchyme (green); WD- wolffian duct (pink).

Bottom panel: illustration of the *Robo2* or *Slit2* knockout, in the absence of SLIT2-ROBO2 signaling (e.g. due to a genetic deletion of either *Slit2* or *Robo2*): the expression of ECM proteins is downregulated, leading to ectopic UB formation.

Interestingly, *Slit3*, a close family member of *Slit2*, has been shown to genetically interact with *Fras1-related extracellular matrix gene 1* (*Frem1*), which encodes an extracellular protein (Beck et al., 2013). A statistically significant increase in the prevalence of renal agenesis phenotype has been found in *Frem1*<sup>-/-</sup>;*Slit3*<sup>+/-</sup> double knockout mice (13.6%) as compared to *Frem1*<sup>-/-</sup> single knockout mice (2.7%, p<0.02). This increase in prevalence was more than an additive effect of homozygosity for the *Frem1*<sup>-/-</sup> (2.7%) and heterozygosity for *Slit3*<sup>+/-</sup> (0%) alone (Beck et al., 2013). This

aggravating genetic interaction may reflect a common role for the ECM proteins FREM1 and SLIT3 in UB outgrowth. Since SLIT3 and SLIT2 share a common ALPS domain structure and high overall sequence homology with one another (Brose et al., 1999), it is possible that SLIT2, like SLIT3, shares functions with other ECM proteins like FREM1 during UB outgrowth.

Although the role of the ECM surrounding the Wolffian duct at the time of UB outgrowth has not been investigated thoroughly, the ECM has been shown to play an important role during branching morphogenesis (Santos and Nigam, 1993). Regulation of the ECM composition is partially controlled by matrix metalloproteases (MMP) that degrade extracellular proteins (Pohl et al., 2000; Riggins et al., 2010). During kidney development, MMPs regulate ureteric bud morphogenesis *in vitro* (Pohl et al., 2000). Some ECM proteins, such as Type IV collagen, heparan sulfate proteoglycans, and vitronectin, can also inhibit kidney branching morphogenesis *in vitro* (Santos and Nigam, 1993). *In vivo*, increased levels of ECM proteins such as collagen IV, laminins, perlecan, and nidogen (e.g. due to a decrease in the matrix metalloproteinase MMP14) are associated with a decrease in UB branching morphogenesis (Riggins et al., 2010). ECM proteins can also signal to the surrounding cells through their interactions with integrins (Zent et al., 2001) or act as co-receptors (Linton et al., 2007). This knowledge about branching morphogenesis suggests that changes in the ECM composition may play an important role in inhibiting ectopic UB outgrowth.



***The Slit2/Robo2 signaling may interact with the TGF- $\beta$ 1 signaling pathway in the ureteric bud***

The results from IPA analysis suggest TGF- $\beta$ 1 as a possible upstream regulator inhibiting gene expression changes observed in the UB and MM of *Robo2*<sup>-/-</sup> and the *Slit2*<sup>-/-</sup> knockout mice. TGF- $\beta$  has been shown in vitro to reduce branching morphogenesis and ureteric bud outgrowth in vitro (Bush et al., 2004), suggesting that TGF- $\beta$ 1 inhibition would lead to more ureteric budding. *ROBO2* mutations have been identified in CAKUT patients with VUR (Lu et al., 2007b). Interestingly, SNPs in *TGF- $\beta$ 1* have also been associated with familial VUR (Kuroda et al., 2007), suggesting that *TGF- $\beta$ 1* may play a role in UB and UVJ formation. TGF- $\beta$ 1 induces *Robo1* expression in mammary epithelial cells and SLIT2-ROBO1 activation inhibits mammary branching morphogenesis (Macias et al., 2011). ROBO2 and TGF- $\beta$  also function as modifiers for Drosophila Dystroglycan-Dystrophin Complex (Kucherenko et al., 2008), suggesting that they might interact in additional cellular environment. Therefore, it is possible that TGF- $\beta$ 1 may also induce *Robo2* expression in the MM during UB outgrowth.

***The Slit2/Robo2 signaling may interact with the Insulin-like receptor during UB outgrowth***

Another upstream regulator identified by IPA analysis is IGF1R, the insulin-like growth factor 1 receptor. IGF1R inhibition and downregulation in vitro reduce the size of kidney explants (Wada et al., 1993), and also decrease the biosynthesis of matrix proteins such as type IV collagen, laminin, and proteoglycans (Wada et al., 1993). Like ROBO2,

IGF1R is expressed in the metanephric mesenchyme (Duong Van Huyen et al., 2003). Interestingly, IGF1R ligand IRS-1 has also been shown to interact with NCK (Lee et al., 1993), suggesting that ROBO2 may form a complex with IGF1R through NCK and IRS-1. So ROBO2 and IGF1R may coordinately induce expression of ECM genes in the MM during UB outgrowth.

***The SLIT2-ROBO2 signaling may be regulated by metalloproteases during UB outgrowth***

Although active SLIT2-ROBO2 signaling may enhance ECM structure in MM to prevent ectopic UB formation, a single normal UB needs to be formed at the correct location in the caudal region of the Wolffian duct during UB outgrowth. This condition requires the SLIT2-ROBO2 signaling not being active in the area of the normal UB budding, but only around the normal budding area to prevent abnormal ectopic UB formation. Regulations of several molecules at transcriptional and translational levels might be needed to accomplish this activity.

First, at the transcriptional level, different isoforms of ROBO2 might be differentially expressed in the area of the normal ureteric bud, which may have different interaction capacity with downstream molecules. For example, we have recently found that alternative splicing of *Robo2* can generate isoforms with or without NCK binding site in the ROBO2 protein and that both isoforms are highly expressed during early kidney development (Anna Pisarek Horowitz and Xueping Fan, unpublished data).

Second, at the protein level, ROBO2 might be inactivated in the area of normal budding by metallopeptidases (MMPs). In our microarray dataset, ADAM10, MMP2 and MMP14 are found to be the top MMPs expressed at E10.5 and E11.5 (Table 4.10). *Adam10* was found to be expressed in kidneys explants in vitro (Stuart et al., 2003) and MMP2 and MMP14 have been shown to be expressed in the metanephric mesenchyme at E12.5 (Legallicier et al., 2001).

**Table 4.10: Top genes encoded metallopeptidase that are expressed in E10.5 and E11.5 UB and MM tissues from *Slit2* and *Robo2* knockout mice.**

		Mean log2					
		E10.5	E10.5	E10.5	E10.5	E11.5	E11.5
		Robo2 <sup>+/+</sup>	Robo2 <sup>-/-</sup>	Slit2 <sup>+/+</sup>	Slit2 <sup>-/-</sup>	Robo2 <sup>+/+</sup>	Robo2 <sup>-/-</sup>
Mmp2	matrix metallopeptidase 2	10.89	10.60	10.88	10.62	11.14	11.05
Mmp14	matrix metallopeptidase 14 MT1-MMP	10.04	9.84	10.14	9.87	10.23	10.10
Adam10	disintegrin and metallopeptidase domain 10	9.66	9.70	9.80	9.61	9.88	9.81

One of our proposed models of post-translational regulation of Robo2 is through the matrix metalloprotease kuzbanian (ADAM10 in mice). In *Drosophila*, kuzbanian /ADAM10 cleaves Robo extracellular domain and activates the SLIT-ROBO signaling (Coleman et al., 2010). ADAM10 may be expressed around the WD but not in the area of the normal UB outgrowth (Illustration 4.3).

Alternatively, metalloproteases may inhibit SLIT2-ROBO2 signaling in the area of normal UB outgrowth. A previous study shows that deletion of the matrix metalloproteinase MT1-MMP (MMP14) lead to increased expression levels of the ECM proteins, including collagen IV, laminins, perlecan, and nidogen (Riggins et al., 2010). Our microarray data showed that MMP14 is also expressed in the UB and MM in E10.5 and E11.5 mice. Therefore, it is possible that MMP14 may inhibit the SLIT2-ROBO2 signaling in the area of normal UB outgrowth, which can reduce the expression of ECM proteins such as collagen and laminins to allow a single UB outgrowth.

#### *4.6.2 Limitations*

The fact that no single gene was significantly differentially expressed in our microarray dataset might be explained by an insufficient enrichment of cells normally affected by the SLIT2-ROBO2 signaling in the tissue collected. If most of the cells in the dissected tissues are not affected by SLIT2-ROBO2 signaling, no significant gene expression change could be detected because of the dilution of the changes. Although there is a need to first validate the gene expression changes using real-time RT-PCR, the changes detected might be very limited and only reflect the subtle difference similar to the microarray data because of the heterogeneity of the tissues collected. Another method to validate the findings could be a staining (either IHC/IF or ISH) showing the composition of the extracellular matrix. However, the microarray data suggest a coordinate decrease of the collagens and laminins expression and not a reduction of one

specific ECM protein. In addition, staining with either IHC or ISH might not be sensitive enough to detect such subtle decrease of expression.

The hypothesis/model developed here presumes that the SLIT2-ROBO2 signaling is not active in the region of normal UB budding. In order to test this hypothesis, further experiments are needed. Since we found that alternative splicing of *Robo2* can affect the NCK binding site of ROBO2 (Anna Pisarek Horowitz / Xueping Fan, unpublished data), in situ hybridization or immunostaining detecting two ROBO2 isoforms may provide new information about the regulation of SLIT2-ROBO2 signaling during UB outgrowth.

Alternatively, protein level modifications by MMPs may also regulate ROBO2 or SLIT2 activities, which might be differentially cleaved in different areas of the metanephric mesenchyme. Immunostaining may also enable to detect cleaved and uncleaved isoforms of ROBO2 or SLIT2. For example, an expression comparison between the Robo2 N-terminal fragment (ROBO2-N) and C-terminal fragment (ROBO2-C) at E10.5-E11.5 may reveal differential expression patterns in the MM around the UB during UB outgrowth.

#### **4.7 Conclusions**

GSEA and IPA analyses in this project enabled us to develop a new hypothesis/model on the role of the SLIT2-ROBO2 signaling during early UB outgrowth. Deletion of *Slit2* and *Robo2* in mice leads to a coordinated downregulation of the expression of ECM protein coding genes. Since ROBO2 is expressed in the metanephric

mesenchyme, this microarray data suggest that the Slit2/Robo2 signaling regulates the ECM composition around the nephric duct during UB outgrowth. Since the Slit/Robo signaling should not be active in the normal UB budding area, the ECM composition might be different in the normal UB outgrowth area when compared to the anterior or posterior regions of the MM surrounding the nephric duct. Previous reports have shown the importance of ECM in UB outgrowth and kidney branching morphogenesis, and GDNF, the main factor regulating UB outgrowth is also secreted into the ECM and may be affected by its composition. Altogether, this project enables the development of a new hypothesis regarding the molecular mechanism through which the SLIT2-ROBO2 signaling may regulate UB outgrowth. Further investigations are warranted to test this hypothesis.

## 5. SUMMARY AND CONCLUSIONS

Congenital kidney birth defects are a relatively common health problem, which account for 20-30% of all anomalies identified in the prenatal period with limited diagnostic and treatment options. Prenatal genetic diagnosis can help in prognosis of the defects observed and genetic counseling for the patient's family. However, most of the patients do not benefit from a genetic diagnosis because the molecular bases of most kidney birth defects remain unclear. To understand the molecular basis of these disorders, it is necessary to study human disease genes in animal models during kidney development. In my thesis research, I studied three disease genes (i.e. *Zeb2*, *Ilk*, *Robo2*) in mice models at three stages of kidney development: nephrogenesis, glomerular podocyte, and early ureteric bud outgrowth.

In the first project of this thesis, we studied a mouse model of a gene causing a human syndrome associated with increased risk for kidney anomalies and identified *Zeb2* as a novel gene important in early nephrogenesis. *Zeb2* conditional knockout mice (*Zeb2 cKO*) develop primary glomerulocystic kidney disease starting at E16.5 days and renal failure by 8 weeks of age. In the *Zeb2 cKO* mice, we observed the presence of atubular glomeruli which explain the formation of primary glomerular cysts in the absence of tubular dilatation. Decreased expression of renal proximal tubular markers was observed at E14.5 preceded cyst formation, suggesting that abnormal tubular development is the

cause for congenital atubular glomeruli formation. This is the first description of a primary glomerulocystic kidney disease caused by congenital atubular glomeruli.

At the molecular level, none of the genes associated with glomerular cysts were differentially expressed in the *Zeb2 cKO* mice at E14.5. It suggests that loss of the transcription factor ZEB2 may affect the expression of genes that have not been identified to be associated with glomerular cysts so far.

After cyst formation, *Pkd1* expression was upregulated in non-cystic glomeruli. Such upregulation has been reported on other cystic kidneys, and might be a non-specific event. In order to examine the effect of this upregulation, we genetically reduced the levels of *Pkd1*. Surprisingly; we found an exacerbated renal cystic phenotype in the *Zeb2-Pkd1 double KO* mice.

Together, our results suggest that ZEB2 and PKD1 may genetically interact during nephron development in mice and ZEB2 might be a novel PKD1 modifier gene. This study also implies that ZEB2 is a novel candidate gene for glomerular cystic disease in patients.

The second and third projects of this thesis explore the function of another two kidney disease genes, *ILK* and *ROBO2*, in the podocytes and during early ureteric bud outgrowth. Our results from the second project showed that integrin-linked kinase (ILK) and ROBO2 form a complex in the podocytes, and that loss of *Robo2* alleviates the survival and the ultrastructural defects of the podocyte and GBM in the *Ilk* podocyte specific knockout mice. Our findings suggest that, in addition to podocyte cytoskeleton,



ROBO2 may affect podocyte adhesion to the GBM and the expression of the GBM components.

In the third project, we also explored the molecular function of ROBO2 on gene expression in early ureteric bud formation. We found that ROBO2 may affect the expression of genes encoding extracellular matrix proteins by the metanephric mesenchyme. These two projects led us to form a new hypothesis that ROBO2 may regulate the expression of extracellular matrix proteins in the glomerular basement membrane and around the Wolffian duct during kidney development.

In conclusion, this thesis exemplifies the strength of combining human and mouse genetics to advance our understanding of functions of human kidney disease genes, and to discover new genes important in kidney development. In the past five years, I found *Zeb2* as a new gene important in kidney development and renal cystic disease, and identified a novel role of *Robo2* in regulating extracellular matrix in the podocytes and during early ureteric bud outgrowth. My thesis research also raises a range of scientific questions regarding the mechanistic roles of *Zeb2*, *Ilk*, and *Robo2* in kidney development, which opens many new research opportunities for future scientific inquiry.

## JOURNALS LIST AND ABBREVIATIONS

Acta Paediatr Scand.....	Acta Paediatrica Scandinavica
Acta Neuropathol .....	Acta Neuropathologica
Am J Hum Genet.....	American Journal of Human Genetics
Am J Kidney Dis .....	American Journal of Kidney Diseases
Am J Med Genet.....	American Journal of Medical Genetics
Am J Med Genet A .....	American Journal of Medical Genetics Part A
Am J Med Genet C .....	Semin Med Genet American Journal of Medical ..... Genetics Part C: Seminars in Medical Genetics
Am J Pathol .....	American Journal of Pathology
Am J Physiol .....	American Journal of Physiology
Am J Physiol Cell Physiol .....	American Journal of Physiology - Cell Physiology
Am J Physiol Renal Physiol .....	American Journal of Physiology: Renal Physiology
Arch Pathol Lab Med .....	Archives of Pathology & Laboratory Medicine
Arch Pediatr Adolesc Med.....	Archives of Pediatrics & Adolescent Medicine
Annu Rev Cell Dev Biol.....	Annual Review of Cell and Developmental Biology
Annu Rev Physiol.....	Annual Review of Physiology
BMB Rep.....	Biochemistry and Molecular Biology Reports
Bioarchitecture	
Bioinformatics	
Biostatistics	
Biotechniques	

## Blood

BMC Dev Biol..... BMC Developmental Biology

## Brain

Br J Ophthalmol..... British Journal of Ophthalmology

Cancer Res..... Cancer Research

## Cell

Cell Biosci .....Cell & Bioscience

## Cell Cycle

Cell Tissue Res..... Cell and Tissue Research

Cell Rep.....Cell Reports

## Cell Stem Cell

Circ Res.....Circulation Research

Clin Genet..... Clinical Genetics

Curr Top Pathol.....Current Topics in Pathology

## Development

Dev Biol..... Developmental Biology

Dev Cell..... Developmental Cell

Dev Dyn..... Developmental Dynamics

EMBO J.....EMBO Journal

EMBO Rep..... EMBO reports

Eur J Hum Genet European.....Journal of Human Genetics

Exp Cell Res..... Experimental Cell Research

Exp Eye Res.....	Experimental Eye Research
Fibrogenesis Tissue Repair	
Front Endocrinol.....	Frontiers in endocrinology
Front Pediatr.....	Frontiers in pediatrics
Genes Cells.....	Genes to Cells
Genes Dev.....	Genes & Development
Genesis	
Genet Med.....	Genetics in Medicine
Genomics	
Genom Data.....	Genomics Data
Histochem Cell Biol.....	Histochemistry and Cell Biology
Hum Genet.....	Human Genetics
Hum Mol Genet.....	Human Molecular Genetics
ILAR J.....	Institute for Laboratory Animal Research Journal
Indian J Nephrol.....	Indian Journal of Nephrology
Int J Mol Med .....	International Journal of Molecular Medicine
Int J Nephrol.....	International Journal of Nephrology
Invest Ophthalmol Vis Sci.....	Investigative Ophthalmology & Visual Science
JAMA .....	Journal of the American Medical Association
J Anat.....	Journal of Anatomy
J Biochem.....	Journal of Biochemistry
J Biol Chem.....	Journal of Biological Chemistry

J Cell Biol .....	Journal of Cell Biology
J Cell Sci .....	Journal of Cell Science
J Am Soc Nephrol .....	Journal of the American Society of Nephrology
J Biol Chem .....	Journal of Biological Chemistry
J Clin Invest .....	Journal of Clinical Investigation
J Histochem Cytochem.....	Journal of Histochemistry & Cytochemistry
J Med Genet.....	Journal of Medical Genetics
J Mol Biol.....	Journal of Molecular Biology
J Pathol.....	Journal of Pathology
J Pediatr .....	Journal of Pediatrics
J Pediatr Surg.....	Journal of Pediatric Surgery
J Pediatr Urol.....	Journal of Pediatric Urology
J Neurosci .....	Journal of Neuroscience
J Urol .....	Journal of Urology
Kidney Int .....	Kidney International
Kidney Int Suppl.....	Kidney International Supplements
Lab Invest.....	Laboratory Investigation
Lancet	
Mech Dev.....	Mechanisms of Development
Methods	
Mol Biol Cell.....	Molecular Biology of the Cell
Mol Cell .....	Molecular Cell

Mol Cell Biol.....	Molecular and Cellular Biology
Mol Med.....	Molecular Medicine
Nature	
Nat Cell Biol.....	Nature Cell Biology
Nat Genet.....	Nature Genetics
Nat Neurosci.....	Nature Neuroscience
Nat Rev Nephrol.....	Nature Reviews Nephrology
Nephrol Dial Transplant.....	Nephrology Dialysis Transplantation
Nephron	
Neuron	
N Engl J Med .....	The New England Journal of Medicine
Nucleic Acids Res.....	Nucleic Acids Research
Oncogene	
Organogenesis	
Orphanet J Rare Dis.....	Orphanet Journal of Rare Diseases
Pathol Int.....	Pathology International
PLoS Biol.....	PLOS Biology
PLoS Genet.....	PLOS Genetics
PLoS One	
Prenat Diagn.....	Prenatal Diagnosis
Proc Natl Acad Sci USA.....	Proceedings of the National Academy of Sciences USA
Pediatrics	

Pediatr Nephrol.....	Pediatric Nephrology
Pediatr Radiol.....	Pediatric Radiology
Radiographics	
Science	
Semin Fetal Neonatal Med.....	Seminars in Fetal and Neonatal Medicine
Semin Nephrol.....	Seminars in Nephrology
Trends Genet.....	Trends in Genetics
Wiley Interdiscip Rev Dev Biol.....	Wiley Interdisciplinary Reviews:
.....	.....Developmental Biology
Wiley Interdiscip Rev Syst Biol Med.....	Wiley Interdisciplinary Reviews
.....	.....Systems Biology and Medicine

## BIBLIOGRAPHY

- (1995). Polycystic kidney disease: the complete structure of the PKD1 gene and its protein. The International Polycystic Kidney Disease Consortium. *Cell* 81, 289-298.
- Abrahamson, D.R. (1985). Origin of the glomerular basement membrane visualized after in vivo labeling of laminin in newborn rat kidneys. *J Cell Biol* 100, 1988-2000.
- Abrahamson, D.R. (2012). Role of the podocyte (and glomerular endothelium) in building the GBM. *Semin Nephrol* 32, 342-349.
- Abrahamson, D.R., Hudson, B.G., Stroganova, L., Borza, D.B., and St John, P.L. (2009). Cellular origins of type IV collagen networks in developing glomeruli. *J Am Soc Nephrol* 20, 1471-1479.
- Abrahamson, D.R., Isom, K., Roach, E., Stroganova, L., Zelenchuk, A., Miner, J.H., and St John, P.L. (2007). Laminin compensation in collagen alpha3(IV) knockout (Alport) glomeruli contributes to permeability defects. *J Am Soc Nephrol* 18, 2465-2472.
- Adam, M.P., Conta, J., and Bean, L.J.H. (1993). Mowat-Wilson Syndrome. *GeneReviews*.
- Ahn, S.Y., Kim, Y., Kim, S.T., Swat, W., and Miner, J.H. (2013). Scaffolding proteins DLG1 and CASK cooperate to maintain the nephron progenitor population during kidney development. *J Am Soc Nephrol* 24, 1127-1138.
- Airik, R., and Kispert, A. (2007). Down the tube of obstructive nephropathies: the importance of tissue interactions during ureter development. *Kidney Int* 72, 1459-1467.
- Albrecht, B., Liebers, M., and Kohlhase, J. (2004). Atypical phenotype and intrafamilial variability associated with a novel SALL1 mutation. *Am J Med Genet A* 125A, 102-104.
- Arnold, S.J., Maretto, S., Islam, A., Bikoff, E.K., and Robertson, E.J. (2006). Dose-dependent Smad1, Smad5 and Smad8 signaling in the early mouse embryo. *Dev Biol* 296, 104-118.
- Arts, H.H., Bongers, E.M., Mans, D.A., van Beersum, S.E., Oud, M.M., Bolat, E., Spruijt, L., Cornelissen, E.A., Schuurs-Hoeijmakers, J.H., de Leeuw, N., *et al.* (2011). C14ORF179 encoding IFT43 is mutated in Sensenbrenner syndrome. *J Med Genet* 48, 390-395.



Arts, H.H., and Knoers, N.V. (2013). Current insights into renal ciliopathies: what can genetics teach us? *Pediatr Nephrol* 28, 863-874.

Ashraf, S., Gee, H.Y., Woerner, S., Xie, L.X., Vega-Warner, V., Lovric, S., Fang, H., Song, X., Cattran, D.C., Avila-Casado, C., *et al.* (2013). ADCK4 mutations promote steroid-resistant nephrotic syndrome through CoQ10 biosynthesis disruption. *J Clin Invest* 123, 5179-5189.

Bachmann-Gagescu, R., Mefford, H.C., Cowan, C., Glew, G.M., Hing, A.V., Wallace, S., Bader, P.I., Hamati, A., Reitnauer, P.J., Smith, R., *et al.* (2010). Recurrent 200-kb deletions of 16p11.2 that include the SH2B1 gene are associated with developmental delay and obesity. *Genet Med* 12, 641-647.

Banas, M.C., Parks, W.T., Hudkins, K.L., Banas, B., Holdren, M., Iyoda, M., Wietecha, T.A., Kowalewska, J., Liu, G., and Alpers, C.E. (2007). Localization of TGF-beta signaling intermediates Smad2, 3, 4, and 7 in developing and mature human and mouse kidney. *J Histochem Cytochem* 55, 275-285.

Basson, M.A., Akbulut, S., Watson-Johnson, J., Simon, R., Carroll, T.J., Shakya, R., Gross, I., Martin, G.R., Lufkin, T., McMahan, A.P., *et al.* (2005). Sprouty1 is a critical regulator of GDNF/RET-mediated kidney induction. *Dev Cell* 8, 229-239.

Batourina, E., Tsai, S., Lambert, S., Sprenkle, P., Viana, R., Dutta, S., Hensle, T., Wang, F., Niederreither, K., McMahan, A.P., *et al.* (2005). Apoptosis induced by vitamin A signaling is crucial for connecting the ureters to the bladder. *Nat Genet* 37, 1082-1089.

Beaulieu, C.L., Huang, L., Innes, A.M., Akimenko, M.A., Puffenberger, E.G., Schwartz, C., Jerry, P., Ober, C., Hegele, R.A., McLeod, D.R., *et al.* (2013). Intellectual disability associated with a homozygous missense mutation in THOC6. *Orphanet J Rare Dis* 8, 62.

Beck, T.F., Shchelochkov, O.A., Yu, Z., Kim, B.J., Hernandez-Garcia, A., Zaveri, H.P., Bishop, C., Overbeek, P.A., Stockton, D.W., Justice, M.J., *et al.* (2013). Novel frem1-related mouse phenotypes and evidence of genetic interactions with gata4 and slit3. *PLoS One* 8, e58830.

Bermejo-Sanchez, E., Cuevas, L., Amar, E., Bakker, M.K., Bianca, S., Bianchi, F., Canfield, M.A., Castilla, E.E., Clementi, M., Cocchi, G., *et al.* (2011). Amelia: a multi-center descriptive epidemiologic study in a large dataset from the International Clearinghouse for Birth Defects Surveillance and Research, and overview of the literature. *Am J Med Genet C Semin Med Genet* 157C, 288-304.

Bernstein, J. (1993). Glomerulocystic kidney disease--nosological considerations. *Pediatr Nephrol* 7, 464-470.

Bertoli-Avella, A.M., Conte, M.L., Punzo, F., de Graaf, B.M., Lama, G., La Manna, A., Polito, C., Grassia, C., Nobili, B., Rambaldi, P.F., *et al.* (2008). ROBO2 gene variants are associated with familial vesicoureteral reflux. *J Am Soc Nephrol* 19, 825-831.

Bingham, C., Bulman, M.P., Ellard, S., Allen, L.I., Lipkin, G.W., Hoff, W.G., Woolf, A.S., Rizzoni, G., Novelli, G., Nicholls, A.J., *et al.* (2001). Mutations in the hepatocyte nuclear factor-1beta gene are associated with familial hypoplastic glomerulocystic kidney disease. *American journal of human genetics* 68, 219-224.

Bissler, J.J., Siroky, B.J., and Yin, H. (2010). Glomerulocystic kidney disease. *Pediatr Nephrol* 25, 2049-2056; quiz 2056-2049.

Bitner-Glindzicz, M., Lindley, K.J., Rutland, P., Blaydon, D., Smith, V.V., Milla, P.J., Hussain, K., Furth-Lavi, J., Cosgrove, K.E., Shepherd, R.M., *et al.* (2000). A recessive contiguous gene deletion causing infantile hyperinsulinism, enteropathy and deafness identifies the Usher type 1C gene. *Nat Genet* 26, 56-60.

Blake, J.A., Bult, C.J., Kadin, J.A., Richardson, J.E., and Eppig, J.T. (2011). The Mouse Genome Database (MGD): premier model organism resource for mammalian genomics and genetics. *Nucleic Acids Res* 39, D842-848.

Blank, U., Seto, M.L., Adams, D.C., Wojchowski, D.M., Karolak, M.J., and Oxburgh, L. (2008). An in vivo reporter of BMP signaling in organogenesis reveals targets in the developing kidney. *BMC Dev Biol* 8, 86.

Bover, J., and Cozzolino, M. (2011). Mineral and bone disorders in chronic kidney disease and end-stage renal disease patients: new insights into vitamin D receptor activation. *Kidney Int Suppl* (2011) 1, 122-129.

Boyer, O., Nevo, F., Plaisier, E., Funalot, B., Gribouval, O., Benoit, G., Huynh Cong, E., Arrondel, C., Tete, M.J., Montjean, R., *et al.* (2011). INF2 mutations in Charcot-Marie-Tooth disease with glomerulopathy. *N Engl J Med* 365, 2377-2388.

Brabletz, S., and Brabletz, T. (2010). The ZEB/miR-200 feedback loop--a motor of cellular plasticity in development and cancer? *EMBO Rep* 11, 670-677.

Bracken, C.P., Gregory, P.A., Kolesnikoff, N., Bert, A.G., Wang, J., Shannon, M.F., and Goodall, G.J. (2008). A double-negative feedback loop between ZEB1-SIP1 and the microRNA-200 family regulates epithelial-mesenchymal transition. *Cancer Res* 68, 7846-7854.

Brenner-Anantharam, A., Cebrian, C., Guillaume, R., Hurtado, R., Sun, T.T., and Herzlinger, D. (2007). Tailbud-derived mesenchyme promotes urinary tract segmentation via BMP4 signaling. *Development* 134, 1967-1975.

Brophy, P.D., Ostrom, L., Lang, K.M., and Dressler, G.R. (2001). Regulation of ureteric bud outgrowth by Pax2-dependent activation of the glial derived neurotrophic factor gene. *Development* 128, 4747-4756.

Brose, K., Bland, K.S., Wang, K.H., Arnott, D., Henzel, W., Goodman, C.S., Tessier-Lavigne, M., and Kidd, T. (1999). Slit proteins bind Robo receptors and have an evolutionarily conserved role in repulsive axon guidance. *Cell* 96, 795-806.

Brunetti-Pierri, N., Berg, J.S., Scaglia, F., Belmont, J., Bacino, C.A., Sahoo, T., Lalani, S.R., Graham, B., Lee, B., Shinawi, M., *et al.* (2008). Recurrent reciprocal 1q21.1 deletions and duplications associated with microcephaly or macrocephaly and developmental and behavioral abnormalities. *Nat Genet* 40, 1466-1471.

Bush, K.T., Sakurai, H., Steer, D.L., Leonard, M.O., Sampogna, R.V., Meyer, T.N., Schwesinger, C., Qiao, J., and Nigam, S.K. (2004). TGF-beta superfamily members modulate growth, branching, shaping, and patterning of the ureteric bud. *Dev Biol* 266, 285-298.

Cain, J.E., Islam, E., Haxho, F., Blake, J., and Rosenblum, N.D. (2011). GLI3 repressor controls functional development of the mouse ureter. *J Clin Invest* 121, 1199-1206.

Cammas, L., Wolfe, J., Choi, S.Y., Dedhar, S., and Beggs, H.E. (2012). Integrin-linked kinase deletion in the developing lens leads to capsule rupture, impaired fiber migration and non-apoptotic epithelial cell death. *Invest Ophthalmol Vis Sci* 53, 3067-3081.

Castori, M., Brancati, F., Rinaldi, R., Adami, L., Mingarelli, R., Grammatico, P., and Dallapiccola, B. (2006). Antenatal presentation of the oculo-auriculo-vertebral spectrum (OAVS). *Am J Med Genet A* 140, 1573-1579.

Caubit, X., Lye, C.M., Martin, E., Core, N., Long, D.A., Vola, C., Jenkins, D., Garratt, A.N., Skaer, H., Woolf, A.S., *et al.* (2008). Teashirt 3 is necessary for ureteral smooth muscle differentiation downstream of SHH and BMP4. *Development* 135, 3301-3310.

CDC (2008). Update on overall prevalence of major birth defects--Atlanta, Georgia, 1978-2005. *MMWR Morb Mortal Wkly Rep* 57, 1-5.

Chaki, S.P., and Rivera, G.M. (2013). Integration of signaling and cytoskeletal remodeling by Nck in directional cell migration. *Bioarchitecture* 3, 57-63.

Chang, Y., Twiss, J.L., Horoupian, D.S., Caldwell, S.A., and Johnston, K.M. (1993). Inherited syndrome of infantile olivopontocerebellar atrophy, micronodular cirrhosis, and renal tubular microcysts: review of the literature and a report of an additional case. *Acta Neuropathol* 86, 399-404.

Chevalier, R.L., and Forbes, M.S. (2008). Generation and evolution of atubular glomeruli in the progression of renal disorders. *J Am Soc Nephrol* 19, 197-206.

Cole, T.R., May, A., and Hughes, H.E. (1991). Alpha thalassaemia/mental retardation syndrome (non-deletional type): report of a family supporting X linked inheritance. *J Med Genet* 28, 734-737.

Coleman, H.A., Labrador, J.P., Chance, R.K., and Bashaw, G.J. (2010). The Adam family metalloprotease Kuzbanian regulates the cleavage of the roundabout receptor to control axon repulsion at the midline. *Development* 137, 2417-2426.

Coles, H.S., Burne, J.F., and Raff, M.C. (1993). Large-scale normal cell death in the developing rat kidney and its reduction by epidermal growth factor. *Development* 118, 777-784.

Colgin, L.M., Hackmann, A.F., Emond, M.J., and Monnat, R.J., Jr. (2002). The unexpected landscape of in vivo somatic mutation in a human epithelial cell lineage. *Proc Natl Acad Sci U S A* 99, 1437-1442.

Colin, E., Huynh Cong, E., Mollet, G., Guichet, A., Gribouval, O., Arrondel, C., Boyer, O., Daniel, L., Gubler, M.C., Ekinici, Z., *et al.* (2014). Loss-of-function mutations in WDR73 are responsible for microcephaly and steroid-resistant nephrotic syndrome: Galloway-Mowat syndrome. *Am J Hum Genet* 95, 637-648.

Comijn, J., Berx, G., Vermassen, P., Verschueren, K., van Grunsven, L., Bruyneel, E., Mareel, M., Huylebroeck, D., and van Roy, F. (2001). The two-handed E box binding zinc finger protein SIP1 downregulates E-cadherin and induces invasion. *Mol Cell* 7, 1267-1278.

Conidi, A., van den Berghe, V., Leslie, K., Stryjewska, A., Xue, H., Chen, Y.G., Seuntjens, E., and Huylebroeck, D. (2013). Four amino acids within a tandem QxVx repeat in a predicted extended alpha-helix of the Smad-binding domain of Sip1 are necessary for binding to activated Smad proteins. *PLoS One* 8, e76733.

Connolly, L.P., Treves, S.T., Connolly, S.A., Zurakowski, D., Share, J.C., Bar-Sever, Z., Mitchell, K.D., and Bauer, S.B. (1997). Vesicoureteral reflux in children: incidence and severity in siblings. *J Urol* 157, 2287-2290.

Cordell, H.J., Darlay, R., Charoen, P., Stewart, A., Gullett, A.M., Lambert, H.J., Malcolm, S., Feather, S.A., Goodship, T.H., Woolf, A.S., *et al.* (2010). Whole-genome linkage and association scan in primary, nonsyndromic vesicoureteric reflux. *J Am Soc Nephrol* 21, 113-123.

- Cormier-Daire, V., Lyonnet, S., Lehnert, A., Martin, D., Salomon, R., Patey, N., Broyer, M., Ricour, C., and Munnich, A. (1995). Craniosynostosis and kidney malformation in a case of Hennekam syndrome. *Am J Med Genet* 57, 66-68.
- Costantini, F. (2010). GDNF/Ret signaling and renal branching morphogenesis: From mesenchymal signals to epithelial cell behaviors. *Organogenesis* 6, 252-262.
- Costantini, F., and Kopan, R. (2010). Patterning a complex organ: branching morphogenesis and nephron segmentation in kidney development. *Dev Cell* 18, 698-712.
- Dai, C., Stolz, D.B., Bastacky, S.I., St-Arnaud, R., Wu, C., Dedhar, S., and Liu, Y. (2006). Essential role of integrin-linked kinase in podocyte biology: Bridging the integrin and slit diaphragm signaling. *J Am Soc Nephrol* 17, 2164-2175.
- Davidson, A.J. (2008). Mouse kidney development. *StemBook*.
- Debiec, H., Kutsche, M., Schachner, M., and Ronco, P. (2002). Abnormal renal phenotype in L1 knockout mice: a novel cause of CAKUT. *Nephrol Dial Transplant* 17 *Suppl* 9, 42-44.
- Deshpande, C., and Hennekam, R.C. (2008). Genetic syndromes and prenatally detected renal anomalies. *Semin Fetal Neonatal Med* 13, 171-180.
- Dickson, B.J., and Gilestro, G.F. (2006). Regulation of commissural axon pathfinding by slit and its Robo receptors. *Annu Rev Cell Dev Biol* 22, 651-675.
- Diez-Roux, G., Banfi, S., Sultan, M., Geffers, L., Anand, S., Rozado, D., Magen, A., Canidio, E., Pagani, M., Peluso, I., *et al.* (2011). A high-resolution anatomical atlas of the transcriptome in the mouse embryo. *PLoS Biol* 9, e1000582.
- Dressler, G.R. (2009). Advances in early kidney specification, development and patterning. *Development* 136, 3863-3874.
- Dressler, G.R., Deutsch, U., Chowdhury, K., Nornes, H.O., and Gruss, P. (1990). Pax2, a new murine paired-box-containing gene and its expression in the developing excretory system. *Development* 109, 787-795.
- Dreyer, S.D., Zhou, G., Baldini, A., Winterpacht, A., Zabel, B., Cole, W., Johnson, R.L., and Lee, B. (1998). Mutations in LMX1B cause abnormal skeletal patterning and renal dysplasia in nail patella syndrome. *Nat Genet* 19, 47-50.
- Duong Van Huyen, J.P., Amri, K., Belair, M.F., Vilar, J., Merlet-Benichou, C., Bruneval, P., and Lelievre-Pegorier, M. (2003). Spatiotemporal distribution of insulin-like growth factor receptors during nephrogenesis in fetuses from normal and diabetic rats. *Cell Tissue Res* 314, 367-379.

- Eccles, M.R., Bailey, R.R., Abbott, G.D., and Sullivan, M.J. (1996). Unravelling the genetics of vesicoureteric reflux: a common familial disorder. *Hum Mol Genet* 5, 1425-1429.
- Eke, T., Woodruff, G., and Young, I.D. (1996). A new oculorenal syndrome: retinal dystrophy and tubulointerstitial nephropathy in cranioectodermal dysplasia. *Br J Ophthalmol* 80, 490-491.
- Eknoyan, G. (2009). A clinical view of simple and complex renal cysts. *J Am Soc Nephrol* 20, 1874-1876.
- El-Aouni, C., Herbach, N., Blattner, S.M., Henger, A., Rastaldi, M.P., Jarad, G., Miner, J.H., Moeller, M.J., St-Arnaud, R., Dedhar, S., *et al.* (2006). Podocyte-specific deletion of integrin-linked kinase results in severe glomerular basement membrane alterations and progressive glomerulosclerosis. *J Am Soc Nephrol* 17, 1334-1344.
- El-Kasti, M.M., Wells, T., and Carter, D.A. (2012). A novel long-range enhancer regulates postnatal expression of *Zeb2*: implications for Mowat-Wilson syndrome phenotypes. *Hum Mol Genet* 21, 5429-5442.
- Elsea, S.H., and Lucas, R.E. (2002). The mousetrap: what we can learn when the mouse model does not mimic the human disease. *ILAR J* 43, 66-79.
- Endris, V., Haussmann, L., Buss, E., Bacon, C., Bartsch, D., and Rappold, G. (2011). *SrGAP3* interacts with lamellipodin at the cell membrane and regulates Rac-dependent cellular protrusions. *J Cell Sci* 124, 3941-3955.
- Engenheiro, E., Moller, R.S., Pinto, M., Soares, G., Nikanorova, M., Carreira, I.M., Ullmann, R., Tommerup, N., and Tumer, Z. (2008). Mowat-Wilson syndrome: an underdiagnosed syndrome? *Clin Genet* 73, 579-584.
- Fan, X., Labrador, J.P., Hing, H., and Bashaw, G.J. (2003). Slit stimulation recruits Dock and Pak to the roundabout receptor and increases Rac activity to regulate axon repulsion at the CNS midline. *Neuron* 40, 113-127.
- Fan, X., Li, Q., Pisarek-Horowitz, A., Rasouly, H.M., Wang, X., Bonegio, R.G., Wang, H., McLaughlin, M., Mangos, S., Kalluri, R., *et al.* (2012). Inhibitory effects of *Robo2* on nephrin: a crosstalk between positive and negative signals regulating podocyte structure. *Cell Rep* 2, 52-61.
- Feather, S.A., Malcolm, S., Woolf, A.S., Wright, V., Blaydon, D., Reid, C.J., Flinter, F.A., Proesmans, W., Devriendt, K., Carter, J., *et al.* (2000). Primary, nonsyndromic vesicoureteric reflux and its nephropathy is genetically heterogeneous, with a locus on chromosome 1. *Am J Hum Genet* 66, 1420-1425.

- Feather, S.A., Winyard, P.J., Dodd, S., and Woolf, A.S. (1997). Oral-facial-digital syndrome type 1 is another dominant polycystic kidney disease: clinical, radiological and histopathological features of a new kindred. *Nephrol Dial Transplant* 12, 1354-1361.
- Fedeles, S.V., Tian, X., Gallagher, A.R., Mitobe, M., Nishio, S., Lee, S.H., Cai, Y., Geng, L., Crews, C.M., and Somlo, S. (2011). A genetic interaction network of five genes for human polycystic kidney and liver diseases defines polycystin-1 as the central determinant of cyst formation. *Nat Genet* 43, 639-647.
- Ferrante, M.I., Zullo, A., Barra, A., Bimonte, S., Messaddeq, N., Studer, M., Dolle, P., and Franco, B. (2006). Oral-facial-digital type I protein is required for primary cilia formation and left-right axis specification. *Nat Genet* 38, 112-117.
- Finger, J.H., Smith, C.M., Hayamizu, T.F., McCright, I.J., Eppig, J.T., Kadin, J.A., Richardson, J.E., and Ringwald, M. (2011). The mouse Gene Expression Database (GXD): 2011 update. *Nucleic Acids Res* 39, D835-841.
- Forbes, M.S., Thornhill, B.A., and Chevalier, R.L. (2011). Proximal tubular injury and rapid formation of atubular glomeruli in mice with unilateral ureteral obstruction: a new look at an old model. *Am J Physiol Renal Physiol* 301, F110-117.
- Forbes, M.S., Thornhill, B.A., Galarreta, C.I., Minor, J.J., Gordon, K.A., and Chevalier, R.L. (2013). Chronic unilateral ureteral obstruction in the neonatal mouse delays maturation of both kidneys and leads to late formation of atubular glomeruli. *Am J Physiol Renal Physiol* 305, F1736-1746.
- Forrester, S., Kovach, M.J., Reynolds, N.M., Urban, R., and Kimonis, V. (2001). Manifestations in four males with and an obligate carrier of the Lenz microphthalmia syndrome. *Am J Med Genet* 98, 92-100.
- Fricke, C., Lee, J.S., Geiger-Rudolph, S., Bonhoeffer, F., and Chien, C.B. (2001). *astray*, a zebrafish roundabout homolog required for retinal axon guidance. *Science* 292, 507-510.
- Funari, V.A., Krakow, D., Nevarez, L., Chen, Z., Funari, T.L., Vatanavicharn, N., Wilcox, W.R., Rimoin, D.L., Nelson, S.F., and Cohn, D.H. (2010). BMPER mutation in diaphanospondylodysostosis identified by ancestral autozygosity mapping and targeted high-throughput sequencing. *Am J Hum Genet* 87, 532-537.
- Galarreta, C.I., Grantham, J.J., Forbes, M.S., Maser, R.L., Wallace, D.P., and Chevalier, R.L. (2014). Tubular obstruction leads to progressive proximal tubular injury and atubular glomeruli in polycystic kidney disease. *Am J Pathol* 184, 1957-1966.
- Gamp, A.C., Tanaka, Y., Lullmann-Rauch, R., Wittke, D., D'Hooge, R., De Deyn, P.P., Moser, T., Maier, H., Hartmann, D., Reiss, K., *et al.* (2003). LIMP-2/LGP85 deficiency

- causes ureteric pelvic junction obstruction, deafness and peripheral neuropathy in mice. *Hum Mol Genet* 12, 631-646.
- Garavelli, L., and Mainardi, P.C. (2007). Mowat-Wilson syndrome. *Orphanet J Rare Dis* 2, 42.
- Gautier, L., Cope, L., Bolstad, B.M., and Irizarry, R.A. (2004). affy--analysis of Affymetrix GeneChip data at the probe level. *Bioinformatics* 20, 307-315.
- Geng, L., Segal, Y., Pavlova, A., Barros, E.J., Lohning, C., Lu, W., Nigam, S.K., Frischauf, A.M., Reeders, S.T., and Zhou, J. (1997). Distribution and developmentally regulated expression of murine polycystin. *Am J Physiol* 272, F451-459.
- George, B., and Holzman, L.B. (2012). Signaling from the podocyte intercellular junction to the actin cytoskeleton. *Semin Nephrol* 32, 307-318.
- Ghoumid, J., Drevillon, L., Alavi-Naini, S.M., Bondurand, N., Rio, M., Briand-Suleau, A., Nasser, M., Goodwin, L., Raymond, P., Yanicostas, C., *et al.* (2013). ZEB2 zinc-finger missense mutations lead to hypomorphic alleles and a mild Mowat-Wilson syndrome. *Human molecular genetics* 22, 2652-2661.
- Gibson, I.W., Downie, T.T., More, I.A., and Lindop, G.B. (1996). Atubular glomeruli and glomerular cysts--a possible pathway for nephron loss in the human kidney? *J Pathol* 179, 421-426.
- Girgert, R., Martin, M., Kruegel, J., Miosge, N., Temme, J., Eckes, B., Muller, G.A., and Gross, O. (2010). Integrin alpha2-deficient mice provide insights into specific functions of collagen receptors in the kidney. *Fibrogenesis Tissue Repair* 3, 19.
- Glessner, J.T., Bick, A.G., Ito, K., Homsy, J.G., Rodriguez-Murillo, L., Fromer, M., Mazaika, E., Vardarajan, B., Italia, M., Leipzig, J., *et al.* (2014). Increased frequency of de novo copy number variants in congenital heart disease by integrative analysis of single nucleotide polymorphism array and exome sequence data. *Circ Res* 115, 884-896.
- Goldenberg, A., Wolf, C., Chevy, F., Benachi, A., Dumez, Y., Munnich, A., and Cormier-Daire, V. (2004). Antenatal manifestations of Smith-Lemli-Opitz (RSH) syndrome: a retrospective survey of 30 cases. *Am J Med Genet A* 124A, 423-426.
- Gong, K.Q., Yallowitz, A.R., Sun, H., Dressler, G.R., and Wellik, D.M. (2007). A Hox-Eya-Pax complex regulates early kidney developmental gene expression. *Mol Cell Biol* 27, 7661-7668.
- Good, D.W., and George, T. (2001). Neurotrophin-3 inhibits HCO absorption via a cAMP-dependent pathway in renal thick ascending limb. *Am J Physiol Cell Physiol* 281, C1804-1811.



Grabitz, A.L., and Duncan, M.K. (2012). Focus on molecules: Smad Interacting Protein 1 (Sip1, ZEB2, ZFH1B). *Exp Eye Res* 101, 105-106.

Greenberg, F., Lewis, R.A., Potocki, L., Glaze, D., Parke, J., Killian, J., Murphy, M.A., Williamson, D., Brown, F., Dutton, R., *et al.* (1996). Multi-disciplinary clinical study of Smith-Magenis syndrome (deletion 17p11.2). *Am J Med Genet* 62, 247-254.

Greka, A., and Mundel, P. (2012). Cell biology and pathology of podocytes. *Annu Rev Physiol* 74, 299-323.

Gribouval, O., Gonzales, M., Neuhaus, T., Aziza, J., Bieth, E., Laurent, N., Bouton, J.M., Feuillet, F., Makni, S., Ben Amar, H., *et al.* (2005). Mutations in genes in the renin-angiotensin system are associated with autosomal recessive renal tubular dysgenesis. *Nat Genet* 37, 964-968.

Grieshammer, U., Le, M., Plump, A.S., Wang, F., Tessier-Lavigne, M., and Martin, G.R. (2004). SLIT2-mediated ROBO2 signaling restricts kidney induction to a single site. *Dev Cell* 6, 709-717.

Grote, D., Boualia, S.K., Souabni, A., Merkel, C., Chi, X., Costantini, F., Carroll, T., and Bouchard, M. (2008). Gata3 acts downstream of beta-catenin signaling to prevent ectopic metanephric kidney induction. *PLoS Genet* 4, e1000316.

Hains, D.S., Sims-Lucas, S., Carpenter, A., Saha, M., Murawski, I., Kish, K., Gupta, I., McHugh, K., and Bates, C.M. (2010). High incidence of vesicoureteral reflux in mice with *Fgfr2* deletion in kidney mesenchyma. *J Urol* 183, 2077-2084.

Halbritter, J., Bizet, A.A., Schmidts, M., Porath, J.D., Braun, D.A., Gee, H.Y., McInerney-Leo, A.M., Krug, P., Filhol, E., Davis, E.E., *et al.* (2013). Defects in the IFT-B component IFT172 cause Jeune and Mainzer-Saldino syndromes in humans. *Am J Hum Genet* 93, 915-925.

Hannibal, M.C., Buckingham, K.J., Ng, S.B., Ming, J.E., Beck, A.E., McMillin, M.J., Gildersleeve, H.I., Bigham, A.W., Tabor, H.K., Mefford, H.C., *et al.* (2011). Spectrum of MLL2 (ALR) mutations in 110 cases of Kabuki syndrome. *Am J Med Genet A* 155A, 1511-1516.

Hannigan, G.E., Leung-Hagesteijn, C., Fitz-Gibbon, L., Coppolino, M.G., Radeva, G., Filmus, J., Bell, J.C., and Dedhar, S. (1996). Regulation of cell adhesion and anchorage-dependent growth by a new beta 1-integrin-linked protein kinase. *Nature* 379, 91-96.

Harding, S.D., Armit, C., Armstrong, J., Brennan, J., Cheng, Y., Haggarty, B., Houghton, D., Lloyd-MacGilp, S., Pi, X., Roochun, Y., *et al.* (2011). The GUDMAP database--an online resource for genitourinary research. *Development* 138, 2845-2853.

- Harris, P.C., and Torres, V.E. (2014). Genetic mechanisms and signaling pathways in autosomal dominant polycystic kidney disease. *J Clin Invest* *124*, 2315-2324.
- Heinritz, W., Zweier, C., Froster, U.G., Strenge, S., Kujat, A., Syrbe, S., Rauch, A., and Schuster, V. (2006). A missense mutation in the ZFHX1B gene associated with an atypical Mowat-Wilson syndrome phenotype. *Am J Med Genet A* *140*, 1223-1227.
- Helal, I., Fick-Brosnahan, G.M., Reed-Gitomer, B., and Schrier, R.W. (2012). Glomerular hyperfiltration: definitions, mechanisms and clinical implications. *Nat Rev Nephrol* *8*, 293-300.
- Higashi, Y., Maruhashi, M., Nelles, L., Van de Putte, T., Verschueren, K., Miyoshi, T., Yoshimoto, A., Kondoh, H., and Huylebroeck, D. (2002). Generation of the floxed allele of the SIP1 (Smad-interacting protein 1) gene for Cre-mediated conditional knockout in the mouse. *Genesis* *32*, 82-84.
- Higgins, A.W., Alkuraya, F.S., Bosco, A.F., Brown, K.K., Bruns, G.A., Donovan, D.J., Eisenman, R., Fan, Y., Farra, C.G., Ferguson, H.L., *et al.* (2008). Characterization of apparently balanced chromosomal rearrangements from the developmental genome anatomy project. *Am J Hum Genet* *82*, 712-722.
- Hildebrandt, F., and Otto, E. (2005). Cilia and centrosomes: a unifying pathogenic concept for cystic kidney disease? *Nat Rev Genet* *6*, 928-940.
- Ho, J. (2014). The regulation of apoptosis in kidney development: implications for nephron number and pattern? *Front Pediatr* *2*, 128.
- Hossain, Z., Ali, S.M., Ko, H.L., Xu, J., Ng, C.P., Guo, K., Qi, Z., Ponniah, S., Hong, W., and Hunziker, W. (2007). Glomerulocystic kidney disease in mice with a targeted inactivation of *Wwtr1*. *Proc Natl Acad Sci U S A* *104*, 1631-1636.
- Huber, C., and Cormier-Daire, V. (2012). Ciliary disorder of the skeleton. *Am J Med Genet C Semin Med Genet* *160C*, 165-174.
- Hughson, M., Farris, A.B., 3rd, Douglas-Denton, R., Hoy, W.E., and Bertram, J.F. (2003). Glomerular number and size in autopsy kidneys: the relationship to birth weight. *Kidney Int* *63*, 2113-2122.
- Irizarry, R.A., Hobbs, B., Collin, F., Beazer-Barclay, Y.D., Antonellis, K.J., Scherf, U., and Speed, T.P. (2003). Exploration, normalization, and summaries of high density oligonucleotide array probe level data. *Biostatistics* *4*, 249-264.
- Ishii, T., Satoh, E., and Nishimura, M. (2001). Integrin-linked kinase controls neurite outgrowth in N1E-115 neuroblastoma cells. *J Biol Chem* *276*, 42994-43003.

- Je, H.S., Yang, F., Ji, Y., Nagappan, G., Hempstead, B.L., and Lu, B. (2012). Role of pro-brain-derived neurotrophic factor (proBDNF) to mature BDNF conversion in activity-dependent competition at developing neuromuscular synapses. *Proc Natl Acad Sci U S A* *109*, 15924-15929.
- Jiang, Q., Fujimura, S., Kobayashi, C., and Nishinakamura, R. (2010). Overexpression of Sall1 in vivo leads to reduced body weight without affecting kidney development. *J Biochem* *147*, 445-450.
- Jonckheere, A.I., Renkema, G.H., Bras, M., van den Heuvel, L.P., Hoischen, A., Gilissen, C., Nabuurs, S.B., Huynen, M.A., de Vries, M.C., Smeitink, J.A., *et al.* (2013). A complex V ATP5A1 defect causes fatal neonatal mitochondrial encephalopathy. *Brain* *136*, 1544-1554.
- Jones, N., Blasutig, I.M., Eremina, V., Ruston, J.M., Bladt, F., Li, H., Huang, H., Larose, L., Li, S.S., Takano, T., *et al.* (2006). Nck adaptor proteins link nephrin to the actin cytoskeleton of kidney podocytes. *Nature* *440*, 818-823.
- Jumlongras, D., Lachke, S.A., O'Connell, D.J., Aboukhalil, A., Li, X., Choe, S.E., Ho, J.W., Turbe-Doan, A., Robertson, E.A., Olsen, B.R., *et al.* (2012). An evolutionarily conserved enhancer regulates Bmp4 expression in developing incisor and limb bud. *PLoS One* *7*, e38568.
- Kaefer, M., Curran, M., Treves, S.T., Bauer, S., Hendren, W.H., Peters, C.A., Atala, A., Diamond, D., and Retik, A. (2000). Sibling vesicoureteral reflux in multiple gestation births. *Pediatrics* *105*, 800-804.
- Kalatzis, V., Abdelhak, S., Compain, S., Vincent, C., and Petit, C. (1996). Characterization of a translocation-associated deletion defines the candidate region for the gene responsible for branchio-oto-renal syndrome. *Genomics* *34*, 422-425.
- Kalluri, R., Shield, C.F., Todd, P., Hudson, B.G., and Neilson, E.G. (1997). Isoform switching of type IV collagen is developmentally arrested in X-linked Alport syndrome leading to increased susceptibility of renal basement membranes to endoproteolysis. *J Clin Invest* *99*, 2470-2478.
- Kam, R.K., Deng, Y., Chen, Y., and Zhao, H. (2012). Retinoic acid synthesis and functions in early embryonic development. *Cell Biosci* *2*, 11.
- Kanasaki, K., Kanda, Y., Palmsten, K., Tanjore, H., Lee, S.B., Lebleu, V.S., Gattone, V.H., Jr., and Kalluri, R. (2008). Integrin beta1-mediated matrix assembly and signaling are critical for the normal development and function of the kidney glomerulus. *Dev Biol* *313*, 584-593.

- Kang, H.S., Beak, J.Y., Kim, Y.S., Herbert, R., and Jetten, A.M. (2009). Glis3 is associated with primary cilia and Wwtr1/TAZ and implicated in polycystic kidney disease. *Mol Cell Biol* 29, 2556-2569.
- Kato, H., Gruenwald, A., Suh, J.H., Miner, J.H., Barisoni-Thomas, L., Taketo, M.M., Faul, C., Millar, S.E., Holzman, L.B., and Susztak, K. (2011). Wnt/beta-catenin pathway in podocytes integrates cell adhesion, differentiation, and survival. *J Biol Chem* 286, 26003-26015.
- Kestila, M., Lenkkeri, U., Mannikko, M., Lamerdin, J., McCready, P., Putaala, H., Ruotsalainen, V., Morita, T., Nissinen, M., Herva, R., *et al.* (1998). Positionally cloned gene for a novel glomerular protein--nephrin--is mutated in congenital nephrotic syndrome. *Mol Cell* 1, 575-582.
- Keymolen, K., Van Damme-Lombaerts, R., Verloes, A., and Fryns, J.P. (2000). Distal limb deficiencies, oral involvement, and renal defect: report of a third patient and confirmation of a distinct entity. *Am J Med Genet* 93, 19-21.
- Kiefer, S.M., Robbins, L., and Rauchman, M. (2012). Conditional expression of Wnt9b in Six2-positive cells disrupts stomach and kidney function. *PLoS One* 7, e43098.
- Kiefer, S.M., Robbins, L., Stumpff, K.M., Lin, C., Ma, L., and Rauchman, M. (2010). Sall1-dependent signals affect Wnt signaling and ureter tip fate to initiate kidney development. *Development* 137, 3099-3106.
- Kobayashi, A., Valerius, M.T., Mugford, J.W., Carroll, T.J., Self, M., Oliver, G., and McMahon, A.P. (2008). Six2 defines and regulates a multipotent self-renewing nephron progenitor population throughout mammalian kidney development. *Cell Stem Cell* 3, 169-181.
- Kohl, S., Hwang, D.Y., Dworschak, G.C., Hilger, A.C., Saisawat, P., Vivante, A., Stajic, N., Bogdanovic, R., Reutter, H.M., Kehinde, E.O., *et al.* (2014). Mild recessive mutations in six Fraser syndrome-related genes cause isolated congenital anomalies of the kidney and urinary tract. *J Am Soc Nephrol* 25, 1917-1922.
- Kreidberg, J.A., Donovan, M.J., Goldstein, S.L., Rennke, H., Shepherd, K., Jones, R.C., and Jaenisch, R. (1996). Alpha 3 beta 1 integrin has a crucial role in kidney and lung organogenesis. *Development* 122, 3537-3547.
- Kucherenko, M.M., Pantoja, M., Yatsenko, A.S., Shcherbata, H.R., Fischer, K.A., Maksymiv, D.V., Chernykh, Y.I., and Ruohola-Baker, H. (2008). Genetic modifier screens reveal new components that interact with the Drosophila dystroglycan-dystrophin complex. *PLoS One* 3, e2418.

Kume, T., Deng, K., and Hogan, B.L. (2000). Murine forkhead/winged helix genes *Foxc1* (*Mf1*) and *Foxc2* (*Mfh1*) are required for the early organogenesis of the kidney and urinary tract. *Development* *127*, 1387-1395.

Kuroda, S., Solari, V., and Puri, P. (2007). Association of transforming growth factor-beta1 gene polymorphism with familial vesicoureteral reflux. *J Urol* *178*, 1650-1653.

Kurschat, C.E., Muller, R.U., Franke, M., Maintz, D., Schermer, B., and Benzing, T. (2014). An approach to cystic kidney diseases: the clinician's view. *Nat Rev Nephrol* *10*, 687-699.

Kvarnung, M., Nilsson, D., Lindstrand, A., Korenke, G.C., Chiang, S.C., Blennow, E., Bergmann, M., Stodberg, T., Makitie, O., Anderlid, B.M., *et al.* (2013). A novel intellectual disability syndrome caused by GPI anchor deficiency due to homozygous mutations in *PIGT*. *J Med Genet* *50*, 521-528.

Lange, A., Wickstrom, S.A., Jakobson, M., Zent, R., Sainio, K., and Fassler, R. (2009). Integrin-linked kinase is an adaptor with essential functions during mouse development. *Nature* *461*, 1002-1006.

Le Merrer, M., David, A., Goutieres, F., and Briard, M.L. (1992). Digito-reno-cerebral syndrome: confirmation of Eronen syndrome. *Clin Genet* *42*, 196-198.

LeBlanc, M.A., Penney, L.S., Gaston, D., Shi, Y., Aberg, E., Nightingale, M., Jiang, H., Gillett, R.M., Fahiminiya, S., Macgillivray, C., *et al.* (2013). A novel rearrangement of *occludin* causes brain calcification and renal dysfunction. *Hum Genet* *132*, 1223-1234.

Lee, C.H., Li, W., Nishimura, R., Zhou, M., Batzer, A.G., Myers, M.G., Jr., White, M.F., Schlessinger, J., and Skolnik, E.Y. (1993). *Nck* associates with the SH2 domain-docking protein IRS-1 in insulin-stimulated cells. *Proc Natl Acad Sci U S A* *90*, 11713-11717.

Legallicier, B., Trugnan, G., Murphy, G., Lelongt, B., and Ronco, P. (2001). Expression of the type IV collagenase system during mouse kidney development and tubule segmentation. *J Am Soc Nephrol* *12*, 2358-2369.

Legate, K.R., Wickstrom, S.A., and Fassler, R. (2009). Genetic and cell biological analysis of integrin outside-in signaling. *Genes Dev* *23*, 397-418.

Lehner, B. (2011). Molecular mechanisms of epistasis within and between genes. *Trends Genet* *27*, 323-331.

Leimeister, C., Bach, A., and Gessler, M. (1998). Developmental expression patterns of mouse sFRP genes encoding members of the secreted frizzled related protein family. *Mech Dev* *75*, 29-42.

- Lennerz, J.K., Spence, D.C., Iskandar, S.S., Dehner, L.P., and Liapis, H. (2010). Glomerulocystic kidney: one hundred-year perspective. *Archives of pathology & laboratory medicine* 134, 583-605.
- Lennon, R., Randles, M.J., and Humphries, M.J. (2014). The importance of podocyte adhesion for a healthy glomerulus. *Front Endocrinol (Lausanne)* 5, 160.
- Leonhard, W.N., Zandbergen, M., Veraar, K., van den Berg, S., van der Weerd, L., Breuning, M., de Heer, E., and Peters, D.J. (2014). Scattered Deletion of PKD1 in Kidneys Causes a Cystic Snowball Effect and Recapitulates Polycystic Kidney Disease. *J Am Soc Nephrol*.
- Levey, A.S., Cattran, D., Friedman, A., Miller, W.G., Sedor, J., Tuttle, K., Kasiske, B., and Hostetter, T. (2009). Proteinuria as a surrogate outcome in CKD: report of a scientific workshop sponsored by the National Kidney Foundation and the US Food and Drug Administration. *Am J Kidney Dis* 54, 205-226.
- Levinson, R.S., Batourina, E., Choi, C., Vorontchikhina, M., Kitajewski, J., and Mendelsohn, C.L. (2005). Foxd1-dependent signals control cellularity in the renal capsule, a structure required for normal renal development. *Development* 132, 529-539.
- Levy, C.M., and Knudtzon, J. (1993). Kallmann syndrome in two sisters with other developmental anomalies also affecting their father. *Clin Genet* 43, 51-53.
- Li, Y., Pawlik, B., Elcioglu, N., Aglan, M., Kayserili, H., Yigit, G., Percin, F., Goodman, F., Nurnberg, G., Cenani, A., *et al.* (2010). LRP4 mutations alter Wnt/beta-catenin signaling and cause limb and kidney malformations in Cenani-Lenz syndrome. *Am J Hum Genet* 86, 696-706.
- Lin, A.E., Semina, E.V., Daack-Hirsch, S., Roeder, E.R., Curry, C.J., Rosenbaum, K., Weaver, D.D., and Murray, J.C. (2000). Exclusion of the branchio-oto-renal syndrome locus (EYA1) from patients with branchio-oculo-facial syndrome. *Am J Med Genet* 91, 387-390.
- Lin, L.F., Doherty, D.H., Lile, J.D., Bektesh, S., and Collins, F. (1993). GDNF: a glial cell line-derived neurotrophic factor for midbrain dopaminergic neurons. *Science* 260, 1130-1132.
- Linton, J.M., Martin, G.R., and Reichardt, L.F. (2007). The ECM protein nephronectin promotes kidney development via integrin alpha8beta1-mediated stimulation of Gdnf expression. *Development* 134, 2501-2509.
- Loftus, H., and Ong, A.C. (2013). Cystic kidney diseases: many ways to form a cyst. *Pediatr Nephrol* 28, 33-49.

- Long, J., Zuo, D., and Park, M. (2005). Pc2-mediated sumoylation of Smad-interacting protein 1 attenuates transcriptional repression of E-cadherin. *J Biol Chem* 280, 35477-35489.
- Lonka-Nevalaita, L., Lume, M., Leppanen, S., Jokitalo, E., Peranen, J., and Saarma, M. (2010). Characterization of the intracellular localization, processing, and secretion of two glial cell line-derived neurotrophic factor splice isoforms. *J Neurosci* 30, 11403-11413.
- Lu, W., Fan, X., Basora, N., Babakhanlou, H., Law, T., Rifai, N., Harris, P.C., Perez-Atayde, A.R., Rennke, H.G., and Zhou, J. (1999). Late onset of renal and hepatic cysts in Pkd1-targeted heterozygotes. *Nat Genet* 21, 160-161.
- Lu, W., Peissel, B., Babakhanlou, H., Pavlova, A., Geng, L., Fan, X., Larson, C., Brent, G., and Zhou, J. (1997). Perinatal lethality with kidney and pancreas defects in mice with a targeted Pkd1 mutation. *Nat Genet* 17, 179-181.
- Lu, W., Quintero-Rivera, F., Fan, Y., Alkuraya, F.S., Donovan, D.J., Xi, Q., Turbe-Doan, A., Li, Q.G., Campbell, C.G., Shanske, A.L., *et al.* (2007a). NFIA haploinsufficiency is associated with a CNS malformation syndrome and urinary tract defects. *PLoS Genet* 3, e80.
- Lu, W., van Eerde, A.M., Fan, X., Quintero-Rivera, F., Kulkarni, S., Ferguson, H., Kim, H.G., Fan, Y., Xi, Q., Li, Q.G., *et al.* (2007b). Disruption of ROBO2 is associated with urinary tract anomalies and confers risk of vesicoureteral reflux. *Am J Hum Genet* 80, 616-632.
- Lu, W., van Eerde, A.M., Fan, X., Quintero-Rivera, F., Kulkarni, S., Ferguson, H.L., Kim, H., Fan, Y., Xi, Q., Li, Q.G., *et al.* (2007c). Disruption of ROBO2 is associated with urinary tract anomalies and confers risk of vesicoureteral reflux. *Am J Hum Genet* 80, 616-632.
- Macias, H., Moran, A., Samara, Y., Moreno, M., Compton, J.E., Harburg, G., Strickland, P., and Hinck, L. (2011). SLIT/ROBO1 signaling suppresses mammary branching morphogenesis by limiting basal cell number. *Dev Cell* 20, 827-840.
- Mackie, G.G., Awang, H., and Stephens, F.D. (1975). The ureteric orifice: the embryologic key to radiologic status of duplex kidneys. *J Pediatr Surg* 10, 473-481.
- MacMullin, A., and Jacobs, J.R. (2006). Slit coordinates cardiac morphogenesis in *Drosophila*. *Dev Biol* 293, 154-164.
- Makita, R., Uchijima, Y., Nishiyama, K., Amano, T., Chen, Q., Takeuchi, T., Mitani, A., Nagase, T., Yatomi, Y., Aburatani, H., *et al.* (2008). Multiple renal cysts, urinary concentration defects, and pulmonary emphysematous changes in mice lacking TAZ. *Am J Physiol Renal Physiol* 294, F542-553.

- Mani, R., St Onge, R.P., Hartman, J.L.t., Giaever, G., and Roth, F.P. (2008). Defining genetic interaction. *Proc Natl Acad Sci U S A* 105, 3461-3466.
- Manthey, A.L., Lachke, S.A., FitzGerald, P.G., Mason, R.W., Scheiblin, D.A., McDonald, J.H., and Duncan, M.K. (2014a). Loss of Sip1 leads to migration defects and retention of ectodermal markers during lens development. *Mech Dev* 131, 86-110.
- Manthey, A.L., Terrell, A.M., Lachke, S.A., Polson, S.W., and Duncan, M.K. (2014b). Development of novel filtering criteria to analyze RNA-sequencing data obtained from the murine ocular lens during embryogenesis. *Genom Data* 2, 369-374.
- Marcussen, N. (1995). Atubular glomeruli in chronic renal disease. *Curr Top Pathol* 88, 145-174.
- Marcussen, N., and Olsen, T.S. (1990). Atubular glomeruli in patients with chronic pyelonephritis. *Lab Invest* 62, 467-473.
- Maruhashi, M., Van De Putte, T., Huylebroeck, D., Kondoh, H., and Higashi, Y. (2005). Involvement of SIP1 in positioning of somite boundaries in the mouse embryo. *Dev Dyn* 234, 332-338.
- Massa, F., Garbay, S., Bouvier, R., Sugitani, Y., Noda, T., Gubler, M.C., Heidet, L., Pontoglio, M., and Fischer, E. (2013). Hepatocyte nuclear factor 1beta controls nephron tubular development. *Development* 140, 886-896.
- Mathew, S., Chen, X., Pozzi, A., and Zent, R. (2012). Integrins in renal development. *Pediatr Nephrol* 27, 891-900.
- McMahon, A.P., Aronow, B.J., Davidson, D.R., Davies, J.A., Gaido, K.W., Grimmond, S., Lessard, J.L., Little, M.H., Potter, S.S., Wilder, E.L., *et al.* (2008). GUDMAP: the genitourinary developmental molecular anatomy project. *J Am Soc Nephrol* 19, 667-671.
- Mefford, H.C., Sharp, A.J., Baker, C., Itsara, A., Jiang, Z., Buysse, K., Huang, S., Maloney, V.K., Crolla, J.A., Baralle, D., *et al.* (2008). Recurrent rearrangements of chromosome 1q21.1 and variable pediatric phenotypes. *N Engl J Med* 359, 1685-1699.
- Mendelsohn, C. (2009). Using mouse models to understand normal and abnormal urogenital tract development. *Organogenesis* 5, 306-314.
- Menon, M.C., Chuang, P.Y., and He, C.J. (2012). The glomerular filtration barrier: components and crosstalk. *Int J Nephrol* 2012, 749010.
- Michos, O., Cebrian, C., Hyink, D., Grieshammer, U., Williams, L., D'Agati, V., Licht, J.D., Martin, G.R., and Costantini, F. (2010). Kidney development in the absence of Gdnf and Spry1 requires Fgf10. *PLoS Genet* 6, e1000809.



Miner, J.H. (2011). Glomerular basement membrane composition and the filtration barrier. *Pediatr Nephrol* 26, 1413-1417.

Miquelajauregui, A., Van de Putte, T., Polyakov, A., Nityanandam, A., Boppana, S., Seuntjens, E., Karabinos, A., Higashi, Y., Huylebroeck, D., and Tarabykin, V. (2007). Smad-interacting protein-1 (*Zfhx1b*) acts upstream of Wnt signaling in the mouse hippocampus and controls its formation. *Proc Natl Acad Sci U S A* 104, 12919-12924.

Miyazaki, Y., Oshima, K., Fogo, A., Hogan, B.L., and Ichikawa, I. (2000). Bone morphogenetic protein 4 regulates the budding site and elongation of the mouse ureter. *J Clin Invest* 105, 863-873.

MOD (2006). March of Dimes global report on birth defects.

Moeller, M.J., Sanden, S.K., Soofi, A., Wiggins, R.C., and Holzman, L.B. (2003). Podocyte-specific expression of cre recombinase in transgenic mice. *Genesis* 35, 39-42.

Morello, R., Zhou, G., Dreyer, S.D., Harvey, S.J., Ninomiya, Y., Thorner, P.S., Miner, J.H., Cole, W., Winterpacht, A., Zabel, B., *et al.* (2001). Regulation of glomerular basement membrane collagen expression by LMX1B contributes to renal disease in nail patella syndrome. *Nat Genet* 27, 205-208.

Mowrey, P.N., Chorney, M.J., Venditti, C.P., Latif, F., Modi, W.S., Lerman, M.I., Zbar, B., Robins, D.B., Rogan, P.K., and Ladda, R.L. (1993). Clinical and molecular analyses of deletion 3p25-pter syndrome. *Am J Med Genet* 46, 623-629.

Murakami, A., Gomi, K., Tanaka, M., Ohyama, M., Itani, Y., Ishikawa, H., Aida, N., Furuya, M., and Tanaka, Y. (2012). Unilateral glomerulocystic kidney disease associated with tuberous sclerosis complex in a neonate. *Pathol Int* 62, 209-215.

Murawski, I.J., and Gupta, I.R. (2006). Vesicoureteric reflux and renal malformations: a developmental problem. *Clin Genet* 69, 105-117.

Murawski, I.J., Myburgh, D.B., Favor, J., and Gupta, I.R. (2007). Vesico-ureteric reflux and urinary tract development in the Pax2 1Neu+/- mouse. *Am J Physiol Renal Physiol* 293, F1736-1745.

Naiki, M., Mizuno, S., Yamada, K., Yamada, Y., Kimura, R., Oshiro, M., Okamoto, N., Makita, Y., Seishima, M., and Wakamatsu, N. (2012). MBTPS2 mutation causes BRESEK/BRESHECK syndrome. *Am J Med Genet A* 158A, 97-102.

Narlis, M., Grote, D., Gaitan, Y., Boualia, S.K., and Bouchard, M. (2007). Pax2 and pax8 regulate branching morphogenesis and nephron differentiation in the developing kidney. *J Am Soc Nephrol* 18, 1121-1129.

- Narumi, Y., Kosho, T., Tsuruta, G., Shiohara, M., Shimazaki, E., Mori, T., Shimizu, A., Igawa, Y., Nishizawa, S., Takagi, K., *et al.* (2010). Genital abnormalities in Pallister-Hall syndrome: Report of two patients and review of the literature. *Am J Med Genet A* 152A, 3143-3147.
- Naylor, R.W., Przepiorski, A., Ren, Q., Yu, J., and Davidson, A.J. (2013). HNF1beta is essential for nephron segmentation during nephrogenesis. *J Am Soc Nephrol* 24, 77-87.
- Negrisol, S., Benetti, E., Centi, S., Della Vella, M., Ghirardo, G., Zanon, G.F., Murer, L., and Artifoni, L. (2011). PAX2 gene mutations in pediatric and young adult transplant recipients: kidney and urinary tract malformations without ocular anomalies. *Clin Genet* 80, 581-585.
- Neild, G.H. (2010). Primary renal disease in young adults with renal failure. *Nephrol Dial Transplant* 25, 1025-1032.
- Nguyen, H.T., Herndon, C.D., Cooper, C., Gatti, J., Kirsch, A., Kokorowski, P., Lee, R., Perez-Brayfield, M., Metcalfe, P., Yerkes, E., *et al.* (2010). The Society for Fetal Urology consensus statement on the evaluation and management of antenatal hydronephrosis. *J Pediatr Urol* 6, 212-231.
- Nie, X., Xu, J., El-Hashash, A., and Xu, P.X. (2011). Six1 regulates Grem1 expression in the metanephric mesenchyme to initiate branching morphogenesis. *Dev Biol* 352, 141-151.
- Niewmierzycka, A., Mills, J., St-Arnaud, R., Dedhar, S., and Reichardt, L.F. (2005). Integrin-linked kinase deletion from mouse cortex results in cortical lamination defects resembling cobblestone lissencephaly. *J Neurosci* 25, 7022-7031.
- Nishimura, H., Yerkes, E., Hohenfellner, K., Miyazaki, Y., Ma, J., Hunley, T.E., Yoshida, H., Ichiki, T., Threadgill, D., Phillips, J.A., 3rd, *et al.* (1999). Role of the angiotensin type 2 receptor gene in congenital anomalies of the kidney and urinary tract, CAKUT, of mice and men. *Mol Cell* 3, 1-10.
- Nishinakamura, R., Matsumoto, Y., Nakao, K., Nakamura, K., Sato, A., Copeland, N.G., Gilbert, D.J., Jenkins, N.A., Scully, S., Lacey, D.L., *et al.* (2001). Murine homolog of SALL1 is essential for ureteric bud invasion in kidney development. *Development* 128, 3105-3115.
- Nishizaki, Y., Takagi, T., Matsui, F., and Higashi, Y. (2014). SIP1 expression patterns in brain investigated by generating a SIP1-EGFP reporter knock-in mouse. *Genesis* 52, 56-67.
- Noe, H.N. (1992). The long-term results of prospective sibling reflux screening. *J Urol* 148, 1739-1742.

- Noe, H.N., Wyatt, R.J., Peeden, J.N., Jr., and Rivas, M.L. (1992). The transmission of vesicoureteral reflux from parent to child. *J Urol* 148, 1869-1871.
- Nonomura, K., Takahashi, M., Wakamatsu, Y., Takano-Yamamoto, T., and Osumi, N. (2010). Dynamic expression of Six family genes in the dental mesenchyme and the epithelial ameloblast stem/progenitor cells during murine tooth development. *J Anat* 216, 80-91.
- O'Meara, Y.M., Natori, Y., Minto, A.W., Goldstein, D.J., Manning, E.C., and Salant, D.J. (1992). Nephrotoxic antiserum identifies a beta 1-integrin on rat glomerular epithelial cells. *Am J Physiol* 262, F1083-1091.
- Ohyama, T., and Groves, A.K. (2004). Generation of Pax2-Cre mice by modification of a Pax2 bacterial artificial chromosome. *Genesis* 38, 195-199.
- Oliverio, M.I., Kim, H.S., Ito, M., Le, T., Audoly, L., Best, C.F., Hiller, S., Kluckman, K., Maeda, N., Smithies, O., *et al.* (1998). Reduced growth, abnormal kidney structure, and type 2 (AT2) angiotensin receptor-mediated blood pressure regulation in mice lacking both AT1A and AT1B receptors for angiotensin II. *Proc Natl Acad Sci U S A* 95, 15496-15501.
- Omori, S., Hida, M., Ishikura, K., Kuramochi, S., and Awazu, M. (2000). Expression of mitogen-activated protein kinase family in rat renal development. *Kidney Int* 58, 27-37.
- Otto, E.A., Hurd, T.W., Airik, R., Chaki, M., Zhou, W., Stoetzel, C., Patil, S.B., Levy, S., Ghosh, A.K., Murga-Zamalloa, C.A., *et al.* (2010). Candidate exome capture identifies mutation of SDCCAG8 as the cause of a retinal-renal ciliopathy. *Nat Genet* 42, 840-850.
- Palsson, R., Sharma, C.P., Kim, K., McLaughlin, M., Brown, D., and Arnaout, M.A. (1996). Characterization and cell distribution of polycystin, the product of autosomal dominant polycystic kidney disease gene 1. *Mol Med* 2, 702-711.
- Pasutto, F., Sticht, H., Hammersen, G., Gillessen-Kaesbach, G., Fitzpatrick, D.R., Nurnberg, G., Brasch, F., Schirmer-Zimmermann, H., Tolmie, J.L., Chitayat, D., *et al.* (2007). Mutations in STRA6 cause a broad spectrum of malformations including anophthalmia, congenital heart defects, diaphragmatic hernia, alveolar capillary dysplasia, lung hypoplasia, and mental retardation. *Am J Hum Genet* 80, 550-560.
- Patel, V., Hajarnis, S., Williams, D., Hunter, R., Huynh, D., and Igarashi, P. (2012). MicroRNAs regulate renal tubule maturation through modulation of Pkd1. *J Am Soc Nephrol* 23, 1941-1948.
- Paul, B.M., and Vanden Heuvel, G.B. (2014). *Kidney: polycystic kidney disease*. Wiley Interdiscip Rev Dev Biol 3, 465-487.

Peeden, J.N., Jr., and Noe, H.N. (1992). Is it practical to screen for familial vesicoureteral reflux within a private pediatric practice? *Pediatrics* 89, 758-760.

Persu, A., Duyme, M., Pirson, Y., Lens, X.M., Messiaen, T., Breuning, M.H., Chauveau, D., Levy, M., Grunfeld, J.P., and Devuyst, O. (2004). Comparison between siblings and twins supports a role for modifier genes in ADPKD. *Kidney Int* 66, 2132-2136.

Peters, C.A., Skoog, S.J., Arant, B.S., Jr., Copp, H.L., Elder, J.S., Hudson, R.G., Khoury, A.E., Lorenzo, A.J., Pohl, H.G., Shapiro, E., *et al.* (2010). Summary of the AUA Guideline on Management of Primary Vesicoureteral Reflux in Children. *J Urol* 184, 1134-1144.

Peters, D.J., Spruit, L., Klingel, R., Prins, F., Baelde, H.J., Giordano, P.C., Bernini, L.F., de Heer, E., Breuning, M.H., and Bruijn, J.A. (1996). Adult, fetal, and polycystic kidney expression of polycystin, the polycystic kidney disease-1 gene product. *Lab Invest* 75, 221-230.

Piontek, K.B., Huso, D.L., Grinberg, A., Liu, L., Bedja, D., Zhao, H., Gabrielson, K., Qian, F., Mei, C., Westphal, H., *et al.* (2004). A functional floxed allele of Pkd1 that can be conditionally inactivated in vivo. *J Am Soc Nephrol* 15, 3035-3043.

Piper, M., Georgas, K., Yamada, T., and Little, M. (2000). Expression of the vertebrate Slit gene family and their putative receptors, the Robo genes, in the developing murine kidney. *Mech Dev* 94, 213-217.

Plessis, G., Le Treust, M., and Le Merrer, M. (1997). Scalp defect, absence of nipples, ear anomalies, renal hypoplasia: another case of Finlay-Marks syndrome. *Clin Genet* 52, 231-234.

Plump, A.S., Erskine, L., Sabatier, C., Brose, K., Epstein, C.J., Goodman, C.S., Mason, C.A., and Tessier-Lavigne, M. (2002). Slit1 and Slit2 cooperate to prevent premature midline crossing of retinal axons in the mouse visual system. *Neuron* 33, 219-232.

Pohl, M., Bhatnagar, V., Mendoza, S.A., and Nigam, S.K. (2002). Toward an etiological classification of developmental disorders of the kidney and upper urinary tract. *Kidney Int* 61, 10-19.

Pohl, M., Sakurai, H., Bush, K.T., and Nigam, S.K. (2000). Matrix metalloproteinases and their inhibitors regulate in vitro ureteric bud branching morphogenesis. *Am J Physiol Renal Physiol* 279, F891-900.

Poley, J.R., and Proud, V.K. (2008). Hardikar syndrome: new features. *Am J Med Genet A* 146A, 2473-2479.

Postigo, A.A. (2003). Opposing functions of ZEB proteins in the regulation of the TGFbeta/BMP signaling pathway. *EMBO J* 22, 2443-2452.

Postigo, A.A., and Dean, D.C. (1999). ZEB represses transcription through interaction with the corepressor CtBP. *Proc Natl Acad Sci U S A* 96, 6683-6688.

Pozzi, A., Jarad, G., Moeckel, G.W., Coffa, S., Zhang, X., Gewin, L., Eremina, V., Hudson, B.G., Borza, D.B., Harris, R.C., *et al.* (2008). Beta1 integrin expression by podocytes is required to maintain glomerular structural integrity. *Dev Biol* 316, 288-301.

Pritchard, L., Sloane-Stanley, J.A., Sharpe, J.A., Aspinwall, R., Lu, W., Buckle, V., Strmecki, L., Walker, D., Ward, C.J., Alpers, C.E., *et al.* (2000a). A human PKD1 transgene generates functional polycystin-1 in mice and is associated with a cystic phenotype. *Human molecular genetics* 9, 2617-2627.

Pritchard, L., Sloane-Stanley, J.A., Sharpe, J.A., Aspinwall, R., Lu, W., Buckle, V., Strmecki, L., Walker, D., Ward, C.J., Alpers, C.E., *et al.* (2000b). A human PKD1 transgene generates functional polycystin-1 in mice and is associated with a cystic phenotype. *Hum Mol Genet* 9, 2617-2627.

Rampoldi, L., Caridi, G., Santon, D., Boaretto, F., Bernascone, I., Lamorte, G., Tardanico, R., Dagnino, M., Colussi, G., Scolari, F., *et al.* (2003). Allelism of MCKD, FJHN and GCKD caused by impairment of uromodulin export dynamics. *Human molecular genetics* 12, 3369-3384.

Raphael, K.L., Strait, K.A., Stricklett, P.K., Miller, R.L., Nelson, R.D., Piontek, K.B., Germino, G.G., and Kohan, D.E. (2009). Inactivation of Pkd1 in principal cells causes a more severe cystic kidney disease than in intercalated cells. *Kidney Int* 75, 626-633.

Rasouly, H.M., and Lu, W. (2013). Lower urinary tract development and disease. *Wiley Interdiscip Rev Syst Biol Med* 5, 307-342.

Rhee, J., Buchan, T., Zukerberg, L., Lilien, J., and Balsamo, J. (2007). Cables links Robo-bound Abl kinase to N-cadherin-bound beta-catenin to mediate Slit-induced modulation of adhesion and transcription. *Nat Cell Biol* 9, 883-892.

Rhee, J., Mahfooz, N.S., Arregui, C., Lilien, J., Balsamo, J., and VanBerkum, M.F. (2002). Activation of the repulsive receptor Roundabout inhibits N-cadherin-mediated cell adhesion. *Nat Cell Biol* 4, 798-805.

Riggins, K.S., Mernaugh, G., Su, Y., Quaranta, V., Koshikawa, N., Seiki, M., Pozzi, A., and Zent, R. (2010). MT1-MMP-mediated basement membrane remodeling modulates renal development. *Exp Cell Res* 316, 2993-3005.

- Romero, R., Bonal, J., Campo, E., Pelegri, A., and Palacin, A. (1993). Glomerulocystic kidney disease: a single entity? *Nephron* 63, 100-103.
- Rosenfeld, J.A., Traylor, R.N., Schaefer, G.B., McPherson, E.W., Ballif, B.C., Klopocki, E., Mundlos, S., Shaffer, L.G., and Aylsworth, A.S. (2012). Proximal microdeletions and microduplications of 1q21.1 contribute to variable abnormal phenotypes. *Eur J Hum Genet* 20, 754-761.
- Rothberg, J.M., and Artavanis-Tsakonas, S. (1992). Modularity of the slit protein. Characterization of a conserved carboxy-terminal sequence in secreted proteins and a motif implicated in extracellular protein interactions. *J Mol Biol* 227, 367-370.
- Routtenberg, A. (1995). Knockout mouse fault lines. *Nature* 374, 314-315.
- Rozen, E.J., Schmidt, H., Dolcet, X., Basson, M.A., Jain, S., and Encinas, M. (2009). Loss of Sprouty1 rescues renal agenesis caused by Ret mutation. *J Am Soc Nephrol* 20, 255-259.
- Ruf, R.G., Berkman, J., Wolf, M.T., Nurnberg, P., Gattas, M., Ruf, E.M., Hyland, V., Kromberg, J., Glass, I., Macmillan, J., *et al.* (2003). A gene locus for branchio-otic syndrome maps to chromosome 14q21.3-q24.3. *J Med Genet* 40, 515-519.
- Ryan, A.K., Goodship, J.A., Wilson, D.I., Philip, N., Levy, A., Seidel, H., Schuffenhauer, S., Oechsler, H., Belohradsky, B., Prieur, M., *et al.* (1997). Spectrum of clinical features associated with interstitial chromosome 22q11 deletions: a European collaborative study. *J Med Genet* 34, 798-804.
- Saadi-Kheddoui, S., Berrebi, D., Romagnolo, B., Cluzeaud, F., Peuchmaur, M., Kahn, A., Vandewalle, A., and Perret, C. (2001). Early development of polycystic kidney disease in transgenic mice expressing an activated mutant of the beta-catenin gene. *Oncogene* 20, 5972-5981.
- Saisawat, P., Kohl, S., Hilger, A.C., Hwang, D.Y., Yung Gee, H., Dworschak, G.C., Tasic, V., Pennimpede, T., Natarajan, S., Sperry, E., *et al.* (2014). Whole-exome resequencing reveals recessive mutations in TRAP1 in individuals with CAKUT and VACTERL association. *Kidney Int* 85, 1310-1317.
- Sakai, T., Li, S., Docheva, D., Grashoff, C., Sakai, K., Kostka, G., Braun, A., Pfeifer, A., Yurchenco, P.D., and Fassler, R. (2003). Integrin-linked kinase (ILK) is required for polarizing the epiblast, cell adhesion, and controlling actin accumulation. *Genes Dev* 17, 926-940.
- Sakaki-Yumoto, M., Kobayashi, C., Sato, A., Fujimura, S., Matsumoto, Y., Takasato, M., Kodama, T., Aburatani, H., Asashima, M., Yoshida, N., *et al.* (2006). The murine homolog of SALL4, a causative gene in Okhiro syndrome, is essential for embryonic

stem cell proliferation, and cooperates with *Sall1* in anorectal, heart, brain and kidney development. *Development* 133, 3005-3013.

Salih, M.A., and Tuvemo, T. (1991). Diabetes insipidus, diabetes mellitus, optic atrophy and deafness (DIDMOAD syndrome). A clinical study in two Sudanese families. *Acta Paediatr Scand* 80, 567-572.

Sampson, M.G., Coughlin, C.R., 2nd, Kaplan, P., Conlin, L.K., Meyers, K.E., Zackai, E.H., Spinner, N.B., and Copelovitch, L. (2010). Evidence for a recurrent microdeletion at chromosome 16p11.2 associated with congenital anomalies of the kidney and urinary tract (CAKUT) and Hirschsprung disease. *Am J Med Genet A* 152A, 2618-2622.

Sanchez, M.P., Silos-Santiago, I., Frisen, J., He, B., Lira, S.A., and Barbacid, M. (1996). Renal agenesis and the absence of enteric neurons in mice lacking GDNF. *Nature* 382, 70-73.

Sanna-Cherchi, S., Ravani, P., Corbani, V., Parodi, S., Haupt, R., Piaggio, G., Innocenti, M.L., Somenzi, D., Trivelli, A., Caridi, G., *et al.* (2009). Renal outcome in patients with congenital anomalies of the kidney and urinary tract. *Kidney Int* 76, 528-533.

Santiago-Martinez, E., Soplop, N.H., Patel, R., and Kramer, S.G. (2008). Repulsion by Slit and Roundabout prevents Shotgun/E-cadherin-mediated cell adhesion during *Drosophila* heart tube lumen formation. *J Cell Biol* 182, 241-248.

Santos, O.F., and Nigam, S.K. (1993). HGF-induced tubulogenesis and branching of epithelial cells is modulated by extracellular matrix and TGF-beta. *Dev Biol* 160, 293-302.

Sanyanusin, P., Schimmenti, L.A., McNoe, L.A., Ward, T.A., Pierpont, M.E., Sullivan, M.J., Dobyns, W.B., and Eccles, M.R. (1995). Mutation of the *PAX2* gene in a family with optic nerve colobomas, renal anomalies and vesicoureteral reflux. *Nat Genet* 9, 358-364.

Sargent, M.A. (2000). What is the normal prevalence of vesicoureteral reflux? *Pediatr Radiol* 30, 587-593.

Sauer, B. (1998). Inducible gene targeting in mice using the Cre/lox system. *Methods* 14, 381-392.

Saxen, L. (1987). *Organogenesis of the kidney* (Cambridge, Cambridge University Press).

Schell, C., Baumhagl, L., Salou, S., Conzelmann, A.C., Meyer, C., Helmstadter, M., Wrede, C., Grahammer, F., Eimer, S., Kerjaschki, D., *et al.* (2013). N-wasp is required for stabilization of podocyte foot processes. *J Am Soc Nephrol* 24, 713-721.

- Schuchardt, A., D'Agati, V., Larsson-Blomberg, L., Costantini, F., and Pachnis, V. (1994). Defects in the kidney and enteric nervous system of mice lacking the tyrosine kinase receptor Ret. *Nature* 367, 380-383.
- Schulman, S.L., Zderic, S., and Kaplan, P. (1996). Increased prevalence of urinary symptoms and voiding dysfunction in Williams syndrome. *J Pediatr* 129, 466-469.
- Scolari, F., Izzi, C., and Ghiggeri, G.M. (2014). Uromodulin: from monogenic to multifactorial diseases. *Nephrol Dial Transplant*.
- Scott, J.E., Swallow, V., Coulthard, M.G., Lambert, H.J., and Lee, R.E. (1997). Screening of newborn babies for familial ureteric reflux. *Lancet* 350, 396-400.
- Seeger, M., Tear, G., Ferres-Marco, D., and Goodman, C.S. (1993). Mutations affecting growth cone guidance in *Drosophila*: genes necessary for guidance toward or away from the midline. *Neuron* 10, 409-426.
- Selicorni, A., Sforzini, C., Milani, D., Cagnoli, G., Fossali, E., and Bianchetti, M.G. (2005). Anomalies of the kidney and urinary tract are common in de Lange syndrome. *Am J Med Genet A* 132, 395-397.
- Senee, V., Chelala, C., Duchatelet, S., Feng, D., Blanc, H., Cossec, J.C., Charon, C., Nicolino, M., Boileau, P., Cavener, D.R., *et al.* (2006). Mutations in *GLIS3* are responsible for a rare syndrome with neonatal diabetes mellitus and congenital hypothyroidism. *Nat Genet* 38, 682-687.
- Seuntjens, E., Nityanandam, A., Miquelajauregui, A., Debruyne, J., Stryjewska, A., Goebbels, S., Nave, K.A., Huylebroeck, D., and Tarabykin, V. (2009). *Sip1* regulates sequential fate decisions by feedback signaling from postmitotic neurons to progenitors. *Nat Neurosci* 12, 1373-1380.
- Shibazaki, S., Yu, Z., Nishio, S., Tian, X., Thomson, R.B., Mitobe, M., Louvi, A., Velazquez, H., Ishibe, S., Cantley, L.G., *et al.* (2008). Cyst formation and activation of the extracellular regulated kinase pathway after kidney specific inactivation of *Pkd1*. *Hum Mol Genet* 17, 1505-1516.
- Shillingford, J.M., Piontek, K.B., Germino, G.G., and Weimbs, T. (2010). Rapamycin ameliorates PKD resulting from conditional inactivation of *Pkd1*. *J Am Soc Nephrol* 21, 489-497.
- Shin, J.O., Kim, E.J., Cho, K.W., Nakagawa, E., Kwon, H.J., Cho, S.W., and Jung, H.S. (2012). BMP4 signaling mediates Zeb family in developing mouse tooth. *Histochem Cell Biol* 137, 791-800.
- Simons, M., and Huber, T.B. (2008). It's not all about nephrin. *Kidney Int* 73, 671-673.



- Singh, L., Singh, G., and Dinda, A.K. (2015). Understanding podocytopathy and its relevance to clinical nephrology. *Indian J Nephrol* 25, 1-7.
- Slavotinek, A.M. (2004). Fryns syndrome: a review of the phenotype and diagnostic guidelines. *Am J Med Genet A* 124A, 427-433.
- Song, X., Di Giovanni, V., He, N., Wang, K., Ingram, A., Rosenblum, N.D., and Pei, Y. (2009). Systems biology of autosomal dominant polycystic kidney disease (ADPKD): computational identification of gene expression pathways and integrated regulatory networks. *Human molecular genetics* 18, 2328-2343.
- St Onge, R.P., Mani, R., Oh, J., Proctor, M., Fung, E., Davis, R.W., Nislow, C., Roth, F.P., and Giaever, G. (2007). Systematic pathway analysis using high-resolution fitness profiling of combinatorial gene deletions. *Nat Genet* 39, 199-206.
- Starremans, P.G., Li, X., Finnerty, P.E., Guo, L., Takakura, A., Neilson, E.G., and Zhou, J. (2008). A mouse model for polycystic kidney disease through a somatic in-frame deletion in the 5' end of Pkd1. *Kidney Int* 73, 1394-1405.
- Stuart, R.O., Bush, K.T., and Nigam, S.K. (2003). Changes in gene expression patterns in the ureteric bud and metanephric mesenchyme in models of kidney development. *Kidney Int* 64, 1997-2008.
- Subramanian, A., Kuehn, H., Gould, J., Tamayo, P., and Mesirov, J.P. (2007). GSEA-P: a desktop application for Gene Set Enrichment Analysis. *Bioinformatics* 23, 3251-3253.
- Subramanian, A., Tamayo, P., Mootha, V.K., Mukherjee, S., Ebert, B.L., Gillette, M.A., Paulovich, A., Pomeroy, S.L., Golub, T.R., Lander, E.S., *et al.* (2005). Gene set enrichment analysis: a knowledge-based approach for interpreting genome-wide expression profiles. *Proc Natl Acad Sci U S A* 102, 15545-15550.
- Sugiyama, N., and Yokoyama, T. (2006). Sustained cell proliferation of renal epithelial cells in mice with *inv* mutation. *Genes Cells* 11, 1213-1224.
- Swanson, S.L., Santen, R.J., and Smith, D.W. (1971). Multiple lentiginos syndrome: new findings of hypogonadotrophism, hyposmia, and unilateral renal agenesis. *J Pediatr* 78, 1037-1039.
- Tan, T.Y., Aftimos, S., Worgan, L., Susman, R., Wilson, M., Ghedia, S., Kirk, E.P., Love, D., Ronan, A., Darmanian, A., *et al.* (2009). Phenotypic expansion and further characterisation of the 17q21.31 microdeletion syndrome. *J Med Genet* 46, 480-489.
- Tanner, G.A., Tielker, M.A., Connors, B.A., Phillips, C.L., Tanner, J.A., and Evan, A.P. (2002). Atubular glomeruli in a rat model of polycystic kidney disease. *Kidney Int* 62, 1947-1957.

Taylor, R.W., Pyle, A., Griffin, H., Blakely, E.L., Duff, J., He, L., Smertenko, T., Alston, C.L., Neeve, V.C., Best, A., *et al.* (2014). Use of whole-exome sequencing to determine the genetic basis of multiple mitochondrial respiratory chain complex deficiencies. *JAMA* *312*, 68-77.

Teo, Z.L., McQueen-Miscamble, L., Turner, K., Martinez, G., Madakashira, B., Dedhar, S., Robinson, M.L., and de Jongh, R.U. (2014). Integrin linked kinase (ILK) is required for lens epithelial cell survival, proliferation and differentiation. *Exp Eye Res* *121*, 130-142.

Terpstra, L., Prud'homme, J., Arabian, A., Takeda, S., Karsenty, G., Dedhar, S., and St-Arnaud, R. (2003). Reduced chondrocyte proliferation and chondrodysplasia in mice lacking the integrin-linked kinase in chondrocytes. *J Cell Biol* *162*, 139-148.

Tessier-Lavigne, M., and Goodman, C.S. (1996). The molecular biology of axon guidance. *Science* *274*, 1123-1133.

Thivierge, C., Kurbegovic, A., Couillard, M., Guillaume, R., Cote, O., and Trudel, M. (2006). Overexpression of PKD1 causes polycystic kidney disease. *Mol Cell Biol* *26*, 1538-1548.

Toka, H.R., Toka, O., Hariri, A., and Nguyen, H.T. (2010). Congenital anomalies of kidney and urinary tract. *Semin Nephrol* *30*, 374-386.

Torres, V.E., Harris, P.C., and Pirson, Y. (2007). Autosomal dominant polycystic kidney disease. *Lancet* *369*, 1287-1301.

Tripathi, P., Wang, Y., Casey, A.M., and Chen, F. (2012). Absence of canonical smad signaling in ureteral and bladder mesenchyme causes ureteropelvic junction obstruction. *J Am Soc Nephrol* *23*, 618-628.

Trowe, M.O., Airik, R., Weiss, A.C., Farin, H.F., Foik, A.B., Bettenhausen, E., Schuster-Gossler, K., Taketo, M.M., and Kispert, A. (2012). Canonical Wnt signaling regulates smooth muscle precursor development in the mouse ureter. *Development* *139*, 3099-3108.

Truett, G.E., Heeger, P., Mynatt, R.L., Truett, A.A., Walker, J.A., and Warman, M.L. (2000). Preparation of PCR-quality mouse genomic DNA with hot sodium hydroxide and tris (HotSHOT). *Biotechniques* *29*, 52, 54.

Tsuchida, S., Matsusaka, T., Chen, X., Okubo, S., Niimura, F., Nishimura, H., Fogo, A., Utsunomiya, H., Inagami, T., and Ichikawa, I. (1998). Murine double nullizygotes of the angiotensin type 1A and 1B receptor genes duplicate severe abnormal phenotypes of angiotensinogen nullizygotes. *J Clin Invest* *101*, 755-760.

Tu, Y., Li, F., and Wu, C. (1998). Nck-2, a novel Src homology2/3-containing adaptor protein that interacts with the LIM-only protein PINCH and components of growth factor receptor kinase-signaling pathways. *Mol Biol Cell* 9, 3367-3382.

Tucker, K., and Lipson, A. (1990). Choanal atresia as a feature of ectrodactyly-ectodermal dysplasia-clefting (EEC) syndrome: a further case. *J Med Genet* 27, 213.

Uetani, N., and Bouchard, M. (2009). Plumbing in the embryo: developmental defects of the urinary tracts. *Clin Genet* 75, 307-317.

Ulinski, T., Lescure, S., Beaufils, S., Guignonis, V., Decramer, S., Morin, D., Clauin, S., Deschenes, G., Bouissou, F., Bensman, A., *et al.* (2006). Renal phenotypes related to hepatocyte nuclear factor-1beta (TCF2) mutations in a pediatric cohort. *J Am Soc Nephrol* 17, 497-503.

Van de Putte, T., Maruhashi, M., Francis, A., Nelles, L., Kondoh, H., Huylebroeck, D., and Higashi, Y. (2003a). Mice lacking ZFH1B, the gene that codes for Smad-interacting protein-1, reveal a role for multiple neural crest cell defects in the etiology of Hirschsprung disease-mental retardation syndrome. *Am J Hum Genet* 72, 465-470.

Van de Putte, T., Maruhashi, M., Francis, A., Nelles, L., Kondoh, H., Huylebroeck, D., and Higashi, Y. (2003b). Mice lacking ZFH1B, the gene that codes for Smad-interacting protein-1, reveal a role for multiple neural crest cell defects in the etiology of Hirschsprung disease-mental retardation syndrome. *Am J Hum Genet* 72, 465-470.

Van den Abbeele, A.D., Treves, S.T., Lebowitz, R.L., Bauer, S., Davis, R.T., Retik, A., and Colodny, A. (1987). Vesicoureteral reflux in asymptomatic siblings of patients with known reflux: radionuclide cystography. *Pediatrics* 79, 147-153.

van Eerde, A.M., Koeleman, B.P., van de Kamp, J.M., de Jong, T.P., Wijmenga, C., and Giltay, J.C. (2007). Linkage study of 14 candidate genes and loci in four large Dutch families with vesico-ureteral reflux. *Pediatr Nephrol* 22, 1129-1133.

Vandewalle, C., Comijn, J., De Craene, B., Vermassen, P., Bruyneel, E., Andersen, H., Tulchinsky, E., Van Roy, F., and Berx, G. (2005). SIP1/ZEB2 induces EMT by repressing genes of different epithelial cell-cell junctions. *Nucleic Acids Res* 33, 6566-6578.

Varelas, X., Sakuma, R., Samavarchi-Tehrani, P., Peerani, R., Rao, B.M., Dembowy, J., Yaffe, M.B., Zandstra, P.W., and Wrana, J.L. (2008). TAZ controls Smad nucleocytoplasmic shuttling and regulates human embryonic stem-cell self-renewal. *Nat Cell Biol* 10, 837-848.

Verschuere, K., Remacle, J.E., Collart, C., Kraft, H., Baker, B.S., Tylzanowski, P., Nelles, L., Wuytens, G., Su, M.T., Bodmer, R., *et al.* (1999). SIP1, a novel zinc

- finger/homeodomain repressor, interacts with Smad proteins and binds to 5'-CACCT sequences in candidate target genes. *J Biol Chem* 274, 20489-20498.
- Visel, A., Thaller, C., and Eichele, G. (2004). GenePaint.org: an atlas of gene expression patterns in the mouse embryo. *Nucleic Acids Res* 32, D552-556.
- Vivante, A., Kohl, S., Hwang, D.Y., Dworschak, G.C., and Hildebrandt, F. (2014). Single-gene causes of congenital anomalies of the kidney and urinary tract (CAKUT) in humans. *Pediatr Nephrol* 29, 695-704.
- Vrljicak, P., Myburgh, D., Ryan, A.K., van Rooijen, M.A., Mummery, C.L., and Gupta, I.R. (2004). Smad expression during kidney development. *Am J Physiol Renal Physiol* 286, F625-633.
- Wada, J., Liu, Z.Z., Alvares, K., Kumar, A., Wallner, E., Makino, H., and Kanwar, Y.S. (1993). Cloning of cDNA for the alpha subunit of mouse insulin-like growth factor I receptor and the role of the receptor in metanephric development. *Proc Natl Acad Sci U S A* 90, 10360-10364.
- Wang, H., Li, Q., Liu, J., Mendelsohn, C., Salant, D.J., and Lu, W. (2011). Noninvasive assessment of antenatal hydronephrosis in mice reveals a critical role for Robo2 in maintaining anti-reflux mechanism. *PLoS One* 6, e24763.
- Wang, Y., Tripathi, P., Guo, Q., Coussens, M., Ma, L., and Chen, F. (2009). Cre/lox recombination in the lower urinary tract. *Genesis* 47, 409-413.
- Ward, C.J., Turley, H., Ong, A.C., Comley, M., Biddolph, S., Chetty, R., Ratcliffe, P.J., Gattner, K., and Harris, P.C. (1996). Polycystin, the polycystic kidney disease 1 protein, is expressed by epithelial cells in fetal, adult, and polycystic kidney. *Proc Natl Acad Sci U S A* 93, 1524-1528.
- Wartiovaara, J., Ofverstedt, L.G., Khoshnoodi, J., Zhang, J., Makela, E., Sandin, S., Ruotsalainen, V., Cheng, R.H., Jalanko, H., Skoglund, U., *et al.* (2004). Nephrin strands contribute to a porous slit diaphragm scaffold as revealed by electron tomography. *J Clin Invest* 114, 1475-1483.
- Weber, S., Landwehr, C., Renkert, M., Hoischen, A., Wuhl, E., Denecke, J., Radlwimmer, B., Haffner, D., Schaefer, F., and Weber, R.G. (2011). Mapping candidate regions and genes for congenital anomalies of the kidneys and urinary tract (CAKUT) by array-based comparative genomic hybridization. *Nephrol Dial Transplant* 26, 136-143.
- Weisschuh, N., Wolf, C., Wissinger, B., and Gramer, E. (2008). A novel mutation in the FOXC1 gene in a family with Axenfeld-Rieger syndrome and Peters' anomaly. *Clin Genet* 74, 476-480.

Weng, Q., Chen, Y., Wang, H., Xu, X., Yang, B., He, Q., Shou, W., Higashi, Y., van den Berghe, V., Seuntjens, E., *et al.* (2012). Dual-mode modulation of Smad signaling by Smad-interacting protein Sip1 is required for myelination in the central nervous system. *Neuron* 73, 713-728.

Wenger, T.L., Harr, M., Ricciardi, S., Bhoj, E., Santani, A., Adam, M.P., Barnett, S.S., Ganetzky, R., McDonald-McGinn, D.M., Battaglia, D., *et al.* (2014). CHARGE-like presentation, craniosynostosis and mild Mowat-Wilson Syndrome diagnosed by recognition of the distinctive facial gestalt in a cohort of 28 new cases. *Am J Med Genet A* 164A, 2557-2566.

Wickstrom, S.A., Lange, A., Montanez, E., and Fassler, R. (2010). The ILK/PINCH/parvin complex: the kinase is dead, long live the pseudokinase! *EMBO J* 29, 281-291.

Williams, G., Fletcher, J.T., Alexander, S.I., and Craig, J.C. (2008a). Vesicoureteral reflux. *J Am Soc Nephrol* 19, 847-862.

Williams, S.S., Cobo-Stark, P., James, L.R., Somlo, S., and Igarashi, P. (2008b). Kidney cysts, pancreatic cysts, and biliary disease in a mouse model of autosomal recessive polycystic kidney disease. *Pediatr Nephrol* 23, 733-741.

Willig, T.N., Draptchinskaia, N., Dianzani, I., Ball, S., Niemeyer, C., Ramenghi, U., Orfali, K., Gustavsson, P., Garelli, E., Brusco, A., *et al.* (1999). Mutations in ribosomal protein S19 gene and diamond blackfan anemia: wide variations in phenotypic expression. *Blood* 94, 4294-4306.

Wilson, G.N., and Oliver, W.J. (1988). Further delineation of the G syndrome: a manageable genetic cause of infantile dysphagia. *J Med Genet* 25, 157-163.

Wong, K., Ren, X.R., Huang, Y.Z., Xie, Y., Liu, G., Saito, H., Tang, H., Wen, L., Brady-Kalnay, S.M., Mei, L., *et al.* (2001). Signal transduction in neuronal migration: roles of GTPase activating proteins and the small GTPase Cdc42 in the Slit-Robo pathway. *Cell* 107, 209-221.

Wood, C.G., 3rd, Stromberg, L.J., 3rd, Harmath, C.B., Horowitz, J.M., Feng, C., Hammond, N.A., Casalino, D.D., Goodhart, L.A., Miller, F.H., and Nikolaidis, P. (2015). CT and MR Imaging for Evaluation of Cystic Renal Lesions and Diseases. *Radiographics* 35, 125-141.

Woolf, A.S. (2000). A molecular and genetic view of human renal and urinary tract malformations. *Kidney Int* 58, 500-512.

Wu, C., and Dedhar, S. (2001). Integrin-linked kinase (ILK) and its interactors: a new paradigm for the coupling of extracellular matrix to actin cytoskeleton and signaling complexes. *J Cell Biol* *155*, 505-510.

Xiao, T., Staub, W., Robles, E., Gosse, N.J., Cole, G.J., and Baier, H. (2011). Assembly of lamina-specific neuronal connections by slit bound to type IV collagen. *Cell* *146*, 164-176.

Xin, B., Puffenberger, E.G., Turben, S., Tan, H., Zhou, A., and Wang, H. (2010). Homozygous frameshift mutation in *TMCO1* causes a syndrome with craniofacial dysmorphism, skeletal anomalies, and mental retardation. *Proc Natl Acad Sci U S A* *107*, 258-263.

Xu, P.X., Adams, J., Peters, H., Brown, M.C., Heaney, S., and Maas, R. (1999). *Eya1*-deficient mice lack ears and kidneys and show abnormal apoptosis of organ primordia. *Nat Genet* *23*, 113-117.

Xu, Y., Ruan, S., Wu, X., Chen, H., Zheng, K., and Fu, B. (2013). Autophagy and apoptosis in tubular cells following unilateral ureteral obstruction are associated with mitochondrial oxidative stress. *Int J Mol Med* *31*, 628-636.

Yamaji, S., Suzuki, A., Sugiyama, Y., Koide, Y., Yoshida, M., Kanamori, H., Mohri, H., Ohno, S., and Ishigatsubo, Y. (2001). A novel integrin-linked kinase-binding protein, affixin, is involved in the early stage of cell-substrate interaction. *J Cell Biol* *153*, 1251-1264.

Yan, C.H., Levesque, M., Claxton, S., Johnson, R.L., and Ang, S.L. (2011). *Lmx1a* and *lmx1b* function cooperatively to regulate proliferation, specification, and differentiation of midbrain dopaminergic progenitors. *J Neurosci* *31*, 12413-12425.

Yang, N., Morrison, C.D., Liu, P., Miecznikowski, J., Bshara, W., Han, S., Zhu, Q., Omilian, A.R., Li, X., and Zhang, J. (2012). TAZ induces growth factor-independent proliferation through activation of EGFR ligand amphiregulin. *Cell Cycle* *11*, 2922-2930.

Yang, Y., Guo, L., Blattner, S.M., Mundel, P., Kretzler, M., and Wu, C. (2005). Formation and phosphorylation of the PINCH-1-integrin linked kinase-alpha-parvin complex are important for regulation of renal glomerular podocyte adhesion, architecture, and survival. *J Am Soc Nephrol* *16*, 1966-1976.

Yoon, P.W., Olney, R.S., Khoury, M.J., Sappenfield, W.M., Chavez, G.F., and Taylor, D. (1997). Contribution of birth defects and genetic diseases to pediatric hospitalizations. A population-based study. *Arch Pediatr Adolesc Med* *151*, 1096-1103.

- Yoshimoto, A., Saigou, Y., Higashi, Y., and Kondoh, H. (2005). Regulation of ocular lens development by Smad-interacting protein 1 involving Foxe3 activation. *Development* 132, 4437-4448.
- Yu, J., Carroll, T.J., and McMahon, A.P. (2002). Sonic hedgehog regulates proliferation and differentiation of mesenchymal cells in the mouse metanephric kidney. *Development* 129, 5301-5312.
- Zent, R., Bush, K.T., Pohl, M.L., Quaranta, V., Koshikawa, N., Wang, Z., Kreidberg, J.A., Sakurai, H., Stuart, R.O., and Nigam, S.K. (2001). Involvement of laminin binding integrins and laminin-5 in branching morphogenesis of the ureteric bud during kidney development. *Dev Biol* 238, 289-302.
- Zha, D., Chen, C., Liang, W., Chen, X., Ma, T., Yang, H., Goor, H., and Ding, G. (2013). Nephritin phosphorylation regulates podocyte adhesion through the PINCH-1-ILK-alpha-parvin complex. *BMB Rep* 46, 230-235.
- Zhang, W., Wu, Y., Wu, C., and Gunst, S.J. (2007). Integrin-linked kinase regulates N-WASp-mediated actin polymerization and tension development in tracheal smooth muscle. *J Biol Chem* 282, 34568-34580.
- Zhang, Y., Chen, K., Tu, Y., Velyvis, A., Yang, Y., Qin, J., and Wu, C. (2002). Assembly of the PINCH-ILK-CH-ILKBP complex precedes and is essential for localization of each component to cell-matrix adhesion sites. *J Cell Sci* 115, 4777-4786.
- Zhou, Y., Huang, J., Cheng, Y.K., Leung, T.Y., Pooh, R.K., Lo, F.M., and Choy, K.W. (2014). Recurrent structural malformations identified among Mowat-Wilson syndrome fetuses. *Prenat Diagn* 34, 296-298.

**CURRICULUM VITAE**

